Universal Couplings in Two–Body Strong and Electromagnetic Meson Decays.

Neville Robert Jones B.Sc. (Hons.)

Submitted in fulfilment
of the requirements
for the degree of
Doctor of Philosophy
University of Tasmania. / Dept of Physics

April, 1997

Declaration

Except as stated herein this thesis contains no material which has been accepted for the award of any other degree or diploma in any University. To the best of my knowledge and belief, this thesis contains no material previously published or written by another person, except where due reference is made in the text of the thesis.

Neville R. Jones

Authority of Access

This thesis may be made available for loan and limited copying in accordance with the *Copyright Act 1968*.

Abstract

The strong and electromagnetic interactions of the ground state hadrons have, since the early 1970's, been known to comply with the tree level approximations given by effective Lagrangians. In more recent years the weak decays of heavy hadrons have been successfully calculated by use of the Heavy Quark Effective Theory (HQET). It is suited to hadrons containing a heavy quark (c, b, t) with light quark partner(s) (u, d, s) and uses the approximation that the hadron momentum is carried by the heavy quark. This resembles a group theoretical approach of constructing relativistic hadron wavefunctions in the mid 1960's, based on $U(2N_f) \otimes U(2N_f) \subset \tilde{U}(4N_f)$ symmetry group, producing wavefunctions whose structure implies that the constituent quarks must be moving collinearly and with the same velocity as the hadron. If one quark is much heavier than the others then it will have most of the momentum, as is the case for HQET. The main difference between the schemes is in the treatment of the light quark momentum, but this is a higher order correction leading only to minor changes.

Given the similarity between the models, but with the present favouritism shown for HQET, we re-investigate the $\tilde{U}(4N_f)$ scheme because of its many advantages. Firstly, since the scheme is a spin extension of the $SU(N_f)$ symmetry, the known mesons (including excited states) are classified into spin-flavour supermultiplets which naturally leads to the reduction of the number of free parameters compared to simple flavour $SU(N_f)$. Secondly, the scheme's interaction Lagrangian is applicable to two-body strong decays with one only needing a single coupling constant for each parent orbital angular momentum state. Vector meson dominance is easily incorporated to enable study of the electromagnetic processes.

In this thesis the $\tilde{U}(4N_f) \times O(3,1)_L$ scheme has been applied to the two-body strong and radiative decays of ground and excited mesons (from $L = 0$ to $L = 3$). We use known decay widths and meson masses to calculate the universal coupling constant involved. Uniformity in the value of supports

the supposed supersymmetry. There is high quality experimental data on the ground states decays and our analysis finds reasonably constant coupling, but there is some small symmetry breaking associated with the parent meson mass. Nonetheless, the breaking is quantifiable and leads to predictions for the D^* and B^* decay rates and branching fractions. From the less accurate experimental data available on excited decays we find good uniformity in the results, especially when taking into account the uniquely large number of processes considered in this work. Thus I have determined that the $\tilde{U}(4N_f)$ scheme appears well suited to describing meson interactions and their excitations and should be useful in studying the weak interactions after appropriate manipulation, as well.

As a contrast to $\tilde{U}(4N_f)$ we develop a quark triangle scheme involving a Feynman graph which provides quark level universal couplings to account for the symmetry breaking effects of unequal quark masses. Due to its complexity it is only applied to the ground state radiative decays, but with considerable success and over a range of processes far exceeding any similar work. Also, whereas other research has used approximations in the derivation of the decay amplitude, ours is exact and lends itself to study of all applicable channels regardless of the mesons involved. Unfortunately it is difficult to apply the method to higher excitations as the quark triangle involved is divergent, and so techniques of renormalization would have to be used.

Acknowledgments

I would like to thank my supervisor, Professor R. Delbourgo for his encouragement, assistance and advice throughout this project. Helping him in this task was Dr. Dongsheng Liu who showed immense patience inspite of my often constant barrage of questions. I wish him a long and fruitful life; if his past is anything to go by, I am sure he will have a very interesting future.

There are several other people of the theory group I would also like to thank. Dr. Peter Jarvis for his inspirational and unusual teaching, Dr. Dirk Kreimer for his appreciation of French cuisine and geography and Dr. Ioannis Tsohantjis for the cookery lessons (and thanks to Dora too) along with his dependency on me whenever his PC was in trouble – it's nice to feel needed! To my once fellow students and now friends, Dr. Tony Waites (`tonestuf`) and Dr. Tim :-) Baker, thanks for the great times. To my office-mate Stuart Corney; how fortunate that we share a like for loud, relatively obnoxious music – our only downfall was that the department staff didn't. There are numerous other people in the department who deserve a thank you, so without naming them all I will simply wish them the best and pass on my gratitude.

Unfortunately there are some friends I have to thank. Some would say I may have completed this project earlier if I had not known them, but I think it's more likely that without them I would never have finished it. They are: Fernando ('The Gimp') Della-Pasqua who keeps me laughing and honours me with his friendship, Shaun ('Big Fella') Hancock for teaching me several great Australian past-times, Peter ('Oh Bo, Oh Dear') Sedwick for his stress handling techniques and Ben ('Bevva') Stockwin for general life tips, mainly for showing what not to do.

It is a very simple task to thank my parents who have always supported my studies free of any pressure. Special thanks to my mother for pretty much everything. To my brothers Dean and Gavin, you guys are amazing. Last, but not least, I am indebted to Suellen for her patience, tolerance and her love.

Contents

List of Tables

List of Figures

Chapter 1

Introduction

Symmetries have played a fundamental role in the present understanding of atomic, nuclear and particle structure. It began when Mendelev first arranged the rapidly growing array of known atoms into the periodic table of the elements. His sorting was based on the regularities in chemical and physical properties of the elements and these symmetries suggested that atoms may have internal structure, motivating the development of several models of the atom. The experimental probing of atoms by Geiger and Marsden confirmed Rutherford's model; that of a dense, heavy, positively charged nucleus with negative charges distributed elsewhere. With this picture in mind, Bohr developed his model of the hydrogen atom in 1913. He assumed the electrons moved about the nucleus in circular orbits under the influence of the Coulomb attraction. These orbits were only at discrete distances from the nucleus and he imposed additional conditions to (attempt to) overcome the conflicts with classical physics. Nonetheless, his model produced predictions which were spectacularly matched by experiment. Unfortunately it did not fare so well for other atoms, but its refined version which seamlessly incorporated the 'new' ideas of quantum physics, yielded much better results. So from an observed symmetry rose a theoretical understanding of the atom with substantial predictive power.

Given that the atomic nucleus is positively charged and contributes to the

majority of the overall mass, the observed charge and mass progressions of the elements were consistent with the nucleus being composed of two particles, the neutron and the proton. The attractive force which binds these particles in the nucleus has to be very strong to overcome the Coulomb repulsion between the protons. This so-called nuclear force was found to be charge independent so that the force between protons and neutrons is the same as the force between protons and protons, or neutrons and neutrons (once other effects such as the Coulomb repulsion and the Pauli exclusion principle were taken into account). This symmetry of the nuclear force suggested the neutron and proton could be treated as related manifestations of the same particle. The new quantum number describing this symmetry was called isospin I (due to its mathematical similarities to the treatment of spin), and the proton was viewed as the isospin up ($I_3 = 1/2$) state, the neutron isospin down ($I_3 = -1/2$) state of the nucleon ($I = 1/2$). This machinery was very powerful in identifying related quantum states in systems with large numbers of nucleons. Symmetries in these systems could be understood on the basis of their isospin composition, and predictive ability spawned hand in hand with the simplifying aspects the symmetry provided. With the discovery of the charged pions in 1947 and the neutral pion in 1950, an understanding of the nuclear interaction based on Yukawa's meson theory of 1935 in terms of the exchange of virtual pions was completely consistent with the strength and short range nature of the nuclear force, as well as its conservation of isospin. At this stage in history, physicists were (once again) content with their understanding of the constituent particles of nature. However, there soon followed a prolification of particles which did not fit into this neat picture.

The 'particle zoo' has continued to expand, and today the number of strongly interacting particles is in the several hundred. In the early sixties, this number was around twenty five and several workers noticed symmetries in their properties. They arranged the particles in groupings much like those of the periodic table of the elements; any gaps in the diagrams representing

missing (unobserved) particles were soon filled and had properties consistent with those predicted by the groupings. Soon after the development of this scheme, it was realized it could be formulated in terms of constituent objects inside the hadrons (strongly interacting particles). These objects were called quarks, and in the mid 1960's three types of quark were required to account for the then known hadrons. As more particles were discovered the number of flavours necessary has grown to six, but most observed hadrons can be accommodated on the basis of the constituent quark model. The quarks are bound by the virtual exchange of gluons described by the gauge field theory of quantum chromodynamics (QCD). This combined with the electroweak theory forms the Standard Model of Elementary Particles, the basis of our present understanding of the forces and particles of nature (excluding gravity).

In all these cases the role played by symmetry considerations has been enormous. The observation of similarities in behaviour points to the possible simplification of the problem. With the development of a theory based on these symmetries one has a powerful predictive tool as few parameters are required to apply it to other situations in which the symmetry is applicable. The more general the symmetry, the fewer the number of parameters are required. Conversely, the discovery of universal parameters from a spectrum of sources indicates the presence of a symmetry. This project is concerned with the two-body strong and electromagnetic decays of the mesons. In recent years there has been a resurgence in the interest in these decays for the heavy mesons due to new tools such as the Heavy Quark Effective Theory. These techniques claim a superiority over those of old, such as $SU(3)$ extended to $SU(4)$ and $SU(5)$ because they exploit symmetries inherent to QCD which only emerge in certain situations.

This project chooses to re-examine as many as possible two-body strong and electromagnetic decays of the mesons using the most up-to-date data available. This analysis will span the ground and orbitally excited state mesons and will attempt to extract universal coupling constants from the

decay data. These couplings constants are universal in that they are the same for all processes considered. Obviously we are highly dependent on the theoretical model used to derive these couplings as to their universality. Since we are searching for couplings most universal in nature we ideally require a technique which embodies as many meson states as possible. To this end we use a relativistic generalisation of the $SU(6)$ quark model which treats the spin zero and spin one mesons of a given angular momentum on an equal footing. In its original conception it was based on three quark flavours, but with the simple extension to an arbitrary number of flavours we can apply it to the heavy meson sector as well as the light. This is a very powerful machinery for computing the couplings, but it has been many years since it was applied to the meson decays. We also examine the electromagnetic decays of the ground state mesons in the context of a quark loop diagram with universal type couplings defined at the meson-quark-antiquark vertices. The accuracy this technique offers is offset by the difficulties in applying this to other processes.

The motivation for determining these couplings is to evaluate the status of some methods which can be applied in the light and heavy meson sector (both ground and excited states). The advantage in this program stems from the opportunity to learn more about the model's abilities to handle different decay types. Our unique approach is to determine the coupling involved in many channels and to compare the values in each instance. In this manner we can immediately see the adherence to universality, and often deviations appear systematic and so can be incorporated into a refined version of the model. This differs from standard approaches relying on universal type couplings. What usually occurs is that the coupling is determined from one decay channel and then immediately used to yield predictions of symmetry related channel widths. These predictions are then compared with their experimental counterpart and a match signifies success. However, this method does not allow for any 'observational' stage and any deviations from the symmetry are much more difficult to determine.

1.1 Structure of the Thesis

This thesis consists of six chapters, this first one detailing the motivation behind the project and what is hoped to be achieved. Chapter 2 deals with the development of relativistic $SU(6)$ theory (and generalization to arbitrary flavour number) which we exploit in later chapters. This development traces the conception of the model based on Wigner's $SU(4)$ theory of nuclear interactions applied to the elementary particles. Since the $SU(6)$ quark model is an extension of the popular $SU(3)$, we directly compare the properties and predictions of both, revealing the many advantages of the $SU(6)$ ideas. To use it as a computational tool, we detail its relativistic generalisation which leads to a meson wavefunction encompassing the vector and pseudoscalar mesons as well as an interaction Lagrangian for the three point coupling of mesons applicable to two-body strong decays. Toward the end of Chapter 2 we discuss the many similarities the method has with some modern techniques, as revealed by several other workers.

Chapter 3 is where we apply the scheme to the ground state meson decays. From the general interaction Lagrangian of Chapter 2, the vertex specific forms are obtained, namely vector to two pseudoscalar (VPP), vector to vector and pseudoscalar (VVP) and vector to two vector (VVV). These in turn yield decay rate formulae which along with experimental data of actual decay widths can be used to extract the coupling constants. However, before doing this we incorporate electromagnetic interactions in the scheme using the notions of vector meson dominance to obtain suitable decay rate relations. After identifying the observed vector and pseudoscalar mesons in terms of the appropriate relativistic wavefunction indices and discussing some of the subtleties of extracting the relative weight of a given decay's coupling constant to the universal couplings we proceed with the analysis of the experimental data. The results show the couplings are quite regular, but there is some scattering of values. However, in most instances any deviations are systematic, and a simple symmetry breaking mechanism effectively restores the universal couplings. With these couplings several predictions are made

about the (presently unmeasured) decays of the D^* mesons, and several of the predictions are compared with other methods.

The decays of the orbitally excited mesons are the focus of Chapter 4. We firstly detail the incorporation of the orbital excitation states into the relativistic $SU(2N_f)$ method and then proceed to derive the permitted interactions and decay rates of the scheme, up to $L = 3$ or the F-wave mesons. With the correct assignment of wavefunction indices to observed mesons we extract couplings from the experimental measure of decay widths. There are a very large number of processes considered and in most cases they support the notion of the universal couplings. However, there are also numerous uncertainties with the data and possible interpretation of states; until the experimentalists reach greater consensus with their data we have problems making conclusive findings. Nonetheless, there are some very encouraging results and we hope the analysis will be performed again in the future.

In Chapter 5 we adopt a new method, that of a quark loop diagram and associated Feynman amplitude. This is applied to the electromagnetic interactions of the ground state mesons, with considerable success. It involves use of effective meson-quark-antiquark couplings constants for various quark flavours and mesons. To the extent that some predictive power is lost due to the prolification of coupling constants, the method offers insight into the symmetry breaking mechanisms at play which may be applicable to the earlier method. It also offers several predictions in the heavy meson realm, and these are directly compared with others.

Finally, Chapter 6 is comprised of a summary of the thesis together with suggestions for further avenues of study.

Chapter 2

History of Relativistic $SU(6)$

This chapter discusses the progression from the $SU(3)$ symmetry of the strong interactions (for three quark flavours) to the nonrelativistic $SU(6)$ model and then the relativistic generalization of this scheme. We detail several of the predictions of the $SU(3)$ symmetry and then contrast these with the extended predictions offered by the 'larger' symmetry of $SU(6)$. After developing the relativistically covariant version of this symmetry, applicable to an arbitrary number of quark flavours, we elaborate on how many modern techniques are very similar, and almost equivalent, to the forms we use.

The $SU(6)$ symmetry scheme of particle classifications was devised in the mid 1960's when researchers were interested in understanding the higher symmetries of the strong interactions. The approach was much like that of Wigner's $SU(4)$ of nuclear structure [117], except applied to the structure of elementary particles. It is therefore convenient to begin with Wigner's $SU(4)$ theory as applied to nucleons and then translate the theory to the elementary particles. We shall also compare the predictions of the $SU(3)$ symmetry scheme of the elementary particles, the so called 'eight-fold way', against those of the $SU(6)$ scheme.

2.1 Wigner's $SU(4)$ of nuclear structure

A fundamental tool of modern particle physics is the use of symmetries to simplify treatment of the ever enlarging 'particle zoo'. These symmetry techniques were first applied to the proton and neutron; the observed charge independence of the nuclear forces implied the proton and neutron were effectively indistinguishable to the nuclear forces (and hence in some sense symmetrical). Thus Heisenberg [67] devised a scheme in which they were considered as different states of the same particle; he gave them a new quantum number called *isotopic spin* (or isospin). The proton was said to be the **isospin up** state, while the neutron had **isospin down**. The observation that the nuclear forces were approximately equal between nucleon pairs is therefore equivalent to saying that the nuclear forces are isospin independent, or they preserve isospin symmetry.

The invariance of the nuclear interactions under isospin transformations was mathematically described by the group $SU(2)$ (the same group as normal spin). These notions of symmetry can be extended by neglecting the forces involving the ordinary spin of the nucleons (tensor and spin-orbit); the spin and space variables are decoupled with regard to the nuclear interactions so that they are invariant under a group $SU(2) \otimes SU(2)$, the direct product of the ordinary spin group and the isospin group. A further approximation can be made if the fundamental part of the nuclear force does not depend on spin and isospin at all (only space) then the interactions are invariant under the larger group of transformations $SU(4)$. The fundamental constituents of the group are a spin-up proton, spin-down proton, spin-up neutron and spin-down neutron and the $SU(4)$ group transforms these amongst themselves. A basis of an irreducible representation of the group $SU(4)$ characterises a supermultiplet of nuclear levels. Such supermultiplets can be reduced to bases of irreducible representations of a subgroup of $SU(4)$, namely $SU(2) \otimes SU(2)$. This reduction is useful for showing what spin and charge multiplets belong to a supermultiplet. Importantly, different spin and charge multiplets can be in the same supermultiplet, as the neutron-proton systems in the $^3S_1$

and ${}^1S_0$ states are (i.e. all spin and isospin states become degenerate).

2.2 Symmetry Groups of Elementary Particles

Provided one is only concerned with isospin and its conservation in nuclear (strong) interactions, $SU(2)$ provides a rudimentary classification of the eight spin 1/2 baryons and eight spin 0 mesons in terms of two doublets and a quartet. Interestingly, the isospin classification of $SU(2)$ was used to predict the existence of the Ξ^0, Σ^0 baryons and of distinct K^0 and $\bar{K}^0$ by Gell-Mann [58] and Nishijima and Nakau [88] in 1953. However, the *conservation* of strangeness (or more correctly hypercharge) by the strong interactions demanded an extended symmetry group beyond $SU(2)$. Gell-Mann [59] and Ne'eman [90] independently produced such a scheme known as the octet model or eightfold way based on the group $SU(3)$. This group transforms components of a fundamental triplet among themselves by unitary unimodular transformations. In such a 3-component representation of $SU(3)$, the mesons were identifiable from the direct product between 3 and $\overline{3}$ ($3 \otimes \overline{3} = 1 \oplus 8$) to produce the physically observed multiplet structure of singlet and octet, while the baryons were obtained from $3 \oplus 3 \oplus 3 = 1 \oplus 8 \oplus 8' \oplus 10$.

In 1964 Gell-Mann [60] and Zweig [120] realized the eightfold way could be more than a convenient classification scheme and might indicate the existence of fundamental constituent particles. Since a triplet was needed to generate $SU(3)$, three elementary particles had to exist and they must possess fractional electric and baryonic charges if they were to comprise the integer charge baryons and mesons. These were named quarks by Gell-Mann and have since received much indirect experimental support. They are necessarily spin 1/2 particles and hence their behaviour with regard to strong interactions possesses some spin dependence in the same way that nuclear forces do. However, if such dependence is minor we may regard the strong interactions as predominantly spin-independent and we can proceed with the

discussion of the elementary particle structure in a way parallel to the nuclear structure mentioned in Section 2.1.

The first approximation we may make is to ignore the tensor and spin-orbit forces so that the strong interactions are invariant under a group $SU(3) \otimes SU(2)$. A further approximation is to neglect all spin dependency so that the strong interactions become invariant under the group $SU(6)$ and we have effectively mixed the $SU(3)$ unitary spin and ordinary spin [65, 94, 101, 64]. The basic representations of $SU(6)$ have dimension 6 and consist of three $SU(3)$ states (quark flavours) having spin up, and three quark flavours with spin down. Thus one can obtain spin 0^- mesons from $q\bar{q}$ combinations in the ${}^1S_0$ state, 1^- mesons from $q\bar{q}$ in the ${}^3S_1$ state, spin 1/2 baryons from $q\uparrow\ q\uparrow\ q\downarrow$, spin 3/2 baryons from $q\uparrow\ q\uparrow\ q\uparrow$. Interestingly, because $SU(6)$ mixes the spin and internal $SU(3)$ spin coordinates, particles with different spin may belong to the same *supermultiplet*. For example, we will proceed to show that the pseudoscalar mesons and vector mesons are in the same supermultiplet in $SU(6)$.

To this end we denote an irreducible representation of the $SU(6)$ group by the dimension of the representation as was done in our discussion of $SU(3)$. Hence 6 will denote a fundamental representation and $\bar{6}$ its conjugate. We wish to reduce various direct products of these into bases of $SU(3) \otimes SU(2)$ so that we can identify $SU(6)$ supermultiplet members with their familiar $SU(3)$ multiplets. To denote such representations of $SU(3) \otimes SU(2)$ we use a pair of numbers (a, α), where a and α characterises the dimension of the $SU(3)$ and $SU(2)$ groups respectively. Hence the spin of a particle belonging to this representation is given by $\frac{1}{2}(\alpha - 1)$. With such notation an irreducible representation of $SU(6)$, "A" may be reduced to irreducible representations of $SU(3) \otimes SU(2)$, (a, α), $(b, \beta), \ldots$ in the following manner:

$$A = (a, \alpha) \oplus (b, \beta) \oplus \ldots$$

and must satisfy the relation $A = a\alpha + b\beta + \ldots$

As stated earlier we assume the pseudoscalar and vector mesons are bound states of a quark and antiquark in the ${}^1S_0$ and ${}^3S_0$ states respectively. Such

a bound state will belong to the representation $6 \otimes \bar{6}$ which can be reduced to 1 and 35 ($6 \otimes \bar{6} = 1 \oplus 35$). The representation 35 maybe further reduced to $(8,1)$, $(1,3)$ and $(8,3)$ representations of $SU(3) \otimes SU(2)$ which we identify with the octet of pseudoscalar mesons, the singlet and octet of vector mesons, respectively. Hence the octet of pseudoscalar mesons ($K^+K^o\pi^+\pi^-\pi^oK^-\bar{K}^0\eta$) and the singlet and octet of vector mesons ($\omega K^{*+}K^{*0}\rho^+\rho^0\rho^-K^{*-}\bar{K}^{*0}\phi$) belong to the *same* supermultiplet in this theory. The singlet pseudoscalar is the η' meson and belongs to the singlet supermultiplet here.

At this stage we have produced a convenient classification scheme for the mesons which groups the normal $SU(3)$ multiplets into $SU(6)$ multiplets by means of "mixing" the normal spin degrees of freedom with the internal degrees of freedom. But is such a scheme physically useful and give us testable predictions? To lead us to such tests we will revisit $SU(3)$ and develop some of the necessary tools in this simpler arena.

2.3 The $SU(3)$ Symmetry Group

In working with $SU(3)$ we have a 3-component spinor

$$q_i = \begin{pmatrix} u \\ d \\ s \end{pmatrix}; \quad \bar{q}_i = (\bar{u},\ \bar{d},\ \bar{s}),$$

with the quantum numbers

	I_3	Y	Q	B
u	$\frac{1}{2}$	$\frac{1}{3}$	$\frac{2}{3}$	$\frac{1}{3}$
d	$-\frac{1}{2}$	$\frac{1}{3}$	$-\frac{1}{3}$	$\frac{1}{3}$
s	0	$-\frac{2}{3}$	$-\frac{1}{3}$	$\frac{1}{3}$

(2.1)

and construct mesons from the direct product

$$q \otimes \bar{q} = q_i\bar{q}^j = M^\alpha_\beta = \begin{pmatrix} u\bar{u} & u\bar{d} & u\bar{s} \\ d\bar{u} & d\bar{d} & d\bar{s} \\ s\bar{u} & s\bar{d} & s\bar{s} \end{pmatrix},$$

which can be separated into scalar and traceless components by manipulation of the diagonal elements:

$$
\begin{aligned}
M^{\alpha}_{\beta} &= \begin{pmatrix} \frac{u\bar{u}+d\bar{d}+s\bar{s}}{3} + \frac{2u\bar{u}-d\bar{d}-s\bar{s}}{3} & u\bar{d} & u\bar{s} \\ d\bar{u} & \frac{u\bar{u}+d\bar{d}+s\bar{s}}{3} + \frac{-u\bar{u}+2d\bar{d}-s\bar{s}}{3} & d\bar{s} \\ s\bar{u} & s\bar{d} & \frac{u\bar{u}+d\bar{d}+s\bar{s}}{3} + \frac{-u\bar{u}-d\bar{d}+2s\bar{s}}{3} \end{pmatrix} \\
&= \underbrace{\frac{1}{\sqrt{3}} \begin{pmatrix} \frac{u\bar{u}+d\bar{d}+s\bar{s}}{\sqrt{3}} & 0 & 0 \\ 0 & \frac{u\bar{u}+d\bar{d}+s\bar{s}}{\sqrt{3}} & 0 \\ 0 & 0 & \frac{u\bar{u}+d\bar{d}+s\bar{s}}{\sqrt{3}} \end{pmatrix}}_{\text{scalarsinglet}} \\
&\quad + \underbrace{\begin{pmatrix} \frac{2u\bar{u}-d\bar{d}-s\bar{s}}{3} & u\bar{d} & u\bar{s} \\ d\bar{u} & \frac{-u\bar{u}+2d\bar{d}-s\bar{s}}{3} & d\bar{s} \\ s\bar{u} & s\bar{d} & \frac{-u\bar{u}-d\bar{d}+2s\bar{s}}{3} \end{pmatrix}}_{\text{tracelesstensoroctet}}.
\end{aligned}
$$

The scalar singlet state is identified as the η' meson while with the octet we perform further manipulations on the diagonal elements,

$$
\begin{aligned}
\frac{2u\bar{u}-d\bar{d}-s\bar{s}}{3} &= \frac{\frac{1}{2}(u\bar{u}+d\bar{d}) + \frac{3}{2}(u\bar{u}-d\bar{d}) - s\bar{s}}{3} \\
&= \frac{u\bar{u}+d\bar{d}-2s\bar{s}}{6} + \frac{u\bar{u}-d\bar{d}}{2} = \frac{\eta}{\sqrt{6}} + \frac{\pi^0}{\sqrt{2}},
\end{aligned}
$$

where we define $\eta = (u\bar{u}+d\bar{d}-2s\bar{s})/\sqrt{6}$ and $\pi^0 = (u\bar{u}-d\bar{d})/\sqrt{2}$. The η and η' both have zero isospin ($I = 0$ from $u\bar{u}+d\bar{d}$) while π^0 has $I = 1$. The requirement that η' be symmetric while η and π^0 be antisymmetric combinations of $u\bar{u}$, $d\bar{d}$, and $s\bar{s}$ gave us the above definitions. The remaining matrix elements of M^{α}_{β} are easily assigned using the quantum numbers of Table 2.1 :

$$
\begin{aligned}
u\bar{d} &\equiv \pi^+, \qquad d\bar{u} \equiv \pi^-, \\
u\bar{s} &\equiv K^+, \qquad d\bar{s} \equiv K^0, \\
s\bar{u} &\equiv K^-, \qquad s\bar{d} \equiv \bar{K}^0,
\end{aligned}
$$

so that for the 0^- mesons

$$M^\alpha_\beta(0^-) = \frac{1}{\sqrt{3}}\delta^\alpha_\beta\eta' + \begin{pmatrix} \frac{\pi^0}{\sqrt{2}} + \frac{\eta}{\sqrt{6}} & \pi^+ & K^+ \\ \pi^- & -\frac{\pi^0}{\sqrt{2}} + \frac{\eta}{\sqrt{6}} & K^0 \\ K^- & \bar{K}^0 & -\frac{2\eta}{\sqrt{6}} \end{pmatrix}, \qquad (2.2)$$

to produce the pseudoscalar meson nonet. In a similar fashion the vector meson nonet is obtained:

$$M^\alpha_\beta(1^-) = \frac{1}{\sqrt{3}}\delta^\alpha_\beta\omega + \begin{pmatrix} \frac{\rho^0}{\sqrt{2}} + \frac{\phi}{\sqrt{6}} & \rho^+ & K^{*+} \\ \rho^- & -\frac{\rho^0}{\sqrt{2}} + \frac{\phi}{\sqrt{6}} & K^{*0} \\ K^{*-} & \bar{K}^{*0} & -\frac{2\phi}{\sqrt{6}} \end{pmatrix}.$$

Thus the $SU(3)$ formalism naturally separates the meson nonets into singlet and octet multiplets (with the assumption that mesons are $q\bar{q}$ bound states). Similarly the baryons (qqq bound states) may be separated by the decomposition $3 \otimes 3 \otimes 3 = 1 \oplus 8 \oplus 8' \oplus 10$. The two octets are of mixed $SU(3)$ symmetry while the decuplet is symmetric. We may identify the decuplet with the ten $J^P = 3/2^+$ baryons: $(\Omega^-, \Xi^{*-}, \Xi^{*0}, \Sigma^{*-}, \Sigma^{*0}, \Sigma^{*+}, \Delta^-, \Delta^0, \Delta^+, \Delta^{++})$,[1] while one or a mixture of the octets contains the eight $J^P = 1/2^+$ baryons: $(n, p, \Sigma^-, \Sigma^0, \Lambda^0, \Sigma^+, \Xi^-, \Xi^0)$. As of yet we cannot say which octet contains these baryons.

So far it has been established that $SU(3)$ is capable of classifying the ground state mesons and baryons into what appears to be sensible groups sharing the same spins, parity and similar mass values. However, if $SU(3)$ were an exact symmetry for the strong interactions these multiplets should each be degenerate in mass (that is, members of multiplets should have identical masses). Experimental observations show that not only are there large splittings amongst the various isospin multiplets composing an $SU(3)$ multiplet, but also small splittings due to the electromagnetic interaction's influence on the strong interaction. These deviations from perfect $SU(3)$ symmetry have many interesting consequences with tangible predictions and we will investigate these with the aim of applying similar ideas in the $SU(6)$ realm.

[1] where $\Xi^* \equiv \Xi(1530)$ and $\Sigma^* \equiv \Sigma(1385)$.

2.3.1 Meson mass relations

The fact that multiplet members are not degenerate in mass led to the famous Gell-Mann Okubo (GMO) mass formula. To derive the relation, we must first define some quantities related to the group structure of $SU(3)$.

Generators of $SU(3)$

An $SU(3)$ octet $\{8\}$, can been written in terms of a set of eight linearly independent 3×3 Hermitian matrices,

$$\{8\} = \frac{1}{\sqrt{2}}(\lambda_i)^b_a M^i = \frac{1}{\sqrt{2}}\vec{\lambda} \cdot \vec{M},$$

where $\{8\}$ is a $SU(3)$ octet, $\vec{M}$ is an object with 8 components and λ_i are the traceless Gell-Mann matrices [59], given in Appendix A.1.1. An infinitesimal $SU(3)$ transformations will then be

$$U = 1 + i\varepsilon^i F_i$$

where $F_i = \lambda_i/2$ are the infinitesimal generators of the group (the λ_i being traceless ensures $\det U = 1$ and hence that we are dealing with $SU(3)$). They obey the commutation relations

$$[F_i, F_j] = i f^k_{ij} F_k \tag{2.3}$$

where f^k_{ij} are the structure constants of $SU(3)$. An alternative representation of $SU(3)$ can be obtained by taking linear combinations of F_i,

$$\begin{aligned} I_\pm &= F_1 \pm iF_2 \\ U_\pm &= F_6 \pm iF_7 \\ V_\pm &= F_4 \mp iF_5 \end{aligned}$$

$$I_3 = F_3, \quad U_3 = \tfrac{\sqrt{3}}{2}F_8 - \tfrac{1}{2}F_3, \quad V_3 = -\tfrac{\sqrt{3}}{2}F_8 - \tfrac{1}{2}F_3,$$

to produce eight independent generators.[2] These generators are the shift operators of $SU(3)$ as they have a one to one correspondence with the particle

[2] Although we have nine generators, $I_3 + U_3 + V_3 = 0$ so they are not independent.

states. Importantly, they show that $SU(3)$ is made out of 3 $SU(2)$ subgroups, I-spin, U-spin and V-spin. Subsequently, an $SU(3)$ triplet can be taken as being made up of an $SU(2)$ doublet plus singlet with respect to each of the spin spaces. For the quark triplet (u, d, s) we find three $SU(2)$ doublets, (u, d), (s, d), and (u, s) corresponding to I-spin, U-spin and V-spin space respectively.

There are some important commutation relations of $I_\pm$, $V_\pm$ and $U_\pm$,

$$\begin{aligned} [I_3, I_\pm] &= \pm I_\pm, \qquad [Y, I_\pm] = 0, \\ [Y, U_\pm] &= \pm U_\pm, \qquad [Q, U_\pm] = 0, \end{aligned} \tag{2.4}$$

so the $I_\pm$ operators change I_3 but do not change the hypercharge $Y = \frac{2}{3}(U_3 - V_3)$, while $U_\pm$ change Y, but not the electric charge $Q = I_3 + \frac{1}{2}Y$. Thus $SU(3)$ multiplet members belong to I-spin multiplets if they have the same hypercharge, or to U-spin multiplets if they have the same charge.

The Medium-Strong Interaction

The fundamental observation which led to the GMO relation is that within $SU(3)$ multiplets I-spin multiplets are almost degenerate in mass (the small difference in mass between isospin multiplets is due to the electromagnetic interaction), while U-spin or V-spin multiplet members have large mass differences. Thus, if we attribute the splitting to a medium-strong interaction (MSI), it must behave as a scalar in I-spin space, but as a vector in U- or V-spin spaces. If we choose to study the MSI in the U-spin space an appropriate mass operator is

$$O_M = M_0 + aU_3, \qquad O_M \psi_\iota = M_i \psi_\iota,$$

where ψ_ι is an $SU(3)$ state of mass M_i and M_0, a are scalars. To obtain U-spin multiplets we rotate the usual baryon octet Y-I_3 representation by $-120°$, as shown in Figure 2.1.

The U_1^0 and U_0^0 states are the central eigenstates of U and are found by

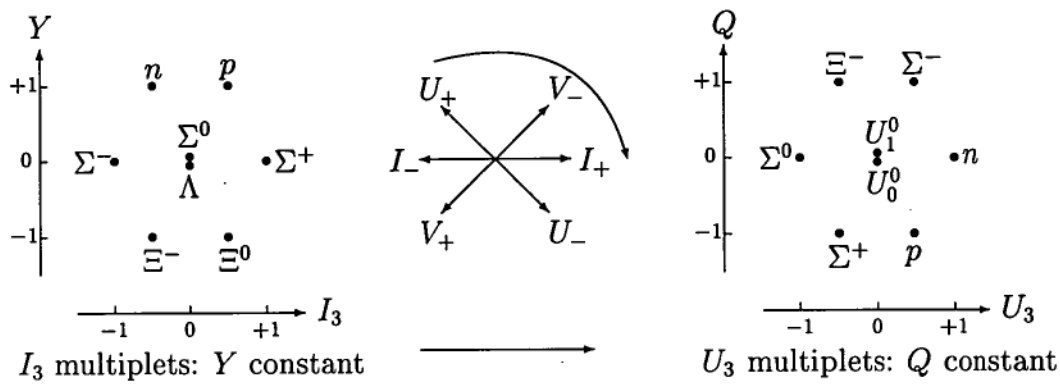

I_3 multiplets: Y constant $\longrightarrow$ U_3 multiplets: Q constant

Figure 2.1: Rotation of the usual baryon octet Y-I_3 representation by $-120°$ (from [83]).

rotating $\begin{pmatrix} \Sigma^0 \\ \Lambda \end{pmatrix}$ by $-120°$:

$$\begin{pmatrix} U_1^0 \\ U_0^0 \end{pmatrix} = \begin{pmatrix} \cos\frac{-2\pi}{3} & \sin\frac{-2\pi}{3} \\ -\sin\frac{-2\pi}{3} & \cos\frac{-2\pi}{3} \end{pmatrix} \begin{pmatrix} \Sigma^0 \\ \Lambda \end{pmatrix} = \begin{pmatrix} 1/2 & -\sqrt{3}/2 \\ \sqrt{3}/2 & 1/2 \end{pmatrix} \begin{pmatrix} \Sigma^0 \\ \Lambda \end{pmatrix},$$

so that $U_1^0 = (\Sigma^0 - \sqrt{3}\Lambda)/2$, $U_0^0 = (\sqrt{3}\Sigma^0 - \Lambda)/2$. Thus if we operate with O_M on the neutral U-spin triplet (Ξ^0, U_1^0, n) with $U_3 = (-1, 0, 1)$, respectively we find,

$$\begin{aligned} M_{\Xi^0} &= \left\langle \Xi^0 \left| O_M \right| \Xi^0 \right\rangle = M_0 - a \qquad (2.5) \\ M_{U_1^0} &= \left\langle \tfrac{\Sigma^0 - \sqrt{3}\Lambda}{2} \middle| O_M \middle| \tfrac{\Sigma^0 - \sqrt{3}\Lambda}{2} \right\rangle = M_0 \qquad (2.6) \\ &= \tfrac{1}{4}\left\langle \Sigma^0 \left| O_M \right| \Sigma^0 \right\rangle + \tfrac{3}{4}\left\langle \Lambda \left| O_M \right| \Lambda \right\rangle = \tfrac{1}{4}M_{\Sigma^0} + \tfrac{3}{4}M_\Lambda \\ M_n &= \left\langle n \left| O_M \right| n \right\rangle = M_0 + a. \qquad (2.7) \end{aligned}$$

Combining (2.5), (2.6) and (2.7) we obtain the Gell-Mann Okubo [59, 93] sum-rule for the baryon octet

$$2(M_n + M_{\Xi^0}) = 3M_{\Lambda^0} + M_{\Sigma^0}. \qquad (2.8)$$

In the context of the quark model, the realization that the MSI is a vector in U-spin space (and therefore $O_M = M_0 + aU_3$) indicates the s quark mass

differs from the u and d quark masses (which must be equivalent if MSI is a scalar in I-spin space and we ignore the electromagnetic interaction). For the pseudoscalar meson octet (2.8) reads $2(M_{K^0} + M_{\bar{K}^0}) = 3M_\eta + M_{\pi^0}$, but since $M_{K^0} = M_{\bar{K}^0}$ by CPT invariance we have

$$M_{K^0} = \tfrac{1}{4}\left(3M_\eta + M_{\pi^0}\right). \tag{2.9}$$

When we actually use these mass rules (2.8) is satisfied very well (4509 MeV compared with 4540 MeV) while (2.9) is only correct to 11% (498 MeV to 444 MeV). But if we replace the mass values by the square of the masses, that is

$$M^2_{K^0} = \tfrac{1}{4}\left(3M^2_\eta + M^2_{\pi^0}\right), \tag{2.10}$$

the agreement is much improved, being of the order 4%. If we try and apply the GMO relation to the vector meson octet, neither the appropriate linear or quadratic forms are satisfied to a reasonable accuracy. Does this mean we must abandon the GMO relation? Fortunately not, as an explanation exists from the mixing of $SU(3)$ states so that the particles we observe are not pure $SU(3)$ states. We note there exists a unitary singlet having the same quantum numbers as the $I_3 = 0$, $I = 0$ member of the octet. It may be possible that these members of different unitary multiplets have been 'mixed' by the MSI. Thus the discrepancy between the GMO relation and the observed masses may be due to the fact that the physical mesons are not pure $SU(3)$ states, but mixtures of singlet and octet states. A mixing angle θ can be defined in terms of the pure $SU(3)$ octet and singlet states, ψ_8 and ψ_1 respectively and the physical octet and singlet states, ψ'_8 and ψ'_1 respectively

$$\begin{aligned} \psi_8 &= \psi'_8 \cos\theta + \psi'_1 \sin\theta \\ \psi_1 &= -\psi'_8 \sin\theta + \psi'_1 \cos\theta, \end{aligned}$$

or

$$\psi = M^{-1}\psi'.$$

The angle θ is calculated from the known physical state masses and assumed validity of the GMO relation in the following manner. Since the Hamiltonian for pure $SU(3)$ states ψ_8, ψ_1 is not necessarily diagonal, but only real, we may write $H\psi = M\psi$ where m is the mass matrix operator (linear in the masses for baryons, linear in the squared masses for the mesons) given by

$$\begin{pmatrix} m_8 & m_{18} \\ m_{81} & m_1 \end{pmatrix}.$$

The observed particles are eigenstates of H so

$$H' \begin{pmatrix} \psi'_8 \\ \psi'_1 \end{pmatrix} = \begin{pmatrix} m'_8 & 0 \\ 0 & m'_1 \end{pmatrix} \begin{pmatrix} \psi'_8 \\ \psi'_1 \end{pmatrix}.$$

The similarity transformation $H' = MHM^{-1}$ diagonalizes the mass matrix by $m = M^{-1}m'M$ from which we obtain $m_8 + m_1 = m'_8 + m'_1$ and

$$\tan\theta = \left(\frac{m'_8 - m_8}{m_8 - m'_1}\right)^{\frac{1}{2}} \tag{2.11}$$

for the baryons. For the mesons, as m is linear in the squared masses we have $m_8^2 + m_1^2 = m_8'^2 + m_1'^2$ and

$$\tan\theta = \left(\frac{m_8'^2 - m_8^2}{m_8^2 - m_1'^2}\right)^{\frac{1}{2}} \tag{2.12}$$

Although we do not know m_8, we assume the GMO relation is accurate so that

$$m_8^2 = \frac{1}{3}(4M_{K^0}^2 - M_{\pi^0}^2),$$

for the pseudoscalars and

$$m_8^2 = \frac{1}{3}(4M_{K^{*0}}^2 - M_{\rho^0}^2)$$

for the vector mesons. If we use the known meson masses [13] we find $\theta \simeq 10.5°$ for pseudoscalar mesons, $\theta \simeq 40°$ for the vector mesons, indicating the pseudoscalar mesons are relatively pure while the vector mesons are substantially mixed.

2.3.2 Magnetic moments of baryons

The small mass differences between members of isospin multiplets within a unitary multiplet are due to electromagnetic interactions. We recall that the $U_\pm$ operators change the hypercharge Y but not the electric charge, as shown by (2.4), so that U-spin multiplets are made of particles with the same coupling to the electromagnetic field. Thus electromagnetic effects should be scalar in U-spin, and consequently the magnetic moments of U-spin multiplet members should be identical. Thus from Figure 2.1 we anticipate

$$\mu_p = \mu_{\Sigma^+}, \quad \mu_{\Sigma^-} = \mu_{\Xi^-}, \quad \mu_n = \mu_{\Xi^0} = \mu_{U_1^0}. \tag{2.13}$$

However, the electromagnetic effects are vector in I-spin space, so that an appropriate form of the magnetic moment μ is

$$\mu = \mu_0 + aI_3.$$

This immediately gives an "equal spacing rule" upon application to the $Y = 0$ I-spin triplet $(\Sigma^-, \Sigma^0, \Sigma^+)$ with $I_3 = (-1, 0, 1)$, respectively

$$\mu_{\Sigma^+} - \mu_{\Sigma^0} = \mu_{\Sigma^0} - \mu_{\Sigma^-}. \tag{2.14}$$

By combining (2.13) and (2.14) we can obtain some interesting relations, but we first need to show how $\mu_{U_1^0}$ is related to μ_Λ and μ_{Σ^0}. To this end,

$$\begin{aligned} \mu_\Lambda &= \langle \Lambda \mid \mu \mid \Lambda \rangle \\ &= \left\langle \frac{\sqrt{3}U_1^0 - U_0^0}{2} \middle| \mu \middle| \frac{\sqrt{3}U_1^0 - U_0^0}{2} \right\rangle = (3\mu_{U_1^0} + \mu_{U_0^0})/4, \end{aligned}$$

and in a similar fashion $\mu_{\Sigma^0} = (\mu_{U_1^0} + 3\mu_{U_0^0})/4$, so that

$$2\mu_{U_1^0} = 3\mu_\Lambda - \mu_{\Sigma^0} = 2\mu_n.$$

This combined with (2.14) and the condition imposed by $SU(3)$ symmetry in the octet, demanding the sum of magnetic moments of the octet members must vanish $\Sigma_i \mu_i = 0$, leads to the predictions

$$\mu_\Lambda = \mu_n/2, \quad \mu_p + \mu_n = -\mu_{\Xi^-},$$

which show some limited adherence in experimental observations [13]:

μ_Λ	$\mu_n/2$	$\mu_p + \mu_n$	$-\mu_{\Xi^-}$
-0.613	-0.957	0.8798	0.6507

We conclude this section with a summary of $SU(3)$ observations and predictions:

- On the assumption that mesons are bound states of $q\bar{q}$ pairs and baryons are qqq bound states, $SU(3)$ predicts the existence of meson singlet and octet structure. In the ground state mesons such structure is seen in the pseudoscalar and vector mesons, which each possess nine members and whose quantum numbers and mass values separate them into octet and singlet groupings. However, the $SU(3)$ model on its own does not reveal how the different spins of the pseudoscalar and vector mesons came about.

- The mass splittings between multiplet members (ignoring electromagnetic differences) appear to be adequately explained by a heavier s quark and equal mass u and d quarks. Such an $SU(3)$ breaking mechanism also explains deviations from the GMO relation, allowing for mixing between octet and singlet members. Observation suggest this mixing is substantial in the vector mesons, but less so in the pseudoscalars.

- The ground state baryon combinations form singlet, octet and decuplet groupings, of which the observed particles occupy the decuplet and octet. However, there is some ambiguity over which theoretical octet is filled by the observed octet of baryons. Nonetheless broken $SU(3)$ produces some predictions for the baryon magnetic moments which are roughly confirmed.

2.4 The $SU(6)$ scheme

In the preceding section we introduced the notion of quarks as a more intuitive way to discuss concepts of $SU(3)$. We now extend their application by making more assumptions about their dynamics and interactions with themselves and other quarks. To begin with we recall $SU(6)$ has a basic representation of dimension 6 which is comprised of three $SU(3)$ states (quarks) with spin up and three $SU(3)$ states with spin down. Thus the ground state mesons are realized as bound $q\bar{q}$ states; the pseudoscalars being in the ${}^1S_0$ state, the vectors in the ${}^3S_1$. Now the decomposition

$$6 \otimes \bar{6} = 1 \oplus 35,$$

and the subsequent reduction $35 = (8,1) \oplus (1,3) \oplus (8,3)$ implicitly shows that the vector meson octet and singlet belong to the same representations, while the pseudoscalar octet and singlet belong to *different* representations, 1 and 35. This is a possible explanation of the large mixing observed in the vector meson masses compared to the comparatively small mixing in the pseudoscalars. The larger degeneracy in the vector meson nonet is a natural consequence of the mass-breaking effects of $SU(6)$, of which the vector mesons are more susceptible than the pseudoscalars. The baryon states in $SU(6)$ formed by three quark states decompose as

$$6 \otimes 6 \otimes 6 = \overbrace{20}^{\text{antisym}} \oplus \overbrace{56}^{\text{sym}} \oplus \overbrace{70 \oplus 70'}^{\text{mixedsym}}, \tag{2.15}$$

and the symmetric 56 reduces to $56 = (8,2) \oplus (10,4)$, an octet of spin $1/2$ and a decuplet of spin $3/2$! Where $SU(3)$ inherently possessed an ambiguity about which octet, 8 or $8'$, contained the observable particles, in $SU(6)$ the problem has disappeared. Subsequently it appears $SU(6)$ is more successful as a classification scheme than $SU(3)$.

There is however, a very important problem with this picture. The decuplet of spin $3/2$ baryons has three interesting states; the Δ^- made up of three $d\uparrow$ quarks, the Δ^{++} of three $u\uparrow$ quarks and the Ω^- of three $s\uparrow$ quarks.

Given that the parities of the quarks are identical and defined as even (which is the only interpretation consistent with the even parity of the baryons), which also implies there is no relative orbital angular momentum between them, all the quarks appear to be in the same quantum state. This immediately suggests they are violating the Pauli exclusion principle in contradiction with their fermionic nature (i.e. the quarks are spin half objects). The only way to restore consistency with the well established exclusion principle is to introduce a new quantum number for the quarks. By necessity this quantum number must be three-valued; each of the quarks in a baryon state must have a different value of this quantum number, but paradoxically it must vanish in the bound state as the quantum number has never been physically observed. That is, a baryon (hadron) state must not possess the quantum number even though their constituents do. This suggests an analogy with the three primary colours which when combined produce white (or an absence of colour). Thus the new three-valued quantum number was given the name "*colour*". This picture can be consistently applied to the mesons; if they are $q\bar{q}$ combinations the colour of the quark cancels the anti-colour of the antiquark (e.g. 'red' + 'anti-red' = 'white') to produce a colourless bound state. Importantly, this quantum number imposes the condition that only colourless combinations of quarks can be observable hadrons. This restricts us to $q\bar{q}$ and qqq bound states[3], which in turn offers some explanation of the binding mechanism of the hadrons.

The common view is that the colour quantum number of the strong interaction has an equivalent role as the charge quantum number does to electromagnetism. Whereas photons are absorbed and emitted by electric charges (the exchange of which leads to the electromagnetic interaction), so to the strong interaction arises by the exchange of *gluons* between colour charges. The gauge field theory of colour, *quantum chromodynamics* (QCD) along

[3]However, exotic states such as $q\bar{q}q\bar{q}$ and $qqqq\bar{q}$ are colourless and thus viable quark combinations. The search continues today for the observation of such states, with some potential candidates in the $a_0(980)$ and $f_0(980)$ and others.

with its electromagnetic counterpart, *quantum electrodynamics* (QED) are two crucial parts of the (generally accepted) modern theory of the elementary particles, the so-called Standard Model. We emphasize that the notion of colour was only introduced when models like $SU(6)$ related the spin of the constituent quarks to the overall spin of the hadron, exposing the conflict with the exclusion principle in the baryons Δ^-, Δ^{++} and Ω^-.

2.4.1 $SU(6)$ Mass Relations

As was the case with $SU(3)$, many of the predictions of the classification scheme come not from its strict adherence in nature, but rather from the way in which it is broken. Obviously $SU(6)$ is more severely broken than $SU(3)$, otherwise we should expect all members of a supermultiplet to be degenerate in mass. Under this condition we would expect the ground state mesons to have identical masses as would all the ground state baryons, which is far from what is observed. Nonetheless, it is possible to quantify the transformation properties of the symmetry breaking interactions and extract some predictions.

Naturally we can reproduce the $SU(3)$ mass relations as the $SU(3)$ multiplet structure is encompassed within the $SU(6)$ supermultiplet structure. The most interesting mass relations are those which span $SU(3)$ multiplets . In the ground state mesons there is the "equal spacing" rule [94, 82, 101]

$$M_{K^*}^2 - M_\rho^2 = M_K^2 - M_\pi^2, \tag{2.16}$$

and the more advanced rule [18]

$$\begin{aligned} M_\omega^2 M_\phi^2 \;\cong\; & \tfrac{1}{2}\left(M_\pi^2 + M_{K^*}^2 - M_K^2\right)\left(3M_{K^*}^2 - M_\rho^2 + M_K^2 - M_\pi^2\right) \\ & -\tfrac{1}{6}\left(4M_{K^*}^2 - M_\rho^2\right)\left(5M_{K^*}^2 - M_\rho^2 + M_\pi^2 - M_K^2 - 2M_\omega^2 - 2M_\phi^2\right) \end{aligned} \tag{2.17}$$

Present mass values [13] show both of these to be well satisfied, with (2.16) and (2.17) yielding $2.09 \times 10^5 = 2.27 \times 10^5$ and $6.35 \times 10^{11} = 6.34 \times 10^{11}$, respectively. The baryons also have "equal spacing" rules:

$$M_{\Xi^*} - M_{\Sigma^*} = M_\Xi - M_\Sigma,$$

and by substituting actual mass values $148 = 127$, we see the prediction is fair.

2.4.2 Baryon Magnetic Moments in $SU(6)$

One of $SU(6)$'s well-known successes is in the prediction of the proton to neutron magnetic moment ratio. As in $SU(3)$ it is assumed the quark magnetic moment operator is proportional to its electric charge so that the d and s quark magnetic moment operators are identical;

$$\mathbf{M}_d = \mathbf{M}_s,$$

and that $\mathbf{M}_u + \mathbf{M}_d + \mathbf{M}_s = 0$ as required by $SU(3)$ symmetry and that the electromagnetic interaction is known to be scalar in I-spin. These determine that the magnetic moment operator has the form

$$\mathbf{M}_q = \mu \frac{e_q}{e} \sigma_q,$$

where e_q and σ_q are the charge and spin operator of quark q and μ is a scale parameter. A hadron's magnetic moment operator is assumed to be given by the sum of the constituent quark magnetic moment operators and hence the magnetic moment of hadron A would be calculated from the expectation value

$$\langle \mu \rangle = \langle \psi(A, s_z) \mid \sum_i \mathbf{M}^z_{q_i} \mid \psi(A, s_z) \rangle, \tag{2.18}$$

where $\psi(A, s_z)$ is the $SU(6)$ wavefunction of hadron A with spin s_z. The baryon decuplet states are fully symmetric under permutations of the three quarks (from Equation (2.15)) and the quark spins must be parallel to give total spin 3/2. Hence the unitary-spin wavefunction must be symmetric to combine with the spin wavefunction to produce an overall symmetric $SU(6)$ wavefunction. One can easily manufacture the wavefunction $\psi(A)$ for a ground state decuplet baryon by combining the spin wavefunctions,

Spin	Wavefunction
$s_z = \frac{3}{2}$	$\lvert\uparrow\uparrow\uparrow\rangle$
$s_z = \frac{1}{2}$	$\frac{1}{\sqrt{3}}\left[\lvert\uparrow\uparrow\downarrow\rangle + \lvert\uparrow\downarrow\uparrow\rangle + \lvert\downarrow\uparrow\uparrow\rangle\right],$

with the quark content of the baryon, for example

$$\psi(\Delta^+, s_z = \tfrac{3}{2}) = \tfrac{1}{\sqrt{3}} \left[|u\uparrow u\uparrow d\uparrow\rangle + |u\uparrow d\uparrow u\uparrow\rangle + |d\uparrow u\uparrow u\uparrow\rangle \right].$$

The octet of baryon states also have an overall symmetric $SU(6)$ wavefunction, but since the total spin of the baryon is $1/2$, the spin and unitary-spin wavefunctions must separately have mixed symmetry. To construct a suitable wavefunction for the spin $1/2$ baryons, one can put two quarks in a spin singlet state and add a third quark with spin up. For example, to build the $SU(6)$ wavefunction for a proton with spin up we would begin with two quarks in a spin singlet state:

$$\frac{1}{\sqrt{2}} (\uparrow\downarrow - \downarrow\uparrow).$$

To produce an overall symmetric combination the quarks have to be in an antisymmetric unitary state and hence for the proton the only possibility is

$$\frac{1}{\sqrt{2}}(ud - du).$$

When we add the final quark, in this case a spin up u flavour we find after symmetrization and normalization that

$$\begin{aligned} \psi(p, s_z = \tfrac{1}{2}) \;=\; & \frac{1}{\sqrt{18}} \left(2\,|u\uparrow d\downarrow u\uparrow\rangle + 2\,|u\uparrow u\uparrow d\downarrow\rangle + 2\,|d\downarrow u\uparrow u\uparrow\rangle \right. \\ & - |u\uparrow u\downarrow d\uparrow\rangle - |u\uparrow d\uparrow u\downarrow\rangle - |u\downarrow d\uparrow u\uparrow\rangle \\ & \left. - |d\uparrow u\downarrow u\uparrow\rangle - |d\uparrow u\uparrow u\downarrow\rangle - |u\downarrow u\uparrow d\uparrow\rangle \right). \end{aligned}$$

In a similar fashion, the neutron $SU(6)$ wavefunction is

$$\begin{aligned} \psi(n, s_z = \tfrac{1}{2}) \;=\; & \frac{1}{\sqrt{18}} \left(-2\,|d\uparrow u\downarrow d\uparrow\rangle + 2\,|d\uparrow d\uparrow u\downarrow\rangle + 2\,|u\downarrow d\uparrow d\uparrow\rangle \right. \\ & + |u\uparrow d\downarrow d\uparrow\rangle + |d\uparrow u\uparrow d\downarrow\rangle + |d\downarrow u\uparrow d\uparrow\rangle \\ & \left. + |d\uparrow d\downarrow u\uparrow\rangle + |u\uparrow d\uparrow d\downarrow\rangle + |d\downarrow d\uparrow u\uparrow\rangle \right). \end{aligned}$$

Thirring [114] supplies a complete list of these constructions for the ground state baryons, as well as the $SU(6)$ wavefunctions for the ground state mesons. With these wavefunctions one can use Equation (2.18) to obtain

$$\mu_p = \mu, \quad \mu_n = -2\mu/3,$$

to give

$$\frac{\mu_p}{\mu_n} = -\frac{3}{2},$$

first quoted by Bég, Lee and Pais [15] and which is in excellent agreement with the experimental ratio of -1.46 [13].

2.4.3 Summary

We summarise aspects of the $SU(6)$ theory discussed above:

- the classification of states is more intuitive is $SU(6)$; the pseudoscalar and vector mesons are bound states of quark and antiquark in the $^1S_0$ and $^3S_1$ states, respectively. The spin 1/2 baryons are bound $q\uparrow\, q\uparrow\, q\downarrow$ states, spin 3/2 baryons are $q\uparrow\, q\uparrow\, q\uparrow$ states.

- There is a lack of appreciable mixing in the η and η' mesons as they belong to different supermultiplets (the 1 and 35, respectively). There is substantial mixing between ϕ and ω because they belong to the same supermultiplet, the 35. The mixing should be 'ideal' [18, 82] in which case $\phi = s\uparrow\, \bar{s}\uparrow$, $\omega = (u\uparrow\, \bar{u}\uparrow + d\uparrow\, \bar{d}\uparrow)/\sqrt{2}$ corresponding to $\theta_V = 35.5°$. This is close to the experimental value $\theta_V = 39.4°$.

- Predictions such as $\mu_p/\mu_n = -3/2$, $M_{\Xi^*} - M_{\Sigma^*} = M_\Xi - M_\Sigma$ and $M^2_{K^*} - M^2_\rho = M^2_K - M^2_\pi$, all of which are well matched by experiment. These results *cannot* be obtained from $SU(3)$ considerations.

The mass breaking effects are substantial from the obvious lack of degeneracy in the masses of the supermultiplets; the pseudoscalar mesons do *not* have the same mass as the vector mesons, nor do the ground state baryons have all the same mass. Nonetheless, $SU(3)$ is badly broken in the multiplet masses, and yet other aspects of the symmetry are regularly applied to provide predictions well matched by experiment. In the same fashion, we intend to apply $SU(6)$ (actually the flavour number independent version) to the two-body decays of the mesons and establish how well prediction compares to

experiment. To this end we must first discuss the relativistic generalization of the symmetry, a necessary step if we wish to obtain an S-matrix theory.

2.5 Covariant $SU(6)$

Our discussion of $SU(6)$ symmetry has been in the non-relativistic domain; in the formulation of the theory the total angular momentum of the hadron was separated into its spin and orbital parts which is not a Lorentz-invariant manoeuver [35]. There were numerous attempts at the relativistic generalization of $SU(6)$, along several paths. Early on, $U(6)\otimes U(6)$ appeared an eligible candidate [57, 8], but it led to parity doubling for the mesons [9] which has the undesirable consequence of the mass term in the free Lagrangian breaking Lorentz invariance [27]. Soon after it was realized that invoking ideas of parity conservation helped alleviate the problems, but at the expense of lack of invariance of the interaction terms [44]. If this group was extended to the non-compact group $U(6,6)$ (appearing as $SU(12)_{\mathcal{L}}$ [97, 17] $M(12)$ [36, 102], and $U(12)$ [105, 104] in the literature) a fully covariant, $SU(6)$ invariant S-matrix could be constructed. There followed discussion about the conflict these methods had with the principle of unitarity of the physical S-matrix [21, 16], leading to a growing loss of enthusiasm for finding a relativistic generalization of $SU(6)$. At the forefront of these concerns was that the finite-dimensional representations of the non-compact $U(6,6)$ were not unitary and so could not be associated with physical particles. However, a physical interpretation could be achieved by subjecting the representations to some equations of motion, effectively projecting out the definite sectors and making the offending terms redundant [105, 104]. In this approach, the authors realized that although the S-matrix could not be $U(6,6)$ invariant, the theory was useful for producing $U(6,6)$ invariant interaction Lagrangians between the corresponding fields. It is for this reason that we shall exploit it in the two-body strong decays of the mesons. We proceed with the derivation of the $U(6,6)$ meson fields and interactions. For a more complete review of

the relativistic generalisation of $SU(6)$, the reader is recommended to that by Dyson [49].

2.5.1 The $\widetilde{U}(12)$ Symmetry

We begin with a discussion of the group $\widetilde{U}(12)$ (or more exactly, $U(6,6)$) and its algebra. To this end we construct the smaller group $U(2,2)$ from which the larger algebra is readily generalizable. The sixteen 4×4 Dirac matrices $\gamma_R, R = 1, \ldots, 16$ consisting of

$$1, \gamma_\mu, \sigma_{\mu\nu}, i\gamma_\mu\gamma_5, \gamma_5,$$

where $\mu, \nu = 0, 1, 2, 3$ and $\sigma_{\mu\nu} = i[\gamma_\mu, \gamma_\nu]/2$, $\gamma_5 = \gamma_0\gamma_1\gamma_2\gamma_3$ along with $\{\gamma_\mu, \gamma_\nu\} = 2g_{\mu\nu}$, $g_{\mu\nu} = (1, -1, -1, -1)_{\text{diag}}$ obey the defining property of the $U(2,2)$ algebra, namely,

$$\gamma_0\gamma_R\gamma_0 = \gamma_R^\dagger,$$

provided γ_0 is hermitian ($\gamma_0 = \gamma_0^\dagger$) and $\vec{\gamma}$ is anti-hermitian ($\vec{\gamma}^\dagger = -\vec{\gamma}$). This is achieved in the Pauli representation in which

$$\gamma_0 = (1, 1, -1, -1)_{\text{diag}}. \tag{2.19}$$

The $U(2,2)$ algebra will be realized by a set of matrices J_R which satisfy the commutation rules analogous to those of the γ_R (Appendix A.1.2). There exists an equivalent basis for the algebra which is useful for generalization to the $U(6,6)$ algebra, or indeed $U(2N_f, 2N_f)$ as we will ultimately require. This basis is defined by the generators

$$J_\beta^\alpha = \frac{1}{2}(\gamma^R)_\alpha^\beta J^R, \qquad \alpha, \beta = 1, 2, 3, 4$$

from which all the commutation rules are summarized to

$$[J_\alpha^\beta, J_\gamma^\delta] = \delta_\alpha^\delta J_\gamma^\beta - \delta_\gamma^\beta J_\alpha^\delta \tag{2.20}$$

and the defining property of $U(2,2)$ is the hermiticity condition

$$(J_\alpha^\beta)^\dagger = (\gamma_0)_\beta^\gamma J_\gamma^\delta (\gamma_0)_\delta^\alpha \tag{2.21}$$

where γ_0 is given in (2.19). It is now a simple step to the $U(6,6)$ algebra. With $\gamma_0 = (\underbrace{1,\ldots,1}_{6},\underbrace{-1,\ldots,-1}_{6})_{\text{diag}}$ and generators J_A^B $(A,B = 1,\ldots,12)$ we obtain the analogues of Equations 2.20 and 2.21, namely the generators satisfy the commutation relations,

$$[J_A^B, J_C^D] = \delta_A^D J_C^B - \delta_C^B J_A^D \tag{2.22}$$

and give the defining property of $U(6,6)$:

$$(J_A^B)^\dagger = (\gamma_0)_B^C J_C^D (\gamma_0)_D^A. \tag{2.23}$$

It is useful to pass to a "hermitian" basis by using the γ_R along with the unitary spin matrices F^i $(i = 0,\ldots,8)$ which define the fundamental $U(3)$ representation. The $F^i = \lambda^i/2$ $(i = 1,\ldots,8)$ were introduced in Section 2.3.1, while $F^0 = 1/\sqrt{6}$. With these definitions, the F^i satisfy

$$F^i F^j = \tfrac{1}{2}(d_k^{ij} + i f_k^{ij}) F^k;\ i,j,k = 0,\ldots,8,$$

which is a direct consequence of (2.3) and the anticommutation relations of F^i, namely $\{F_i, F_j\} = d_{ij}^k F_k$ where d_{ij}^k $(i,j,k = 1,\ldots,8)$ are structure constants of $SU(3)$, and $f_k^{0j} = 0$, $d_k^{0j} = \sqrt{\frac{2}{3}}\delta_k^j$. We then construct the generators

$$J_R^i = (\gamma_R)_\alpha^\beta (F^i)_a^b J_B^A,$$

$$A = \alpha a,\ B = \beta b;\ \alpha,\beta = 1,\ldots,4;\ a,b = 1,2,3.$$

Quark spinors in $U(6,6)$

We take as the fundamental particle of strong interactions a 12-component (Dirac) quark, $\psi_A = \psi_{a\alpha}$ $(A = a\alpha,\ a = 1,2,3,\ \alpha = 1,...,4)$ which under a homogenous $U(6,6)$ transformation undergoes the change

$$\psi_A \longrightarrow \psi'_A = S_A^B \psi_B$$

with

$$S = \exp(i\epsilon_R^j J_R^j) = \exp(i\epsilon_B^A J_B^A),$$

where all 144 ϵ's are real, ensuring $\bar{\psi}^A\psi_A$ is invariant under $U(6,6)$ transformations, provided the antiquark spinor is defined by

$$\bar{\psi}^A = \bar{\psi}^{a\alpha} = (\psi_{a\beta})^\dagger(\gamma_0)^\alpha_\beta = (\psi^{a\beta})^*(\gamma_0)^\alpha_\beta$$

and the * denotes complex conjugation. To obtain fields of higher rank with the aim of describing particles of different quark number and spin (for example mesons and baryons) we construct multi-index spinor fields (multispinors). To this end, the direct products between quarks and antiquarks produces finite-dimensional non-unitary representations of $U(6,6)$ which transform according to the rule

$$\Psi^{CD\ldots}_{AB\ldots} = S^{A'}_A S^{B'}_B \ldots (S^{-1})^C_{C'}(S^{-1})^D_{D'} \ldots \Psi^{C'D'\ldots}_{A'B'\ldots}.$$

Of particular importance to this project are the multispinor fields representing the ground state mesons (quark and antiquark), $\Psi^B_A = \Phi^B_A$ with dimensionality 143 (from the decomposition of $U(6,6)$ to $SU(6,6)$: $12 \otimes \overline{12} = 1 \oplus 143$). The baryons formed from the multispinor $\Psi_{\{ABC\}}$, have dimensionality 364 (from $12 \otimes 12 \otimes 12 = 220 \oplus 364 \oplus 572 \oplus 572$).

Physical Interpretation from the Bargmann–Wigner equations

Since U(6,6) is non-compact, its unitary representations are infinite dimensional and cannot be associated with physical particles. However the non-unitary finite-dimensional representations can be tied to particle states by projecting out a particular sector through the application of equations of motion which the spinors must satisfy. Despite the apparent restrictive nature of such a projection, all presently known particles can be accommodated in the scheme so there appears to be no disadvantage in using such a method.

We proceed along this path with the definition of the invariant scalar product between multispinors $\phi^{B_1\ldots}_{A_1A_2\ldots}$ belonging to some irreducible representation of $U(6,6)$,

$$\phi^{B_1\ldots}_{A_1A_2\ldots}\bar{\phi}^{A_1A_2\ldots}_{B_1\ldots} = \phi^{B_1\ldots}_{A_1A_2\ldots}(\gamma_0)^{B'_1}_{B_1}\ldots(\phi^{A'_1A'_2\ldots}_{B'_1\ldots})^*(\gamma_0)^{A_1}_{A'_1}(\gamma_0)^{A_2}_{A'_2}\ldots, \qquad (2.24)$$

where $(\gamma_0)^B_A = (\gamma_0)^\beta_\alpha \delta^b_a$. The form of the scalar product (2.24) is not positive definite but a definite subspace can be projected out by imposing the set $\phi^{B_1\ldots}_{A_1A_2\ldots}$ to those on which γ_0 takes one value. For lower indices we choose

$$(\gamma_0)^{A'_n}_{A_n} \phi^{B_1\ldots}_{A_1A_2\ldots A'_n\ldots} = \phi^{B_1\ldots}_{A_1A_2\ldots A_n\ldots}, \tag{2.25}$$

and for upper indices

$$(\gamma_0)^{B_n}_{B'_n} \phi^{B_1B_2\ldots B'_n\cdots}_{A_1\ldots} = -\phi^{B_1B_2\ldots B_n\cdots}_{A_1\ldots}. \tag{2.26}$$

The multispinors which satisfy (2.25) and (2.26) are not invariant under the full group $U(6,6)$ but instead belong to the subgroup consisting of those matrices S^B_A for which

$$S\gamma_0 S^{-1} = \gamma_0,$$

or equivalently

$$S^{-1} = S^\dagger,$$

which is the maximal compact subgroup $U(6) \otimes U(6)$. Hence the original indefinite space of the $U(6,6)$ representation has been reduced to a definite subspace invariant under $U(6) \otimes U(6)$.

If these multispinors are taken to represent particle states at rest, we can set them in motion by applying the appropriate relativistic boost. Denote by L_p a family of Lorentz matrices for which

$$L_p \gamma_0 L_p^{-1} = \not{p}/m = p_\mu \gamma^\mu / m$$

where m is the rest mass $p^2 = m^2$. Then a multispinor state with momentum p_μ is given by

$$\phi^{B_1\ldots}_{A_1A_2\ldots}(p) = (L_p)^{A'_1}_{A_1}(L_p)^{A'_1}_{A_1} \ldots \phi^{B'_1\ldots}_{A'_1A'_2\ldots}(L_p^{-1})^{B_1}_{B'_1} \ldots .$$

The boosted versions of (2.25) and (2.26) are

$$\not{p}^{A'_n}_{A_n} \phi^{B_1\ldots}_{A_1A_2\ldots A'_n\ldots}(p) = m\phi^{B_1\ldots}_{A_1A_2\ldots A_n\ldots}(p)$$

for lower indices and

$$\not{p}^{B_n}_{B'_n} \phi^{B_1B_2\ldots B'_n\cdots}_{A_1\ldots}(p) = -m\phi^{B_1B_2\ldots B_n\cdots}_{A_1\ldots}(p)$$

for upper indices, which with minimal manipulation are seen to be the Bargmann–Wigner equations [11] which describe particles of a definite mass m and definite spin. In the same way that $U(6,6)$ was reduced to the subgroup $U(6) \otimes U(6)$ by (2.25) and (2.26), the Bargmann–Wigner equations have reduced the boosted multispinors to $(U(6) \otimes U(6))_p$, defined as the subgroup for which

$$S \not{p} S^{-1} = \not{p}.$$

If we then apply these equations to the specific multispinors we can simplify their form. For the moment we shall examine the traceless $U(6,6)$ state meson forms. A multispinor of rank 2 (representing the ground state mesons) could be written in the most general form:

$$\Phi_A^B = \phi_\alpha^{j\beta} F_{ja}^b = (\phi^j + \gamma_5 \phi_5^j + i\gamma^\mu \gamma_5 \phi_{\mu 5}^j + \gamma^\mu \phi_\mu^j + \tfrac{1}{2}\sigma^{\mu\nu} \phi_{\mu\nu}^j)_\alpha^\beta F_{ja}^b$$

and upon application of the B-W equations, where it is assumed the meson is free with mass m we find

$$\begin{aligned} \phi^j &= 0, \\ p_\mu \phi_5^j = im\phi_{\mu 5}^j, \qquad & p^\mu \phi_{\mu 5}^j = -im\phi_5^j \\ p_\mu \phi_\nu^j - p_\nu \phi_\mu^j = im\phi_{\mu\nu}^j, \qquad & p^\nu \phi_{\nu\mu}^j = -im\phi_\mu^j \end{aligned} \tag{2.27}$$

so that $(\phi_5, \phi_{\mu 5})$ together form a 5-component field describing a pseudoscalar particle and $(\phi_\mu, \phi_{\mu\nu})$ a 10-component field describing a vector particle [80]. By using (2.27) Φ_A^B simplifies as

$$\Phi_A^B = \phi_{a\alpha}^{b\beta} = \frac{1}{2m}(\not{p} + m)(\gamma^\mu \phi_{\mu a}^b - \gamma_5 \phi_{5a}^b)_\alpha^\beta. \tag{2.28}$$

The relations (2.27) also show $p^\mu \phi_\mu = 0$ and subsequently $\phi_{\mu a}^b$ and ϕ_{5a}^b correspond to the 1^- and 0^- parts of the multiplet respectively. Each contains an $SU(3)$ singlet and octet[4] so the meson supermultiplet field Φ_A^B encompasses all known ground state mesons. The parity assignments have come

[4]from the decomposition $SU(6,6) \to SU(6) \otimes SU(6) \to SU(6) \otimes SU(3) \otimes SU(2)$.

about because the parity operation (which is contained within the $U(6,6)$ transformations) defined by

$$\psi^{\beta_1\ldots}_{\alpha_1\alpha_2\ldots}(\mathbf{p}) \rightarrow (\gamma_0)^{\gamma_1}_{\alpha_1}(\gamma_0)^{\gamma_2}_{\alpha_2}\ldots(\gamma_0)^{\beta_1}_{\delta_1}\ldots\psi^{\delta_1\ldots}_{\gamma_1\gamma_2\ldots}(-\mathbf{p}),$$

readily gives the intrinsic parity of a $U(6,6)$ multiplet as $(-1)^n$ where n denotes the number of upper indices [106].

Thus the $\tilde{U}(12)$ scheme naturally incorporates all the ground state mesons in a single supermultiplet, and from this perspective is very attractive if one is attempting to derive universal factors of the mesons. In this pursuit,we are particularly interested in strong two–body decays of the mesons and as such the $\tilde{U}(12)$ scheme provides a convenient framework for studying these vertices.

2.5.2 Interaction Lagrangians in $\tilde{U}(12)$

The three point couplings of the ground state mesons form $U(6,6)$ invariant expressions [43] from which we form the interaction Lagrangian

$$\mathcal{L}_{\text{int}} = 2G\Phi^B_A(p_1)\Phi^C_B(p_2)\Phi^A_C(p_3),$$

with G having the dimension of mass. If we implement the ideas of charge conjugation invariance (a property external to the scheme, unlike parity which belongs to the $U(6,6)$ transformations) we can show the three meson term is unique. Firstly we require a lowering operator $C_{\alpha\beta}$ and raising operator $(C^{-1})^{\alpha\beta}$ which are defined by $(C^{-1})^{\alpha\beta}(\gamma_\mu)^\gamma_\beta C_{\gamma\delta} = -(\gamma_\mu)^\alpha_\delta$ and $(C^{-1})^{\alpha\beta}C_{\beta\gamma} = \delta^\alpha_\gamma$ [106]. Then under charge conjugation

$$\phi^{\beta b}_{\alpha a} \rightarrow C_{\alpha\alpha'}\phi^{\alpha' b}_{\beta' a}(C^{-1})^{\beta'\beta},$$

to be consistent with the 'normal' C-parity ($C\pi^0C^{-1} = +\pi^0$, $C\rho^0C^{-1} = -\rho^0$ or $\phi_5 \rightarrow \phi_5$, $\phi_\mu \rightarrow \phi_\mu$) so that $\Phi^B_A(p_1)\Phi^C_B(p_2)\Phi^A_C(p_3) \rightarrow \Phi^A_B(p_1)\Phi^B_C(p_2)\Phi^C_A(p_3)$ and $\text{Tr}[\Phi\Phi\Phi]$ can be replaced by $\frac{1}{2}\text{Tr}[\Phi\{\Phi,\Phi\}]$. This leads us to the phenomenological interaction Lagrangian for the three-point meson function,

$$\mathcal{L}_{\text{int}} = G\Phi^B_A(p_1)\left\{\Phi^C_B(p_2)\Phi^A_C(p_3) + \Phi^C_B(p_3)\Phi^A_C(p_2)\right\}. \qquad (2.29)$$

2.5.3 Extension from 3 to N_f flavours

Although our development of the covariant meson wavefunctions has assumed three quark flavours, the theory can be *easily* extended to an arbitrary number of quark flavours, N_f. The $U(2N_f, 2N_f)$ algebra with

$$\gamma_0 = (\underbrace{1, \ldots, 1}_{2N_f}, \underbrace{-1, \ldots, -1}_{2N_f})_{\text{diag}},$$

and generators J_A^B $(A, B = 1, \ldots, 4N_f)$ obeying (2.22) and (2.23) will yield multispinors (2.28) applicable to the charm ($N_f = 4$) [40] and bottom ($N_f = 5$) mesons as well as their Zweig allowed interactions (2.29).

2.6 Covariant $SU(6)$ as the basis for other models of hadrons

There are many modern applications which have at their core the $\tilde{U}(12)$ scheme. Some are used with this knowledge by the researcher, others without. In this section, these applications are highlighted and discussed as further evidence of the power of the scheme.

One of the large obstacles in constructing relativistic hadronic wavefunctions is in the number of degrees of freedom which arise when the quarks and gluons are permitted relativistic velocities. Nonetheless, the many successes of the non–relativistic quark model empowered the search for a relativistic version of the constituent quark model. The typical approximations that necessarily enter involve regarding the quark composites as almost moving collinearly with equal velocity. This, as we shall see, is intrinsically related to the dynamical interpretation of the $\tilde{U}(12)$ fields.

The multispinor fields we have constructed did not, per se, depend on quark constituents. Moreover, they are relativistic fields describing pointlike particles of definite mass and spin. It is difficult to relate such fields with the modern perception of the hadrons consisting of physical quarks and gluons. Such internal structure naturally excludes description of the hadrons in terms

of a local field. Present day endeavours work around this problem by giving the constituent quarks an effective mass with the gluons incorporated into some confining potential. A necessary condition is that in the limit of zero momentum the wavefunction reduces to those of non–relativistic $SU(6)$.

Many of these simplifications are inherently related to reinterpretation of the multispinor fields in terms of physical quark constituents with the necessary condition that the quarks all have the same velocity [70]. This is the only means by which a relativistic wavefunction satisfying the Bargmann–Wigner equations can be attributed to a hadron with internal structure. To explicitly see this consider a system of N free massive quarks and antiquarks with momenta p_i, $i = 1, \ldots, N$, total mass $m = \sum_{i=1}^{N} m_i$ ($m_i \neq 0 \; \forall i$), and total momentum $p = \sum_{i=1}^{N} p_i$. The mass–shell condition $p^2 = m^2$ infers that all the quarks and antiquarks are moving collinearly with the same velocity, as in a rigid body,

$$\frac{p_1}{m_1} = \frac{p_2}{m_2} = \ldots = \frac{p_N}{m_N} = \frac{p}{m}. \tag{2.30}$$

At rest, the wavefunction of the whole system can be written as the direct product of free quark and antiquark wavefunctions at zero momentum

$$\Psi^{\rho\sigma\cdots}_{\alpha\beta\ldots}(\underline{0}) = \Psi_\alpha(\underline{0})\Psi_\beta(\underline{0}) \ldots \Psi^\rho(\underline{0})\Psi^\sigma(\underline{0}) \ldots,$$

with n lower and $N - n$ upper indices corresponding to n quarks and $N - n$ antiquarks. A general product wavefunction for N free quarks and antiquarks with momenta p_i is

$$\Psi^{\rho\sigma\cdots}_{\alpha\beta\ldots}(p_1, p_2, \ldots, p_N) \equiv \Psi_\alpha(p_1)\Psi_\beta(p_2) \ldots \Psi^\rho(p_{n+1})\Psi^\sigma(p_{n+2}) \ldots,$$

but is related to the rest wavefunction by individual Lorentz boosts applied to each quark so that

$$\Psi^{\rho\sigma\cdots}_{\alpha\beta\ldots}(p_1, p_2, \ldots, p_N) = S^{\alpha'}_{\alpha}(\Lambda_1)S^{\beta'}_{\beta}(\Lambda_2) \ldots \Psi^{\rho'\sigma'\cdots}_{\alpha'\beta'\ldots}(\underline{0})S^{-1}(\Lambda_{n+1})^{\rho}_{\rho'} \ldots.$$

However, in the rigid body situation all the composites are moving with the same velocity (2.30) so that all boost factors Λ_i are identical and the

wavefunction transforms covariantly,

$$\begin{aligned}\Psi^{\rho\sigma\cdots}_{\alpha\beta\ldots}(p) &\equiv \Psi^{\rho\sigma\cdots}_{\alpha\beta\ldots}(p_1, p_2, \ldots, p_N) \\ &= S^{\alpha'}_{\alpha}(\Lambda) S^{\beta'}_{\beta}(\Lambda) \ldots \Psi^{\rho'\sigma'\cdots}_{\alpha'\beta'\ldots}(0) S^{-1}(\Lambda)^{\rho}_{\rho'} S^{-1}(\Lambda)^{\sigma}_{\sigma'} \ldots\end{aligned}$$

where Λ is a boost from rest to p. Now since each quark satisfies the Dirac equation,

$$(\not{p}_1 - m_1)^{\alpha'}_{\alpha} \Psi^{\rho\sigma\cdots}_{\alpha'\beta\ldots}(p) = 0$$

the Bargmann–Wigner equations readily follow as $p_i/m_i = p/m$ for all i so,

$$(\not{p} - m)^{\alpha'}_{\alpha} \Psi^{\rho\sigma\cdots}_{\alpha'\beta\ldots}(p) = 0.$$

Hence our relativistically covariant multispinor does not necessarily describe a point particle, but rather may describe the centre of mass of a system of quarks all moving collinearly with the same velocity! Another important point is that the composite quarks do not have to have the same mass, only the same velocity.

The interpretation of the multispinor wavefunctions in this fashion explains why many seemingly different methods for generating relativistic hadronic wavefunctions produce similar results. Hussain *et al.* [70] discuss several models in the modern literature with the common thread of a weak–binding approximation, $m = \sum m_i$, which in turn implies the free motion of the constituent quarks all having the same velocity. It is shown that many of the preferred tools of today are nothing more than the one model with slightly different perturbative methods and for this reason it is hardly surprising that they give results within 5% of each other. They discuss Bethe–Salpeter wavefunctions for onium , the null–plane method and the helicity matching method in a relativistic spectator quark model. In all these cases a weak binding approximation is used at some stage in the derivation, the only difference between them the way in which one perturbs around the approximation using different momentum wavefunctions, and distributions.

2.6.1 Heavy Quark Effective Theory

The publication of two papers by Isgur and Wise in late 1989 and early 1990 [71, 72] on the weak decays of heavy mesons was quickly followed by the extensive adoption of their technique in what is now known as the Heavy Quark Effective Theory (HQET). The method exploits symmetries which emerge in the low energy effective Lagrangian for QCD applied to heavy hadrons to obtain relations between weak hadronic matrix elements. In these heavy hadrons, containing one quark of mass much larger than the QCD parameter $\Lambda_{\rm QCD}$, most of the hadron momentum is assumed to be possessed by the heavy quark and interactions with the light quark(s) are not believed to significantly alter the heavy quark velocity. Thus in the hadron's rest frame the heavy quark effectively acts as a static source of gluons being characterized by its flavour and colour quantum numbers, but not its mass. The model also admits a spin symmetry so that the properties of the heavy hadrons are independent of the spin and mass of the heavy source of colour. The HQET translates these assumptions into an effective theory of QCD, whereby its Green's functions match those of QCD to leading order $\Lambda_{\rm QCD}/m_Q$, where m_Q is the heavy quark mass.

The HQET is undoubtedly a powerful machinery and has been applied to many aspects of particle physics, in particular the weak interactions of the B and D mesons. However, it's results can be obtained from other methods given the scenario of the dynamics outlined above. Hussain *et al.* [69] demonstrate the equivalence between the Bloch–Nordsieck model, a Bethe-Salpeter wavefunction calculation and the HQET for the evaluation of semi-leptonic exclusive decays of heavy hadrons. However, their most relevant finding for this project is that the corresponding weak matrix elements, in the very heavy quark mass limit, can be written as a trace over $\tilde{U}(4N_f)$ wavefunctions like (2.28) multiplied by a universal form factor. This is because of the obvious similarities in the dynamical approximations exploited by both models. The supermultiplet scheme in the context of the quark model, (as we have seen) necessarily has the composite quarks moving collinearly with

equal velocity. In the special case of a heavy hadron with one quark much heavier than the other(s), this equal velocity condition implies it has large momentum by virtue of its large mass. In the limit of infinite quark mass, the quark momentum will be exactly the hadron momentum, as anticipated in HQET.

The $\tilde{U}(4N_f)$ approach is advocated as the most appropriate technique for formulating the first approximation of the decays of heavy hadrons; what is a few line calculation involving taking the trace of the weak current between $\tilde{U}(4N_f)$ wavefunctions can become a complex computation in other techniques [70]. Although these techniques produce higher order corrections, the simplicity with which the $\tilde{U}(4N_f)$ scheme yields the leading order contribution makes it a very attractive computational method.

2.7 Summary

We have established that the extension from $SU(3)$ symmetry notions of the elementary particles to those based on $SU(6)$ yields many additional predictions, often well matched by experiment. It also offers a superior understanding of the origin of the spin states of the ground state mesons and baryons. The observed nonets of vector (spin 1) and pseudoscalar (spin 0) mesons interpreted as bound quark-antiquark in the ${}^3S_0$ and ${}^1S_0$ states, respectively, which are beautifully accommodated in the $SU(6)$ supermultiplet structure; the $SU(3)$ octet of spin 1/2 baryons are bound $q\uparrow\ q\uparrow\ q\downarrow$ states while the $SU(3)$ decuplet of spin 3/2 baryons are bound $q\uparrow\ q\uparrow\ q\uparrow$ states, both of which fill the symmetric 56-plet of $SU(6)$. It also requires the existence of an extra quantum number (colour) to be consistent with Pauli's exclusion principle in states such as $\Delta^{++} = u\uparrow\ u\uparrow\ u\uparrow$ whereas $SU(3)$ alone does not (unless the internal spin of the quarks is related to the spin of the hadron).

To exploit the extra predictive power of the $SU(6)$ scheme, we have used its relativistic generalization to obtain a usable field theory in the context of $U(6,6)$ invariant phenomenological interaction Lagrangians and relativistic

multispinor fields describing the three meson vertex and meson supermultiplet, respectively. To go beyond the three quark flavour limit of $\tilde{U}(12)$, we generalised it to $\tilde{U}(4N_f)$ and we are now prepared to test the technology by applying it to the two-body strong (and electromagnetic with the help of vector meson dominance) decays of the ground state mesons. Importantly, the $\tilde{U}(4N_f)$ scheme relates all such OZI decays by a single coupling constant, so it is very suited to the search for 'universal' couplings.

The final section concentrated on the similarities between the $\tilde{U}(4N_f)$ scheme and many modern techniques. It showed that these yielded identical predictions in the leading order to those of the supermultiplet method. Moreover, the speed and ease with which the leading order result could be derived with the $\tilde{U}(4N_f)$ method proves its worth.

Chapter 3

Ground State Meson Decays

The ground state mesons are the natural starting point for the investigation of universal couplings of strong and electromagnetic decays. The decay widths of the mesons composed of u, d and s quarks are well known, especially in the strong regime, so they provide a stringent test of the $\tilde{U}(12)$ ideas. The heavier mesons composed of c and b quarks along with a lighter companion quark are presently under the scrutiny of experimentalists. With the simple extension of $\tilde{U}(12)$ to $\tilde{U}(4N_f)$, up to N_f quark flavours can be supported allowing us to provide testable predictions in the heavy meson arena ($N_f = 5$). Unfortunately, most experimental interest lies in the weak–interactions of these heavier mesons due to the high number of decay channels and the sensitive tests of the Standard Model they offer, but strong and electromagnetic data are gradually being gathered. There has recently been considerable theoretical interest in the strong and electromagnetic decays of the D^* and B^* mesons from HQET and QCD sum rule perspectives. We provide a summary of these predictions and compare those which arise from our own work. Once the experimentalists reach a consensus on the results, many of the current theoretical methods will be resolved.

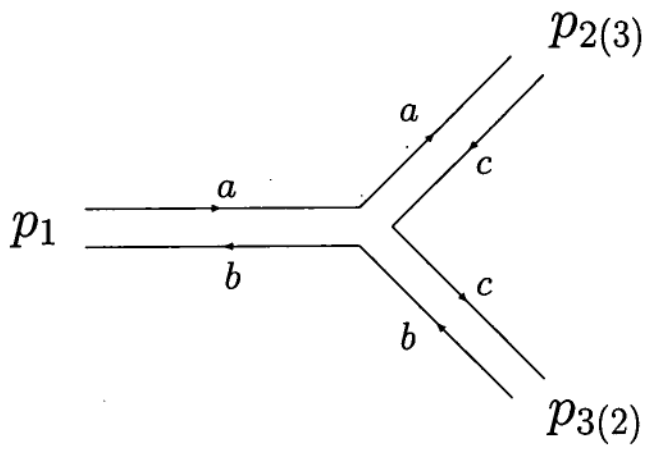

Figure 3.1: Duality diagram for incoming mesons with momenta p_i. The labels a, b and c correspond to the quark flavours.

3.1 Ground state interactions

Taking the ground state superfield $\Phi_A^B(p)$ of Equation (2.28) along with the general three meson interaction Lagrangian (2.29) we expand the implied trace using Dirac's trace algebra (Appendix A.2) along with the momentum conditions

$$p_1 + p_2 + p_3 = 0; \quad p_i^2 = m_i^2, \quad p_i^\mu \phi_\mu(p_i) = 0, \tag{3.1}$$

as the mesons are on–shell and all momenta are incoming to be consistent with Zweig's rules and the duality diagram counterpart of Figure 3.1 [66, 99]. In this figure flavour labels (carried by the line) have been included to demonstrate the automatic conservation of flavour. The momentum crossed terms arise under the exchange $p_2 \leftrightarrow p_3$.

In the early stages of the expansion the various interactions are seen to emerge, namely the vector to two pseudoscalars (VPP vertex), vector to vector plus pseudoscalar (VVP vertex), vector into two vectors (VVV vertex) and pseudoscalar into two pseudoscalars (PPP vertex),

$$\begin{aligned}\mathcal{L}_{\text{int}} &= G\text{Tr}\left[(\not{p}_1 + m_1)\left(\gamma^\mu \phi^b_{\mu a}(p_1) - \gamma_5 \phi^b_{5a}(p_1)\right)\right. \\ &\quad \left.\times(\not{p}_2 + m_2)\left(\gamma^\nu \phi^c_{\nu b}(p_2) - \gamma_5 \phi^c_{5b}(p_2)\right)\right.\end{aligned}$$

$$\times (\not{p}_3 + m_3)\,(\gamma^\sigma \phi^a_{\sigma c}(p_3) - \gamma_5 \phi^a_{5c}(p_3)) + \text{terms with } \Phi(p_2) \leftrightarrow \Phi(p_3)]\,,$$

and we have not included the spin indices associated with vector wave functions as this does not affect the trace. To continue with the expansion we shall handle each vertex separately to clarify the methods used in each technique.

3.1.1 Three Meson Vertex Expansions

The four unique vertex types are expanded by use of general trace results and those particular to the Dirac algebra (Appendix A.2). The antisymmetric or Levi–Civita tensor $\epsilon_{\mu\nu\rho\sigma}$ is taken as antisymmetric in each pair of adjacent indices with $\epsilon_{0123} = 1$.

VPP vertex expansion

The VPP vertex is calculated using elementary Dirac algebra rules in conjunction with the trace algebra result and when subjected to the momentum conditions of (3.1) expand as

$$\begin{aligned}
\mathcal{L}_{\text{int}} &= G\,\text{Tr}\,[\not{p}_1\gamma^\mu m_2\gamma_5 m_3\gamma_5 + m_1\gamma^\mu \not{p}_2\gamma_5 m_3\gamma_5 + m_1\gamma^\mu m_2\gamma_5 \not{p}_3\gamma_5 + \ldots \\
&\qquad \not{p}_1\gamma^\mu \not{p}_2\gamma_5 \not{p}_3\gamma_5]\,\phi^b_{\mu a}(p_1)\,[\phi^c_{5b}(p_2)\phi^a_{5c}(p_3) + (p_2 \leftrightarrow p_3)]\,/8\prod_i m_i \\
&= G\sum_i m_i q^\mu \phi^b_{\mu a}(p_1)\,[\phi^c_{5b}(p_2)\phi^a_{5c}(p_3) - \phi^c_{5b}(p_3)\phi^a_{5c}(p_2)]\,/4m_2m_3, \qquad (3.2)
\end{aligned}$$

where the negative sign on the final term $\phi^c_{5b}(p_3)\phi^a_{5c}(p_2)$ arises from the presence of the momentum transfer term $q = (p_2 - p_3)$ which is obviously antisymmetric under the interchange $p_2 \leftrightarrow p_3$. Hence, as expected by charge conjugation invariance of the strong interactions, the antisymmetric or "F–type" Yukawa coupling of the VPP vertex is observed in the interaction term.

VVP vertex expansion

The term which contributes to the VVP vertex requires somewhat delicate handling of the crossed term $\Phi(p_2) \leftrightarrow \Phi(p_3)$ as shown,

$$\begin{aligned}
\mathcal{L}_{\rm int} &= G\,{\rm Tr}\,[(\not{p}_1\gamma^\mu\,\not{p}_2\gamma^\nu m_3\gamma_5 + \not{p}_1\gamma^\mu m_2\gamma^\nu\,\not{p}_3\gamma_5 + m_1\gamma^\mu\,\not{p}_2\gamma^\nu\,\not{p}_3\gamma_5) \\
&\qquad \times\phi^b_{\mu a}(p_1)\phi^c_{\nu b}(p_2)\phi^a_{5c}(p_3) \\
&\quad + (\not{p}_1\gamma^\mu\,\not{p}_3\gamma_5 m_2\gamma^\nu + \not{p}_1\gamma^\mu m_3\gamma_5\,\not{p}_2\gamma^\nu + m_1\gamma^\mu\,\not{p}_3\gamma_5\,\not{p}_2\gamma^\nu) \\
&\qquad \times\phi^b_{\mu a}(p_1)\phi^c_{5b}(p_2)\phi^a_{\nu c}(p_3)\big]\,/8m_1m_2m_3 \\
&\;\;\vdots \\
&= \frac{G\sum_i m_i}{2m_1m_2m_3}\epsilon^{\mu\nu\kappa\lambda}p_{1\kappa}p_{2\lambda}\phi^b_{\mu a}(p_1)\,\{\phi^c_{\nu b}(p_2)\phi^a_{5c}(p_3) + \phi^c_{5b}(p_2)\phi^a_{\nu c}(p_3)\} \qquad (3.3)
\end{aligned}$$

and the interaction preserves the anticipated symmetric or "D-type" coupling.

VVV vertex expansion

The trace algebra rules restrict the terms in the three vector interaction to those comprising four or six γ matrices; all others vanish under the trace. Hence we are left with

$$\begin{aligned}
\mathcal{L}_{\rm int} &= \frac{G}{8\prod_i m_i}{\rm Tr}[\,\not{p}_1\gamma^\mu m_2\gamma^\nu m_3\gamma^\sigma + m_1\gamma^\mu\,\not{p}_2\gamma^\nu m_3\gamma^\sigma + m_1\gamma^\mu m_2\gamma^\nu\,\not{p}_3\gamma^\sigma \\
&+ \not{p}_1\gamma^\mu\,\not{p}_2\gamma^\nu\,\not{p}_3\gamma^\sigma]\phi^b_{\mu a}(p_1)\,\{\phi^c_{\nu b}(p_2)\phi^a_{\sigma c}(p_3) + \Phi(p_2) \leftrightarrow \Phi(p_3)\} \\
&= \frac{G\sum_i m_i}{4\prod_i m_i}\,[(p_2-p_3)^\mu g^{\nu\sigma}m_1 + (p_3-p_1)^\nu g^{\sigma\mu}m_2 + (p_1-p_2)^\sigma g^{\mu\nu}m_3 \\
&\qquad + \frac{2}{\sum_i m_i}\,(p_2-p_3)^\mu(p_3-p_1)^\nu(p_1-p_2)^\sigma] \\
&\qquad \phi^b_{\mu a}(p_1)\,[\phi^c_{\nu b}(p_2)\phi^a_{\sigma c}(p_3) - \phi^c_{\sigma b}(p_3)\phi^a_{\nu c}(p_2)]\,, \qquad (3.4)
\end{aligned}$$

which preserves the anticipated F-type coupling. We also note that the interaction does not preserve gauge invariance if $m_1 \neq m_2 \neq m_3$.

PPP vertex expansion

The three pseudoscalar vertex contains the trace,

$$\mathrm{Tr}\left[(\not{p}_1 + m_1)\gamma_5(\not{p}_2 + m_2)\gamma_5(\not{p}_3 + m_3)\gamma_5\right],$$

and all terms fall into the categories of Equations (A.1) so that there are no non–zero terms. Hence the three pseudoscalar interaction vanishes, conforming with parity conservation.

Summary of three meson interaction terms

The $\tilde{U}(4N_f)$ scheme has reproduced the known three meson vertices, VPP, VVP and VVV (as well as confirming the vanishing PPP vertex). To provide a summary of these interactions we firstly associate the meson couplings in (3.2,3.3) and (3.4) with their more familiar covariant equivalents, namely g_{VPP}, g_{VVP} and g_{VVV},

$$\begin{aligned} g_{VPP} &= \frac{G\sum_i m_i}{4m_2m_3} \\ g_{VVP} &= \frac{G\sum_i m_i}{2m_1m_2m_3} \\ g_{VVV} &= \frac{G\sum_i m_i}{4m_1m_2m_3} \end{aligned} \quad . \tag{3.5}$$

By compiling our results we see the overall three meson interaction Lagrangian is composed of the distinct vertices,

$$\mathcal{L}_{\mathrm{int}} = g_{VPP}q_{23}^{\mu}\langle\phi_\mu(p_1)[\phi_5(p_2),\phi_5(p_3)]\rangle \tag{3.6}$$

$$+g_{VVP}\epsilon^{\mu\nu\kappa\lambda}p_{1\kappa}p_{2\lambda}\langle\phi_\mu(p_1)\{\phi_\nu(p_2),\phi_5(p_3)\}\rangle \tag{3.7}$$

$$+g_{VVV}\left[q_{23}^{\mu}g^{\nu\sigma}m_1 + q_{31}^{\nu}g^{\sigma\mu}m_2 + q_{12}^{\sigma}g^{\mu\nu}m_3 + \frac{2q_{23}^{\mu}q_{31}^{\nu}q_{12}^{\sigma}}{\sum_i m_i}\right] \langle\phi_\mu(p_1)[\phi_\nu(p_2),\phi_\sigma(p_3)]\rangle \tag{3.8}$$

where $q_{ij} = p_i - p_j$ and $\langle\rangle$ stands for a trace over the internal symmetry indices, corresponding to a joining of quark lines in a duality diagram. For instance, such a trace for flavour indices would expand as

$$\phi^b_{\mu a}(p_1)[\phi^c_{5b}(p_2)\phi^a_{5c}(p_3) - \phi^c_{5b}(p_3)\phi^a_{5c}(p_2)]$$

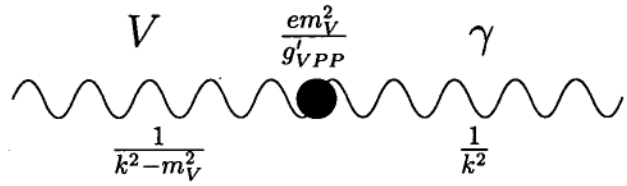

Figure 3.2: Vector meson dominance model.

for the VPP vertex. We have introduced the three distinct covariant coupling constants as at this stage we are alert to the possibility that symmetry breaking may affect each piece differently (that is, we have introduced three separate constants depending on the type of decay).

3.1.2 Electromagnetic Interactions

We now have an adequate formalism for describing various strong interaction decays amongst ground state mesons. To extend the applications of the supermultiplet theory we invoke the ideas of the vector meson dominance model to enable the study of the electromagnetic interactions of our mesons. Vector meson dominance (VMD) is derived from the fact that vector mesons with the same C-parity of the photon (namely $\rho^0, \omega, \phi, J/\psi, \Upsilon$) can undergo direct photon-vector transitions. In the standard way [103], we assume the effective coupling between a vector meson flavour singlet V, and a photon is of the form

$$g_{V\gamma}(k^2 = 0) = em_V^2/g'_{VPP}, \tag{3.9}$$

as shown in Figure 3.2. With this definition the strength of the ρ resonance in the electric form factor of the pion is g_{VPP}/g'_{VPP}, which is of the order of unity if the ρ resonance dominates the form factor [61], hence the notation. When extrapolating away from $k^2 = 0$ we expect the coupling to decrease and as such have denoted the coupling by em_V^2/g'_{VPP} to allow for such change. That is, we anticipate g'_{VPP} will vary with k^2 due to intermediate virtual particle contributions and its value at $k = 0$ equals the g_{VPP} of Equation

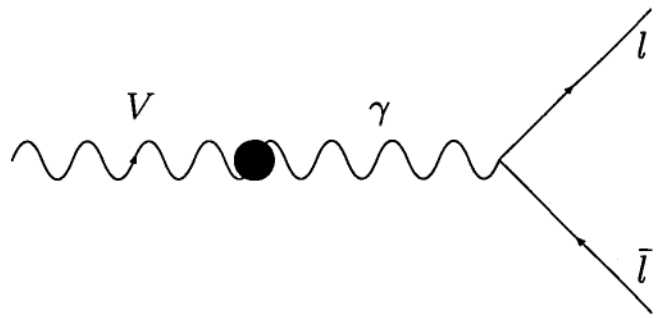

Figure 3.3: Photon dominated leptonic decay modes of vector mesons (adapted from [107]).

3.6. Direct measures of g'_{VPP} come from the electromagnetic decays $\rho^0 \to l\bar{l}, \omega \to l\bar{l}$ and so on, via the photon pole graphs of Figure 3.3.

Given the interaction

$$\mathcal{L}_{Vl\bar{l}} = \frac{e^2}{g'_{VPP}} \bar{u}_l(p_2)\gamma^\mu v_{\bar{l}}(p_1)\varepsilon_\mu(p_1+p_2),$$

the decay rate for such processes is

$$\Gamma_{V\to l\bar{l}} = \left(\frac{e^2}{g'_{VPP}}\right)^2 \frac{(m_V^2 - 4m_l^2)^{1/2}}{12\pi}\left(1 - \frac{m_l^2}{m_V^2}\right) \tag{3.10}$$

3.1.3 Decay Rates

Since we only consider strong meson decays, tree-level calculations in perturbation theory given by (3.6, 3.7, 3.8) suffice which leads to the general formula for a two-body decay,

$$\Gamma_{1\to 2,3} = \frac{\lambda^{1/2}(m_1^2, m_2^2, m_3^2)}{16\pi m_1^3}|\mathcal{M}|^2, \tag{3.11}$$

where $|\mathcal{M}|^2 = \frac{1}{2J_1+1}\sum_\lambda |\mathcal{L}_{\text{int}}|^2$ and J_1 is the spin of the parent meson and

$$\lambda(m_1^2, m_2^2, m_3^2) = m_1^4 + m_2^4 + m_3^4 - 2m_1^2m_2^2 - 2m_1^2m_3^2 - 2m_2^2m_3^2.$$

Upon substitution of the interaction Lagrangian in the form of Equations (3.6,3.7,3.8) into the decay rate formula (3.11), we derive the following widths

for the various decays:

$$\Gamma_{V\to PP} = \frac{g_{VPP}^2\lambda^{3/2}(m_1^2,m_2^2,m_3^2)}{48\pi m_1^5} \tag{3.12}$$

$$\Gamma_{V\to VP} = \frac{g_{VVP}^2\lambda^{3/2}(m_1^2,m_2^2,m_3^2)}{96\pi m_1^3} \tag{3.13}$$

$$\Gamma_{V\to VV} = \frac{g_{VVV}^2\lambda^{3/2}(m_1^2,m_2^2,m_3^2)}{192\pi m_1^5}\frac{\mathcal{Y}(m_1,m_2,m_3)}{m_2^2m_3^2}, \tag{3.14}$$

where

$$\begin{aligned}\mathcal{Y}(m_1,m_2,m_3) &= 9\left(\sum_{1\le i<j\le 3}(m_i+m_j)^2(m_i-m_j)^4-\sum_{i=1}^{3}m_i^6\right)\\ &\quad+\prod_{i=1}^{3}m_i\left(98\sum_{i=1}^{3}m_i^3-16\sum_{1\le i<j\le 3}(m_i+m_j)^3\right)+142\prod_{i=1}^{3}m_i^2.\end{aligned}$$

Electromagnetic decay rates

The vector meson dominance model, used in conjunction with our decay rate formulae (3.12,3.13,3.14), gives the following rates for the various processes:

$$\Gamma_{V\to P\gamma} = \left(\frac{eg_{VVP}}{g'_{VPP}}\right)^2\frac{(m_V^2-m_P^2)^3}{96\pi m_V^3}, \tag{3.15}$$

$$\Gamma_{P\to V\gamma} = \left(\frac{eg_{VVP}}{g'_{VPP}}\right)^2\frac{(m_P^2-m_V^2)^3}{32\pi m_P^3}, \tag{3.16}$$

$$\Gamma_{P\to\gamma\gamma} = \left(\frac{e^2g_{VVP}}{g'_{VPP}g'_{VPP}}\right)^2\frac{m_P^3}{64\pi}, \tag{3.17}$$

thereby greatly extending the original scope of the supermultiplet scheme. In going from our purely strong interaction decay rates to the radiative ones, we have used the gauge invariance of our interaction Lagrangian and simply substituted a mass of zero for those vectors connecting with the photon. However, the three vector interaction (3.8) is only gauge invariant for the case $m_2 = m_3$ so strictly we should only apply it to radiative examples for which the virtual vector meson satisfies this condition. Unfortunately, since the photon only couples to flavour singlet states the condition $m_2 =$

m_3 also implies the daughter vector mesons are identical. Due to the F–type coupling between daughter states in the interaction Lagrangian (3.8) such vertices vanish. It is for this reason we have not included a $V \to V\gamma$ term above, despite possible experimental observation of such processes (e.g. $\Gamma_{\phi\to\rho\gamma}/\Gamma_{\phi\to\text{all}} < 2\%$; but we note this measure is only an upper bound so a zero width is not excluded, as expected by $\tilde{U}(4N_f)$). We now go on to apply the formalism to the ground state mesons.

3.2 Application of the $\tilde{U}(4N_f)$ scheme

In order to test the supermultiplet scheme to the two-body decays of the ground state mesons we must identify physical mesons with their $\tilde{U}(4N_f)$ states and derive Clebsch–Gordan coefficients which relate the coupling constant obtained from the analysis of a particular decay to the generic couplings g_{VPP}, g_{VVP} or g_{VVV}. The first task is relatively simple, and is only complicated by singlet-octet mixing, while the derivation of Clebsch–Gordan constants can be somewhat more involved, particularly in the electromagnetic processes.

3.2.1 Ground State Nonet Assignments

A crucial step in using the supermultiplet scheme is in the correct identification of flavour labels with the mesons. This is a simple process for the ground states, but is significantly more difficult in the excited meson realm due to controversial quark model assignments, as we shall see. For the ground states, the pseudoscalar nonet is taken as:

$$\phi^b_{5a} \xrightarrow{0^-} \begin{pmatrix} \frac{\pi^0}{\sqrt{2}} + \frac{\eta_8}{\sqrt{6}} + \frac{\eta_0}{\sqrt{3}} & \pi^+ & K^+ \\ \pi^- & -\frac{\pi^0}{\sqrt{2}} + \frac{\eta_8}{\sqrt{6}} + \frac{\eta_0}{\sqrt{3}} & K^0 \\ K^- & \bar{K}^0 & -\frac{2\eta_8}{\sqrt{6}} + \frac{\eta_0}{\sqrt{3}} \end{pmatrix}, \tag{3.18}$$

where η_8 and η_0 are the pure $SU(3)$ octet and singlet states with $I_3 = 0$, $I = 0$ and are related to the physical states η and η' by the pseudoscalar

mixing angle θ_P defined by

$$|\eta_8\rangle = \cos\theta_P|\eta\rangle + \sin\theta_P|\eta'\rangle \tag{3.19}$$

$$|\eta_0\rangle = -\sin\theta_P|\eta\rangle + \cos\theta_P|\eta'\rangle. \tag{3.20}$$

The vector nonet is similarly given by

$$\phi^b_{\mu a} \xrightarrow{1^-} \begin{pmatrix} \frac{\rho^0}{\sqrt{2}} + \frac{\omega_8}{\sqrt{6}} + \frac{\omega_0}{\sqrt{3}} & \rho^+ & K^{*+} \\ \rho^- & -\frac{\rho^0}{\sqrt{2}} + \frac{\omega_8}{\sqrt{6}} + \frac{\omega_0}{\sqrt{3}} & K^{*0} \\ K^{*-} & \bar{K}^{*0} & -\frac{2\omega_8}{\sqrt{6}} + \frac{\omega_0}{\sqrt{3}} \end{pmatrix}, \tag{3.21}$$

where

$$|\omega_8\rangle = \cos\theta_V|\phi\rangle + \sin\theta_V|\omega\rangle \tag{3.22}$$

$$|\omega_0\rangle = -\sin\theta_V|\phi\rangle + \cos\theta_V|\omega\rangle, \tag{3.23}$$

and θ_V is the vector mixing angle as determined using the Gell-Mann–Okubo (GMO) mass relation, as discussed in Section 2.3.1. From the vector nonet (3.21) the octet and singlet fields are expressed in terms of the supermultiplet vector as

$$\sqrt{6}\omega_8 = \phi^1_{\mu 1} + \phi^2_{\mu 2} - 2\phi^3_{\mu 3}, \qquad \sqrt{3}\omega_0 = \phi^1_{\mu 1} + \phi^2_{\mu 2} + \phi^3_{\mu 3}.$$

Hence, from Equations 3.22 and 3.23

$$\sqrt{6}\phi = (\cos\theta_V - \sqrt{2}\sin\theta_V)(\phi^1_{\mu 1} + \phi^2_{\mu 2}) - (2\cos\theta_V + \sqrt{2}\sin\theta_V)\phi^3_{\mu 3}.$$

In the case of "ideal mixing" $\phi = \phi^3_{\mu 3}$ so that

$$\cos\theta_V - \sqrt{2}\sin\theta_V = 0 \text{ or } \tan\theta_V = \sqrt{1/2}$$

leaving us two options for θ_V; either $0 < \theta_V < \pi/2$ or $\pi < \theta_V < 3\pi/2$. The first case implies $\cos\theta_V = \sqrt{2/3}$, $\sin\theta_V = \sqrt{1/3}$ so that $\phi = -\phi^3_{\mu 3}$ while the second region gives the desired result of $\phi = \phi^3_{\mu 3}$. Since the general solution to (2.12) is $\theta_V + n\pi$ where n is any integer, the range $\pi < \theta_V < 3\pi/2$ is an entirely consistent choice of mixing angle.

The above arguments for the determination of the vector mixing angle can be applied to the pseudoscalar nonet with the substitutions $\omega_8 \to \eta_8$, $\omega_0 \to \eta_0$, $\phi \to \eta$, $\omega \to \eta'$. Using the condition $\pi < \theta_V < 3\pi/2$ and a similarly derived expression for the pseudoscalar angle, $-\pi/2 < \theta_P < \pi/2$, we obtain the results

$$\begin{aligned} \theta_V &= 219.4^\circ \pm 0.1^\circ \\ \theta_P &= -10.54^\circ \pm 0.05^\circ, \end{aligned}$$

where the errors have been determined by assuming uncorrelated errors in the masses involved in (2.12). The mixing angles we have obtained may seem accurate, but as was pointed out in Section 2.3.1, the GMO relation is extremely sensitive to symmetry breaking mechanisms.

3.2.2 Tests of the $\tilde{U}(4N_f)$ scheme

With the structure now in place, it is a relatively simple process to test the supermultiplet theory. To do so we calculate the standard coupling constants g_{VPP} and g_{VVP} and compare their similarity between different processes. From Equation (3.5) we could in fact determine the coupling constant G from numerous channels. However, if we try and do this using physical masses m_1, m_2 and m_3 in a decay $1 \to 2 + 3$ the values tend to be wildly distributed. Instead we believe the appropriate masses to use should be $m_{1,2,3} = m$ where m is the so-called central meson mass and is defined as the degenerate mass of a supermultiplet, that is it is the mass all members of a supermultiplet have before mass breaking effects shift individual members apart. This assumption leads to the following relation between the covariant couplings:

$$2g_{VPP} = mg_{VVP} = 2mg_{VVV}. \tag{3.24}$$

and shall test for this in the results. This methodology contrasts usual practice in which a value for the coupling is determined from a single channel and then the symmetry conditions are invoked to calculate decay rates for other

channels. The test of the symmetry comes when the predicted widths are compared with experiment. This technique has not been adopted because:

1. we are investigating the universality of the couplings. Any universality will be much more apparent by presenting the couplings and not relations between decay widths,

2. any systematic deviation from the symmetry is much more obvious.

3.2.3 Clebsch–Gordan factors

In practice we take the decay width and particle masses as input and determine the coupling constant associated with the decay via (3.12) and (3.13). The simplicity of the supermultiplet method is that Clebsch–Gordan type factors and mixing angles are automatically accounted for. One simply chooses an appropriate strong or electromagnetic decay process, determines the correct flavour indices a, b and c of the parent and daughter mesons via matrices (3.18) and (3.21). With these flavour indices substituted into the appropriate vertex of the interaction Lagrangian (3.6, 3.7, or 3.8) the fields ϕ_μ or ϕ_5 are then replaced by their matrix counterpart and after simplification one is left with the meson interaction and its relative strength in the form of Clebsch–Gordan factors.

As an example, the decay $\rho^+ \to \pi^+\pi^0$ involves the field indices $a = 1, b = 2, c = 1, 2$ and upon substitution of the fields into Equation 3.6 a factor of $\sqrt{2}$ emerges, indicating the coupling of the interaction, $g_{\rho^+\pi^+\pi^0}$ is $\sqrt{2}$ times the standard coupling of a VPP vertex, g_{VPP}. Subsequently the coupling we determine for this decay process must be normalised by the factor $\sqrt{2}$ to obtain the standard coupling constant. This procedure is repeated for all appropriate physical decays. Table 3.1 includes all such Clebsch–Gordan factors of $V \to PP$ decays for which there is some experimental data. Mixing has been easily accommodated by using the relations (3.19,3.20,3.22,3.23) to replace the pure fields by the physical mesons.

Decay process	Clebsch–Gordan factor
$\rho^{\pm} \to \pi^{\pm}\pi^0$	$\sqrt{2}$
$\rho^0 \to \pi^{\pm}\pi^{\mp}$	$\sqrt{2}$
$K^* \to K\pi^0, K\pi^{\pm}$	$\sqrt{1/2}, 1$
$\phi \to K^{\pm}K^{\mp}$	$\sqrt{3/2}\cos\theta_V$
$\phi \to K_L^0 K_S^0$	$\sqrt{\frac{3}{2}}\frac{1+\lvert\epsilon\rvert^2}{1-\lvert\epsilon\rvert^2}\cos\theta_V$
$\phi \to \rho^0\pi^0, \rho^{\pm}\pi^{\mp}$	$\sqrt{2/3}(\cos\theta_V - \sqrt{2}\sin\theta_V)$
$D^{*\pm} \to D^0\pi^{\pm}, D^{\pm}\pi^0$	$1, \sqrt{1/2}$
$D^{*0} \to D^0\pi^0$	$\sqrt{1/2}$

Table 3.1: Clebsch–Gordan factors for $V \to PP$ decay processes.

$V \to l\bar{l}$ decay process	Clebsch–Gordan factor
$\rho^0 \to e^+e^-, \mu^+\mu^-$	$\sqrt{1/2}$
$\omega \to e^+e^-, \mu^+\mu^-$	$\sqrt{\frac{1}{6}}\sin\theta_V$
$\phi \to e^+e^-, \mu^+\mu^-$	$\sqrt{\frac{1}{6}}\cos\theta_V$
$J/\psi \to e^+e^-, \mu^+\mu^-$	$2/3$
$\Upsilon \to e^+e^-, \mu^+\mu^-, \tau^+\tau^-$	$1/3$

Table 3.2: Clebsch–Gordan factors for $V \to l\,\bar{l}$ decay processes.

In radiative decays of the type $V \to l\,\bar{l}$ we allow for the coupling of the photon to the quark. Using the following electromagnetic charge projectors

$$Q_a^b = \begin{pmatrix} \frac{2}{3} & 0 & 0 \\ 0 & -\frac{1}{3} & 0 \\ 0 & 0 & -\frac{1}{3} \end{pmatrix},$$

we may likewise determine the Clebsch–Gordan coupling factor as shown in Table 3.2.

Radiative modes such as $V \to P\gamma$ require some delicacy in normalising the coupling constant. To elicit a clear understanding of the method we include an example of the procedure for the decay $\rho^0 \to \eta\gamma$. Firstly, we recognise ρ^0 is a combination of $\phi^1_{\mu 1}(p_1)$ and $\phi^2_{\mu 2}(p_1)$, so we require terms in

the interaction Lagrangian (3.7) with $a = 1, b = 1$ and $a = 2, b = 2$. For each of these cases we determine the third flavour index c such that $\phi_\nu(p_2)$ is a flavour singlet which may couple to a photon (thus $c = 1, 2$). Substituting these values into formula 3.7 we pick out the uncharged parts;

$$\begin{aligned}
\mathcal{L}_{\text{int}} &\propto g_{VVP}\left[\phi^1_{\mu 1}(p_1)\left\{\phi^1_{\nu 1}(p_2), \phi^1_{51}(p_3)\right\} + \phi^2_{\mu 2}(p_1)\left\{\phi^2_{\nu 2}(p_2), \phi^2_{52}(p_3)\right\}\right] \\
&= g_{VVP}\left[\frac{\rho^0(p_1)}{\sqrt{2}} 2\left(\frac{\rho^0(p_2)}{\sqrt{2}} + \frac{\omega_8(p_2)}{\sqrt{6}}\right)\left(\frac{\eta_8(p_3)}{\sqrt{6}} + \frac{\eta_0(p_3)}{\sqrt{3}}\right)\right. \\
&\quad \left. -\frac{\rho^0(p_1)}{\sqrt{2}} 2\left(-\frac{\rho^0(p_2)}{\sqrt{2}} + \frac{\omega_8(p_2)}{\sqrt{6}}\right)\left(\frac{\eta_8(p_3)}{\sqrt{6}} + \frac{\eta_0(p_3)}{\sqrt{3}}\right)\right] \\
&= \sqrt{\frac{2}{3}} g_{VVP}\rho^0(p_1)\rho^0(p_2)\left[\eta_8(p_3) + \sqrt{2}\eta_0(p_3)\right] \\
&= \sqrt{\frac{2}{3}}\left(\cos\theta_P - \sqrt{2}\sin\theta_P\right) g_{VVP}\rho^0(p_1)\rho^0(p_2)\eta(p_3),
\end{aligned}$$

where, in particular, we have used relations (3.19,3.20) to arrive at the final result. The form shows that the coupling between two ρ^0 mesons and a pseudoscalar η is related to the standard VVP coupling by

$$g_{\rho^0\rho^0\eta} = \sqrt{\frac{2}{3}}\left(\cos\theta_P - \sqrt{2}\sin\theta_P\right) g_{VVP}$$

The virtual vector meson is immediately identifiable as $\rho^0(p_2)$, and we must necessarily allow for the coupling between this and the photon. Since $\rho^0 = (u\bar{u} + d\bar{d})/\sqrt{2}$ then $g_{\rho^0\gamma} = g_{V\gamma}/\sqrt{2}$, which in turn implies $g'_{\rho^0 PP} = \sqrt{2} g'_{VPP}$ from (3.9). Subsequently, the coupling between a ρ^0, η and photon is related to our standard couplings by

$$\begin{aligned}
g_{\rho^0\eta\gamma} &= e g_{\rho^0\rho^0\eta}/g'_{\rho^0 PP} \\
&= \frac{e\sqrt{\frac{2}{3}}\left(\cos\theta_P - \sqrt{2}\sin\theta_P\right) g_{VVP}}{\sqrt{2} g'_{VPP}} \\
&= \frac{1}{\sqrt{3}}\left(\cos\theta_P - \sqrt{2}\sin\theta_P\right)\frac{e g_{VVP}}{g'_{VPP}}
\end{aligned}$$

In other decays, it is possible that the radiative mode may proceed via more than one virtual vector meson. The above method is still used to

Radiative decay process	Clebsch–Gordan factor
$\rho^{\pm,0} \to \pi^{\pm,0}\gamma$	$1/3$
$\rho^0 \to \eta\gamma$	$(\cos\theta_P - \sqrt{2}\sin\theta_P)/\sqrt{3}$
$\omega \to \pi^0\gamma$	$(\cos\theta_V + \sin\theta_V)/\sqrt{3}$
$\omega \to \eta\gamma$	$(\sqrt{2}\cos(\theta_V + \theta_P) + \sin\theta_V\cos\theta_P)/3$
$\phi \to \pi^0\gamma$	$(\cos\theta_V - \sqrt{2}\sin\theta_V)/\sqrt{3}$
$\phi \to \eta\gamma$	$-(\sqrt{2}\sin(\theta_V + \theta_P) + \cos\theta_V\cos\theta_P)/3$
$\phi \to \eta'\gamma$	$(\sqrt{2}\cos(\theta_V + \theta_P) - \cos\theta_V\sin\theta_P)/3$
$K^{*\pm,0} \to K^{\pm,0}\gamma$	$1/3, -2/3$
$D^{*\pm,0} \to D^{\pm,0}\gamma$	$1/3, 4/3$
$D_s^{*\pm} \to D_s^{\pm}\gamma$	$1/3$
$J/\psi \to \eta_c\gamma$	$4/3$
$\eta' \to \rho^0\gamma$	$(\sqrt{2}\cos\theta_P + \sin\theta_P)/\sqrt{3}$
$\eta' \to \omega\gamma$	$(\sin\theta_P\sin\theta_V + \sqrt{2}\sin(\theta_P + \theta_V))/3$
$\pi^0 \to \gamma\gamma$	$\sqrt{2}/3$
$\eta \to \gamma\gamma$	$\sqrt{2/3}(-2\sqrt{2}\sin\theta_P + \cos\theta_P)/3$
$\eta' \to \gamma\gamma$	$\sqrt{2/3}(2\sqrt{2}\cos\theta_P + \sin\theta_P)/3$
$\eta_c \to \gamma\gamma$	$8/9$

Table 3.3: Clebsch–Gordan factors for $V \to P\gamma$, $P \to V\gamma$ and $P \to \gamma\gamma$ process.

determine each virtual vector meson contribution and the appropriate linear combination is taken to produce the Clebsch–Gordan factors given in Table 3.3.

3.3 Results and Analysis

There is an abundant amount of accurate data on the two-body strong decays of the light-sector ground state mesons, as many of the processes have been under the scrutiny of experimentalists for up to 30 years. Fortunately the Particle Data Group publish a review of the known experimental measures

pertaining to particle physics every even-numbered year, the current edition covering all data up to January 1996 [13]. Our approach is to adopt the measures provided in the Summary Tables which are the best values from the many studies they have analysed (often referred to as the "world averages"). Importantly, the data we use are particle masses, decay widths and branching fractions. In our tables of results we include additional columns which are derived from using world averages from earlier editions (namely 1992 and 1994, [68, 87], respectively) as they show the change in our results with time as more experimental data is gathered on a decay process.[1] In situations where the 1992 or 1994 world average is the *same* as the 1996, (and hence our results have not differed) *we use the* $\leftarrow$ *symbol* to indicate the later world average applies to the earlier; the presence of an entry in the 1992 or 1994 column indicates the old data has been used. Some of the results from the 1992 data have been previously reported by this author [76].

3.3.1 VPP vertex coupling

Table 3.4 summarises the experimental determinations of the VPP vertex coupling. The upper half of Table 3.4 details purely strong interaction two-body decays, while the second lists the coupling constant g'_{VPP} obtained from the vector meson dominance extrapolation. For the processes $V \to e^+e^-$ we use the widths $\Gamma_{ee} \equiv \Gamma_{V\to e^+e^-}$ provided in the Summary Tables of the Particle Data Reviews, while other leptonic decays like $V \to \mu^+\mu^-$ use the branching fraction $Br(V \to \mu^+\mu^-) \stackrel{\text{def}}{=} \Gamma_{V\to\mu^+\mu^-}/\Gamma_{V\to\text{all}}$ in conjunction with the full width $\Gamma_{V\to\text{all}}$ to determine the partial width $\Gamma_{V\to\mu^+\mu^-}$.

Two important features are apparent:

- the g_{VPP} coupling is reasonably regular, and the light meson sector obeys the symmetry quite well. Nonetheless there is some symmetry breaking mechanism at play, but fortunately it appears to be a *regular*

[1] This is particularly true for results about the heavy mesons, as much of the world data is relatively new and is being constantly updated.

Decay process		g_{VPP} (MeV)	
$V \to PP$	1992 [68]	1994 [87]	1996 [13]
$\rho^{\pm} \to \pi^{\pm}\pi^0$	4.24 ± 0.05	$\leftarrow$	4.24 ± 0.04
$\rho^0 \to \pi^+\pi^-$	4.30 ± 0.03	$\leftarrow$	4.28 ± 0.02
$K^{*\pm} \to (K\pi)^{\pm}$	$\leftarrow$	$\leftarrow$	4.59 ± 0.04
$K^{*0} \to (K\pi)^0$	$\leftarrow$	$\leftarrow$	4.55 ± 0.03
$\phi \to K^+K^-$	4.82 ± 0.05	$\leftarrow$	4.83 ± 0.04
$\phi \to K_L^0 K_S^0$	4.99 ± 0.06	$\leftarrow$	4.97 ± 0.05
$D^{*+} \to D^0\pi^+$	$< 27.2 \pm 2.9$	$< 10.6 \pm 1.0$	$< 10.5 \pm 1.0$
$D^{*+} \to D^+\pi^0$	$< 28.5 \pm 3.2$	$< 10.6 \pm 0.9$	$< 10.4 \pm 1.1$
$D^{*0} \to D^0\pi^0$	$< 44.9 \pm 7.1$	$< 50.2 \pm 3.9$	$< 49.6 \pm 3.9$
$V \to l\bar{l}$		g'_{VPP} (MeV)	
$\rho^0 \to e^+e^-$	$\leftarrow$	$\leftarrow$	3.56 ± 0.08
$\rho^0 \to \mu^+\mu^-$	3.41 ± 0.11	3.41 ± 0.10	3.41 ± 0.11
$\omega \to e^+e^-$	$\leftarrow$	$\leftarrow$	4.41 ± 0.07
$\omega \to \mu^+\mu^-$	$\leftarrow$	$\leftarrow$	> 2.70
$\phi \to e^+e^-$	$\leftarrow$	$\leftarrow$	4.07 ± 0.07
$\phi \to \mu^+\mu^-$	4.46 ± 0.31	$\leftarrow$	4.47 ± 0.31
$J/\psi \to e^+e^-$	7.57 ± 0.21	$\leftarrow$	7.64 ± 0.27
$J/\psi \to \mu^+\mu^-$	7.72 ± 0.31	7.63 ± 0.27	7.65 ± 0.25
$\Upsilon \to e^+e^-$	13.23 ± 0.20	13.33 ± 0.15	13.33 ± 0.25
$\Upsilon \to \mu^+\mu^-$	13.47 ± 0.32	$\leftarrow$	13.42 ± 0.30
$\Upsilon \to \tau^+\tau^-$	11.63 ± 0.72	11.59 ± 0.71	12.23 ± 0.53

Table 3.4: Determination of g_{VPP} and g'_{VPP} from two body strong and leptonic decays respectively. We take $\theta_V = 219.4°, \theta_P = -10.5°$ and $\epsilon \approx 3.4 \times 10^{-3}$.

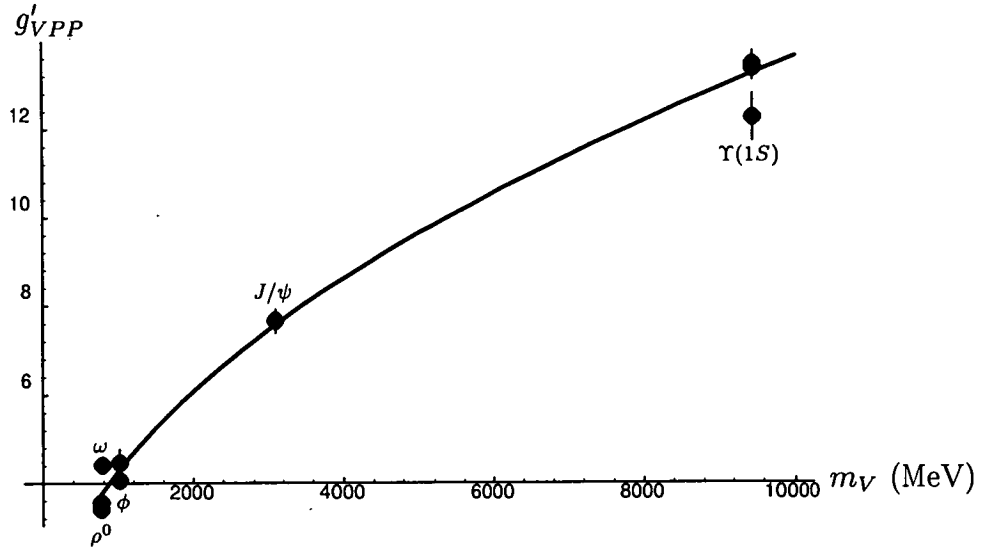

Figure 3.4: The coupling g'_{VPP}, derived from leptonic decay processes $V \to l\bar{l}$, plotted against parent vector meson mass, m_V. The curve represents the fit $g'_{VPP}(V) = 0.1359 m_V^{1/2}$.

one as the numbers appear to be groupable in terms of the parent vector meson.

- the g'_{VPP} coupling is more regular in the light meson sector, but deviates strongly in the heavy meson cases. However, there is a very obvious pattern to the symmetry breaking here.

On closer inspection the coupling appears to obey, $g'_{VPP} \propto m_V^{1/2}$ as seen in Figure 3.4 where a weighted fit (of $g'_{VPP}(V) = (0.1359 \pm 0.0036) m_V^{1/2}$)[2] has been superposed on the experimental data of 1996.

The fit is seen to be exceptionally well satisfied in the heavy meson realm with only the g'_{VPP} from the $\Gamma_{\Upsilon(1S)\to\tau^+\tau^-}$ data outside the fit. However, one should notice in Table 3.4 that in progressive data sets (1992→1994→1996) this measure is moving closer to those from $\Gamma_{\Upsilon(1S)\to e^+e^-}$ and $\Gamma_{\Upsilon(1S)\to\mu^+\mu^-}$. It

[2]The notation $g_{VPP}(V)$ indicates the 'universal' coupling constant g_{VPP} for parent vector meson state V with mass m_V. The indices VPP in g_{VPP} make no reference to the vector meson state flavour.

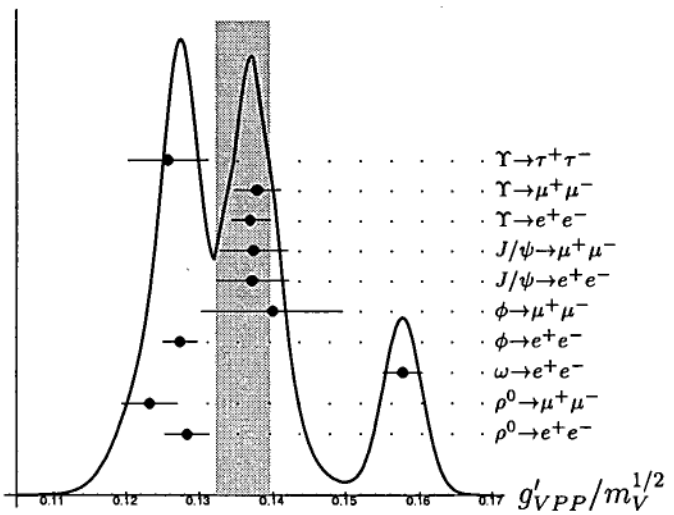

Figure 3.5: Ideogram of the data fit for the g'_{VPP} results.

is not so obvious from Figure 3.4 as to how well the fit matches the data in the light meson sector. This is more clearly seen in Figure 3.5 which is an ideogram, much like that found in the Particle Data Tables. Each 1996 experimental determination of g'_{VPP} of Table 3.4 has been divided by $m_V^{1/2}$ (where $V = \rho^0, \omega, \phi, J/\psi$ or $\Upsilon(1S)$). Then from each data set (x_i, σ_i) we plot

$$\sum_{i=1}^{N} \frac{1}{\sigma_i^2\sqrt{2\pi}} \exp\left(-\frac{(-x+x_i)^2}{2\sigma_i^2}\right)$$

and at the same time superpose the data x_i with error bars of width σ_i. As can be seen the light meson results are distributed just outside the mean value, which is indicated by the shaded zone. The most controversial result comes from the width $\Gamma_{\omega\to e^+e^-}$, leading to a g'_{VPP} which falls well outside the fit. Unfortunately the $\omega \to \mu^+\mu^-$ width is only known to an upper bound. More accurate experimental determination of this value would help in understanding this large deviation.

It appears that regardless of the symmetry breaking mechanism at play, $g'_{VPP}(V) \propto m_V^{1/2}$. Importantly we will be able to exploit this regularity in the symmetry breaking to make predictions about other processes. Given that the coupling g'_{VPP} follows this pattern, should we not expect this pattern

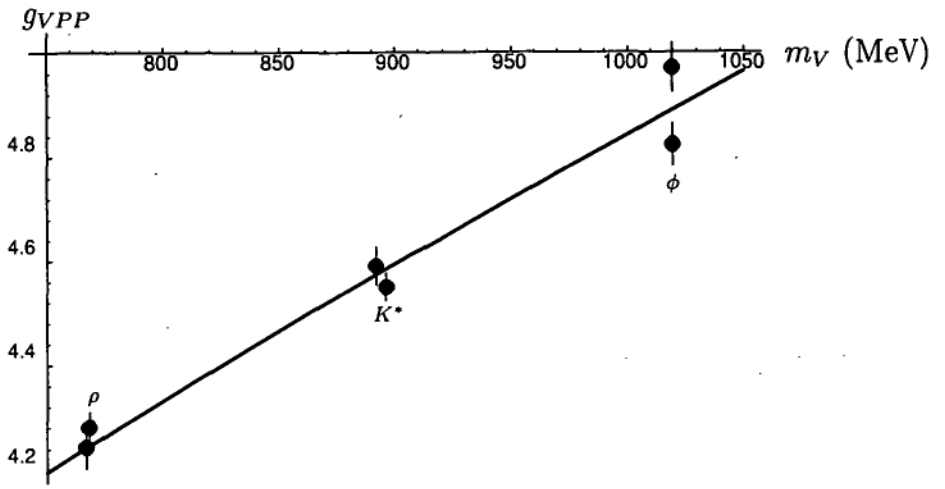

Figure 3.6: The coupling g_{VPP}, derived from purely strong decay processes, $V \to PP$, plotted against parent vector meson mass, m_V. The curve represents the fit $g_{VPP} = 0.15319 m_V^{1/2}$.

to be repeated in the g_{VPP} coupling? By performing a similar analysis as above, we first plot the g_{VPP} against the parent vector meson mass and at the same time superpose the weighted fit function $g_{VPP} \propto m_V^{1/2}$. This is shown in Figure 3.6 and demonstrates an adequate fit is achievable although it does not appear remarkably different to a linear fit over the mass range considered. However, the fit parameters slightly support an $m_V^{1/2}$ relation over that of a m_V fit as shown in the following data:

Fit Parameters:	$m_V^{1/2}$ fit	m_V fit
Adjusted R^2:	0.999893	0.96431
Estimated variance:	1.8195	1.91978

The estimated variance is $\chi^2/(N-1)$, where χ^2 is the weighted residual sum of squares, $\chi^2 = \sum_{i=1}^{N} w_i(\bar{x} - x_i)^2$. This results in the fit $g_{VPP}(V) = (0.15319 \pm 0.00065) m_V^{1/2}$ where the original error was scaled by the factor $S = [\chi^2/(N-1)]^{1/2}$. (This is identical to the way in which the Particle Data Group handle their errors.) Once again an ideogram of the fit has been produced in Figure 3.7, and clearly demonstrates it is the $\phi \to K\bar{K}$ measures

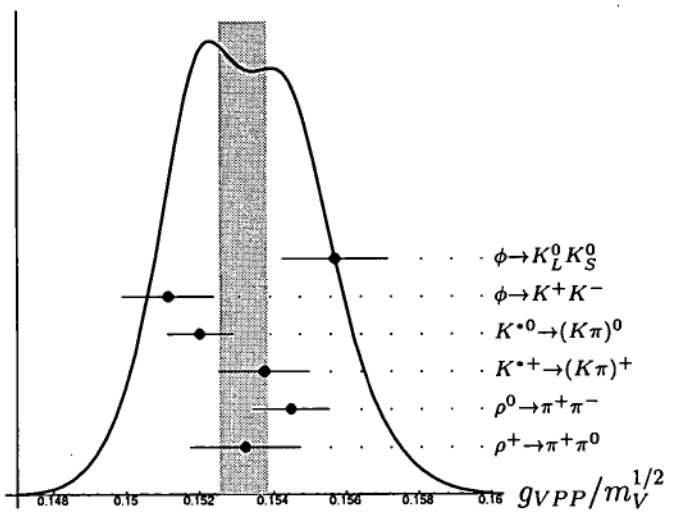

Figure 3.7: Ideogram of data fit for the g_{VPP} results.

which are the most problematic.

If we adopt the fit $g_{VPP}(V) \propto m_V^{1/2}$ we must ask ourselves are there any theoretical grounds behind the relation. Fortunately there are, and it is most easily shown by use of the heavy quark effective theory although the result can be derived from models of strong interactions. We begin by defining the pseudoscalar form factor f_P for the pseudoscalar meson–vacuum transition

$$\left\langle 0 \mid A_\mu^{(0)} \mid P(p) \right\rangle = f_P p_\mu, \tag{3.25}$$

where $A_\mu = \bar{q}\gamma_\mu\gamma_5 q'$ is the axial current, and the meson P is normalized in the standard relativistic way,

$$\langle P(p') \mid P(p) \rangle = 2E\delta^{(3)}(\mathbf{p} - \mathbf{p}'). \tag{3.26}$$

Now if we were to formulate the interaction in the HQET, $q' = Q$, we would instead be working in velocity space and hence use an effective pseudoscalar decay constant $\tilde{f}_P$ defined by

$$\left\langle 0 \mid \tilde{A}_\mu^{(0)} \mid \tilde{P}(v) \right\rangle = \tilde{f}_P v_\mu, \tag{3.27}$$

where $\tilde{A}_\mu^{(0)} \sim A_\mu^{(0)}$ is the heavy-light axial current. In the HQET, the pseudo-

scalar state is normalized to $2E/M_P$

$$\left\langle \tilde{P}(v') \mid \tilde{P}(v) \right\rangle = 2v^0 \delta^{(3)}(\mathbf{v} - \mathbf{v}')$$

which, when compared with (3.26), shows the covariant states are related to the HQET states by

$$|P(p)\rangle = \sqrt{M_P} \left| \tilde{P}(v) \right\rangle . \tag{3.28}$$

In the HQET the normalization of states and dynamics has been rendered independent of the heavy quark mass, M_Q so that $\tilde{f}_P$ is too. Hence we can assume that it is an invariant object with regard to quark content of the mesons, provided one is heavy, the other light. By writing $v_\mu = p_\mu / M_P$ and using the relation between normalizations of Equation (3.28), one can move from Equation (3.27) to (3.25) to show

$$f_P = \tilde{f}_P / \sqrt{M_P},$$

provided $\tilde{A}_\mu^{(0)} = A_\mu^{(0)}$ (techniques of renormalization can be employed to obtain an expression independent of this assumption [62]). The crucial point is that since $\tilde{f}_P$ is independent of M_Q, then so is $f_P \sqrt{M_P}$, and we conclude f_P scales as $1/\sqrt{M_P}$. We can now apply similar techniques to the interaction $V \to PP$ to determine a theoretical scaling behaviour in g_{VPP}. We begin with the definition of the matrix element in the covariant normalization,

$$\langle P(p_2) P'(p_3) \mid V(p_2 + p_3, \epsilon) \rangle = g_{VPP} (p_2 - p_3)^\mu \epsilon_\mu,$$

which in the language of HQET would be expressed as

$$\left\langle \tilde{P}(v_2) \tilde{P}'(v_3) \mid \tilde{V}(v_2 + v_3, \epsilon) \right\rangle = \tilde{g}_{VPP} (v_2 - v_3)^\mu \epsilon_\mu.$$

In the special case $P = P'$ (daughter pseudoscalars are the same so $M_P = M_{P'}$ which in turn implies $v_{2,3}^\mu = p_{2,3}^\mu / M_P$) we find

$$\langle P(p_2) P(p_3) \mid V(p_2 + p_3, \epsilon) \rangle = \sqrt{M_V} \tilde{g}_{VPP} (p_2 - p_3)^\mu \epsilon_\mu$$

which implies

$$g_{VPP} = \sqrt{M_V} \tilde{g}_{VPP}, \tag{3.29}$$

so that g_{VPP} scales as $\sqrt{M_V}$ as observed. It is important to note that this scaling behaviour *is evident in the light mesons*, whereas the theoretical method above is only assumed applicable in the heavy meson arena. The scaling behaviour of g'_{VPP} mirrors that of g_{VPP}, as it should based on their relation to one another. The data shows that the scaling is obeyed to some degree in the light meson sector (with the possible exception in $\omega \to e^+e^-$) with excellent adherence in the heavy mesons.

We now move on to Table 3.5 which predominantly lists the estimates of g_{VVP} using vector meson dominance and radiative decay data. The first entry in the table is from the decay $\phi \to \rho\pi$ and leads to a direct determination of g_{VVP}. In fact, we use it to test the supermultiplet prediction $2g_{VPP} = mg_{VVP}$, the results of which are shown in Figure 3.8 which has the difference $mg_{VVP} - 2g_{VPP}$ plotted against vector mixing angle θ_V. Since all interactions we have examined involve a vector meson parent we have chosen an average vector mass of 866 MeV (average of ρ, ω, K^*, ϕ) and an average $g_{VPP} \approx 4.58$ from Table 3.4. The figure clearly demonstrates the supermultiplet rule is satisfied at $\theta_V \approx 219.35°$, very close to the accepted value $\theta_V = 219.4°$.

The remaining g_{VVP} estimates in Table 3.5 are derived from radiative decays in which the coupling is related to the ratio g_{VVP}/g'_{VPP}. From our experience and understanding of the scaling behaviour of g'_{VPP} we safely employ the relation $g'_{VPP} \approx 0.1359 m_V^{1/2}$ to obtain g_{VVP} on its own. This relation applies to the virtual vector meson so that any process mediated via the ideal field ω_8 we have to use its mass of approximately 932 MeV. The data shows that once again the coupling is quite regular, but now the symmetry breaking appears to obey a power law relation $g_{VVP} \propto m_1^{-n}$ where $1/2 < n < 3/2$. It is worth noting that the estimates of g_{VVP} from the processes $J/\psi \to \eta_c\gamma$ and $\eta_c \to \gamma\gamma$ are in fair agreement, particularly for the 1996 data set. This is reassuring as they are described by the same vertex in the $\tilde{U}(4N_f)$ scheme. The results for the D^* and D_s^* radiative widths are derived from the upper bounds on the full widths and as such await more accurate measurement.

Decay process	g_{VVP} ($\times 10^{-2}$ MeV^{-1})		
	1992 [68]	1994 [87]	1996 [13]
$\phi \to \rho\pi$	1.062 ± 0.030	$\leftarrow$	1.062 ± 0.030
$\rho^{\pm} \to \pi^{\pm}\gamma$	0.922 ± 0.057	0.924 ± 0.056	0.921 ± 0.057
$\rho^0 \to \pi^0\gamma$	1.214 ± 0.157	1.217 ± 0.157	1.212 ± 0.157
$\rho^0 \to \eta\gamma$	0.982 ± 0.094	0.986 ± 0.094	0.982 ± 0.095
$\omega \to \pi^0\gamma$	0.877 ± 0.035	0.880 ± 0.034	0.878 ± 0.035
$\omega \to \eta\gamma$	0.916 ± 0.028	1.221 ± 0.157	1.218 ± 0.158
$\phi \to \pi^0\gamma$	0.729 ± 0.041	0.730 ± 0.041	0.722 ± 0.041
$\phi \to \eta\gamma$	0.603 ± 0.021	0.605 ± 0.021	0.608 ± 0.022
$\phi \to \eta'\gamma$	< 1.68	$\leftarrow$	< 1.69
$K^{*\pm} \to K^{\pm}\gamma$	0.903 ± 0.047	0.906 ± 0.046	0.904 ± 0.047
$K^{*0} \to K^0\gamma$	0.732 ± 0.037	0.734 ± 0.037	0.733 ± 0.038
$D^{*\pm} \to D^{\pm}\gamma$	$< 130 \pm 15$	$< 11.1 \pm 7.9$	$< 11.0 \pm 11.1$
$D^{*0} \to D^0\gamma$	$< 4.68 \pm 0.34$	$< 4.24 \pm 0.19$	$< 4.34 \pm 0.20$
$D_s^{*\pm} \to D_s^{\pm}\gamma$	$< 349 \pm 9$	$< 350 \pm 8.7$	$< 228 \pm 6.3$
$J/\psi \to \eta_c\gamma$	0.308 ± 0.050	0.313 ± 0.050	0.310 ± 0.050
$\eta' \to \rho^0\gamma$	0.691 ± 0.041	0.699 ± 0.036	0.698 ± 0.037
$\eta' \to \omega\gamma$	0.697 ± 0.051	0.702 ± 0.048	0.701 ± 0.049
$\pi^0 \to \gamma\gamma$	0.908 ± 0.040	0.914 ± 0.040	0.910 ± 0.041
$\eta \to \gamma\gamma$	0.865 ± 0.051	0.873 ± 0.050	0.866 ± 0.052
$\eta' \to \gamma\gamma$	0.724 ± 0.052	0.725 ± 0.044	0.722 ± 0.045
$\eta_c \to \gamma\gamma$	0.480 ± 0.334	0.484 ± 0.337	0.385 ± 0.106

Table 3.5: Determination of g_{VVP} from two body strong and electromagnetic decays. We take $\theta_V = 219.4°, \theta_P = -10.5°$.

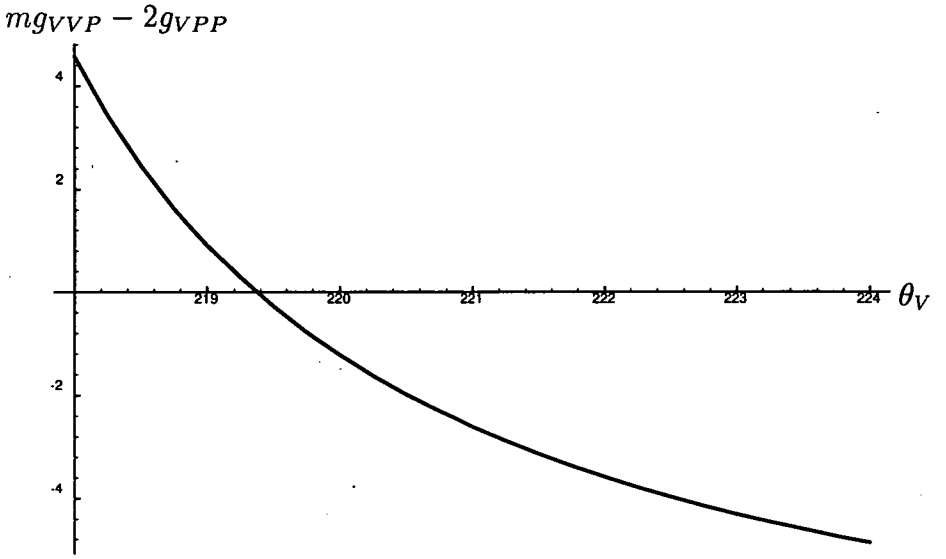

Figure 3.8: The $\tilde{U}(12)$ relation, $2g_{VPP} = mg_{VVP}$ receives strong experimental support near the vector mixing angle $\theta_V = 219.4°$ for $m = 866$ MeV.

Arguments similar to those which lead to the predicted scaling of g_{VPP} in Equation (3.29), if applied to the VVP interaction lead to the expectation

$$g_{VVP}(V, V', P) = \sqrt{\frac{M_P}{M_V M_{V'}}}\tilde{g}_{VPP},$$

but this does not appear to be reflected in the experimental results. However, it is difficult to draw reasonable conclusions from the data because we are using many decay processes along with the uncertainties inherent with vector meson dominance. There is a very real chance that higher order effects play a more significant role in the electromagnetic processes, and this notion is supported in Chapter 5.

3.4 Predictions

With the newfound understanding of the effect of the symmetry breaking on the coupling constants g_{VPP} and g'_{VPP} we can make numerous predictions.

We concentrate our efforts on making predictions about non-Zweig allowed decays and heavy meson strong and radiative decay widths and branching fractions.

3.4.1 Non-Zweig allowed Decay Widths

There are several non-Zweig allowed decays which may proceed by virtual photon mediation. For example $\omega \to \pi^+\pi^-, \phi \to \pi^+\pi^-$ and $\Upsilon(1S) \to \pi^+\pi^-$, can be realized by a virtual photon coupling between the parent vector meson and a ρ^0 meson. Thus in the case $\omega \to \pi^+\pi^-$ we have the overall coupling of

$$g_{\omega\pi^+\pi^-} = \frac{e^2 m_{\rho^0}^2 g_{\rho^0\pi^+\pi^-}}{g'_{\omega PP}(m_\omega^2 - m_{\rho^0}^2) g'_{\rho^0 PP}}$$

and for $\phi \to \pi^+\pi^-$ we have

$$g_{\phi\pi^+\pi^-} = \frac{e^2 m_{\rho^0}^2 g_{\rho^0\pi^+\pi^-}}{g'_{\phi PP}(m_\phi^2 - m_{\rho^0}^2) g'_{\rho^0 PP}}$$

and for $\Upsilon(1S) \to \pi^+\pi^-$

$$g_{\Upsilon(1S)\pi^+\pi^-} = \frac{e^2 m_{\rho^0}^2 g_{\rho^0\pi^+\pi^-}}{g'_{\Upsilon(1S)PP}(m_{\Upsilon(1S)}^2 - m_{\rho^0}^2) g'_{\rho^0 PP}}.$$

Using

$$\begin{aligned}
g_{\rho^0\pi^+\pi^-} &= \sqrt{2}(0.15319 \pm 0.00065) m_{\rho^0}^{1/2} \\
g'_{\rho^0 PP} &= \sqrt{2}(0.1359 \pm 0.0036) m_{\rho^0}^{1/2} \\
g'_{\omega PP} &= \sqrt{6}(0.1359 \pm 0.0036) m_\omega^{1/2} / \sin\theta_V \\
g'_{\phi PP} &= \sqrt{6}(0.1359 \pm 0.0036) m_\phi^{1/2} / \cos\theta_V \\
g'_{\Upsilon(1S)PP} &= 3(0.1359 \pm 0.0036) m_{\Upsilon(1S)}^{1/2},
\end{aligned}$$

we predict

$$\begin{aligned}
\Gamma_{\omega\to\pi^+\pi^-} &= (1.58 \pm 0.17) \times 10^{-1} \text{ MeV} \\
\Gamma_{\phi\to\pi^+\pi^-} &= (5.86 \pm 0.62) \times 10^{-4} \text{ MeV} \\
\Gamma_{\Upsilon(1S)\to\pi^+\pi^-} &= (1.87 \pm 0.20) \times 10^{-8} \text{ MeV},
\end{aligned}$$

which compare favourably with the 1996 accepted values [13]

$$\begin{aligned}\Gamma_{\omega\to\pi^+\pi^-} &= (1.86 \pm 0.25) \times 10^{-1}\ \text{MeV} \\ \Gamma_{\phi\to\pi^+\pi^-} &= (3.5 \pm 2.8) \times 10^{-4}\ \text{MeV} \\ \Gamma_{\Upsilon(1S)\to\pi^+\pi^-} &< (2.63 \pm 0.09) \times 10^{-5}\ \text{MeV}.\end{aligned}$$

3.4.2 Heavy meson coupling constants

There are many works which concentrate on the calculation of the heavy meson-π meson coupling constants, $g_{H^*H\pi}$ where H is a heavy meson (i.e. $H = D$ or B). In our case, these couplings are simply derived from the relation $g_{H^*H\pi} = c(0.15319 \pm 0.00065)m_{H^*}^{1/2}$ where c is a Clebsch-Gordan factor. We tabulate our predictions against those of other research in Table 3.6. The table details the couplings $g_{D^*D\pi}$ and $g_{B^*B\pi}$ where

$$g_{H^*H\pi} \equiv g_{H^{*+}H^0\pi^+} = \sqrt{2}g_{H^{*+}H^+\pi^0} = g_{H^{*0}H^+\pi^-} = -\sqrt{2}g_{H^{*0}H^0\pi^0}.$$

Many of the other research papers use a different coupling constant (often indicated by g, g_A), but this can be related to our covariant coupling by comparison between their and our decay rate formulas. Any work marked with an arrow next to their coupling value have had it rescaled by us. The rescaling used is indicated by:

Symbol	Rescaling factor
$\xrightarrow{\dagger}$	m_{H^*}/f_π
$\xrightarrow{\ddagger}$	m_H/f_π
$\xrightarrow{\sqrt{\dagger\ddagger}}$	$\sqrt{m_{H^*}m_H}/f_\pi$,

where $f_\pi \simeq 131$ MeV. For any research which only details a coupling value in reference to D^* decays, we only apply the rescaling to produce their equivalent $g_{D^*D\pi}$ and do not use it to estimate $g_{B^*B\pi}$. For papers which only produce a decay width prediction, we use (3.12) to convert this to a coupling constant and indicate that we have done so with the symbol: $^\Gamma$. In some instances other research will quote a coupling constant $g_{H^*H\pi}$ and a decay rate value

which are not consistent with our formula. In such works the decay rate formulas are typically a factor of 4 smaller than ours so their coupling constants are a factor of 2 greater to achieve the same width result. For these cases we list their quoted value of $g_{H^*H\pi}$ and ours determined from the decay width using (3.12). Once again we mark these with the $^\Gamma$ symbol. At present there are no experimental measures, apart from upper bounds, with which to validate our predictions. Our predictions fare quite well when compared to the numerous other ones, although our value $g_{B^*B\pi}$ appears to be consistently lower than most. Unfortunately there is unlikely to be a direct measure of this coupling as the process is kinematically forbidden by the available phase space.

3.4.3 $H^* \to H\gamma$ decays and coupling ratios

The symmetry breaking effects we have observed also lead to a measurable consequence in the radiative decays of heavy mesons. We begin by re-examining the decays $K^{*\pm} \to K^\pm\gamma$ and $K^{*0} \to K^0\gamma$. Experimentally, the K^* branching fraction is

$$\Gamma_{K^{*0}\to K^0\gamma}/\Gamma_{K^{*\pm}\to K^\pm\gamma} = 2.31 \pm 0.29,$$

and allowing for phase space factors this translates into a coupling constant ratio of

$$|g_{K^{*0}K^0\gamma}/g_{K^{*\pm}K^\pm\gamma}| = 1.514 \pm 0.095,$$

and as such is far from the exact $SU(3)$ ratio of 2. Under the supermultiplet scheme, one can show the decays proceed via two intermediate vector mesons, ρ^0 and ω_8. Following the procedure we described for determining the Clebsch–Gordan factors, one finds

$$g_{K^{*\pm}K^\pm\gamma} = e\left(\frac{g_{K^{*\pm}\rho^0K^\pm}}{g'_{\rho^0PP}} + \frac{g_{K^{*\pm}\omega_8K^\pm}}{g'_{\omega_8PP}}\right), \tag{3.30}$$

$$g_{K^{*0}K^0\gamma} = e\left(\frac{g_{K^{*0}\rho^0K^0}}{g'_{\rho^0PP}} + \frac{g_{K^{*0}\omega_8K^0}}{g'_{\omega_8PP}}\right). \tag{3.31}$$

Research and method[a]	Paper's constant and scaling used	$g_{D^*D\pi}$	$g_{B^*B\pi}$
This		6.87 ± 0.03	11.18 ± 0.05
Exp. [13]		$< 10.5 \pm 1.0$	
[75] RQM		8.78	22.92
[38] B-S		8.29	
[79] SQM(c)		6.97	
[98]		8.35	
[100] H-LS		8.36^{Γ}	
[50] H-LS		$\sim 8^{\Gamma}$	
[91] H-LS		≈ 11.8	≈ 36
[78] H-LS		$\sim 4.2^{\Gamma}$	
[89] HHCT	$0.25 - 0.5 \overset{\uparrow}{\rightarrow}$	$3.54 - 7.08$	
[81] QCDSR		12.5 ± 1 $6.25 \pm 0.5^{\Gamma}$	29 ± 3
[113] $SU(4)$		6.34 ± 0.22 $4.48 \pm 0.16^{\Gamma}$	
[63] HHCT	$0.2 - 0.7 \overset{\uparrow}{\rightarrow}$	$3.0 - 10.7$	
[52] QCDSR		6.1 ± 1.4	
[5] HHCT	$\leq \sqrt{0.5} \overset{\uparrow}{\rightarrow}$	≤ 10.8	
[109] RQM	$0.28(D), 0.32(B) \overset{2\times\sqrt{\uparrow\uparrow}}{\rightarrow}$	8.29	25.96
[19] QCDSR		12.5 ± 1 $6.25 \pm 0.5^{\Gamma}$	29 ± 3
[31] HQET	$0.4 \pm 0.08 \overset{\uparrow}{\rightarrow}$	6.1 ± 0.2	16.1 ± 3.2
[34] QCDSR		7 ± 1	15 ± 4
[32] RPM	$0.4 \left\{ \begin{array}{l} \overset{2\times\uparrow}{\rightarrow} \\ \overset{\uparrow}{\rightarrow} \end{array} \right.$	12.3 6.2^{Γ}	31.7 16^{Γ}
[10] HHCT	$0.56 \overset{\uparrow}{\rightarrow}$	8.38	
[92] RLFQM	0.6	9.23	
[73] HHCT	$0.53 \overset{\uparrow}{\rightarrow}$	8.07	
[28] RQM	$0.4 - 0.6 \left\{ \begin{array}{l} \overset{2\times\uparrow}{\rightarrow} \\ \overset{\uparrow}{\rightarrow} \end{array} \right.$	$12 - 18$ $6 - 9^{\Gamma}$	$32 - 48$ $16 - 24^{\Gamma}$
[48] QCDSR		6.3 ± 1.9	14 ± 4
[30] HHCT	$\left. \begin{array}{l} 0.66 \pm 0.47 \\ 0.58 \pm 0.41 \end{array} \right\} \overset{\sqrt{\uparrow\uparrow}}{\rightarrow}$	$\left\{ \begin{array}{l} 9.7 \pm 6.9 \\ 8.5 \pm 6.0 \end{array} \right.$	
[95] QM	$3/4 \overset{\uparrow}{\rightarrow}$	11.5	
[86] Bag		$8.1 \pm 0.8^{\Gamma}$	

[a]Abbreviations: R=Relativistic, QM=Quark Model, B-S=Bethe-Salpeter, SQM=Simple QM, H-LS=Heavy-Light System, HHCT=Heavy Hadron Chiral Theory, QCDSR=QCD Sum Rules, PM=Potential Model, LF=Light Front

Table 3.6: Summary of theoretical estimates for couplings $g_{H^*H\pi}$.

If one assumes g'_{VPP} is constant then

$$g_{K^{*\pm}K^{\pm}\gamma} = e\left(\frac{1/\sqrt{2}}{\sqrt{2}} + \frac{-1/\sqrt{6}}{\sqrt{6}}\right) g_{VVP}/g'_{VPP} = g_{VP\gamma}/3,$$
$$g_{K^{*0}K^{0}\gamma} = e\left(\frac{-1/\sqrt{2}}{\sqrt{2}} + \frac{-1/\sqrt{6}}{\sqrt{6}}\right) g_{VVP}/g'_{VPP} = -2g_{VP\gamma}/3,$$

and we arrive at the exact $SU(3)$ prediction. If instead we use a symmetry breaking g'_{VPP} we must substitute $g'_{\rho^0 PP} = \sqrt{2}\,k\,m_{\rho^0}^{1/2}$ and $g'_{\omega_8 PP} = \sqrt{6}\,k\,m_{\omega_8}^{1/2}$ in Equations (3.30) and (3.31). Thus

$$\frac{g_{K^{*0}K^{0}\gamma}}{g_{K^{*\pm}K^{\pm}\gamma}} = -\frac{m_{\rho^0}^{-1/2} + m_{\omega_8}^{-1/2}/3}{m_{\rho^0}^{-1/2} - m_{\omega_8}^{-1/2}/3} = -1.868 \pm 0.001, \tag{3.32}$$

and notice the result is independent of the proportionality constant between g_{VPP} and $m_V^{1/2}$. Although not matching the experimental result, it is an improvement on exact $SU(3)$. Actually, the most satisfactory explanation of the symmetry breaking mechanism comes from Bramon and Scadron [25]. They attribute the deviation from exact $SU(3)$ to the constituent mass difference between the strange and non-strange quarks in the loop of a quark triangle diagram. As $K^* \to K\gamma$ excite both strange and non-strange quarks, such a difference must be accounted for. With these corrections, the experimental ratio is found to match theoretical estimates very well. We shall develop this method and apply it to many other meson cases in Chapter 5 as a contrast to the $\tilde{U}(4N_f)$ scheme.

Let us continue to use the observed mass scaling of g_{VPP} and g'_{VPP} in the heavy meson sector. Upon application to the D^* and B^* mesons we obtain

$$\frac{g_{D^{*0}D^{0}\gamma}}{g_{D^{*+}D^{+}\gamma}} = \frac{3m_{\rho^0}^{-1/2} + m_{\omega_8}^{-1/2} + 4m_{J/\psi}^{-1/2}}{-3m_{\rho^0}^{-1/2} + m_{\omega_8}^{-1/2} + 4m_{J/\psi}^{-1/2}} \approx -59.16 \pm 1.48, \tag{3.33}$$

$$\frac{g_{B^{*0}B^{0}\gamma}}{g_{B^{*+}B^{+}\gamma}} = \frac{-3m_{\rho^0}^{-1/2} + m_{\omega_8}^{-1/2} - 2m_{\Upsilon}^{-1/2}}{3m_{\rho^0}^{-1/2} + m_{\omega_8}^{-1/2} - 2m_{\Upsilon}^{-1/2}} \approx -0.7973 \pm 0.0002, \tag{3.34}$$

which are significantly different from the exact $SU(5)$ predictions of

$$g_{D^{*0}D^{0}\gamma}/g_{D^{*+}D^{+}\gamma} = 4,$$
$$g_{B^{*0}B^{0}\gamma}/g_{B^{*+}B^{+}\gamma} = -2,$$

and as such require better experimental data to test the results.

3.4.4 D^* and B^* Decay Widths

In addition to these relative decay rate predictions, the supermultiplet scheme can be easily adapted to decay width calculations. Scattered amongst Tables 3.4 and 3.5 are various constants determined by extending the supermultiplets to include the charm and bottom quark mesons. In particular, using the upper bound of 131 keV for the D^{*+} decay width (ACCMOR Collab., [12]) we have found $g_{VPP} < 10$. Conversely, we can use our knowledge of the effects of symmetry breaking to predict the VPP coupling constant for D^{*+}. We find

$$g_{VPP}(D^{*+}) \approx (0.15319 \pm 0.00065)(2010)^{1/2} = 6.87 \pm 0.03,$$

similar to a heavy quark prediction of 7 ± 1 by Colangelo *et al.* [34]. We can use the value for D^{*+} to calculate the total decay width of the $D^{*+} \to PP$ channels. The $\tilde{U}(4N_f)$ trace technique provides all the Zweig allowed decay channels of D^{*+} into two pseudoscalars; however, the available kinematical phase space restricts these to $D^{*+} \to D^0\pi^+$ and $D^{*+} \to D^+\pi^0$ so that the width must be

$$\begin{aligned}
\Gamma_{D^{*+}\to PP} &= \Gamma_{D^{*+}\to D^0\pi+} + \Gamma_{D^{*+}\to D^+\pi^0} \\
&= \frac{g^2_{VPP}}{48\pi m^5_{D^{*+}}} \left[\lambda^{3/2}(m^2_{D^{*+}}, m^2_{D^0}, m^2_{\pi^+}) + \frac{1}{2}\lambda^{3/2}(m^2_{D^{*+}}, m^2_{D^+}, m^2_{\pi^0})\right] \\
&= 55.88 \pm 0.47 \text{ keV}.
\end{aligned}$$

We compare this with the radiative width $D^{*+} \to D^+\gamma$ in the following ratio:

$$\begin{aligned}
&\frac{\Gamma_{D^{*+}\to D^+\gamma}}{\Gamma_{D^{*+}\to PP}} \\
&= \frac{(g_{VP\gamma}/g'_{VPP})^2(m^2_{D^{*+}} - m^2_{D^+})^3/96\pi m^3_{D^{*+}}}{\left[\lambda^{3/2}(m^2_{D^{*+}}, m^2_{D^0}, m^2_{\pi^+}) + \frac{1}{2}\lambda^{3/2}(m^2_{D^{*+}}, m^2_{D^+}, m^2_{\pi^0})\right]/48\pi m^5_{D^{*+}}} \\
&\approx \frac{\left[e(-3m_{\rho^0}^{-1/2} + m_{\omega_8}^{-1/2} + 4m_{J/\psi}^{-1/2})/(6 \times 0.1359)\right]^2 (m^2_{D^{*+}} - m^2_{D^+})^3}{\lambda^{3/2}(m^2_{D^{*+}}, m^2_{D^0}, m^2_{\pi^+}) + \frac{1}{2}\lambda^{3/2}(m^2_{D^{*+}}, m^2_{D^+}, m^2_{\pi^0})} \\
&\approx (9.90 \pm 0.52) \times 10^{-5},
\end{aligned}$$

where in particular we have used the supermultiplet prediction $g_{VVP}/g_{VPP} = 2/m_{D^{*+}}$. Here we have assumed that the central meson mass m is significantly higher when the charm mesons are included in the supermultiplet. Since $\Gamma_{D^{*+}\to\text{all}} = \Gamma_{D^{*+}\to PP} + \Gamma_{D^{*+}\to D^+\gamma}$, the above result implies that the dominant decay modes in D^{*+} decay are the PP channels and therefore approximately compose the full width, that is $\Gamma_{D^{*+}\to PP} \cong \Gamma_{D^{*+}\to\text{all}}$. Thus the radiative branching fraction $\Gamma_{D^{*+}\to D^+\gamma}/\Gamma_{D^{*+}\to\text{all}}$ is very small which is not inconsistent with the present experimental fraction of $(1.1 \pm 2.1 \pm 0.7)\%$[13]. However, our prediction does conflict with other theoretical models [79, 32, 92, 73]. Under the assumption $\Gamma_{D^{*+}\to PP} = \Gamma_{D^{*+}\to\text{all}}$, branching fraction calculations for the two PP channels yield

$$\begin{aligned} \Gamma_{D^{*+}\to D^0\pi^+}/\Gamma_{D^{*+}\to\text{all}} &\approx 68.8\%, \\ \Gamma_{D^{*+}\to D^+\pi^0}/\Gamma_{D^{*+}\to\text{all}} &\approx 31.2\% \end{aligned}$$

which compare well with other models and the present experimental result [13]:

$$\begin{aligned} \Gamma_{D^{*+}\to D^0\pi^+}/\Gamma_{D^{*+}\to\text{all}} &= (68.3 \pm 1.4)\%, \\ \Gamma_{D^{*+}\to D^+\pi^0}/\Gamma_{D^{*+}\to\text{all}} &= (30.6 \pm 2.5)\%. \end{aligned}$$

We are able to employ similar methods in the decays of the D^{*0} vector meson. In this instance, the possible PP decay channels are restricted by phase space to $D^{*0} \to D^0\pi^0$. We calculate this width to be 24.9 ± 0.2 keV, where we used $g_{D^{*0}D^0\pi^0} = (0.15319 \pm 0.00065)(2006.7)^{1/2}/\sqrt{2}$. To determine the radiative width $D^{*0} \to D^0\gamma$ we apply relation (3.33) along with a small correction for the change in phase space to derive

$$\Gamma_{D^{*0}\to D^0\gamma} \approx (3630 \pm 182) \times \Gamma_{D^{*+}\to D^+\gamma} = (20.1 \pm 1.5) \text{ keV}.$$

Thus if these two partials are the only decay channels available for D^{*0} decay the total D^{*0} width is (45.0 ± 1.5) keV, although the result is sensitive to the supermultiplet prediction $g_{VVP}(D^*)/g_{VPP}(D^*) = 2/m_{D^*}$. Consequently we

predict the following branching fractions:

$$\begin{aligned}\Gamma_{D^{*0}\to D^0\pi^0}/\Gamma_{D^{*0}\to \text{all}} &\approx (55.3 \pm 1.9)\%, \\ \Gamma_{D^{*0}\to D^0\gamma}/\Gamma_{D^{*+}\to \text{all}} &\approx (44.7 \pm 3.7)\%,\end{aligned}$$

which are in fair agreement with the Particle Data Group's average [13] data:

$$\begin{aligned}\Gamma_{D^{*0}\to D^0\pi^0}/\Gamma_{D^{*0}\to \text{all}} &\approx (61.9 \pm 2.9)\%, \\ \Gamma_{D^{*0}\to D^0\gamma}/\Gamma_{D^{*+}\to \text{all}} &\approx (38.1 \pm 2.9)\%.\end{aligned}$$

3.5 Summary

This study of two-body ground state meson decays has shown that the supermultiplet method unifies meson decays quite well, even for the light quarks. The most significant finding is that the coupling between mesons is susceptible to symmetry breaking mechanisms, but in a *regular* way, allowing us to successfully extrapolate to decay rates for other processes. In particular, the methods are readily applicable to heavy quark examples, as highlighted by our examination of D^* processes.

Chapter 4

Excited state meson decays

The excited mesons are the next testing ground for the $\tilde{U}(4N_f)$ method and associated investigation of universal coupling constants. The $\tilde{U}(4N_f)$ wavefunctions for the excited mesons are constructed by combining the spin-flavour symmetry with the $O(3,1)$ group corresponding to relativistic orbital angular momentum. The methods we shall use to determine the coupling constants of various decays closely resemble those of Chapter 3, and it is the ease with which notions of Clebsch–Gordan factors, mixing angles and so forth are accommodated that the $\tilde{U}(4N_f)$ trace method once again demonstrates its appeal.

4.1 Excited meson wavefunctions

The extension of the $\tilde{U}(4N_f)$ scheme to include orbital excitation states (and not "quark-excitation" types) was first considered in the context of incorporating higher–symmetry ideas into the phenomenology of Regge poles [45]. These ideas were latter refined by Delbourgo and Liu [41] and we follow their derivation of the excited state meson wavefunctions. These are most easily constructed by boosting quark-antiquark systems at rest. In the rest frame, the meson's four-velocity is a unit timelike vector pointing along the time axis with spatial $SU(2)$ (the little group of the full Lorentz group) the

only surviving space-time symmetry, of which the mesons are irreducible representations. The quantum numbers of the meson can only be the $SU(2)_J$ labels, so that the meson state is given by

$$\left[\phi_a^b\right]_{\{m_1 \ldots m_L\}},$$

where m is an $O(3)$ vector index corresponding to orbital excitation L, and a, b are the usual two-component spinors corresponding to flavour. $\{\ldots\}$ signifies a symmetrised tensor product and it is assumed that all Kronecker traces over the m indices are zero to ensure the orbital state is irreducible with respect to $O(3)$. As the quarks and antiquarks can be acted on by different spin groups, we need to reduce the multispinors into total spin states, that is $\frac{1}{2} \otimes \frac{1}{2} = 0 \oplus 1$,

$$\phi_a^b = \left[\phi_5 \delta_a^b + (\sigma_m)_a^b \phi_m\right], \tag{4.1}$$

where the orbital quantum numbers have been disregarded. ϕ_5 and ϕ_m are the familiar pseudoscalar and vector states (in the rest frame). To produce the orbital excitation states, L is combined with spin S to form representations of total spin J. The pseudoscalar meson excitations are simply $\phi_{5\{m_1 \ldots m_L\}}$ while the vector meson excitations $(1 \otimes L)$ are reducible to states with $J = L+1, L, L-1$ as shown

$$\begin{aligned} \phi_{m\{m_1 \ldots m_L\}} &= \phi^{(L+1)}_{\{m m_1 \ldots m_L\}} + \tfrac{1}{\sqrt{2L}} \sum_k i\epsilon_{m m_k n} \phi^{(L)}_{\{m_1 \ldots \bar{k} \ldots m_L n\}} \\ &+ \tfrac{1}{L}\sqrt{\tfrac{2L-1}{2L+1}} \sum_k \left[\delta_{m m_k} \phi^{(L-1)}_{\{m_1 \ldots \bar{k} \ldots m_L\}} - \tfrac{2}{2L-1} \sum_l \delta_{m_k m_l} \phi^{(L-1)}_{\{m_1 \ldots \bar{k}\bar{l} \ldots m_L\}}\right], \end{aligned} \tag{4.2}$$

where a bar over an $O(3)$ index, like $\bar{k}$, signifies that m_k is missing from the tensor. The pseudoscalar and vector excitations have parity $P = (-1)^{L+1}$ and charge conjugation $C = (-1)^{L+S}$. If we boost these non-relativistic wavefunctions we shall obtain the fully Lorentz covariant wavefunctions. The important point to realize is that an incoming meson must contain the projection factors $[(1+\gamma_0)/2]\Gamma[(1-\gamma_0)/2]$ in the rest frame. This ensures the upper two components of the quark and the lower two components of the

antiquark (which form the meson) are picked out. By these considerations, we obtain the boosted version of the wavefunction (4.1)

$$[\phi(p)]^{\beta}_{\alpha} = \frac{(\not{p}+m)}{2m}\left[\gamma^{\mu}\phi_{\mu}(p) - \gamma_5\phi_5(p)\right]^{\beta}_{\alpha},$$

which, as expected, is identical to the original derivation (2.28). Hence an excited meson of orbital angular momentum L and momentum p has the $\tilde{U}(4N_f) \otimes O(3,1)_L$ structure

$$\Phi^{B}_{A\{\mu_1\ldots\mu_L\}}(p) = \frac{1}{2m}(\not{p}+m)\left[\gamma^{\mu}\phi^{b}_{\mu\{\mu_1\ldots\mu_L\}a}(p) - \gamma_5\phi^{b}_{5\{\mu_1\ldots\mu_L\}a}(p)\right]^{\beta}_{\alpha}, \quad (4.3)$$

and from (4.2) the vector meson excitations reduce to states with $J = L+1, L, L-1$ in the following manner

$$\begin{aligned}
\phi_{\mu\{\mu_1\ldots\mu_L\}}(p) \;=\; & \phi^{(L+1)}_{\{\mu\mu_1\ldots\mu_L\}}(p) \\
& -\frac{i}{L\sqrt{2}}\frac{p^{\lambda}}{m}\sum_{k=1}^{L}\epsilon_{\lambda\mu\mu_k\nu}g^{\nu\nu'}\phi^{(L)}_{\{\mu_1\ldots\bar{k}\ldots\mu_L\nu'\}}(p) \\
& +\frac{1}{L}\sqrt{\frac{2L-1}{2L+1}}\sum_{k=1}^{L}\Big[(-g_{\mu\mu_k}+p_{\mu}p_{\mu_k}/m^2)\phi^{(L-1)}_{\{\mu_1\ldots\bar{k}\ldots\mu_L\}}(p) \\
& -\frac{2}{2L-1}\sum_{l=1}^{k}(-g_{\mu_k\mu_l}+p_{\mu_k}p_{\mu_l}/m^2)\phi^{(L-1)}_{\{\mu\mu_1\ldots\bar{k}\bar{l}\ldots\mu_L\}}(p)\Big] \quad (4.4)
\end{aligned}$$

where $\phi^{(J)}$ denotes the J value of the state.

4.2 Excited meson interactions and decays

The interaction Lagrangian for the excited meson decays are similar to that of the ground states, except for extra terms which must be introduced to contract the new indices associated with the orbital momentum quantum number and hence construct a covariant interaction. The majority of data is for decays of the type

$$\Phi_{\{\mu_1\ldots\mu_L\}}(p_1) \to \Phi(-p_2) + \Phi(-p_3),$$

where p_i is incoming, so that the final states are both ground state mesons. In this instance, the only $U(2N_f) \otimes U(2N_f) \otimes 0(2)$ symmetry conserving covariant interaction consistent with Bose statistics is

$$G_L q^{\mu_1} \ldots q^{\mu_L} \Phi^B_{A\{\mu_1 \ldots \mu_L\}}(p_1) \left[\Phi^C_B(p_2)\Phi^A_C(p_3) + (-1)^L \Phi^C_B(p_3)\Phi^A_C(p_2)\right].$$

Since these momentum terms are external to the trace many of the derivations of Section A.2 are valid here. For other decay types, where daughter particles involve excited meson states as well, the forms of covariant interaction are more complex and cumbersome. Nonetheless, they are still describable in terms of the $\tilde{U}(4N_f) \otimes O(3,1)_L$ wavefunctions signifying the adaptability of the scheme.

As stated previously, the experimental data for two-body strong decays of the excited mesons is most abundant in decays to the ground states. Although this leads to the 'simplest' of the excited interaction Lagrangians, the increased complexity enters in the derivations of the decay rate formulae, as polarizations sums become progressively more difficult. Fortunately, general methods for calculating the polarization sums of a spin J meson have been devised [41] and we use various guises of these in the proceeding sections. The two main results we use are

$$\sum_\lambda \left| q^{\mu_1} \ldots q^{\mu_J} \phi^{(\lambda)}_{\mu_1 \ldots \mu_J}(p_1) \right|^2 = \frac{2^J (J!)^2}{(2J)!} \frac{\lambda^J(m_1^2, m_2^2, m_3^2)}{m_1^{2J}}, \tag{4.5}$$

for a summation with all indices contracted (where $q = p_2 - p_3$) and for instances in which an index remains uncontracted,

$$\sum_\lambda q^{\mu_2} \ldots q^{\mu_J} \phi^{(\lambda)}_{\mu\mu_2 \ldots \mu_J}(p_1) \phi^{(\lambda)*}_{\mu'\mu'_2 \ldots \mu'_J}(p_1) q^{\mu'_2} \ldots q^{\mu'_J} = \frac{2^J (J!)^2}{(2J)!} \left(\frac{\lambda^{1/2}}{m_1}\right)^{2(J-1)}$$
$$\times \left[\frac{(J+1)}{2J} d_{\mu\mu'}(p) + \frac{(J-1)}{2J} \frac{(q_\mu - \frac{q \cdot p_1 p_{1\mu}}{m_1^2})(q_{\mu'} - \frac{q \cdot p p_{\mu'}}{m^2})}{\lambda(m_1^2, m_2^2, m_3^2)/m^2} \right], \tag{4.6}$$

where $d_{\mu\mu'}(p) = -g_{\mu\mu'} + p_\mu p_{\mu'}/m^2$, $p^2 = m^2$.

We shall investigate mesons of $L = 1$ to $L = 4$ and thus span a considerable range of the known mesons. There are many Zweig allowed two-body

decays of the excited mesons, but not all of these have been experimentally observed. Since we are always "chasing" experimental measures to calculate the universal couplings, we concentrate our study on the observed processes, but it is important to realise that there are many potential channels which could be studied in terms of the $\tilde{U}(4N_f) \otimes O(3,1)_L$ scheme which may not be mentioned in our analysis simply because of the lack of data.

4.2.1 $L = 1$ meson interactions

There is considerable data on two-body strong decays of the $L = 1$ excited state mesons ($J^{PC} = 2^{++}, 1^{++}, 0^{++}, 1^{+-}$). Most channels are of the type $\mathsf{P} \to PP$ or $\mathsf{P} \to VP$ where P denotes an $L = 1$ meson (from the $^{2S+1}L_J$ terminology) while $V(P)$ denotes a vector(pseudoscalar) meson. Subsequently, we need only consider the interaction Lagrangian

$$\mathcal{L}_{\text{int}} = G_{\mathsf{P}}(p_2 - p_3)^{\mu_1} \Phi^B_{A\mu_1}(p_1) \left[\Phi^C_B(p_2)\Phi^A_C(p_3) - \Phi^C_B(p_3)\Phi^A_C(p_2)\right], \qquad (4.7)$$

where $\Phi^B_A(p)$ is a ground state wavefunction of Equation (2.28). The $L = 1$ superfield as derived from (4.3) and (4.4) is

$$\Phi^B_{A\mu_1}(p_1) = \frac{1}{2m_1}(\not{p}_1 + m_1)(\gamma^\mu \phi_{\mu\mu_1}(p) - \gamma_5 \phi_{5\mu_1}(p))$$

where $\phi_{\mu\mu_1}$ decomposes as

$$\phi_{\mu\mu_1}(p_1) = \phi^{(2)}_{\{\mu\mu_1\}}(p_1) - \frac{i}{\sqrt{2}}\frac{p_1^\lambda}{m_1}\epsilon_{\lambda\mu\mu_1\kappa} g^{\kappa\kappa'} \phi^{(1)}_{\kappa'}(p_1) + \frac{1}{\sqrt{3}} d_{\mu\mu_1}\phi^{(0)}(p_1) \qquad (4.8)$$

The trace in (4.7) is expanded in much the same manner as those of the previous chapter, it is only in the final stages of the expansion that one need substitute the form (4.8).

$\mathsf{P} \to PP$ interactions

The $\mathsf{P} \to PP$ interactions (where P denotes the ground state pseudoscalar mesons) compose the major fraction of the $L = 1$ two-body strong decays. Fortunately the $\tilde{U}(4N_f)$ trace methodology and corresponding wavefunctions

account for many of these channels. To begin with we consider decays of the type $1^{+-} \to PP$, of which the interaction term,

$$\begin{aligned}\mathcal{L}_{\rm int} &= \frac{G_{\mathsf{P}}}{8\prod_{i=1}^{3} m_i}(p_2-p_3)^{\mu}\mathrm{Tr}\left[(\not{p}_1+m_1)\gamma_5(\not{p}_2+m_2)\gamma_5(\not{p}_3+m_3)\gamma_5\right. \\ &\qquad \left.\times\,\phi_{5\mu}(p_1)\left(\phi_5(p_2)\phi_5(p_3)-(p_2\leftrightarrow p_3)\right)\right]\end{aligned}$$

disappears in agreement with parity conservation considerations, so we predict strong suppression of such widths in the experimental data. The other $\mathsf{P} \to PP$ terms do not vanish, but expand like Equation (3.2) so that

$$\mathcal{L}_{\rm int} = -\frac{G_{\mathsf{P}}\sum_{i=1}^{3} m_i}{4m_2m_3}q^{\mu}q^{\mu_1}\left\langle\phi_{\mu\mu_1}(p_1)\left\{\phi_5(p_2),\phi_5(p_3)\right\}\right\rangle,$$

where $q^{\mu}=(p_2-p_3)^{\mu}$. Upon substitution of (4.4) into this term, we find the surviving terms

$$\begin{aligned}\mathcal{L}_{\rm int} &= -\frac{G_{\mathsf{P}}\sum_i m_i}{4m_2m_3}q^{\mu}q^{\mu_1}\left\{\phi^{(2)b}_{\{\mu\mu_1\}a}(p_1)+\tfrac{1}{\sqrt{3}}(-g_{\mu\mu_1}+p_{1\mu}p_{1\mu_1}/m_1^2)\phi^{(0)b}_{a}(p_1)\right\} \\ &\qquad \times\left[\phi^{c}_{5b}(p_2)\phi^{a}_{5c}(p_3)+\phi^{c}_{5b}(p_3)\phi^{a}_{5c}(p_2)\right],\end{aligned}$$

so that $2^{++} \to PP$ and $0^{++} \to PP$ decays are adequately described by the above Lagrangian, while $1^{++} \to PP$ processes are suppressed. This finding is supported by the experimental data as we shall see.

We define a universal coupling $g_{\mathsf{P}PP}$ in terms of the G_{P} and meson masses via

$$g_{\mathsf{P}PP} = \frac{G_{\mathsf{P}}\sum_i m_i}{4m_2m_3}$$

to determine the decay rate forms for the two processes as follows.

$2^{++} \to PP$ decay rate From the general two-body decay rate formula (3.11), along with the general polarization sum (4.5), the sum in this instance reduces to

$$\begin{aligned}|\mathcal{L}_{\rm int}|^2 &= \frac{g^2_{\mathsf{P}PP}}{2.2+1}\sum_{\lambda}q^{\mu}q^{\mu_1}\phi^{(\lambda)}_{\{\mu\mu_1\}}(p_1)\phi^{(\lambda)*}_{\{\mu'\mu'_1\}}(p_1)q^{\mu'}q^{\mu'_1} \\ &= \frac{g^2_{\mathsf{P}PP}}{5}\frac{2^2(2!)^2}{(2.2)!}\frac{\lambda^2(m_1^2,m_2^2,m_3^2)}{m_1^4}\end{aligned}$$

so that the decay rate is

$$\Gamma_{2^{++}\to PP} = \frac{g_{\mathsf{P}PP}^2}{120\pi}\frac{\lambda^{5/2}(m_1^2,m_2^2,m_3^2)}{m_1^7} \tag{4.9}$$

$0^{++} \to PP$ decay rate There is no polarization sum in this instance; we have the simple contraction

$$\begin{aligned}|\mathcal{L}_{\text{int}}|^2 &= \frac{g_{\mathsf{P}PP}^2}{2.0+1}q^{\mu}q^{\mu_1}\frac{1}{3}\left(-g_{\mu\mu_1}+\frac{p_{1\mu}p_{1\mu_1}}{m_1^2}\right)\left(-g_{\mu'\mu_1'}+\frac{p_{1\mu'}p_{1\mu_1'}}{m_1^2}\right)q^{\mu'}q^{\mu_1'}\\ &= \frac{g_{\mathsf{P}PP}^2}{3}\frac{\lambda^2(m_1^2,m_2^2,m_3^2)}{m_1^4}\end{aligned}$$

resulting in the decay rate formula

$$\Gamma_{0^{++}\to PP} = \frac{g_{\mathsf{P}PP}^2}{48\pi}\frac{\lambda^{5/2}(m_1^2,m_2^2,m_3^2)}{m_1^7} \tag{4.10}$$

$\mathsf{P} \to VP$ interactions

Lagrangian terms for decays of the type $2^{++}, 1^{++}, 0^{++} \to VP$ are similar to those of Equation (3.3) and after expansion and substitution reduce to

$$\begin{aligned}\mathcal{L}_{\text{int}} &= -\frac{G_{\mathsf{P}}\sum_i m_i}{2m_1m_2m_3}q^{\mu_1}\epsilon^{\mu\nu\rho\sigma}p_{1\rho}p_{2\sigma}\left\langle\phi_{\mu\mu_1}(p_1)\left[\phi_\nu(p_2),\phi_5(p_3)\right]\right\rangle\\ &= -\frac{G_{\mathsf{P}}\sum_i m_i}{2m_1m_2m_3}q^{\mu_1}\epsilon^{\mu\nu\rho\sigma}p_{1\rho}p_{2\sigma}\left\{\phi^{(2)b}_{\{\mu\mu_1\}a}(p_1)-\frac{i}{\sqrt{2}}\frac{p_1^\lambda}{m_1}\epsilon_{\lambda\mu\mu_1\kappa}g^{\kappa\kappa'}\phi^{(1)b}_{\kappa'a}(p_1)\right\}\\ &\qquad\times\left[\phi^c_{vb}(p_2)\phi^a_{5c}(p_3)-\phi^c_{5b}(p_3)\phi^a_{vc}(p_2)\right],\end{aligned}$$

accounting for $2^{++}, 1^{++} \to VP$ decays, while the $0^{++} \to VP$ interaction is absent. The decays $1^{+-} \to VP$ are contained within the term

$$\begin{aligned}\mathcal{L}_{\text{int}} &= \frac{G_{\mathsf{P}}}{8m_1m_2m_3}q^{\mu_1}\text{Tr}[(\not{p}_1+m_1)\gamma_5(\not{p}_2+m_2)\gamma_\nu(\not{p}_2+m_2)\gamma_5\\ &\qquad\times\phi_{5\mu_1}(p_1)\left\{\phi_\nu(p_2)\phi_5(p_3)+\phi_5(p_3)\phi_\nu(p_2)\right\}],\end{aligned}$$

and by standard trace methods reduce to

$$\mathcal{L}_{\text{int}} = -\frac{G_{\mathsf{P}}\sum_i m_i}{2m_1m_3}q^{\mu_1}(p_1-p_3)^\nu\left\langle\phi_{5\mu_1}(p_1)\left\{\phi_\nu(p_2),\phi_5(p_3)\right\}\right\rangle.$$

The definition

$$g_{\mathsf{P}VP} = \frac{G_{\mathsf{P}}\sum_i m_i}{2m_1m_2m_3},$$

allows us to express our decay rate forms in terms of a universal coupling constant.

$2^{++} \to VP$ **decay rate** The sum

$$|\mathcal{L}_{\rm int}|^2 = \frac{g^2_{PVP}}{2.2+1}\sum_\lambda \epsilon^{\mu\nu\alpha\beta}p_{1\alpha}p_{2\beta}q^{\mu_1}\phi^{(\lambda)}_{\{\mu\mu_1\}}(p_1)\phi^{(\lambda)}_{\nu}(p_2) \times\phi^{(\lambda)*}_{\{\mu'\mu'_1\}}(p_1)\phi^{(\lambda)*}_{\nu'}(p_2)\epsilon^{\mu'\nu'\alpha'\beta'}p_{1\alpha'}p_{2\beta'}q^{\mu'_1},$$

is most easily solved using the first principles,

$$\begin{aligned}\sum_\lambda \phi^{(\lambda)}_{\{\mu\mu_1\}}(p_1)\phi^{(\lambda)*}_{\{\mu'\mu'_1\}}(p_1) &= \tfrac{1}{2}\left[d_{\mu\mu'}(p_1)d_{\mu_1\mu'_1}(p_1)+d_{\mu\mu'_1}(p_1)d_{\mu'\mu_1}(p_1)\right.\\ &\quad \left.-\tfrac{2}{3}d_{\mu\mu_1}(p_1)d_{\mu'\mu'_1}(p_1)\right]\\ \sum_\lambda \phi^{(\lambda)}_{\nu}(p_2)\phi^{(\lambda)*}_{\nu'}(p_2) &= d_{\nu\nu'}(p_2),\end{aligned}$$

so that

$$\Gamma_{2^{++}\to VP} = \frac{g^2_{PVP}}{320\pi}\frac{\lambda^{5/2}(m_1^2,m_2^2,m_3^2)}{m_1^5}. \tag{4.11}$$

$1^{++} \to VP$ **decay rate** The sum

$$|\mathcal{L}_{\rm int}|^2 = \frac{g^2_{PVP}}{2.1+1}\sum_\lambda \epsilon^{\mu\nu\alpha\beta}p_{1\alpha}p_{2\beta}q^{\mu_1}\frac{-i}{\sqrt{2}}\frac{p_1^\lambda}{m_1}\epsilon_{\lambda\mu\mu_1\kappa}g^{\kappa\kappa'}\phi^{(1)}_{\kappa'}(p_1)\phi^{(\lambda)}_{\nu}(p_2) \times\phi^{(\lambda)*}_{\kappa''}(p_1)\phi^{(\lambda)*}_{\nu'}(p_2)\frac{i}{\sqrt{2}}\frac{p_1^{\lambda'}}{m_1}\epsilon_{\lambda'\mu'\mu'_1\kappa'}g^{\kappa'\kappa''}\epsilon^{\mu'\nu'\alpha'\beta'}p_{1\alpha'}p_{2\beta'}q^{\mu'_1},$$

is best solved using the properties of the antisymmetric tensor (using in particular (A.3)), to obtain

$$\Gamma_{1^{++}\to VP} = \frac{g^2_{PVP}}{192\pi}\frac{\lambda^{5/2}(m_1^2,m_2^2,m_3^2)}{m_1^5}. \tag{4.12}$$

$1^{+-} \to VP$ **decay rate** The polarization sum

$$|\mathcal{L}_{\rm int}|^2 = \frac{g^2_{PVP}m_3^2}{2.1+1}\sum_\lambda q^{\mu_1}(p_1-p_3)^\nu\phi^{(\lambda)}_{5\mu_1}(p_1)\phi^{(\lambda)}_{\nu}(p_2)\phi^{(\lambda)*}_{5\mu'_1}(p_1)\phi^{(\lambda)*}_{\nu'}(p_1-p_3)^{\nu'}q^{\mu'_1},$$

is relatively simple and upon expansion and reduction enables us to derive

$$\Gamma_{1^{+-}\to VP} = \frac{g^2_{PVP}}{192\pi}\frac{\lambda^{5/2}(m_1^2,m_2^2,m_3^2)}{m_1^5}. \tag{4.13}$$

$\mathsf{P} \to VV$ interactions

The final case of $L = 1$ meson vertices we wish to investigate is that accounting for decays into two vectors. The expansion of the interaction term trace for the ${}^3P$ mesons follows that of (3.4), reducing to

$$\begin{aligned}\mathcal{L}_{\rm int} &= \frac{G_{\mathsf{P}}\sum_i m_i}{4\prod_i m_i} q^{\mu_1}\Big\{(p_2-p_3)^{\mu}g^{\nu\rho}m_1+(p_3-p_1)^{\nu}g^{\rho\mu}m_2 \\ &\quad +(p_3-p_1)^{\rho}g^{\mu\nu}m_3+\frac{2}{\sum_i m_i}(p_2-p_3)^{\mu}(p_3-p_1)^{\nu}(p_3-p_1)^{\rho}\Big\} \\ &\quad \times\langle\phi_{\mu\mu_1}(p_1)\{\phi_{\nu}(p_2),\phi_{\rho}(p_3)\}\rangle\,,\end{aligned}$$

and all ${}^3P$ parent states can decay into two vector daughters. Although we have shown that interactions of this sort are permissible in the $\tilde{U}(4N_f)\otimes O(3,1)_L$ scheme, experimental observation of such processes has not occurred. This is mainly due to the lack of kinematical phase space available for these decay types to proceed, thus suppressing the widths. Therefore we shall not continue to derive the possible decay rate relations.

4.2.2 $L = 2$ meson interactions

The D-wave or $L = 2$ mesons ($J^{PC} = 3^{--}, 2^{--}, 1^{--}, 2^{-+}$) undergo transitions to the ground state mesons, but in addition some members also decay to combinations of $L = 1$ excited states and ground state mesons. This provides another hunting ground for universal couplings; however, the predominant data is in decays to the ground state. Hence we are primarily interested in the interaction Lagrangian,

$$\mathcal{L}_{\rm int} = G_{\mathsf{D}} q^{\mu_1} q^{\mu_2}\phi^B_{\mu_1\mu_2 A}(p_1)\left\{\phi^C_B(p_2)\phi^A_C(p_3)+\phi^C_B(p_3)\phi^A_C(p_2)\right\},$$

and this combined with the $L = 2$ meson superfield,

$$\phi^B_{A\mu_1\mu_2}(p_1) = \frac{1}{2m_1}(\not{p}_1+m_1)(\gamma^{\mu}\phi_{\mu\mu_1\mu_2}(p)-\gamma_5\phi_{5\mu_1\mu_2}(p)), \qquad (4.14)$$

accounts for all the Zweig allowed two body strong decays of the D-wave states into ground state mesons. The vector components of (4.14) decompose

to $J = 3, 2$ and 1 states as:

$$\begin{aligned}\phi_{\mu\mu_1\mu_2}(p_1) &= \phi^{(3)}_{\{\mu\mu_1\mu_2\}}(p_1) \\ &-\tfrac{i}{2\sqrt{2}}\tfrac{p_1^\lambda}{m_1} g^{\kappa\kappa'}\left(\epsilon_{\lambda\mu\mu_1\kappa}\phi^{(2)}_{\{\mu_2\kappa'\}}(p_1) + \epsilon_{\lambda\mu\mu_2\kappa}\phi^{(2)}_{\{\mu_1\kappa'\}}(p_1)\right) \\ &+\tfrac{\sqrt{3}}{2\sqrt{5}}\left(d_{\mu\mu_1}(p_1)\phi^{(1)}_{\mu_2}(p_1) + d_{\mu\mu_2}(p_1)\phi^{(1)}_{\mu_1}(p_1) - \tfrac{2}{3}d_{\mu_1\mu_2}(p_1)\phi^{(1)}_{\mu}(p_1)\right).\end{aligned} \tag{4.15}$$

D $\to PP$ interactions

In the same manner that the expansion of the $L = 1$ parent to two pseudoscalar trace led to the exclusion of $1^{++}, 1^{+-} \to PP$ interactions, so too are the $2^{--}, 2^{-+} \to PP$ decays suppressed. The non-zero terms in the expansion are

$$\begin{aligned}\mathcal{L}_{\rm int} &= -\frac{G_{\rm D}\sum_i m_i}{4m_2m_3} q^\mu q^{\mu_1} q^{\mu_2}\left\{\phi^{(3)b}_{\{\mu\mu_1\mu_2\}a}(p_1) + \tfrac{\sqrt{3}}{2\sqrt{5}}\left(d_{\mu\mu_1}(p_1)\phi^{(1)b}_{\mu_2 a}(p_1) + \right.\right. \\ &\qquad \left.\left. + d_{\mu\mu_2}(p_1)\phi^{(1)b}_{\mu_1 a}(p_1) - \tfrac{2}{3}d_{\mu_1\mu_2}(p_1)\phi^{(1)b}_{\mu a}(p_1)\right)\right\} \\ &\qquad \times\left[\phi^c_{5b}(p_2)\phi^a_{5c}(p_3) - \phi^c_{5b}(p_3)\phi^a_{5c}(p_2)\right],\end{aligned}$$

clearly attributing for $3^{--}, 1^{--} \to PP$ decays. We define

$$g_{\mathrm{D}PP} = \frac{G_{\rm D}\sum_i m_i}{4m_2m_3},$$

and proceed to derive the $3^{--}, 1^{--} \to PP$ decay amplitudes.

$3^{--} \to PP$ decay rate By use of (4.5), the polarisation sum

$$|\mathcal{L}_{\rm int}|^2 = \frac{g^2_{\mathrm{D}PP}}{2.3+1}\sum_\lambda \left|q^\mu q^{\mu_1} q^{\mu_2}\phi^{(\lambda)}_{\{\mu\mu_1\mu_2\}}(p_1)\right|^2,$$

is readily reduced to obtain the decay rate

$$\Gamma_{3^{--}\to PP} = \frac{g^2_{\mathrm{D}PP}}{280\pi}\frac{\lambda^{7/2}(m_1^2, m_2^2, m_3^2)}{m_1^9}. \tag{4.16}$$

$1^{--} \to PP$ decay rate The sum

$$\begin{aligned}|\mathcal{L}_{\rm int}|^2 &= \frac{g^2_{\mathrm{D}PP}}{2.1+1}\sum_\lambda \left|q^\mu q^{\mu_1} q^{\mu_2}\tfrac{\sqrt{3}}{2\sqrt{5}}\right. \\ &\qquad \left.\times\left(d_{\mu\mu_1}(p_1)\phi^{(1)b}_{\mu_2 a}(p_1) + d_{\mu\mu_2}(p_1)\phi^{(1)b}_{\mu_1 a}(p_1) - \tfrac{2}{3}d_{\mu_1\mu_2}(p_1)\phi^{(1)b}_{\mu a}(p_1)\right)\right|^2,\end{aligned}$$

is relatively simple despite the quantity of terms, and ultimately leads to the decay rate

$$\Gamma_{1^{--}\to PP} = \frac{g_{\mathsf{D}PP}^2}{180\pi}\frac{\lambda^{7/2}(m_1^2,m_2^2,m_3^2)}{m_1^9}. \tag{4.17}$$

$\mathsf{D}\to VP$ interactions

The $S=1$ D-wave states may decay into a vector plus pseudoscalar state, the corresponding interaction Lagrangian reducing to

$$\begin{aligned}\mathcal{L}_{\text{int}} &= \frac{G_{\mathsf{D}}\sum_i m_i}{2\prod_i m_i}q^{\mu_1}q^{\mu_2}\epsilon^{\mu\nu\alpha\beta}p_{1\alpha}p_{2\beta}\left\{\phi^{(3)b}_{\{\mu\mu_1\mu_2\}a}(p_1)\right.\\
&\quad -\frac{i}{2\sqrt{2}}\frac{p_1^\lambda}{m_1}g^{\kappa\kappa'}\left(\epsilon_{\lambda\mu\mu_1\kappa}\phi^{(2)b}_{\{\mu_2\kappa'\}a}(p_1)+\epsilon_{\lambda\mu\mu_2\kappa}\phi^{(2)b}_{\{\mu_1\kappa'\}a}(p_1)\right)\\
&\quad \left.-\frac{1}{\sqrt{15}}\left(-g_{\mu_1\mu_2}+p_{1\mu_1}p_{1\mu_2}/m_1^2\right)\phi^{(1)b}_{\mu a}(p_1)\right\}\\
&\quad \times\left\{\phi^c_{\nu b}(p_2)\phi^a_{5c}(p_3)+\phi^c_{5b}(p_3)\phi^a_{\nu c}(p_2)\right\},\end{aligned}$$

accounting for $3^{--},2^{--},1^{--}\to VP$ decays. The $S=0$ D-wave state, $J^{PC}=2^{-+}$ can also undergo transitions to a $V+P$ final state and the term

$$\mathcal{L}_{\text{int}} = \frac{G_{\mathsf{D}}\sum_i m_i}{2m_1m_2m_3}q^{\mu_1}q^{\mu_2}(p_1-p_3)^\nu\phi^b_{5\mu_1\mu_2a}(p_1)\left[\phi^c_{\nu b}(p_2)\phi^a_{5c}(p_3)-\phi^c_{5b}(p_3)\phi^a_{\nu c}(p_2)\right],$$

describes such a vertex. After defining the coupling $g_{\mathsf{D}VP}=\frac{G_{\mathsf{D}}\sum_i m_i}{2m_1m_2m_3}$, we proceed onto the decay amplitudes.

$3^{--}\to VP$ decay rate In this case the polarisation sum

$$|\mathcal{L}_{\text{int}}|^2 = \frac{g_{\mathsf{D}VP}^2}{2.3+1}\sum_\lambda\left|q^{\mu_1}q^{\mu_2}\epsilon^{\mu\nu\alpha\beta}p_{1\alpha}p_{2\beta}\phi^{(\lambda)}_{\{\mu\mu_1\mu_2\}}(p_1)\phi^{(\lambda)}_\nu(p_2)\right|^2,$$

is best solved using (4.6), and leads to the decay rate

$$\Gamma_{3^{--}\to VP} = \frac{g_{\mathsf{D}VP}^2}{840\pi}\frac{\lambda^{7/2}(m_1^2,m_2^2,m_3^2)}{m_1^7}. \tag{4.18}$$

$2^{--} \to VP$ **decay rate** The numerous terms of the sum

$$|\mathcal{L}_{\rm int}|^2 = \frac{g_{\rm DVP}^2}{2.2+1}\sum_\lambda \left| q^{\mu_1} q^{\mu_2} \epsilon^{\mu\nu\alpha\beta} p_{1\alpha} p_{2\beta} \frac{-i}{2\sqrt{2}} \frac{p_1^\lambda}{m_1} \right.$$
$$\left. \times\, g^{\kappa\kappa'} \left(\epsilon_{\lambda\mu\mu_1\kappa} \phi^{(2)}_{\{\mu_2\kappa'\}}(p_1) + \epsilon_{\lambda\mu\mu_2\kappa} \phi^{()}_{\{\mu_1\kappa'\}}(p_1) \right) \phi_\nu^{(\lambda)}(p_2) \right|^2,$$

involve extensive use of (4.6) along with the properties of the antisymmetric tensor, to yield

$$\Gamma_{2^{--}\to VP} = \frac{g_{\rm DVP}^2}{640\pi} \frac{\lambda^{7/2}(m_1^2, m_2^2, m_3^2)}{m_1^7}. \tag{4.19}$$

$1^{--} \to VP$ **decay rate** The sum

$$|\mathcal{L}_{\rm int}|^2 = \frac{g_{\rm DVP}^2}{2.1+1} \frac{1}{15} \sum_\lambda \left| q^{\mu_1} q^{\mu_2} \epsilon^{\mu\nu\alpha\beta} p_{1\alpha} p_{2\beta} d_{\mu_1\mu_2}(p_1) \phi_\mu(p_1) \phi_v(p_2) \right|^2,$$

is relatively simple, and leads to the rate

$$\Gamma_{1^{--}\to VP} = \frac{g_{\rm DVP}^2}{1440\pi} \frac{\lambda^{7/2}(m_1^2, m_2^2, m_3^2)}{m_1^7}. \tag{4.20}$$

$2^{-+} \to VP$ decay rate

From the basic sum

$$|\mathcal{L}_{\rm int}|^2 = \frac{g_{\rm DVP}^2 m_3^2/4}{2.2+1} \sum_\lambda \left| q^{\mu_1} q^{\mu_2} (p_1 - p_3)^\nu \phi^{(\lambda)}_{5\mu_1\mu_2}(p_1) \phi_\nu^{(\lambda)}(p_2) \right|^2,$$

the decay rate turns out to be

$$\Gamma_{2^{-+}\to VP} = \frac{g_{\rm DVP}^2}{480\pi} \frac{\lambda^{7/2}(m_1^2, m_2^2, m_3^2)}{m_1^7}. \tag{4.21}$$

4.2.3 $L = 3$ meson interactions

As the kinematical phase space increases with increasing parent meson mass the possible daughter mesons can attain higher masses and in conjunction different excitation states, unfortunately experimental investigation of these high excitation mesons is limited, and we are mostly bereft of useful decay width measurements, except in the $J^{PC} = 4^{++}$ case. For this reason alone we

shall restrict the daughter mesons to the ground state, $L = 0$, but future experimental results could fuel useful application of the supermultiplet method to these interesting channels. The interaction Lagrangian for the vertex we are primarily interested in is thus

$$\mathcal{L}_{\text{int}} = G_{\mathsf{F}} q^{\mu_1} q^{\mu_2} q^{\mu_3} \phi^B_{A\mu_1\mu_2\mu_3}(p_1) \left[\phi^C_B(p_2)\phi^A_C(p_3) - \phi^C_B(p_3)\phi^A_C(p_2)\right], \quad (4.22)$$

where the $L = 3$ supermultiplet wavefunction has the form

$$\phi^B_{A\mu_1\mu_2\mu_3}(p_1) = \frac{1}{2m_1}(\not{p}_1 + m_1)\left(\gamma^\mu \phi_{\mu\mu_1\mu_2\mu_3}(p_1) - \gamma_5 \phi_{5\mu_1\mu_2\mu_3}(p_1)\right),$$

of which the $S = 1$ components decompose into their $J = 4, 3$ and 2 components as

$$\begin{aligned}
\phi_{\mu\mu_1\mu_2\mu_3} \;=\; & \phi^{(4)}_{\mu\mu_1\mu_2\mu_3} \\
& -\tfrac{i}{3\sqrt{2}} \frac{p^\lambda}{m} g^{\kappa\kappa'} \left(\epsilon_{\lambda\mu\mu_1\kappa}\phi^{(3)}_{\{\mu_2\mu_3\kappa'\}} + \epsilon_{\lambda\mu\mu_2\kappa}\phi^{(3)}_{\{\mu_1\mu_3\kappa'\}} + \epsilon_{\lambda\mu\mu_3\kappa}\phi^{(3)}_{\{\mu_1\mu_2\kappa'\}}\right) \\
& +\tfrac{1}{3}\sqrt{\tfrac{5}{7}}\left\{d_{\mu\mu_1}\phi^{(2)}_{\{\mu_2\mu_3\}} + d_{\mu\mu_1}\phi^{(2)}_{\{\mu_2\mu_3\}} + d_{\mu\mu_1}\phi^{(2)}_{\{\mu_2\mu_3\}}\right. \\
& \left. -\tfrac{2}{5}\left[d_{\mu_1\mu_2}\phi^{(2)}_{\{\mu\mu_3\}} + d_{\mu_1\mu_3}\phi^{(2)}_{\{\mu\mu_2\}} + d_{\mu_2\mu_3}\phi^{(2)}_{\{\mu\mu_1\}}\right]\right\}.
\end{aligned}$$

Since there only exists some experimental data for the $J^{PC} = 4^{++}$ mesons we further restrict the derivation of interaction vertices to these cases, but as one can see the supermultiplet scheme produces wavefunctions and interaction vertices for all the $L = 3$ mesons, so one can in principle obtain any required Zweig allowed interaction from the above.

$4^{++} \to PP$ interaction and decay rate

Expanding and calculating the implied trace in (4.22) one obtains

$$\mathcal{L}_{\text{int}} = \frac{G_{\mathsf{F}} \sum_i m_i}{4m_2m_3} q^\mu q^{\mu_1} q^{\mu_2} q^{\mu_3} \left\langle \phi^{(4)}_{\mu\mu_1\mu_2\mu_3}(p_1) \left\{\phi_5(p_2), \phi_5(p_3)\right\}\right\rangle,$$

and with the identification $g_{\mathsf{F}PP} = \frac{G_{\mathsf{F}} \sum_i m_i}{4m_2m_3}$ along with the polarization sum calculation,

$$\begin{aligned}
|\mathcal{L}_{\text{int}}|^2 \;&=\; \frac{g^2_{\mathsf{F}PP}}{2.4+1} \sum_\lambda \left| q^\mu q^{\mu_1} q^{\mu_2} q^{\mu_3} \phi^{(\lambda)}_{\mu\mu_1\mu_2\mu_3}(p_1)\right|^2 \\
&=\; \frac{8 g^2_{\mathsf{F}PP}}{315} \frac{\lambda^4(m_1^2, m_2^2, m_3^2)}{m_1^8},
\end{aligned}$$

the decay rate is found to be

$$\Gamma_{4^{++}\to PP} = \frac{g^2_{\mathsf{F}PP}}{630\pi}\frac{\lambda^{9/2}(m_1^2,m_2^2,m_3^2)}{m_1^{11}}. \tag{4.23}$$

$4^{++} \to VP$ interaction and decay rate

In this channel, the interaction vertex reduces to the form

$$\mathcal{L}_{\text{int}} = -\frac{G_{\mathsf{F}}\sum_i m_i}{2m_1m_2m_3}q^{\mu_1}q^{\mu_2}q^{\mu_3}\epsilon^{\mu\nu\alpha\beta}p_{1\alpha}p_{2\beta}\left\langle\phi^{(4)}_{\mu\mu_1\mu_2\mu_3}(p_1)\left[\phi_\nu(p_2),\phi_5(p_3)\right]\right\rangle,$$

and by using the rule (4.6) along with the definition $g_{\mathsf{F}VP} = \frac{G_{\mathsf{F}}\sum_i m_i}{2m_1m_2m_3}$, the polarisation sum calculation is completed:

$$\begin{aligned}|\mathcal{L}_{\text{int}}|^2 &= \frac{g^2_{\mathsf{F}VP}}{2.4+1}\sum_\lambda q^{\mu_1}q^{\mu_2}q^{\mu_3}\epsilon^{\mu\nu\alpha\beta}p_{1\alpha}p_{2\beta}\phi^{(\lambda)}_{\mu\mu_1\mu_2\mu_3}(p_1)\phi^{(\lambda)}_{\nu}(p_2)\\ &\quad\times\phi^{(\lambda)*}_{\mu'\mu'_1\mu'_2\mu'_3}(p_1)\phi^{(\lambda)*}_{\nu'}(p_2)q^{\mu'_1}q^{\mu'_2}q^{\mu'_3}\epsilon^{\mu'\nu'\alpha'\beta'}p_{1\alpha'}p_{2\beta'}\\ &= \frac{8g^2_{\mathsf{F}VP}}{126}\frac{\lambda^4(m_1^2,m_2^2,m_3^2)}{m_1^6},\end{aligned}$$

from which the decay rate formula is obtained

$$\Gamma_{4^{++}\to VP} = \frac{g^2_{\mathsf{F}VP}}{2016\pi}\frac{\lambda^{9/2}(m_1^2,m_2^2,m_3^2)}{m_1^9}. \tag{4.24}$$

$4^{++} \to VV$ interaction and decay rate

From the expansion of the vertex

$$\begin{aligned}\mathcal{L}_{\text{int}} &= \frac{G_{\mathsf{F}}\sum_i m_i}{2m_1m_2m_3}q^{\mu_1}q^{\mu_2}q^{\mu_3}\left\{(p_2-p_3)^\mu g^{\nu\rho}m_1+(p_3-p_1)^\nu g^{\rho\mu}m_2\right.\\ &\quad\left.+(p_3-p_1)^\rho g^{\mu\nu}m_3+\frac{2}{\sum_i m_i}(p_2-p_3)^\mu(p_3-p_1)^\nu(p_3-p_1)^\rho\right\}\\ &\quad\times\left\langle\phi^{(4)}_{\mu\mu_1\mu_2\mu_3}(p_1)\left\{\phi_\nu(p_2),\phi_\rho(p_3)\right\}\right\rangle,\end{aligned}$$

the polarisation sum calculation is quite complex and employs relation (4.6) to produce the decay rate

$$\Gamma_{4^{++}\to VV} = \frac{g^2_{\mathsf{F}VV}}{2520}\frac{\lambda^{9/2}(m_1^2,m_2^2,m_3^2)}{m_1^{11}m_2^2m_3^2}\left(\mathcal{Y}(m_1,m_2,m_3)-6m_1^2m_2^2m_3^2\right), \tag{4.25}$$

where $g_{\mathsf{F}VV} = \frac{G_{\mathsf{F}}\sum_i m_i}{2m_1m_2m_3}$.

4.2.4 Summary of decay rate formulae

We quickly list the multitude of decay rate formula we have generated. We shall shortly use these in conjunction with experimental data to obtain estimates of the coupling constants involved.

$$
\begin{array}{l}
L=1 \\ \text{mesons}
\end{array}
\left\{
\begin{array}{l}
\mathsf{P} \to PP: \left\{
\begin{array}{l}
\Gamma_{2^{++}\to PP} = \frac{g^2_{\mathsf{P}PP}}{120\pi} \frac{\lambda^{5/2}(m_1^2,m_2^2,m_3^2)}{m_1^7} \\
\Gamma_{0^{++}\to PP} = \frac{g^2_{\mathsf{P}PP}}{48\pi} \frac{\lambda^{5/2}(m_1^2,m_2^2,m_3^2)}{m_1^7}
\end{array}
\right. \\
\mathsf{P} \to VP: \left\{
\begin{array}{l}
\Gamma_{2^{++}\to VP} = \frac{g^2_{\mathsf{P}VP}}{320\pi} \frac{\lambda^{5/2}(m_1^2,m_2^2,m_3^2)}{m_1^5} \\
\Gamma_{1^{++}\to VP} = \frac{g^2_{\mathsf{P}VP}}{192\pi} \frac{\lambda^{5/2}(m_1^2,m_2^2,m_3^2)}{m_1^5} \\
\Gamma_{1^{+-}\to VP} = \frac{g^2_{\mathsf{P}VP}}{192\pi} \frac{\lambda^{5/2}(m_1^2,m_2^2,m_3^2)}{m_1^5}
\end{array}
\right.
\end{array}
\right.
$$

$$
\begin{array}{l}
L=2 \\ \text{mesons}
\end{array}
\left\{
\begin{array}{l}
\mathsf{D} \to PP: \left\{
\begin{array}{l}
\Gamma_{3^{--}\to PP} = \frac{g^2_{\mathsf{D}PP}}{280\pi} \frac{\lambda^{7/2}(m_1^2,m_2^2,m_3^2)}{m_1^9} \\
\Gamma_{1^{--}\to PP} = \frac{g^2_{\mathsf{D}PP}}{180\pi} \frac{\lambda^{7/2}(m_1^2,m_2^2,m_3^2)}{m_1^9}
\end{array}
\right. \\
\mathsf{D} \to VP: \left\{
\begin{array}{l}
\Gamma_{3^{--}\to VP} = \frac{g^2_{\mathsf{D}VP}}{840\pi} \frac{\lambda^{7/2}(m_1^2,m_2^2,m_3^2)}{m_1^7} \\
\Gamma_{2^{--}\to VP} = \frac{g^2_{\mathsf{D}VP}}{640\pi} \frac{\lambda^{7/2}(m_1^2,m_2^2,m_3^2)}{m_1^7} \\
\Gamma_{1^{--}\to VP} = \frac{g^2_{\mathsf{D}VP}}{1440\pi} \frac{\lambda^{7/2}(m_1^2,m_2^2,m_3^2)}{m_1^7} \\
\Gamma_{2^{-+}\to VP} = \frac{g^2_{\mathsf{D}VP}}{480\pi} \frac{\lambda^{7/2}(m_1^2,m_2^2,m_3^2)}{m_1^7}
\end{array}
\right.
\end{array}
\right. \qquad (4.26)
$$

$$
\begin{array}{l}
L=3 \\ \text{mesons}
\end{array}
\left\{
\begin{array}{l}
4^{++} \to PP: \left\{ \Gamma_{4^{++}\to PP} = \frac{g^2_{\mathsf{F}PP}}{630\pi} \frac{\lambda^{9/2}(m_1^2,m_2^2,m_3^2)}{m_1^{11}} \right. \\
4^{++} \to VP: \left\{ \Gamma_{4^{++}\to VP} = \frac{g^2_{\mathsf{F}VP}}{2016\pi} \frac{\lambda^{9/2}(m_1^2,m_2^2,m_3^2)}{m_1^9} \right. \\
4^{++} \to VV: \left\{
\begin{array}{l}
\Gamma_{4^{++}\to VV} = \frac{g^2_{\mathsf{F}VV}}{2520} \frac{\lambda^{9/2}(m_1^2,m_2^2,m_3^2)}{m_1^{11}m_2^2m_3^2} \\
\qquad \times \left(\mathcal{Y}(m_1,m_2,m_3) - 6m_1^2m_2^2m_3^2\right)
\end{array}
\right.
\end{array}
\right.
$$

The supermultiplet scheme predicts

$$2g_{LPP} = mg_{LVP} = 2mg_{LVV},$$

where $L = \mathsf{P}, \mathsf{D}, \mathsf{F}$ for the P, D and F-wave mesons, respectively. m is the central meson mass.

4.3 Application of $\tilde{U}(4N_f) \otimes O(3,1)_L$ to excited meson decays

As in the previous Chapter, derivation of Clebsch–Gordan type factors is crucial to the normalisation of our coupling constants. As demonstrated in Section 3.2.3, these factors are easily generated in the $\tilde{U}(4N_f)$ scheme using the trace over flavours in the Lagrangian, and precisely the same technique is used for the excited mesons. We begin with the identification of multiplet members with our $\tilde{U}(4N_f)$ fields.

4.3.1 Excited meson multiplet identifications

In the excited mesons, there are many as of yet, unidentified or missing multiplet members. Some experimentalists report observation of these mesons and the data appears in the full listings of Particle Data tables. However, the Particle Data Group stipulate that for many of these cases, the assignments of J^{PC} values are not confirmed so there is always some uncertainty as to which multiplets these mesons belong. Additionally, very few of the heavy excited mesons have been observed so we will mainly restrict ourselves to $N_f = 3$ and hence with the identification of nonet members to the super-wavefunctions' flavour indices. Section 4.5.2 details some predictions about excited heavy meson interactions, where we consider up to $N_f = 5$. In making our nonet identifications, we mention all of the mesons which complete the structure, using the naming scheme as used in the 1996 edition of the Particle Data Review [13].

The medium strong interaction continues to operate at the excited meson level, and leads to the mixing between the central states, namely the $I = Y = 0$ members of the nonets. We use the standard definitions of the mixing angles and derive their present mass determined values once we have identified our multiplets. We use the unambiguous naming convention $\theta_{L_{JC}}$ for the mixing angle of the meson multiplet with angular momentum L, total spin J and

sign C under charge conjugation. Note that the C label is only used to distinguish between the $S = 0$ and $S = 1$ meson multiplets (e.g. between the 1^{+-} and 1^{++} multiplets in the $L = 1$ mesons); if there is no ambiguity the label is not included.

$L = 1$ multiplets

The $L = 1$ mesons have been extensively studied; their masses and decay rate widths are usually well-known and there are few missing multiplet members. A noticeable inclusion in the 1996 tables was the σ-meson (or $f_0(400-1200)$). This leads to significant problems of interpretation in the 0^{++} nonet, as we shall see. We begin with the 1^{+-} mesons, and work our way to the 2^{++} states via the 0^{++} and 1^{++} mesons.

Several of the axial-vector mesons, $J^{PC} = 1^{+-}$, have been experimentally observed and some of their properties measured. Unfortunately there are some suspect spin assignments in the multiplet, particularly the $h_1(1380)$ meson. There is the additional complication of more complicated mixing phenomena in this multiplet, whereby the strange members of the $^3P_1$ nonet mix with the strange members of the $^1P_1$ nonet through $SU(3)$ breaking of $I = Y = 0$. We shall discuss this further when the mixing angles are determined. The nonet of 1^{+-} mesons is thus taken as

$$\phi^b_{5\mu 1a} \overset{1^{+-}}{=} \begin{pmatrix} \frac{b_1^0(1235)}{\sqrt{2}} + \frac{h_8}{\sqrt{6}} + \frac{h_1}{\sqrt{3}} & b_1^+(1235) & K_{1B}^+ \\ b_1^-(1235) & -\frac{b_1^0(1235)}{\sqrt{2}} + \frac{h_8}{\sqrt{6}} + \frac{h_1}{\sqrt{3}} & K_{1B}^0 \\ K_{1B}^- & \bar{K}_{1B}^0 & -\frac{2h_8}{\sqrt{6}} + \frac{h_1}{\sqrt{3}} \end{pmatrix},$$

where

$$\begin{aligned} |h_8\rangle &= \cos\theta_{P_{1-}} |h_1(1380)\rangle + \sin\theta_{P_{1-}} |h_1(1170)\rangle \\ |h_1\rangle &= -\sin\theta_{P_{1-}} |h_1(1380)\rangle + \cos\theta_{P_{1-}} |h_1(1170)\rangle , \end{aligned}$$

and

$$|K_{1B}\rangle = \cos\theta_K |K_1(1270)\rangle - \sin\theta_K |K_1(1400)\rangle .$$

Particle assignments in the scalar meson nonet $J^{PC} = 0^{++}$ are very difficult. There is an abundance of non-$q\bar{q}$ meson candidates and the re-introduction of the σ meson to the tables confuses the issue even further. In the 1994 tables the following assignments were speculated

$$\phi_a^{(0)b\ 0^{++}} \stackrel{=}{=} \begin{pmatrix} \frac{a_0^0(980)}{\sqrt{2}} + \frac{f_{08}}{\sqrt{6}} + \frac{f_{01}}{\sqrt{3}} & a_0^+(980) & K_0^{*+}(1430) \\ a_0^-(980) & -\frac{a_0^0(980)}{\sqrt{2}} + \frac{f_{08}}{\sqrt{6}} + \frac{f_{01}}{\sqrt{3}} & K_0^{*0}(1430) \\ K_0^{*-}(1430) & \bar{K}_0^{*0}(1430) & -\frac{2f_{08}}{\sqrt{6}} + \frac{f_{01}}{\sqrt{3}} \end{pmatrix}, \quad (4.27)$$

where

$$\begin{aligned} |f_{08}\rangle &= \cos\theta_{P_0}\,|f_0(1370)\rangle + \sin\theta_{P_0}\,|f_0(980)\rangle \\ |f_{01}\rangle &= -\sin\theta_{P_0}\,|f_0(1370)\rangle + \cos\theta_{P_0}\,|f_0(980)\rangle\,. \end{aligned}$$

The 1996 review contests this picture following improved support for the σ-meson (listed in the Data Tables as $f_0(400-1200)$). The $K^*(1430)$ retains its assignment as the $I = 1/2$ member of the nonet, but the identification of the $I = 0$ and $I = 1$ members of the nonet is very controversial. There are two main models [13]:

1. The $f_0(980)$ and $a_0(980)$ are $K\bar{K}$ bound states [116], the $f_0(1370)$ is the $\phi_1^1 + \phi_2^2$ state, the $a_0(1450)$ is the ϕ_1^2 state and the mainly ϕ_3^3 has still not been observed (possibly the $f_J(1710)$). The $f_0(400-1200)$ is then left as a background structure.

2. The physically observed light scalars are different manifestations of the quark model $q\bar{q}$ states. An application of this model [115] fits the $f_0(400-1200)$, $f_0(980)$, $f_0(1370)$, $a_0(980)$, $a_0(1450)$, and $K^*(1430)$ as unitarized remnants of $q\bar{q}\ ^3P_0$ states. The $f_0(400-1200)$ is simultaneously the $u\bar{u} + d\bar{d}$ state, the chiral partner of the π , and the Higgs boson of QCD; $f_0(980)$ and $f_0(1300)$ are two different manifestations of the unitarized $s\bar{s}$ state; $a_0(980)$ and $a_0(1450)$ are two manifestations of $u\bar{d}$.

Given the confusing experimental status of this nonet, we choose to limit our analysis to the 1994 interpretation of the states, despite how unsatisfactory this may be. In the future, if a clear understanding of the scalars emerges, the supermultiplet scheme could be readily applied to the decay modes. We wish to state that this omission in the analysis is not significant. Even if we had managed to incorporate one of the potential interpretations of the scalars given above, the experimental data on branching fractions and decay widths (and in some instances masses) is so scant to render analysis almost impossible.

The axial vector nonet $J^{PC} = 1^{++}$ is reasonably well accounted for and has as its multiplet structure

$$\phi^{(1)b}_{\mu_1 a} \overset{1^{++}}{=} \begin{pmatrix} \frac{a_1^0(1260)}{\sqrt{2}} + \frac{f_{18}}{\sqrt{6}} + \frac{f_{11}}{\sqrt{3}} & a_1^+(1260) & K_{1A}^+ \\ a_1^-(1260) & -\frac{a_1^0(1260)}{\sqrt{2}} + \frac{f_{18}}{\sqrt{6}} + \frac{f_{11}}{\sqrt{3}} & K_{1A}^0 \\ K_{1A}^- & \bar{K}_{1A}^0 & -\frac{2f_{18}}{\sqrt{6}} + \frac{f_{11}}{\sqrt{3}} \end{pmatrix},$$

where

$$\begin{aligned} |f_{18}\rangle &= \cos\theta_{P_{1+}} |f_1(1510)\rangle + \sin\theta_{P_{1+}} |f_1(1285)\rangle \\ |f_{11}\rangle &= -\sin\theta_{P_{1+}} |f_1(1510)\rangle + \cos\theta_{P_{1+}} |f_1(1285)\rangle , \end{aligned}$$

and

$$|K_{1A}\rangle = \sin\theta_K |K_1(1270)\rangle + \cos\theta_K |K_1(1400)\rangle .$$

The tensor nonet, $J^{PC} = 2^{++}$, is probably the most extensively studied of the excited states with well determined multiplet masses, decay widths and branching fractions. The multiplet structure is

$$\phi^{(2)b}_{\mu\mu_1 a} \overset{2^{++}}{=} \begin{pmatrix} \frac{a_2^0(1320)}{\sqrt{2}} + \frac{f_{28}}{\sqrt{6}} + \frac{f_{21}}{\sqrt{3}} & a_2^+(1320) & K_2^{*+}(1430) \\ a_2^-(1320) & -\frac{a_2^0(1320)}{\sqrt{2}} + \frac{f_{28}}{\sqrt{6}} + \frac{f_{21}}{\sqrt{3}} & K_2^{*0}(1430) \\ K_2^{*-}(1430) & \bar{K}_2^{*0}(1430) & -\frac{2f_{28}}{\sqrt{6}} + \frac{f_{21}}{\sqrt{3}} \end{pmatrix},$$

where

$$\begin{aligned} |f_{28}\rangle &= \cos\theta_{P_2} |f_2'(1525)\rangle + \sin\theta_{P_2} |f_2(1270)\rangle \\ |f_{21}\rangle &= -\sin\theta_{P_2} |f_2'(1525)\rangle + \cos\theta_{P_2} |f_2(1270)\rangle . \end{aligned}$$

(We realize θ_{P_2} is commonly called θ_T, but we use our labelling scheme for consistency.)

$L = 2$ multiplets

The $L = 2$ meson multiplets are somewhat sparser than the lower states, in particular the 2^{--} nonet is mostly empty, with only the strange members, $K_2(1820)$ having been observed with any real certainty. The 3^{--} multiplet is full, while the 1^{--} and 2^{-+} are partly complete. Following are the identifications:

$$\phi^{b}_{5\mu_1\mu_2 a} \overset{2^{-+}}{=} \begin{pmatrix} \frac{\pi_2^0(1670)}{\sqrt{2}} & \pi_2^+(1670) & K_2^+(1430) \\ \pi_2^-(1670) & -\frac{\pi_2^0(1670)}{\sqrt{2}} & K_2^0(1820) \\ K_2^-(1820) & \bar{K}_2^0(1820) & \end{pmatrix},$$

$$\phi^{(1)b}_{\mu a} \overset{1^{--}}{=} \begin{pmatrix} \frac{\rho^0(1700)}{\sqrt{2}} + \frac{\omega_{18}}{\sqrt{6}} + \frac{\omega_{11}}{\sqrt{3}} & \rho^+(1700) & K^{*+}(1680) \\ \rho^-(1700) & -\frac{\rho^0(1700)}{\sqrt{2}} + \frac{\omega_{18}}{\sqrt{6}} + \frac{\omega_{11}}{\sqrt{3}} & K^{*0}(1680) \\ K^{*-}(1680) & \bar{K}^{*0}(1680) & \frac{-2\omega_{18}}{\sqrt{6}} + \frac{\omega_{11}}{\sqrt{3}} \end{pmatrix}.$$

The singlet $I = Y = 0$ symmetric and antisymmetric states have not been confidently identified in the 2^{-+} multiplet and only the $\omega(1600)$ particle in the 1^{--} multiplet, where

$$|\omega(1600)\rangle = \sin\theta_{\mathsf{D}_1}\,|\omega_{18}\rangle + \cos\theta_{\mathsf{D}_1}\,|\omega_{11}\rangle\,.$$

The 2^{--} multiplet is mostly empty, with only the strange candidate $K_2(1820)$ being identified,

$$\phi^{(2)b}_{\mu\nu a} \overset{2^{--}}{=} \begin{pmatrix} & & K_2^+(1820) \\ & & K_2^0(1820) \\ K_2^-(1820) & \bar{K}_2^0(1820) & \end{pmatrix}.$$

Finally the 3^{--} nonet has the assignments,

$$\phi^{(3)b}_{\{\mu\mu_1\mu_2\}a} \overset{3^{--}}{=} \begin{pmatrix} \frac{\rho_3^0(1690)}{\sqrt{2}} + \frac{\omega_{38}}{\sqrt{6}} + \frac{\omega_{31}}{\sqrt{3}} & \rho_3^+(1690) & K_3^{*+}(1780) \\ \rho_3^-(1690) & -\frac{\rho_3^0(1690)}{\sqrt{2}} + \frac{\omega_{38}}{\sqrt{6}} + \frac{\omega_{31}}{\sqrt{3}} & K_3^{*0}(1780) \\ K_3^{*-}(1780) & \bar{K}_3^{*0}(1780) & -\frac{2\omega_{38}}{\sqrt{6}} + \frac{\omega_{31}}{\sqrt{3}} \end{pmatrix},$$

where

$$
\begin{aligned}
|\omega_{38}\rangle &= \cos\theta_{\mathsf{D}_3}\,|\phi_3(1850)\rangle + \sin\theta_{\mathsf{D}_3}\,|\omega_3(1670)\rangle \\
|\omega_{31}\rangle &= -\sin\theta_{\mathsf{D}_3}\,|\phi_3(1850)\rangle + \cos\theta_{\mathsf{D}_3}\,|\omega_3(1670)\rangle\,.
\end{aligned}
$$

$L = 3$ multiplets

The few F-wave mesons identified so far belong to the $J^{PC} = 4^{++}$ multiplet, and are labelled as

$$
\phi^{(4)b}_{\{\mu\mu_1\mu_2\mu_3\}a} \overset{4^{++}}{=} \begin{pmatrix} \frac{a_4^0(2040)}{\sqrt{2}} + \frac{f_{48}}{\sqrt{6}} + \frac{f_{48}}{\sqrt{3}} & a_4^+(2040) & K_4^{*+}(2045) \\ a_4^-(2040) & -\frac{a_4^0(2040)}{\sqrt{2}} + \frac{f_{48}}{\sqrt{6}} + \frac{f_{41}}{\sqrt{3}} & K_4^{*0}(2045) \\ K_4^{*-}(2045) & \bar{K}_4^{*0}(2045) & -\frac{2f_{48}}{\sqrt{6}} + \frac{f_{41}}{\sqrt{3}} \end{pmatrix},
$$

with the $SU(3)$ pure octet and singlet states f_{48} and f_{41} related to the physical states via the mixing angle definition,

$$
\begin{aligned}
|f_{48}\rangle &= \cos\theta_{\mathsf{F}_4}\,|f_4(2220)\rangle + \sin\theta_{\mathsf{F}_4}\,|f_4(2050)\rangle \\
|f_{41}\rangle &= -\sin\theta_{\mathsf{F}_4}\,|f_4(2220)\rangle + \cos\theta_{\mathsf{F}_4}\,|f_4(2050)\rangle\,.
\end{aligned}
$$

4.3.2 Excited state mixing angles

The determination of the mixing angles follows the procedure established in Section 2.3.1; we assume the GMO relation is obeyed by multiplet members and use it to calculate the mass of the $I = Y = 0$ octet member, m_8 from the mass of the $I \neq 0$ members, $m_8^2 = \frac{1}{3}(4m_{I=1/2}^2 - m_{I=1}^2)$ and then solve

$$
\tan\theta = \left(\frac{m_8'^2 - m_8^2}{m_8^2 - m_1'^2}\right)^{\frac{1}{2}}
$$

where m_8' and m_1' is the mass of the physical $I = Y = 0$ octet and singlet members respectively. To first determine the mixing angles $\theta_{\mathsf{P}_{1-}}$ and $\theta_{\mathsf{P}_{1+}}$ we need to know the masses K_{1A} and K_{1B}, the ideal $SU(3)$ $^3P_1$ and $^1P_1$ strange states. The same medium strong interaction which leads to mixing of the $I = Y = 0$ members of a multiplet can also mix these ideal states. Thus

with masses $m_{K_{1A}}$ and $m_{K_{1B}}$ the angle θ_K is given by

$$\cos 2\theta_K = \frac{m^2_{K_{1A}} - m^2_{K_{1B}}}{m^2_{K_1(1400)} - m^2_{K_1(1270)}}. \tag{4.28}$$

Unfortunately, we cannot easily derive θ_K as there is an undetermined system of equations; to compute the masses $m_{K_{1A}}$ and $m_{K_{1B}}$ one must know the masses of the pure states m_8 and m_1 which are given by the GMO relation using the masses $m_{K_{1A}}$ and $m_{K_{1B}}$! To overcome this conundrum one must make assumptions about the singlet-octet mixing (e.g. it is ideal [110]) or use a model-dependent calculation to derive the masses $m_{K_{1A}}$ and $m_{K_{1B}}$ (e.g. via the relativized quark model [22]). Another approach is to use an experimental result which is sensitive to θ_K. Such a sensitive, yet reliable measure is given by the ratio

$$\Gamma_{\tau\to K_1(1270)}/\Gamma_{\tau\to K_1(1400)},$$

but the limited data available only restricts the angle to $-30° \leq \theta_K \leq 50°$ at 68% confidence level [14, 22]. We decide to choose a mixing angle of $\theta_K = 45°$ which is consistent with the majority of results [22, 13]. By the center-of-gravity rule,

$$m^2_{K_1(1270)} + m^2_{K_1(1400)} = m^2_{K_{1A}} + m^2_{K_{1B}},$$

and the degeneracy $m_{K_{1A}} = m_{K_{1B}}$ inherent to the choice $\theta_K = 45°$ (from (4.28)), we find

$$m_{K_{1A,B}} = 1339 \pm 5 \text{ MeV}.$$

We can then use this value to derive the singlet-octet mixing angles for the 1^{+-} and 1^{++} nonets.

In Table 4.1 we list the masses of all the excited meson nonet members used to compute the singlet-octet mixing angle (errors are derived from the uncorrelated errors of the meson masses). Controversial meson assignments are signified by italic face. The masses used are those given in the 1996 edition of the Particle Data Tables [13].

J^{PC}	Experimental input masses (MeV)[13]				Mixing angle
	$m_{I=1}$	$m_{I=1/2}$	m'_8	m'_1	$\theta_{\mathrm{L}_{JC}}$
1^{+-}	1231 ± 10	1339 ± 5	*1380 ± 20*	1170 ± 20	$11° \pm 16°$
0^{++}					
1^{++}	1230 ± 40	1339 ± 5	1512 ± 4	1282.2 ± 0.7	$-37.9° \pm 3.5°$
2^{++}	1318.1 ± 0.7	1428 ± 1	1525 ± 5	1275 ± 5	$31.1° \pm 1.1°$
2^{+-}	1670 ± 20	1773 ± 8			
1^{--}	1700 ± 20	1714 ± 20		1649 ± 24	
2^{--}		1816 ± 13			
3^{--}	1691 ± 5	1770 ± 10	1854 ± 7	1667 ± 4	$34.7° \pm 4.7°$
4^{++}	2037 ± 26	2045 ± 9	*2225 ± 6*	2044 ± 11	$-8° \pm 20°$

Table 4.1: Mixing angles of the excited mesons. $n = 0, \pm 1, \pm 2, \ldots$. Masses for controversial meson assignments are shown in italic face.

The absence of several mass values prevent the determination of all the mixing angles. For these cases we will be unable to adequately account for the potential mixing of states in the decay rates. The mixing angle for scalar nonet $J^{PC} = 0^{++}$ has not been determined because their understanding in terms of $q\bar{q}$ bound states is clouded at present. If we use the 1994 assignments (4.27) and corresponding masses the mixing angle is imaginary as $m_8 > m'_8$.

4.3.3 Excited state Clebsch–Gordan factors

With the multiplets identified and the mixing angle relations defined, we can now resume compiling the Clebsch–Gordan type factors crucial to normalising the coupling constants. The method for determining these factors is identical to that for the ground states as the form of the trace over the flavour indices has not changed. Hence given a Zweig allowed two-body decay process and via the matrices in Section (4.3.1) we can determine the flavour indices in the process and substitute these into the interaction Lagrangian. After simplification the coupling constant for the process may effectively be

scaled by an isospin or mixing angle factor. Experimental decay width measurements lead to the determination of this scaled coupling, so to return to the standard coupling we normalise the results by each channel's Clebsch–Gordan factor. We once again provide all these factors in table form, and as $\Gamma \propto g^2$, the sign of the Clebsch–Gordan factors is not so important to us so the entries in the tables are not always of the correct sign[1]. Unless the table specifies the charge characteristics of parent and daughter mesons, the reader can assume that any charge assignments not in conflict with conservation of charge are permissible and that the single Clebsch–Gordan coefficient associated with such entries applies to all these possible charge assignments. The large range of mesons we now consider lead to numerous such factors.

Factors for $L = 1$ meson two-body decays

Table 4.2 lists the normalisation factors for the experimentally observed transitions of the type $\mathsf{P} \to PP$.

In contrast with the ground state mesons, the $L = 1$ mesons readily undergo $\mathsf{P} \to VP$ type transitions due to the extra phase space available with increasing parent mass. Table 4.3 details the Clebsch–Gordan factors for these interactions. There are an additional two processes which could not be listed, namely $K_1(1270) \to \omega K$ and $K_1(1400) \to \omega K$, because these involve a combination of 1^{+-} and $1^{++} \to VP$ processes. Recall $K_1(1270)$ and $K_1(1400)$ are mixtures of the pure 1^{+-} and 1^{--} states, K_{1B} and K_{1A}, and after combining the contributions of each channel one finds

$$\begin{aligned}
\Gamma_{K_1(1270)\to\omega K} &= \frac{g_{PVP}}{192\pi}\left[\frac{\cos^2\theta_K}{6}(2\sqrt{2}\cos\theta_V - \sin\theta_V)^2 + \frac{3}{2}\sin^2\theta_K\sin^2\theta_V\right] \\
&\qquad \times\lambda^{5/2}(m^2_{K_1(1270)}, m^2_\omega, m^2_K)/m^5_{K_1(1270)}, \\
\Gamma_{K_1(1400)\to\omega K} &= \frac{g_{PVP}}{192\pi}\left[\frac{\sin^2\theta_K}{6}(2\sqrt{2}\cos\theta_V - \sin\theta_V)^2 + \frac{3}{2}\cos^2\theta_K\sin^2\theta_V\right] \\
&\qquad \times\lambda^{5/2}(m^2_{K_1(1400)}, m^2_\omega, m^2_K)/m^5_{K_1(1400)}
\end{aligned}$$

[1]The choice of signs for some channels is quite arbitrary, and because we cannot determine the sign of the coupling from decay width measures this arbitrariness does not affect our results.

Decay process $\mathsf{P} \to PP$	Clebsch–Gordan factor
$a_0(980) \to \eta\pi$	$\sqrt{\frac{2}{3}}\left(\cos\theta_P - \sqrt{2}\sin\theta_P\right)$
$a_0^{\pm}(980) \to K^{\pm}K^0$	1
$a_0^0(980) \to (K\bar{K})^0$	$\sqrt{1/2}$
$f_0(980) \to \pi\pi$	$\sqrt{\frac{2}{3}}\left(\sqrt{2}\cos\theta_{\mathsf{P}_0} + \sin\theta_{\mathsf{P}_0}\right)$
$f_0(980) \to K\bar{K}$	$\sqrt{\frac{1}{6}}\left(2\sqrt{2}\cos\theta_{\mathsf{P}_0} - \sin\theta_{\mathsf{P}_0}\right)$
$f_0(1370) \to \pi\pi$	$\sqrt{\frac{2}{3}}\left(\cos\theta_{\mathsf{P}_0} - \sqrt{2}\sin\theta_{\mathsf{P}_0}\right)$
$f_0(1370) \to K\bar{K}$	$-\sqrt{\frac{1}{6}}\left(\cos\theta_{\mathsf{P}_0} + 2\sqrt{2}\sin\theta_{\mathsf{P}_0}\right)$
$K_0^*(1430) \to K\pi^0, K\pi^{\pm}$	$\sqrt{1/2}, 1$
$a_2^{\pm}(1320) \to K^{\pm}K^0$	1
$a_2^0(1320) \to (K\bar{K})^0$	$\sqrt{1/2}$
$a_2(1320) \to \eta\pi$	$\sqrt{\frac{2}{3}}\left(\cos\theta_P - \sqrt{2}\sin\theta_P\right)$
$a_2(1320) \to \eta'\pi$	$\sqrt{\frac{2}{3}}\left(\sqrt{2}\cos\theta_P + \sin\theta_P\right)$
$f_2(1270) \to \pi\pi$	$\sqrt{\frac{2}{3}}\left(\sqrt{2}\cos\theta_{\mathsf{P}_2} + \sin\theta_{\mathsf{P}_2}\right)$
$f_2(1270) \to K\bar{K}$	$\sqrt{\frac{1}{6}}\left(2\sqrt{2}\cos\theta_{\mathsf{P}_2} - \sin\theta_{\mathsf{P}_2}\right)$
$f_2(1270) \to \eta\eta$	$-\sqrt{\frac{2}{3}}\{\sin\theta_{\mathsf{P}_2}\cos\theta_P \times$ $\times\left(2\sqrt{2}\sin\theta_P + \cos\theta_P\right) - \sqrt{2}\cos\theta_{\mathsf{P}_2}\}$
$f_2'(1525) \to \pi\pi$	$\sqrt{\frac{2}{3}}\left(\cos\theta_{\mathsf{P}_2} - \sqrt{2}\sin\theta_{\mathsf{P}_2}\right)$
$f_2'(1525) \to K\bar{K}$	$-\sqrt{\frac{1}{6}}\left(\cos\theta_{\mathsf{P}_2} + 2\sqrt{2}\sin\theta_{\mathsf{P}_2}\right)$
$f_2'(1525) \to \eta\eta$	$-\sqrt{\frac{2}{3}}\{\cos\theta_{\mathsf{P}_2}\cos\theta_P \times$ $\times\left(2\sqrt{2}\sin\theta_P + \cos\theta_P\right) + \sqrt{2}\sin\theta_{\mathsf{P}_2}\}$
$K_2^*(1430) \to K\pi^0, K\pi^{\pm}$	$\sqrt{1/2}, 1$
$K_2^*(1430) \to K\eta$	$-\sqrt{\frac{1}{6}}\left(\cos\theta_P + 2\sqrt{2}\sin\theta_P\right)$

Table 4.2: Clebsch–Gordan factors for $\mathsf{P} \to PP$ processes.

Decay process $\mathsf{P} \to VP$	Clebsch–Gordan factor
$b_1(1235) \to \omega\pi$	$\sqrt{\frac{2}{3}}\left(\sqrt{2}\cos\theta_V + \sin\theta_V\right)$
$b_1(1235) \to \rho\eta$	$\sqrt{\frac{2}{3}}\left(\cos\theta_P - \sqrt{2}\sin\theta_P\right)$
$b_1(1235) \to \phi\pi$	$\sqrt{\frac{2}{3}}\left(\cos\theta_V - \sqrt{2}\sin\theta_V\right)$
$h_1(1170) \to \rho\pi$	$\sqrt{\frac{2}{3}}\left(\sqrt{2}\cos\theta_{\mathsf{P}_{1-}} + \sin\theta_{\mathsf{P}_{1-}}\right)$
$K_1(1270) \to \rho^0 K, \rho^\pm K$	$\sqrt{1/2}, 1$
$K_1(1270) \to K^*\pi^0, K^*\pi^\pm$	$\sqrt{1/2}, 1$
$a_1(1260) \to \rho\pi$	$\sqrt{2}$
$a_1^{\pm,0}(1260) \to K^*\bar{K}$	$1, \sqrt{1/2}$
$f_1(1510) \to K^*\bar{K} + c.c.$	$\sqrt{\frac{3}{2}}\cos\theta_{\mathsf{P}_{1+}}$
$K_1(1400) \to \rho^0 K, \rho^\pm K$	$\sqrt{1/2}, 1$
$K_1(1400) \to K^*\pi^0, K^*\pi^\pm$	$\sqrt{1/2}, 1$
$a_2(1320) \to \rho\pi$	$\sqrt{2}$
$K_2^*(1430) \to K^*\pi^0, K^*\pi^\pm$	$\sqrt{1/2}, 1$
$K_2^*(1430) \to \rho^0 K, \rho^\pm K$	$\sqrt{1/2}, 1$
$K_2^*(1430) \to \omega K$	$-\sqrt{\frac{3}{2}}\sin\theta_V$

Table 4.3: Clebsch–Gordan factors for $\mathsf{P} \to VP$ processes.

Factors for $L = 2$ meson two-body decays

With the increase in mass associated with going to even higher excited states one anticipates a greater variety of decay channels to sample, but unfortunately we are also moving into less well–charted territory. The experimentalists are overwhelmed by difficulties of broad resonance peaks and a deluge of processes to observe, so unfortunately the data does not match our expectations. Nonetheless there are some interesting channels to study, particularly in the strange realm where results are more easily determined. In Table 4.4 and 4.5 we provide the Clebsch–Gordan factors necessary for the normalisation of the processes we can analyse.

Decay process $\mathsf{D} \to PP$	Clebsch–Gordan factor
$\rho^{\pm,0}(1700) \to \pi^{\pm}\pi^{0,\mp}$	$\sqrt{2}$
$\rho^{\pm}(1700) \to K^{\pm}K^{0}$	1
$\rho^{0}(1700) \to K\bar{K}$	$\sqrt{1/2}$
$K^{*}(1680) \to K\pi^{0}, K\pi^{\pm}$	$\sqrt{1/2}, 1$
$\rho_3^{\pm,0}(1690) \to \pi^{\pm}\pi^{0,\mp}$	$\sqrt{2}$
$\rho_3^{\pm}(1690) \to K^{\pm}K^{0}$	1
$\rho_3^{0}(1690) \to K\bar{K}$	$\sqrt{1/2}$
$\phi_3(1850) \to K\bar{K}$	$\sqrt{\frac{3}{2}}\cos\theta_{\mathsf{D}_3}$
$K_3^{*}(1780) \to K\pi^{0}, K\pi^{\pm}$	$\sqrt{1/2}, 1$
$K_3^{*}(1780) \to K\eta$	$\sqrt{\frac{3}{2}}\cos\theta_{P}$

Table 4.4: Clebsch–Gordan factors for $\mathsf{D} \to PP$ processes.

Factors for $L = 3$ meson two-body decays

The F-wave mesons are only experimentally known by the 4^{++} mesons and hence we restrict the determination of Clebsch–Gordan factors to this set, and they are given in Tables 4.6 and 4.7.

4.4 Results and Analysis

During the course of study into the excited mesons, two releases of the Particle Data Reviews occurred, the 1994 edition [87] and the 1996 edition [13]. From the experimental decay widths along with the appropriate decay rate formula (4.26) and Clebsch–Gordan factors the coupling constants were determined for both the 1994 and 1996 data sets. Errors quoted for the coupling constants are calculated from the assumption of uncorrelated errors in the meson masses (parent and daughters), decay widths and branching fractions. The contribution to the error from the mixing angle uncertainties, shown in Table 4.1, are not taken into account; for processes involving mixed states we typically comment on the sensitivity to the angle. In situations

Decay process $\mathsf{D} \to VP$	Clebsch–Gordan factor
$\pi_2^{\pm,0}(1670) \to \rho^{\pm}\pi^{0,\mp}$	$\sqrt{2}$
$\pi_2^{0,\pm}(1670) \to K^*\bar{K} + c.c.$	$\sqrt{1/2}, 1$
$K_2(1770) \to K^*\pi^0, K^*\pi^{\pm}$	$\sqrt{1/2}, 1$
$K_2(1770) \to \omega K$	$-\sqrt{\frac{3}{2}}\sin\theta_V$
$K_2(1770) \to \phi K$	$\sqrt{\frac{3}{2}}\cos\theta_V$
$\rho^{0,\pm}(1700) \to K^*\bar{K} + c.c.$	$\sqrt{1/2}, 1$
$\rho(1700) \to \rho\eta$	$\sqrt{\frac{2}{3}}\left(\cos\theta_P - \sqrt{2}\sin\theta_P\right)$
$\omega(1600) \to \rho\pi$	1
$K^*(1680) \to K^*\pi^0, K^*\pi^{\pm}$	$\sqrt{1/2}, 1$
$K^*(1680) \to \rho^0 K, \rho^{\pm} K$	$\sqrt{1/2}, 1$
$K_2(1820) \to K^*\pi^0, K^*\pi^{\pm}$	$\sqrt{1/2}, 1$
$K_2(1820) \to \omega K$	$\sqrt{\frac{1}{6}}\left(2\sqrt{2}\cos\theta_V - \sin\theta_V\right)$
$K_2(1820) \to \phi K$	$-\sqrt{\frac{1}{6}}\left(\cos\theta_V + 2\sqrt{2}\sin\theta_V\right)$
$\rho_3(1690) \to \omega\pi$	$\sqrt{\frac{2}{3}}\left(\sqrt{2}\cos\theta_V + \sin\theta_V\right)$
$\omega_3(1670) \to \rho\pi$	$\sqrt{\frac{2}{3}}\left(\sqrt{2}\cos\theta_{\mathsf{D}_3} + \sin\theta_{\mathsf{D}_3}\right)$
$\phi_3(1850) \to K^*\bar{K} + c.c.$	$-\sqrt{\frac{1}{6}}\left(\cos\theta_{\mathsf{D}_3} + 2\sqrt{2}\sin\theta_{\mathsf{D}_3}\right)$
$K_3^*(1780) \to K^*\pi^0, K^*\pi^{\pm}$	$\sqrt{1/2}, 1$
$K_3^*(1780) \to \rho^0 K, \rho^{\pm} K$	$\sqrt{1/2}, 1$

Table 4.5: Clebsch–Gordan factors for $\mathsf{D} \to VP$ processes.

Decay process $\mathsf{F} \to PP$	Clebsch–Gordan factor
$f_4(2050) \to \pi\pi$	$\sqrt{\frac{2}{3}}\left(\sqrt{2}\cos\theta_{\mathsf{F}_4} + \sin\theta_{\mathsf{F}_4}\right)$
$f_4(2050) \to K\bar{K}$	$\sqrt{\frac{1}{6}}\left(2\sqrt{2}\cos\theta_{\mathsf{F}_4} - \sin\theta_{\mathsf{F}_4}\right)$
$f_4(2050) \to \eta\eta$	$\frac{1}{3}\sqrt{\frac{2}{3}}\left(\sqrt{2}\cos\theta_{\mathsf{F}_4} + \sin\theta_{\mathsf{F}_4}\right)\left(\cos\theta_P - \sqrt{2}\sin\theta_P\right)^2$
$K_4^*(2045) \to K\pi^0, K\pi^{\pm}$	$\sqrt{1/2}, 1$

Table 4.6: Clebsch–Gordan factors for $\mathsf{F} \to PP$ processes.

Decay process $\mathsf{F} \to VV$	Clebsch–Gordan factor
$f_4(2050) \to \omega\omega$	$\frac{1}{3}\sqrt{\frac{2}{3}}\left(\sqrt{2}\cos\theta_{\mathsf{F}_4} + \sin\theta_{\mathsf{F}_4}\right)\left(\sqrt{2}\cos\theta_V + \sin\theta_V\right)^2$
$K_4^*(2045) \to \phi K^*(892)$	$-\sqrt{\frac{1}{6}}\left(2\sqrt{2}\sin\theta_V + \cos\theta_V\right)$

Table 4.7: Clebsch–Gordan factors for $\mathsf{D} \to VV$ processes.

where the 1994 world average is the *same* as the 1996, (and hence our results have not differed) *we use the* $\leftarrow$ *symbol* to indicate the later world average applies to the earlier; the presence of an entry in the 1994 column indicates the old data has been used.

In some instances there are problems associated with calculating the coupling constants. These spring from large uncertainty of masses (and this is also related to the determination of mixing angles), decay widths and branching fractions. Often the only test we can apply to these difficult cases is to use relative branching fraction measurements where the problems of mixing angles and decay widths are irrelevant. This method assumes a universal coupling constant exists and then we predict relations between branching fractions. Then any experimental deviation from the prediction indicates the deviation from universality.

4.4.1 Coupling constants of the P-wave mesons

The $L = 1$ supermultiplet is probably the best studied of all the orbital angular momentum excitation modes of the mesons. Decay widths are reasonably well determined, but there are some notable gaps in the data set. As mentioned earlier, the most troublesome mesons are the scalar mesons, and our analysis assumes the assignments are based on the 1994 Data Tables [87].

Experimental measures of $g_{\mathsf{P}PP}$ and $g_{\mathsf{P}VP}$

Table 4.8 lists the determination of the $g_{\mathsf{P}PP}$ coupling constant from $0^{++} \to PP$ and $2^{++} \to PP$ processes via the decay rate formulae (4.10) and (4.9).

There are several problematic mesons in the 0^{++} nonet.

Decay process	g_{PPP} ($\times 10^{-3}$ MeV^{-1})	
$P \to PP$	1994 [87]	1996 [13]
$a_0(980) \to \eta\pi$	< 19.7	< 11.4
$f_0(980) \to \pi\pi$	depend on	
$f_0(1370) \to \pi\pi$	unknown mixing	
$f_0(1370) \to K\bar{K}$	angle θ_{P_0}	
$K_0^{*\pm}(1430) \to (K\pi)^{\pm}$	$\leftarrow$	4.33 ± 0.30
$K_0^{*0}(1430) \to (K\pi)^0$	$\leftarrow$	4.32 ± 0.30
$a_2^{\pm}(1320) \to K^{\pm}K^0$	$\leftarrow$	2.63 ± 0.22
$a_2^0(1320) \to (K\bar{K})^0$	$\leftarrow$	2.63 ± 0.22
$a_2^{\pm}(1320) \to \eta\pi^{\pm}$	$\leftarrow$	2.66 ± 0.13
$a_2^0(1320) \to \eta\pi^0$	$\leftarrow$	2.65 ± 0.13
$a_2^{\pm}(1320) \to \eta'\pi^{\pm}$	$\leftarrow$	2.58 ± 0.26
$a_2^0(1320) \to \eta'\pi^0$	2.54 ± 0.25	2.55 ± 0.25
$f_2(1270) \to \pi\pi$	2.84 ± 0.16	2.84 ± 0.16
$f_2(1270) \to K\bar{K}$	$\leftarrow$	3.61 ± 0.32
$f_2(1270) \to \eta\eta$	$\leftarrow$	2.61 ± 0.33
$f_2'(1525) \to \pi\pi$	1.86 ± 0.22	1.86 ± 0.21
$f_2'(1525) \to K\bar{K}$	3.56 ± 0.26	3.98 ± 0.28
$f_2'(1525) \to \eta\eta$	4.04 ± 0.36	2.47 ± 0.40
$K_2^{*\pm}(1430) \to (K\pi)^{\pm}$	$\leftarrow$	2.95 ± 0.05
$K_2^{*0}(1430) \to (K\pi)^0$	$\leftarrow$	3.06 ± 0.08
$K_2^{*\pm}(1430) \to K^{\pm}\eta$	$\leftarrow$	1.82 ± 1.91
$K_2^{*0}(1430) \to K^0\eta$	$\leftarrow$	1.90 ± 2.00

Table 4.8: Results from $P \to PP$ decays.

- the $f_0(1370)$ mass has a large uncertainty (m = 1000 to 1500 MeV:1994, 1200 to 1500 MeV: 1996) and decay width (Γ = 150 to 400 MeV:1994, 300 to 500 MeV: 1996).

- the $f_0(980)$ decay width has large uncertainty (Γ = 40 to 400 MeV:1994, 40 to 100 MeV:1996)

- the $a_0(980)$ decay width has some uncertainty (Γ = 50 to 300 MeV:1994, 50 to 100 MeV:1996)

The $\mathsf{P} \to VP$ decays are well represented, particularly in the $J^P = 1^+$ nonets and the strange members therein. The branching fractions for the decays $b_1(1235) \to \omega\pi$ and $b_1(1235) \to \phi\pi$ are only known to upper bounds. Also the fraction for $a_1(1260) \to \rho\pi$ is only known to dominate the possible channels from a given total width of $\Gamma \sim 400$ MeV. Hence we simply assume $\Gamma_{a_1(1260)\to\rho\pi} < 400$ MeV. In a similar fashion the process $f_1(1510) \to K^*\bar{K}$ has only been 'seen' in the total width of $\Gamma = 35 \pm 15$ MeV, so we assume $\Gamma_{f_1(1510)\to K^*\bar{K}} < 35 \pm 15$ MeV. With these approximations, we obtain upper bounds on the coupling constants for these processes. These as well as better determinations of $g_{\mathsf{P}VP}$ from more accurate channels are given in Table 4.9. The electromagnetic decays of the $L = 1$ mesons also provide some estimates of the $g_{\mathsf{P}VP}$ coupling constant. The decay rate formula

$$\Gamma_{\mathsf{P}\to P\gamma} = \frac{g^2_{\mathsf{P}P\gamma}}{320\pi}\frac{(m^2_{\mathsf{P}} - m^2_P)^5}{m^5_{\mathsf{P}}},$$

when used in conjunction with the VMD relation, $g_{\mathsf{P}P\gamma} = eg_{\mathsf{P}VP}/g'_{VPP}$ and

Decay process	g_{PVP} ($\times 10^{-6}\mathrm{MeV}^{-2}$)	
$P \to VP$	1994 [87]	1996 [13]
$b_1^{\pm}(1235) \to \omega\pi^{\pm}$	$\leftarrow$	$< 16.22 \pm 0.99$
$b_1^0(1235) \to \omega\pi^0$	$\leftarrow$	$< 16.07 \pm 0.97$
$b_1(1235) \to \rho\eta$	phase space limited	
$b_1^{\pm}(1235) \to \phi\pi^{\pm}$	$\leftarrow$	$< 245 \pm 49$
$b_1^0(1235) \to \phi\pi^0$	$\leftarrow$	$< 230 \pm 44$
$h_1(1170) \to \rho\pi$	$\leftarrow$	$< 21.4 \pm 2.9$
$K_1^{\pm}(1270) \to (\rho K)^{\pm}$	$\leftarrow$	435 ± 1041
$K_1^0(1270) \to (\rho K)^0$	$\leftarrow$	359 ± 722
$K_1^{\pm}(1270) \to (K^*\pi)^{\pm}$	$\leftarrow$	8.67 ± 2.07
$K_1^0(1270) \to (K^*\pi)^0$	$\leftarrow$	8.59 ± 2.04
$K_1(1270) \to \omega K$	phase space limited	
$a_1^{\pm}(1260) \to (\rho\pi)^{\pm}$	$\leftarrow$	$< 17.9 \pm 8.9$
$a_1^0(1260) \to \rho^{\pm}\pi^{\mp}$	$\leftarrow$	$< 18.0 \pm 3.7$
$f_1(1510) \to K^*\bar{K} + c.c$	$\leftarrow$	$< 9.3 \pm 2.0$
$K_1^{\pm}(1400) \to (\rho K)^{\pm}$	$\leftarrow$	5.29 ± 2.77
$K_1^0(1400) \to (\rho K)^0$	$\leftarrow$	5.23 ± 2.74
$K_1^{\pm}(1400) \to (K^*\pi)^{\pm}$	$\leftarrow$	14.24 ± 1.34
$K_1^0(1400) \to (K^*\pi)^0$	$\leftarrow$	14.15 ± 1.33
$K_1^{\pm}(1400) \to \omega^{\pm}K$	$\leftarrow$	5.9 ± 3.1
$K_1^0(1400) \to \omega^0 K$	$\leftarrow$	6.1 ± 3.1
$a_2^{\pm}(1320) \to \rho^0\pi^{\pm}, \rho^{\pm}\pi^0$	6.67 ± 0.21	6.68 ± 0.21
$a_2^0(1320) \to \rho^{\pm}\pi^{\mp}$	6.67 ± 0.20	6.68 ± 0.21
$K_2^{*\pm}(1430) \to (K^*\pi)^{\pm}$	$\leftarrow$	6.44 ± 0.25
$K_2^{*0}(1430) \to (K^*\pi)^0$	$\leftarrow$	6.54 ± 0.28
$K_2^{*\pm}(1430) \to (\rho K)^{\pm}$	$\leftarrow$	7.14 ± 0.38
$K_2^{*0}(1430) \to (\rho K)^0$	$\leftarrow$	7.04 ± 0.39
$K_2^{*\pm}(1430) \to \omega K^{\pm}$	$\leftarrow$	7.11 ± 0.99
$K_2^{*0}(1430) \to \omega K^0$	$\leftarrow$	7.25 ± 1.02

Table 4.9: Results from $P \to VP$ decays.

$g'_{VPP}(V) = (0.1359 \pm 0.0036) m_V^{1/2}$ yield the following estimates:

Decay process $\mathsf{P} \to P\gamma$	Conversion factor	g_{PVP} ($\times 10^{-6}$MeV^{-2}) 1994, 1996 [87, 13]
$b_1(1235) \to \pi^{\pm}\gamma$	$e/(0.1359 m_{\omega_8}^{1/2})$	3.12 ± 0.40
$a_1(1260) \to \pi\gamma$	$e/(0.1359 m_{\rho^0}^{1/2})$	$\begin{cases} < 119 \\ 4.8 \pm 1.0 \end{cases}$
$a_2(1320) \to \pi^{\pm}\gamma$	$e/(0.1359 m_{\rho^0}^{1/2})$	3.52 ± 0.40
$K_2^{*\pm}(1430) \to K^{\pm}\gamma$	$e\frac{(1/\sqrt{m_{\rho^0}}+1/\sqrt{m_{\omega_8}})}{-2\times 0.1359}$	3.61 ± 0.38
$K_2^{*0}(1430) \to K^0\gamma$	$e\frac{(1/\sqrt{m_{\rho^0}}-1/\sqrt{m_{\omega_8}})}{-2\times 0.1359}$	< 47

Analysis of the g_{PPP} and g_{PVP} experimental measures

The $L = 1$ meson results support the notion of excited meson supermultiplets as the coupling constants are reasonably uniform, even though we have spanned several J^{PC} multiplets. The following general observations can be made:

- The g_{PPP} coupling determined from $\mathsf{P} \to PP$ decays is quite uniform, with only a few channels producing spurious results. These include channels with a high sensitivity to mixing angles, such as $f_2'(1270) \to \pi\pi$ which with $\Delta\theta_{\mathsf{P}_2} = 1.5°$ leads to $g_{PPP} \simeq 2.88 \times 10^{-3}$ MeV^{-1}, putting it much nearer the other calculated values. The scalar mesons require more experimental attention to help resolve the confusion over multiplet assignments. The $K_0^*(1430)$ results are inconsistent with a uniform g_{PPP}, but this may be due to the lack of experimental study of this meson, with only one project [7] successfully measuring the full decay width and branching fraction. It is difficult to determine if symmetry breaking leads to a predictable mass variation in g_{PPP} because the parent meson masses are quite similar, and the data is not precise enough. The results of Table 4.8 suggest an approximate average of $g_{PPP} \simeq 2.65 \times 10^{-3}$ MeV^{-1}.

- The $g_{\mathsf{P}VP}$ coupling constants are also mostly uniform, with only the $K_1(1400) \to K^*\pi$ channel data in conflict with an approximate average of $g_{\mathsf{P}VP} \simeq 6.65 \times 10^{-6}$ MeV^{-2}. The unusual values obtained from $K_1(1270) \to \rho K$ have arisen because the decay mode is at the point of exclusion given the available kinematical phase space. Fortunately the large errors associated with these channels indicate the results are still consistent with our approximate average. Not forgetting the supermultiplet prediction, $g_{\mathsf{P}PP}/g_{\mathsf{P}VP} = m/2$, these two averages imply $m \sim 800 - 900$ MeV.

- The electromagnetic processes $\mathsf{P} \to P\gamma$ give us more estimates of the $g_{\mathsf{P}VP}$ couplings via VMD. These are very uniform, but tend to be somewhat less than their counterparts determined from purely strong interactions. The upper bound from $a_1(1260) \to \pi\gamma$ corresponds to using the full width $\Gamma_{a_1(1260)\to\text{all}}$, while the smaller value $g_{\mathsf{P}VP} = (4.8 \pm 1.0) \times 10^{-6}$ MeV^{-2} is obtained from the partial width $\Gamma_{a_1(1260)\to\pi\gamma} = 640 \pm 246$ keV [119].

- The $L = 1$ mesons have provided us with the first true test of the supermultiplet scheme; we are no longer combining the scheme with VMD to get some idea of the $\phi_\mu\phi_\nu\phi_5$ vertex; we now have direct measures which, with the exception of a single channel, are remarkably uniform. This implies the supermultiplet scheme could describe all $\mathsf{P} \to \mathsf{SS}$ interactions (where S is a $L = 0$ meson) by a single coupling constant.

- We make the observations $g_{\mathsf{P}PP}/g_{VPP} \simeq 1700$ MeV and $g_{\mathsf{P}VP}/g_{VPP} \simeq 1600$ MeV for future comment.

4.4.2 Coupling constants of the D-wave mesons

The $L = 2$ supermultiplet has significant gaps in the data set. Unfortunately many channels have only been observed without direct measure of the decay width. At present, the 3^{--} nonet is the most comprehensively studied for

which the branching fractions of most of the viable processes are known. For the other nonets, data for the strange members is typically forthcoming, while for the non-strange entities it is mostly nonexistent.

Experimental measures of g_{DPP} and g_{DVP}

Tables 4.10 and 4.11 list the determinations the couplings constants g_{DPP} and g_{DVP},respectively. In these Tables the upper bounds have come from the branching fraction bounds:

$$\begin{aligned}
\Gamma_{\rho(1700)\to K\bar{K},K^*\bar{K}} &< 235 \pm 50 \text{ MeV}, \\
\Gamma_{\rho(1700)\to \rho\eta}/\Gamma_{\rho(1700)\to \text{all}} &< 0.04, \qquad (4.29) \\
\Gamma_{\omega(1600)\to\rho\pi} &< \begin{cases} 280 \pm 24 \text{ MeV (1994)} \\ 220 \pm 35 \text{ MeV (1996)}, \end{cases} \\
\Gamma_{K_2(1820)\to K^*\pi,\omega K,\phi K} &< 276 \pm 35 \text{ MeV}, \\
\Gamma_{K_2(1770)\to K^*\pi,\omega K,\phi K} &< 186 \pm 14 \text{ MeV}, \\
\Gamma_{\omega_3(1670)\to\rho\pi} &< \begin{cases} 173 \pm 11 \text{ MeV (1994)} \\ 168 \pm 10 \text{ MeV (1996)}, \end{cases} \\
\Gamma_{\phi_3(1850)\to K\bar{K},K\bar{K}^*} &< 87 \pm 36.2 \text{ MeV},
\end{aligned}$$

where the measure (4.29) comes from the Particle Data Group full listings [47]. We also assume $\omega(1600) = (\phi_1^1 + \phi_2^2)/\sqrt{2}$ (ideally mixed) as there is no means to obtain a GMO mass determined mixing angle.

There are also some other interesting results in the full particle listings of the Particle Data Tables. For instance the measure [6]

$$\Gamma_{\phi_3(1850)\to K^*\bar{K}}/\Gamma_{\phi_3(1850)\to K\bar{K}} = 0.55 \pm {}^{0.85}_{0.45} \qquad (4.30)$$

gives a direct determination of the g_{DPP}/g_{DVP} ratio via the relation

$$\begin{aligned}
\frac{\Gamma_{\phi_3(1850)\to K^*\bar{K}}}{\Gamma_{\phi_3(1850)\to K\bar{K}}} &= \frac{2}{27}\frac{\left(\cos\theta_{D_3} + 2\sqrt{2}\sin\theta_{D_3}\right)^2}{\cos^2\theta_{D_3}}\left(\frac{g_{DVP}}{g_{DPP}}\right)^2 m^2_{\phi_3(1850)} \\
&\times \frac{\left[\lambda^{7/2}(m^2_{\phi_3}, m^2_{K^{*\pm}}, m^2_{K^{\mp}}) + \lambda^{7/2}(m^2_{\phi_3}, m^2_{K^{*0}}, m^2_{\bar{K}^0})\right]}{\left[\lambda^{7/2}(m^2_{\phi_3}, m^2_{K^{\pm}}, m^2_{K^{\mp}}) + \lambda^{7/2}(m^2_{\phi_3}, m^2_{K^{0}}, m^2_{\bar{K}^0})\right]}.
\end{aligned}$$

Decay process	g_{DPP} ($\times 10^{-6}$ MeV^{-2})	
$D \to PP$	1994 [87]	1996 [13]
$\rho^0(1700) \to \pi^\pm\pi^\mp$	$\leftarrow$	$< 2.27 \pm 0.25$
$\rho^\pm(1700) \to K^\pm K^0$	$\leftarrow$	$< 6.33 \pm 0.75$
$\rho^0(1700) \to (K\bar{K})^0$	$\leftarrow$	$< 6.33 \pm 0.71$
$K^*(1680) \to K\pi$	$\leftarrow$	2.50 ± 0.45
$\rho_3^\pm(1690) \to \pi^\pm\pi^0$	1.331 ± 0.073	1.148 ± 0.049
$\rho_3^0(1690) \to \pi^\pm\pi^\mp$	1.333 ± 0.073	1.150 ± 0.049
$\rho_3^\pm(1690) \to K^\pm K^0$	0.971 ± 0.093	0.838 ± 0.074
$\rho_3^0(1690) \to (K\bar{K})^0$	0.971 ± 0.094	0.838 ± 0.076
$\phi_3(1850) \to (K\bar{K})^0$	$\leftarrow$	$< 2.37 \pm 0.50$
$K_3^{*\pm}(1780) \to (K\pi)^\pm$	$\leftarrow$	1.415 ± 0.089
$K_3^{*0}(1780) \to (K\pi)^0$	$\leftarrow$	1.412 ± 0.089
$K_3^{*\pm}(1780) \to K^\pm\eta$	$\leftarrow$	1.425 ± 0.157
$K_3^{*0}(1780) \to K^0\eta$	$\leftarrow$	1.435 ± 0.158

Table 4.10: Results from $D \to PP$ decays.

Decay process	g_{DVP} ($\times 10^{-9}$ MeV^{-3})	
$D \to VP$	1994 [87]	1996 [13]
$\rho(1700) \to K^*\bar{K}$	$\leftarrow$	$< 27.4 \pm 7.9$
$\rho^{\pm}(1700) \to \rho^{\pm}\eta$	$\leftarrow$	$< 5.09 \pm 0.75$
$\rho^0(1700) \to \rho^0\eta$	$\leftarrow$	$< 5.12 \pm 0.76$
$\omega(1600) \to \rho\pi$	$< 8.8 \pm 1.8$	$< 7.8 \pm 1.8$
$K^*(1680) \to \rho K$	$\leftarrow$	10.9 ± 2.8
$K^*(1680) \to K^*\pi$	$\leftarrow$	8.3 ± 2.0
$K_2^{\pm}(1820) \to (K^*\pi)^{\pm}$	$\leftarrow$	$< 14.88 \pm 0.65$
$K_2^0(1820) \to (K^*\pi)^0$	$\leftarrow$	$< 14.81 \pm 0.65$
$K_2^{\pm}(1820) \to \omega K^{\pm}$	$\leftarrow$	$< 15.9 \pm 1.3$
$K_2^0(1820) \to \omega K^0$	$\leftarrow$	$< 16.0 \pm 1.3$
$K_2^{\pm}(1820) \to \phi K^{\pm}$	$\leftarrow$	$\ll 25.8 \pm 2.7$
$K_2^0(1820) \to \phi K^0$	$\leftarrow$	$\ll 26.3 \pm 2.8$
$\pi_2^{\pm}(1670) \to (\rho\pi)^{\pm}$	2.12 ± 0.28	2.19 ± 0.29
$\pi_2^0(1670) \to \rho^{\pm}\pi^{\mp}$	2.12 ± 0.21	2.19 ± 0.22
$\pi_2(1670) \to K^*K$	3.99 ± 1.38	4.14 ± 1.43
$K_2(1770) \to K^*\pi$	$\leftarrow$	$< 5.41 \pm 0.34$
$K_2^{\pm}(1770) \to \phi K^{\pm}$	$\leftarrow$	$< 27.4 \pm 1.9$
$K_2^0(1770) \to \phi K^0$	$\leftarrow$	$< 28.0 \pm 2.0$
$K_2^{\pm}(1770) \to \omega K^{\pm}$	$\leftarrow$	$< 10.90 \pm 0.55$
$K_2^0(1770) \to \omega K^0$	$\leftarrow$	$< 11.01 \pm 0.55$
$\rho_3(1690) \to \omega\pi$	2.61 ± 0.51	2.26 ± 0.43
$\omega_3(1670) \to \rho\pi$	$< 3.52 \pm 0.14$	$< 3.47 \pm 0.13$
$\phi_3(1850) \to K^*\vec{K}$	$\leftarrow$	$< 4.04 \pm 0.88$
$K_3^{*\pm}(1780) \to (K^*\pi)^{\pm}$	$\leftarrow$	3.55 ± 0.36
$K_3^{*0}(1780) \to (K^*\pi)^0$	$\leftarrow$	3.53 ± 0.35
$K_3^{*\pm}(1780) \to (\rho K)^{\pm}$	$\leftarrow$	5.60 ± 0.56
$K_3^{*0}(1780) \to (\rho K)^0$	$\leftarrow$	5.58 ± 0.56

Table 4.11: Results from $D \to VP$ decays.

The result in (4.30) leads to $g_{DPP}/g_{DVP} = 275 \pm 240$ MeV or $m = 550 \pm 480$ MeV after invoking the supermultiplet prediction $g_{DPP}/g_{DVP} = m/2$.

Analysis of the g_{DPP} and g_{DVP} experimental measures

The $L = 2$ mesons have provided some useful estimates of the coupling constants g_{DPP} and g_{DVP}, from which we make the observations:

- The depth of experimental results for determinations of g_{DPP} is limited and we would benefit greatly by more accurate measures, particularly in the $J^{PC} = 1^{--}$ mesons. This aside, the 3^{--} mesons suggest a uniform coupling constant is apparent, with an approximate average of $g_{DPP} \sim 1.4 \times 10^{-6}$ MeV^{-2}. There are two estimates noticeably outside this average, that from $\rho_3(1690) \to K\bar{K}$ and $K^*(1680) \to K\pi$ (the latter with a comparatively large error). However, investigation of the $\rho_3(1690)$ full listing entry in the Particle Data Tables show the measures of the $K\bar{K}$ and $\pi\pi$ channels are quite volatile. The total width changed from 215 ± 20 MeV in 1994 to 160 ± 10 MeV in 1996 and more interestingly in both years the branching ratio $\Gamma_{\rho_3(1690)\to K\bar{K}}/\Gamma_{\rho_3(1690)\to\pi\pi}$ significantly varies between the overall data fit of all decay channel measures ($\Gamma_{\rho_3(1690)\to K\bar{K}}/\Gamma_{\rho_3(1690)\to\pi\pi} = 0.067 \pm 0.011$) and the average of the direct measures of the ratio ($\Gamma_{\rho_3(1690)\to K\bar{K}}/\Gamma_{\rho_3(1690)\to\pi\pi} = 0.118 \pm \frac{0.039}{0.032}$). If we assume a uniform coupling constant exists, then this branching fraction is given by

$$\frac{\Gamma_{\rho_3(1690)\to K\bar{K}}}{\Gamma_{\rho_3(1690)\to\pi\pi}} = \frac{1}{4}\frac{\left[\lambda^{7/2}(m^2_{\rho_3}, m^2_{K^\pm}, m^2_{K^\mp}) + \lambda^{7/2}(m^2_{\rho_3}, m^2_{K^0}, m^2_{\bar{K}^0})\right]}{\lambda^{7/2}(m^2_{\rho_3}, m^2_{\pi^\pm}, m^2_{\pi^\mp})},$$

which with present mass values calculates to

$$\Gamma_{\rho_3(1690)\to K\bar{K}}/\Gamma_{\rho_3(1690)\to\pi\pi} = 0.126,$$

much closer to the average value than the fit value. Importantly it is the fit value which is used in the summary listings so this inconsistency may be the main reason for the mismatched $\rho_3(1690) \to K\bar{K}$ result.

- There is a large number of $g_{\mathsf{D}VP}$ determinations in Table 4.11, but most of them are upper bound values. The most important aspect of these results is that all parent D-wave states have been represented, that is all $2^{+-}, 1^{--}, 2^{--}, 3^{--} \rightarrow VP$ channels have been studied in the context of the excited supermultiplet wavefunctions with a single coupling constant $g_{\mathsf{D}VP}$. The poorest results come from $1^{--} \rightarrow VP$, in particular $K^*(1680) \rightarrow VP$. We wish to add that this is a controversial identification, being a possible candidate for the 2^3S_1 nonet. Also, there is much uncertainty in the full width measure ($\Gamma = 323 \pm 110$ MeV, where the very large scale factor of $S = 4.2$ has been applied [13]). Hence it is hard to say if the poor results in Table 4.11 reflect a fault in the supermultiplet scheme, or if it is simply due to incorrect assignment or poor experimental data. *The* D*-wave mesons certainly deserve more intense experimental attention.* If we ignore the $K^*(1680)$ results, the data suggests a very approximate average $g_{\mathsf{D}VP} \sim 3 \times 10^{-9}$ MeV^{-3}. In turn this, along with our estimate $g_{\mathsf{D}PP} \sim 1.4 \times 10^{-6}$ MeV^{-2}, implies $m \sim 900$ MeV via $g_{\mathsf{D}PP}/g_{\mathsf{D}VP} = m/2$. As a final note, we remark that there are no observed electromagnetic interactions of the type $\mathsf{D} \rightarrow P\gamma$ with which to make extra determinations of $g_{\mathsf{D}VP}$ via VMD.

- The ratio $g_{\mathsf{P}PP}/g_{\mathsf{D}PP}$ or $g_{\mathsf{P}VP}/g_{\mathsf{D}VP}$ is of the order of 2000 MeV which compares well with the ratio $g_{VPP}/g_{\mathsf{P}PP}$ or $g_{VPP}/g_{\mathsf{P}VP}$.

4.4.3 Coupling constants of the F-wave mesons

As mentioned earlier, only the 4^{++} nonet of the $L = 3$ supermultiplet has been experimentally studied to any degree. Hence the results are limited to those given in Table 4.12 and 4.13.

Analysis of the $g_{\mathsf{F}PP}$ and $g_{\mathsf{F}VV}$ experimental measures

Given the lack of experimental results only the following generalizations can be made:

Decay process	$g_{\mathsf{F}PP}$ ($\times 10^{-10}$ MeV^{-3})
$\mathsf{F} \to PP$	1994, 1996 [87, 13]
$f_4(2050) \to \pi\pi$	4.90 ± 0.28
$f_4(2050) \to K\bar{K}$	4.67 ± 1.34
$f_4(2050) \to \eta\eta$	3.08 ± 0.60
$K_4^{*\pm}(2045) \to (K\pi)^{\pm}$	5.60 ± 1.09
$K_4^{*0}(2045) \to (K\pi)^0$	5.59 ± 1.09

Table 4.12: Results from $\mathsf{F} \to PP$ decays.

Decay process	$g_{\mathsf{F}VV}$ ($\times 10^{-13}$ MeV^{-4})
$\mathsf{F} \to VV$	1994, 1996 [87, 13]
$f_4(2050) \to \omega\omega$	7.31 ± 0.87
$K_4^*(2045) \to \phi K^*(892)$	28.6 ± 7.5

Table 4.13: Results from $\mathsf{F} \to VV$ decays.

- The g_{FPP} coupling constants are quite uniform; the only result inconsistent with the value $g_{FPP} \simeq 5 \times 10^{-10}$ MeV^{-3} is from the channel $f_4(2050) \to \eta\eta$. This calculation depends on the mixing angles $\theta_{F_4} = -8° \pm 20°$ and $\theta_P = 10.5°$ so there is room for variation in this value by symmetry breaking effects. We also note that $g_{DPP}/g_{FPP} \sim 2500$ MeV from our rough estimates, which is similar to the previous ratios g_{PPP}/g_{DPP} and g_{VPP}/g_{PPP}.

- We are finally provided with a direct measure of a coupling constant of the type g_{LVV} in the decays $F \to VV$. The large disparity in the measures in Table 4.13 is most likely due to the fact that the process $K_4^*(2045) \to \phi K^*(892)$ is not strictly applicable in the supermultiplet scheme as the daughter mesons have unequal masses; in the scheme at least two mesons must have the same mass to form a gauge invariant vertex interaction. If we use the value $g_{FVV} = (7.31 \pm 0.87) \times 10^{-13}$ MeV^{-4} and the average $g_{FPP} \simeq 5 \times 10^{-10}$ MeV^{-3}, the supermultiplet relation $g_{FPP}/g_{FVV} = m$ yields $m \simeq 680 \pm 80$ MeV.

4.5 Beyond $N_f = 3$: Excited heavy mesons

The extension from $N_f = 3$ to $N_f = 4$ and 5 is not a difficult one, but the number of excited heavy mesons identified are so few as to make such an extension unwarranted in the preceding sections. Here we wish to report and analyse these few excited heavy meson states and where appropriate, make some predictions about decay rates and branching fractions.

4.5.1 Excited heavy meson states

The identified excited meson states are assigned the following super-wave-function flavour indices:

$$
\begin{aligned}
{}^1P_1 \text{ mesons, } J^{PC} &= 1^{+-} \rightarrow \left\{ \begin{array}{ll} a,b & \phi^b_{5\mu_1 a} \\ 4,1 & \bar{D}^0_1(2420) \\ 4,2 & D^+_1(2420) \\ 4,3 & D^+_{s1}(2536) \\ 4,4 & h_c(1P) \end{array} \right. , \\
{}^3P_0 \text{ mesons, } J^{PC} &= 0^{++} \rightarrow \left\{ \begin{array}{ll} a,b & \phi^{(0)b}_a \\ 4,4 & \chi_{c0}(1P) \\ 5,5 & \chi_{b0}(1P) \end{array} \right. , \\
{}^3P_1 \text{ mesons, } J^{PC} &= 1^{++} \rightarrow \left\{ \begin{array}{ll} a,b & \phi^{(1)b}_{\mu a} \\ 4,4 & \chi_{c1}(1P) \\ 5,5 & \chi_{b1}(1P) \end{array} \right. , \\
{}^3P_2 \text{ mesons, } J^{PC} &= 2^{++} \rightarrow \left\{ \begin{array}{ll} a,b & \phi^{(2)b}_{\mu\mu_1 a} \\ 4,1 & \bar{D}^{*0}_2(2460) \\ 4,2 & D^{*+}_2(2460) \\ 4,3 & D^+_{sJ}(2573) \\ 4,4 & \chi_{c2}(1P) \\ 5,5 & \chi_{b2}(1P) \end{array} \right. , \\
{}^3D_1 \text{ mesons, } J^{PC} &= 1^{--} \rightarrow \left\{ \begin{array}{ll} a,b & \phi^{(1)b}_a \\ 4,4 & \psi(3770) \end{array} \right. ,
\end{aligned}
$$

where any charge conjugate mesons are obtained by swapping $a \leftrightarrow b$. Any mesons shown in italic face are controversial assignments and are awaiting confirmation of J^{PC} values. There is some experimental data available on the strong decay modes of these mesons, namely in the form of upper bounds on the decay widths and observations of the decay channels. We provide the corresponding upper bounds on the coupling constants determined from these interactions in Table 4.14. For brevity we include the Clebsch-Gordan factors in this table.

Decay process	C–G factor	Coupling constant 1994 [87]	1996 [13]
$\mathsf{P} \to PP$		$g_{\mathsf{P}PP}$ ($\times 10^{-3}$ MeV^{-1})	
$D_2^{*\pm}(2460) \to D^0\pi^\pm$	1	$< 7.0 \pm 1.6$	$< 7.3 \pm 1.5$
$D_2^{*0}(2460) \to D^\pm\pi^\mp$	1	$< 6.82 \pm 0.81$	$< 7.10 \pm 0.77$
$\mathsf{P} \to VP$		$g_{\mathsf{P}VP}$ ($\times 10^{-6}$ MeV^{-2})	
$D_1^\pm(2420) \to D^{*0}(2007)\pi^\pm$	1	$< 10.1 \pm 2.6$	$< 9.2 \pm 1.3$
$D_1^0(2420) \to D^{*\pm}(2010)\pi^\mp$	1	$< 7.8 \pm 1.6$	$< 8.0 \pm 1.2$
$D_{s1}^\pm(2536) \to D^{*\pm}(2010)K^0$	1	$\leftarrow$	< 23.9
$D_{s1}^\pm(2536) \to D^{*0}(2007)K^\pm$	1	$\leftarrow$	< 17.9
$D_2^{*\pm}(2460) \to D^{*0}(2007)\pi^\pm$	1	$< 8.9 \pm 2.0$	$< 9.3 \pm 2.0$
$D_2^{*0}(2460) \to D^{*\pm}(2010)\pi^\mp$	1	$< 8.8 \pm 1.0$	$< 9.09 \pm 0.99$
$\mathsf{D} \to PP$		$g_{\mathsf{D}PP}$ ($\times 10^{-6}$ MeV^{-2})	
$\psi(3770) \to D\bar{D}$	1	$\leftarrow$	$< 92 \pm 27$

Table 4.14: Upper bounds of excited heavy meson coupling constants provided by experimental measures.

The main purpose of Table 4.14 is to show the upper bound measures are consistent with the light meson results, and it is unfortunate that no definite measures of branching fractions have been collated for us to study. However, there are a few interesting results in the full listings of the Particle Data Tables,

$$\Gamma_{D_2^{*+}(2460)\to D^0\pi^+}/\Gamma_{D_2^{*+}(2460)\to D^{*0}(2007)\pi^+} = 1.9 \pm 1.1 \pm 0.3, \quad (4.31)$$

$$\Gamma_{D_2^{*0}(2460)\to D^+\pi^-}/\Gamma_{D_2^{*0}(2460)\to D^{*+}(2010)\pi^-} = 2.3 \pm 0.6. \quad (4.32)$$

These ratios in the supermultiplet theory are given by

$$\frac{\Gamma_{D_2^{*+}(2460)\to D^0\pi^+}}{\Gamma_{D_2^{*+}(2460)\to D^{*0}(2007)\pi^+}} = \left(\frac{g_{PPP}}{g_{PVP}}\right)^2 \frac{8}{3m^2_{D_2^{*+}}} \frac{\lambda^{5/2}(m^2_{D_2^{*+}}, m^2_{D^0}, m^2_{\pi^+})}{\lambda^{5/2}(m^2_{D_2^{*+}}, m^2_{D^{*0}}, m^2_{\pi^+})},$$

$$\frac{\Gamma_{D_2^{*0}(2460)\to D^+\pi^-}}{\Gamma_{D_2^{*0}(2460)\to D^{*+}(2010)\pi^-}} = \left(\frac{g_{PPP}}{g_{PVP}}\right)^2 \frac{8}{3m^2_{D_2^{*0}}} \frac{\lambda^{5/2}(m^2_{D_2^{*0}}, m^2_{D^+}, m^2_{\pi^-})}{\lambda^{5/2}(m^2_{D_2^{*0}}, m^2_{D^{*+}}, m^2_{\pi^-})},$$

and from the symmetry condition $g_{PPP}/g_{PVP} = m/2$, the results (4.31) and (4.32) imply

$$m = 2153 \pm 623 \pm 170 \text{ MeV}, \quad (4.33)$$

$$m = 2368 \pm 309 \text{ MeV}, \quad (4.34)$$

respectively. These are significantly different from the mass determined from the studies of the light mesons for which $N_f = 3$. They are consistent with $m \to m_{D_2^*(2460)}$, which may be associated with an increase in the central meson mass in going from $N_f = 3$ to $N_f = 4$. It may also be indicative of some symmetry breaking mechanism which leads to a mass scaling behaviour in g_{PPP} and/or g_{PVP}. Unfortunately, the results (4.31) and (4.32) provide no means of determining whether both or only one coupling is subject to mass scaling behaviour. This restricts our ability to supply predictions about decay widths and so forth. Nonetheless, we can make some interesting predictions after some reasonable assumptions about the decay modes of the heavy excited mesons.

4.5.2 Predictions of excited heavy meson decay widths

If we assume two body strong and electromagnetic interactions are the predominant decay modes for the excited heavy mesons we can use the measured full width to calculate the coupling constants involved. This enables us to easily make partial width predictions.

We begin with the $D_2^*(2460)$ meson as the results (4.31) and (4.32) give us crucial information about the ratio g_{PPP}/g_{PVP}. If we account for all two-body strong and electromagnetic decays permitted by phase space then we should have an approximation to the full decay width as these processes should dominate over non-Zweig allowed and weak interactions. Unfortunately, the method ignores the three-body meson decays, which may be a significant contribution. This may be particularly true for the two pion widths like $D_2^* \to D^*\pi\pi$ (as seen in the $K_2^*(1430)$ decays where $\mathrm{Br}(K_2^* \to K^*\pi\pi) = 13\%$), so at best we shall produce upper bounds on the two body processes. However, there is some theoretical evidence to suggest the two pion width for $D_2^*(2460)$ is small [53] so our predictions should be comparable to those of other studies which also ignore the three body decay modes [51, 33]. If this project had included study of three-body processes in the $\tilde{U}(4N_f)$ scheme we could have included these contributions in the prediction.

The allowed two-body transitions of the $D_2^*(2460)$ meson are listed in Table 4.15 along with corresponding Clebsch–Gordan factors. If these are the only contributions to the full width, then

$$\Gamma_{D_2^*(2460)\to\mathrm{all}} = \Gamma_{D_2^*(2460)\to PP} + \Gamma_{D_2^*(2460)\to VP} + \Gamma_{D_2^*(2460)\to P\gamma}. \qquad (4.35)$$

Using the experimental full widths, $\Gamma_{D_2^{*\pm}(2460)\to\mathrm{all}} = 25 \pm 8 \pm 7$ MeV and $\Gamma_{D_2^{*0}(2460)\to\mathrm{all}} = 23 \pm 5$ MeV [13] along with the $\tilde{U}(4N_f) \times 0(3)_L$ relation $g_{PPP}/g_{PVP} = m/2$ and VMD, we can evaluate all the kinematical factors in Equation (4.35) to evaluate g_{PPP}. We choose $m = 2330 \pm 280$ MeV[2] to derive

$$g_{PPP} = (4.94 \pm 1.21) \times 10^{-3}\ \mathrm{MeV}^{-1} \text{ from } \Gamma_{D_2^{*\pm}(2460)\to\mathrm{all}},$$

[2]the weighted average of (4.33) and (4.34), so our mass value is consistent with the results (4.31) and (4.32).

Decay process	Clebsch-Gordan factor
$D_2^*(2460) \to D\pi^{\pm,0}$	$1, \sqrt{1/2}$
$D_2^*(2460) \to D\eta$	$\sqrt{\frac{1}{6}}\left(\cos\theta_P - \sqrt{2}\sin\theta_P\right)$
$D_2^*(2460) \to D^*\pi^{\pm,0}$	$1, \sqrt{1/2}$
$D_2^{*\pm}(2460) \to D^{\pm}\gamma$	$\frac{e}{6\times 0.1359}\left(-\frac{3}{m_{\rho^0}^{1/2}} + \frac{1}{m_{\omega_8}^{1/2}} - \frac{4}{m_{J/\psi}^{1/2}}\right)$
$D_2^{*0}(2460) \to D^0\gamma$	$\frac{e}{6\times 0.1359}\left(-\frac{3}{m_{\rho^0}^{1/2}} - \frac{1}{m_{\omega_8}^{1/2}} + \frac{4}{m_{J/\psi}^{1/2}}\right)$

Table 4.15: Two-body decays of the $D_2^*(2460)$ meson and corresponding Clebsch–Gordan factors.

$$g_{PPP} \;=\; (4.77 \pm 0.77) \times 10^{-3}\ \text{MeV}^{-1} \text{ from } \Gamma_{D_2^{*0}(2460)\to \text{all}}.$$

A weighted average of these results is $g_{PPP} = (4.82 \pm 0.65) \times 10^{-3}$ MeV^{-1}, which is of comparable magnitude with our rough average from the light meson sector $g_{PPP} \simeq 2.9 \times 10^{-3}$ MeV^{-1}, with some indication of a mass scaling behaviour. If we assume this coupling to apply to all charm heavy mesons with $L = 1$, then we can predict numerous partial widths as provided in Table 4.16 and 4.17, where we have also compared these to experimental measures and other theoretical predictions.

Most of our predictions are not dissimilar to those of other techniques. The full width prediction for the $D_1(2420)$ meson is significantly lower than the measured value. This may be due to large contributions from two pion widths and other processes not considered (including transitions to excited and ground state mesons). Other research with similarly low predictions [53, 33] attribute the disparity to mixing between the D_1 and D_1' ($^3P_2$) states, much like that of the K_{1B} and K_{1A}. In a recent analysis [54], such a suggestion seems to be disfavoured by the experimental evidence (but not ruled out).

Decay mode		Width (typically MeV)				
$^2P_3$ parent	$\tilde{U}(4N_f) \times O(3,1)_L$	[13][a]	[51][b]	[39][c]	[96][d]	Various
$D_2^{*+} \to D^+\pi^0$	5.4 ± 1.5		16	15	6	22.3 [100][e]
$D_2^{*+} \to D^0\pi^+$	11.0 ± 3.0					
$D_2^{*+} \to D^+\eta$	21.5 ± 5.8 keV		0.1			
$D_2^{*+} \to D^{*+}\pi^0$	2.43 ± 0.66		9	6.8	18	14.6 [100][e]
$D_2^{*+} \to D^{*0}\pi^+$	5.0 ± 1.4					
$D_2^{*+} \to D^+\gamma$	61 ± 17 keV					38 ± 19 keV [112][f]
$D_2^{*+} \to$ all	23.8 ± 3.6	$25 \pm {}^{8}_{7}$	28		33	
$D_2^{*0} \to D^0\pi^0$	5.6 ± 1.5		16	15	6	22.3 [100][e]
$D_2^{*0} \to D^+\pi^-$	10.6 ± 2.9					
$D_2^{*0} \to D^0\eta$	28.1 ± 7.6 keV					
$D_2^{*0} \to D^{*0}\pi^0$	2.51 ± 0.68		9	6.8	18	14.6 [100][e]
$D_2^{*0} \to D^{*+}\pi^-$	4.8 ± 1.3					
$D_2^{*0} \to D^0\gamma$	14 ± 3.8 keV					13 ± 7 keV [112][f]
$D_2^{*0} \to$ all	23.5 ± 3.5	23 ± 5	28		33	21 ± 5 [33][g]
$D_{sJ}^+ \to D^+K^0$	4.2 ± 1.1		7	7.5		
$D_{sJ}^+ \to D^0K^+$	4.7 ± 1.3					
$D_{sJ}^+ \to D_s^+\eta$	85 ± 23 keV		0.1			
$D_{sJ}^+ \to D^{*+}K^0$	0.38 ± 0.10		< 1	0.67		
$D_{sJ}^+ \to D^{*0}K^+$	0.50 ± 0.13					
$D_{sJ}^+ \to D_s^+\gamma$	62 ± 17 keV					
$D_{sJ}^+ \to$ all	10.0 ± 1.7	$15 \pm {}^{5}_{4}$	7			

[a] Experimental measures
[b] using HQET
[c] using relativistic Bethe-Salpeter approach
[d] using $SU(4)$
[e] using Heavy-Light System assumptions
[f] using Finite Energy Sum Rule techniques
[g] using QCD Sum Rule methods

Table 4.16: Predicted decay rates of the $^3P_2$ heavy charm mesons, $D_2^*(2460)$ and $D_{sJ}^*(2573)$. Widths typically MeV except when stated otherwise.

Table 4.17: Predicted decay rates of the $^1P_1$ heavy charm mesons, $D_1(2420)$ and $D_{s1}(2536)$.. Widths typically MeV except when stated otherwise.

Decay mode	Width (typically MeV) from model[a]					
	$\tilde{U}(4N_f) \times O(3,1)_L$	Exp.	HQET	QCDSR	HQET	HQET	B-S
$^1P_1$ parent		[13]	[51]	[33]	[55]	[31]	[39]
$D_1^+ \to D^{*+}\pi^0$	5.6 ± 1.5		11				8.0
$D_1^+ \to D^{*0}\pi^+$	2.76 ± 0.75						
$D_1^+ \to D^+\gamma$	$(48 \pm 13)/10^6$				0.69 keV	< 2.3 keV	
$D_1^+ \to$ all	8.4 ± 1.7	28 ± 8	18	~ 6			
$D_1^0 \to D^{*0}\pi^0$	5.1 ± 1.4		11				8.0
$D_1^0 \to D^{*+}\pi^-$	2.71 ± 0.73						
$D_1^0 \to D^0\gamma$	166 ± 45 keV				410 keV	14 ± 6 keV	
$D_1^0 \to$ all	$\approx 8.0 \pm 1.6$	$18.9 \pm {}^{4.6}_{3.5}$	18	~ 6			
$D_{s1}^+ \to D^{*+}K^0$	0.069 ± 0.018		< 1				0.16
$D_{s1}^+ \to D^{*0}K^+$	0.123 ± 0.033						
$D_{s1}^+ \to D_s^+\gamma$	$(1.63 \pm 0.44)/10^4$						
$D_{s1}^+ \to$all	$\approx 0.192 \pm 0.033$	< 2.3					

[a]Abbreviations: Exp.=Experiment, HQET=Heavy Quark Effective Theory, QCDSR=QCD Sum Rule,B-S=Bethe Salpeter

4.6 Summary

The supermultiplet scheme has been applied to all known $N = 1$ orbitally excited mesons consistent with a $q\bar{q}$ bound state. For each orbital excitation number L we found the possible 36 mesons from the 4 nonets ${}^3L_{L+1}$, ${}^3L_L$, ${}^3L_{L-1}$ and ${}^1L_L$ were describable in terms of a single super-wavefunction (4.3) and that the physical mesons occupied these nonets satisfactorily; vacancies are due to the lack of experimental observation of the states. The only nonet which posed particular problems was the ${}^3P_0$ mesons, or scalars. This was mainly due to the confusion regarding the possible $q\bar{q}$ assignments of the scalar mesons. Hopefully, the situation will be rectified in the next few years and if the states can be understood in terms of $q\bar{q}$ bound states, there would be nothing preventing their study in the context of the supermultiplet scheme.

The main test of the supermultiplet scheme for the excited mesons has been in its application to the two-body strong decays from excited meson parent to ground state daughters. By all accounts the scheme is very successful; the uniformity in coupling constants for a large range of processes indicates the symmetry is good. The experimental data suggests that for a given value of parent orbital angular momentum L, all decays to two pseudoscalars, PP can be calculated by the single coupling constant $g_{\mathsf{L}PP}$; all decays to a vector and pseudoscalar, VP by $g_{\mathsf{L}VP}$. The exact $\tilde{U}(4N_f) \otimes O(3,1)_L$ symmetry predicts $g_{\mathsf{L}PP}/g_{\mathsf{L}VP} = m/2$, and for $\mathsf{L} = \mathsf{P}$ and D we found $m = 800 - 900$ MeV, in the light sector. This is also consistent with the value derived from the study of the two-body strong decays of the ground state mesons. With the limited data available for the F-wave mesons, we could test the relation $g_{\mathsf{L}PP}/g_{\mathsf{L}VV} = m$ and obtained $m \simeq 700$ MeV.

There were some deviations from uniformity in the coupling constants, but usually this could be attributed to a possible problem with the experimental data. Unfortunately study of the light sector excited states is difficult and not the priority of many experimentalists. We can only hope this situation improves; the increased theoretical attention on the P-wave heavy

mesons may spur them on. We found the supermultiplet scheme easily accommodated the heavy states (with $N_f = 4$) and we provided numerous calculations on the two-body strong and electromagnetic partial decay widths of these states. Many of these were consistent with experiment, and the comparison with other theoretical predictions in Tables 4.16 and 4.17 will be interesting to look upon in the future.

There were indications of a higher symmetry group acting on the excited mesons. This was observed in the consistent scaling of $g_{\mathsf{LSS}}/g_{(\mathsf{L}+1)\mathsf{SS}}$ where S is a ground state meson. Typically the ratio was found to be $g_{\mathsf{LSS}}/g_{(\mathsf{L}+1)\mathsf{SS}} \sim$ 2000 MeV for $\mathsf{L} = \mathsf{S}, \mathsf{P}, \mathsf{D}$ and F which encompasses an extraordinary range of the known mesons. This consistency may originate from a higher symmetry group. Consideration of the dynamical approximations of the supermultiplet scheme may expose the source of this interesting scaling; a potential source of further study.

Chapter 5

Meson decays in a quark triangle scheme

The earlier chapters have all relied on the $\tilde{U}(4N_f) \times O(3,1)_L$ scheme as a means of obtaining the *most* general coupling constants at the meson level. The work indicates this notion is relatively successful as we have observed uniform coupling constants from $L = 0$ to $L = 4$. In the ground states, any deviations from the perfect symmetry were seen to follow a set breaking mechanism which was then harnessed to provide additional predictions, showing that no predictive power had been lost. What was most striking in the studies of the ground and excited state mesons was the inadequacy of combined VMD and supermultiplet scheme to account for the electromagnetic decays.

This inadequacy was best seen in the large, unexpected deviation from $\tilde{U}(12)$ theory in the $K^* \to K\gamma$ decays as discussed in Section 3.4.3. The supermultiplet theory (without a "mass scaling" g'_{VPP}) matches the exact $SU(3)$ prediction: $g_{K^{*0}K^0\gamma}/g_{K^{*+}K^+\gamma} = -2$. However, experimentalists report $|g_{K^{*0}K^0\gamma}/g_{K^{*+}K^+\gamma}| = 1.51 \pm 0.13$, a substantial difference. A possible explanation for this difference stems from the unknown form of vector meson dominance in the $q^2 \to 0$ limit; it is only accurately known for $q^2 = m_V^2$ from $V \to l\bar{l}$ decays. Hence there is some uncertainty in extrapolating vec-

tor meson dominance to the off–shell case. Another reason for the disparity may have been in the "mass scaling" behaviour of g'_{VPP} where from $V \to l\bar{l}$ transitions we observed $g'_{VPP}(V) \propto m_V^{1/2}$. When we introduced this symmetry breaking mechanism into the analysis, the theoretical expectation became $g_{K^{*0}K^0\gamma}/g_{K^{*+}K^+\gamma} = -1.87$, closer to experiment, but still substantially different.

This conflict, along with the need to better understand the electromagnetic interactions of the mesons, provides the motivation for this Chapter. We sought a method which easily allowed for arbitrary off–shell propagation of the quarks; a factor excluded in the effective dynamics of the $\tilde{U}(4N_f)$ model. A convenient and apparently successful method for doing this was by use of a quark triangle diagram; which has given accurate predictions for $\pi^0 \to \gamma\gamma$ decay widths [4] and pion and kaon charge radii [4, 111]. It has also been applied to the K^* radiative decay problem *in a form which used chiral and isospin symmetry* [25]. The loop integral arising from the triangle diagram could incorporate different quark masses and hence propagators in the loop; in so doing it matched the experimental result with reasonable quark mass values.

The quark triangle diagram uses meson–quark–antiquark vertex couplings of the form $g_{Pqq'}\gamma_5$ for the pseudoscalar meson and $g_{Vqq'}\gamma^\mu$ for the vector meson. These are the universal coupling constants we shall now examine; we anticipate them to be more stable than the meson level couplings considered in the previous chapters, but this stability is at the expense of many more couplings required for the various quark flavours. To examine these couplings we *formulate an approximation free form* of the quark loop integral and apply it to known $P \to \gamma\gamma$ decays to determine $g_{Pqq'}$ and then to $V \to P\gamma$ decays to obtain the product $g_{Vq\bar{q}'}g_{Pq\bar{q}'}$ for different quark flavors. As a final check, we test the method on $\phi \to \rho\pi$ decay.

The results indicate that the meson–quark–antiquark couplings in VVP vertex type interactions determined from different channels which involve common constituent quarks are remarkably uniform, suggesting that the ef-

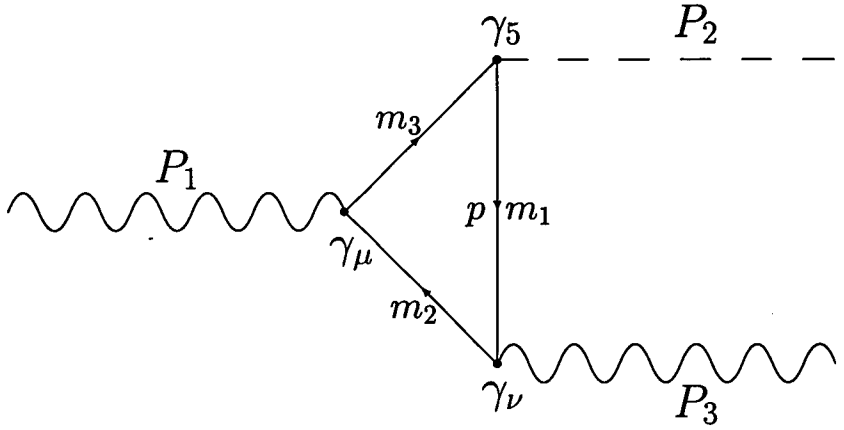

Figure 5.1: Quark triangle diagram.

fective vertex in the quark triangle diagram is valid. The data also demonstrates that the triangle method should be highly predictive due to the stability of the couplings. Finally we use the method in the heavy meson sector to predict coupling ratios of the form $g_{V^0P^0\gamma}/g_{V^+P^+\gamma}$ where the only free parameters required are the constituent quark masses. Our result for D^* decays fall within other theoretical estimates, while that of B^* is sensitive to b quark mass.

5.1 The quark triangle integral

There are three types of ground state mesonic transitions which can be described in terms of a non-divergent Feynman one-loop graph, namely $V \to VP$, $V \to P\gamma$ (or equivalently $P \to V\gamma$) and $P \to \gamma\gamma$. These can be treated by the same Feynman graph, but with differing vertex couplings and external momenta P_i where $P_1 = P_2 + P_3$. The quark triangle of Figure 5.1, shows the one-loop diagram of the three particle vertex.

The three external particles are composed of two spin 1 particles (vector mesons or photons) and one spin 0 particle, the pseudoscalar meson. The internal propagators of the loop are the spin $\frac{1}{2}$ quarks of mass m_i. In the

constituent quark model the higher-order gluonic corrections effectively dress the current quarks so m_i are the *constituent* quark masses, and this assumption is supported by studies into the meson charge radii using the quark triangle approach [111, 3, 4]). The quark triangle diagram corresponds to the Feynman loop integral

$$\int \frac{d^4p}{(2\pi)^4} \mathrm{Tr}\left[\gamma_\nu \frac{1}{\not p - m_1}\gamma^5 \frac{1}{\not p + \not P_2 - m_3}\gamma_\mu \frac{1}{\not p - \not P_3 - m_2}\right], \tag{5.1}$$

$$= 4\epsilon^{\mu\nu\rho\sigma}\int \frac{d^4p}{(2\pi)^4}\frac{p_\rho(P_{2\sigma}m_2 + P_{3\sigma}m_3) + P_{1\rho}(p-P_3)_\sigma m_1}{[p^2-m_1^2]\,[(p+P_2)^2-m_3^2]\,[(p-P_3)^2-m_2^2]}. \tag{5.2}$$

where the possible coupling factors $g_{Vqq'}, eQ_i, g_{Pqq'}$ for the vector, photon and pseudoscalar vertex respectively, have been omitted from the above (Q_i is the charge of the quark and anti-quark of mass m_i at the photon vertex). These couplings are included in the Feynman amplitude depending on which specific transition type is under scrutiny. We use Feynman's parametrization to re-express the denominator,

$$\begin{aligned}
&\frac{1}{[p^2-m_1^2]\,[(p+P_2)^2-m_3^2]\,[(p-P_3)^2-m_2^2]} \\
&\quad = 2\int_0^1 x\,dx\int_0^1 dy\left[(p^2-m_1^2)xy + \left((p+P_2)^2-m_3^2\right)x(1-y)\right. \\
&\qquad\qquad \left. + \left((p-P_3)^2-m_2^2\right)(1-x)\right]^{-3} \\
&\quad = 2\int_0^1 x\,dx\int_0^1 dy\left[p'^2 - M'^2\right]^{-3}
\end{aligned}$$

where p' is the momentum shift and M' the effective mass

$$\begin{aligned}
p' &= p + P_2x(1-y) - P_3(1-x), \\
M'^2 &= m_1^2xy + m_2^2(1-x) + m_3^2x(1-y) \\
&\quad -P_1^2x(1-y)(1-x) - P_2^2x^2y(1-y) - P_3^2xy(1-y).
\end{aligned}$$

With these definitions, the momentum integral (5.2) can be completed via

$$\int \frac{d^4p'}{(2\pi)^4}\frac{1}{[p'^2-M'^2]^3} = \frac{i}{2(4\pi)^2}\left(-\frac{1}{M'^2}\right),$$

and with the change of variables $u = x(1-y)$, $v = 1-x$, the most economical version of the overall result is

$$\frac{-i}{4\pi^2}\epsilon_{\mu\nu\rho\sigma}P_1^\rho P_3^\sigma \int_0^1 du \int_0^{1-u} dv\,[m_1 + (m_3 - m_1)u + (m_2 - m_1)v]\,/ \\ \left[m_1^2 + (m_3^2 - m_1^2)u + (m_2^2 - m_1^2)v - M_1^2 uv - (M_2^2 u + M_3^2 v)(1-u-v)\right]$$

where the external particles are on-shell, so we replace $P^2 = M^2$. By defining the quantity

$$\begin{aligned} & J_{m_1,m_2,m_3}(M_1, M_2, M_3) \\ & \quad \equiv \; m_1 \int_0^1 du \int_0^{1-u} dv\,[m_1 + (m_3 - m_1)u + (m_2 - m_1)v]\,/ \\ & \qquad \left[m_3^2 u + m_2^2 v - M_1^2 uv + (m_1^2 - M_2^2 u - M_3^2 v)(1-u-v)\right] \end{aligned} \quad (5.3)$$

where the external m_1 ensures a massless dimension, we can write down the Feynman amplitudes for the three types of decays:

$$\begin{aligned} A(V \;\to\; PV') &= i\tfrac{N_C}{4\pi^2} g_{Vq_2q_3}\varepsilon^\mu \varepsilon'^\nu P_V^\rho P_{V'}^\sigma \epsilon_{\mu\nu\rho\sigma} \times \\ &\quad [g_{Vq_1q_2} g_{Pq_1q_3} J_{m_1,m_2,m_3}(M_V, M_P, M_{V'})/m_1 + (m_2 \leftrightarrow m_3)] \quad (5.4) \\ A(V \;\to\; P\gamma) &= i\tfrac{N_C}{4\pi^2} g_{Vq\bar{q}} g_{Pq\bar{q}} e\varepsilon^\mu \varepsilon^\nu P_V^\rho P_\gamma^\sigma \epsilon_{\mu\nu\rho\sigma} \times \\ &\quad [Q J_{m,m,\bar{m}}(M_V, M_P, M_\gamma)/m + \bar{Q} J_{\bar{m},\bar{m},\bar{m}}(M_V, M_P, 0)/\bar{m}] \quad (5.5) \\ A(\gamma \;\to\; P\gamma) &= i\tfrac{N_C}{2\pi^2} g_{Pq\bar{q}} e^2 Q^2 \varepsilon^\mu \varepsilon'^\nu P_\gamma^\rho P_{\gamma'}^\sigma \epsilon_{\mu\nu\rho\sigma} J_{m,m,m}(0, M_P, 0)/m \quad (5.6) \end{aligned}$$

where ε is the vector or photon polarization vector, $P_V(M_V)$, $P_P(M_P)$, $P_\gamma(0)$ is the on-shell vector, pseudoscalar and photon four-momenta(mass), respectively, $g_{Vqq'}(g_{Pqq'})$ is the vector–quark–antiquark (pseudoscalar–quark–antiquark) coupling constant and eQ is the electric charge of the quark of mass m in the loop. We now go on to solve each case in the most general terms possible.

5.1.1 $V \to PV'$ loop integral

The most complex loop integral of those considered is $J_{m_1,m_2,m_3}(M_V, M_P, M_{V'})$. Although not intractable [46], it is nonetheless very difficult without the help

of simplifying assumptions. There is only one experimentally known transition of this type we can apply the quark triangle technique to $\phi \to \rho\pi$, so it is not of substantial benefit to solve the most general case. Thus we use some very reasonable approximations; since this channel only involves u or d quark flavours in the loop at any one time and as isospin is a good symmetry, we can assume $m_u = m_d = m$. Under this assumption (5.3) simplifies to

$$\begin{aligned} & J_{m,m,m}(M_V, M_P, M_{V'}) \\ &= \int_0^1 dx \int_0^{1-y} dy \frac{m^2}{m^2 - M_V^2 xy - (M_P^2 x + M_{V'}^2 y)(1-x-y)}. \end{aligned}$$

This case is solvable, but a fair degree of complexity remains. If we use the further approximation $M_\pi^2 = 0$ (soft pion limit) the solution is much easier to obtain. By reversing the order of integration we find

$$\begin{aligned} & J_{m,m,m}(M_V, M_\pi, M_{V'}) \\ &\simeq J_{m,m,m}(M_V, 0, M_{V'}) \\ &= \frac{-m^2}{M_V^2 - M_{V'}^2} \int_0^1 \frac{dx}{x} \left(\ln \left| m^2 - M_V^2 x + M_V^2 x^2 \right| \right. \\ &\qquad \left. - \ln \left| m^2 - M_{V'}^2 x + M_{V'}^2 x^2 \right| \right), \\ &= \frac{m^2}{M_V^2 - M_{V'}^2} \sum_{k=\pm} \mathrm{Li}_2(v_m^k(M_V)) - \mathrm{Li}_2(v_m^k(M_{V'})), \end{aligned} \tag{5.7}$$

with $v_m^\pm(M) = \left(M^2 \pm \sqrt{M^4 - 4M^2 m^2} \right) / m^2$ provided $M > 2m$ (which is quite reasonable with the ρ and ϕ mesons and the u and d quarks, $m_{u,d} < 380$ MeV).

If we compare (5.4) with the standard covariant form,

$$A(V \to PV') = i g_{VPP} \varepsilon^\mu \varepsilon'^\nu P_V^\rho P_{V'}^\sigma \epsilon_{\mu\nu\rho\sigma}$$

we find a direct relation between the quark level and covariant couplings,

$$\begin{aligned} g_{VVP} &= -i \frac{N_c}{4\pi^2} g_{Vq_2q_3} \left[g_{Vq_1q_2} g_{Pq_1q_3} J_{m_1,m_2,m_3}(M_V, M_P, M_{V'})/m_1 \right. \\ &\qquad \left. + (q_2, m_2 \leftrightarrow q_3, m_3) \right]. \end{aligned}$$

In the case we have considered, where $m_1 = m_2 = m_3 \equiv m$ and $M_P \to 0$, this general form simplifies to

$$g_{VVP} = -\frac{2N_c}{4\pi^2} g_{Vqq}^2 g_{Pqq} J_{m,m,m}(M_V, 0, M_{V'})/m,$$

where $J_{m,m,m}(M_V, 0, M_{V'})$ is stated in (5.7).

5.1.2 $V \to P\gamma$ loop integral

The transition $V \to P\gamma$ places two constraints on J, which are beneficial to finding the solution. Firstly, as the quarks at the photon vertex must be of the same flavour (to annihilate to form a photon) they are therefore of the same mass. Secondly, the external photon is on-shell so $P_\gamma^2 = 0$. Thus we need to evaluate

$$J_{m,m,\bar{m}}(M_V, M_P, 0) = m \int_0^1 dx \int_0^{1-x} dy \frac{m + (\bar{m} - m)x}{m^2 + (\bar{m}^2 - m^2)x - M_V^2 xy - M_P^2 x(1 - x - y)} \quad (5.8)$$

where m is the mass of the quarks at the photon vertex (that is, $m_1 = m_2 \equiv m$) and $\bar{m} \equiv m_3$ is the only other quark mass in the loop. Performing the integrations,

$$\begin{aligned} J_{m,m,\bar{m}}(M_V, M_P, 0) &= \\ &\frac{-m^2}{M_V^2 - M_P^2} \int_0^1 dx\, (\delta + 1/x) \left[\ln \left| \left(m^2 - (m^2 - \bar{m}^2 + M_V^2)x + M_V^2 x^2 \right) / m^2 \right| \right. \\ &\qquad \left. - \ln \left| \left(m^2 - (m^2 - \bar{m}^2 + M_P^2)x + M_P^2 x^2 \right) / m^2 \right| \right] \\ &= \frac{m^2}{M_V^2 - M_P^2} \sum_{h=a,b} j_{m,\bar{m}}^h(M_V) - j_{m,\bar{m}}^h(M_P), \end{aligned}$$

where

$$\begin{aligned} \delta &= \frac{m - \bar{m}}{m}, \\ j_{m,\bar{m}}^a(M) &= -\int_0^1 \frac{dx}{x} \ln \left| \left(m^2 - (m^2 - \bar{m}^2 + M^2)x + M^2 x^2 \right) / m^2 \right|, \\ j_{m,\bar{m}}^b(M) &= -\delta \int_0^1 dx \ln \left| \left(m^2 - (m^2 - \bar{m}^2 + M^2)x + M^2 x^2 \right) / m^2 \right|. \end{aligned}$$

The terms j^k can be calculated rather easily with some assumptions about the size of quark masses in relation to meson masses. However, we intend to use $J_{m,m,\bar{m}}(M_V, M_P, 0)$ across a wide range of prospective mass values, so we wish to obtain the most general expression. To this end, we evaluate the components j^k generally.

Determination of j^a

j^a turns out to be expressible in terms of the dilogarithm function, $\mathrm{Li}_2(z)$ [84]. To see this we factorize the argument of the natural logarithm,

$$j^a_{m,\bar{m}}(M) = -\int_0^1 \frac{dx}{x}\left(\ln\left|1 - v^+_{m,\bar{m}}(M)x\right| + \ln\left|1 - v^-_{m,\bar{m}}(M)x\right|\right)$$

where

$$\begin{aligned} v^\pm_{m,\bar{m}}(M) &= \left(-\delta^2 + 2\delta - (M/m)^2\right. \\ &\quad \left. \mp[(\delta^2 + 2\delta - (M/m)^2)^2 - (2M/m)^2]^{1/2}\right)/2 \qquad (5.9) \\ &= \left[m^2 - \bar{m}^2 + M^2 \pm \lambda^{1/2}(m^2, \bar{m}^2, M^2)\right]/2m^2, \qquad (5.10) \end{aligned}$$

and

$$\lambda(m^2, \bar{m}^2, M^2) = [M^2 - (m + \bar{m})^2][M^2 - (m - \bar{m})^2] \qquad (5.11)$$

is the function introduced in Section 3.1.3. The factorization we have performed does not necessarily lead to real $v^\pm_{m,\bar{m}}(M)$ as $\lambda(m^2, \bar{m}^2, M^2)$ may be negative. We consider both cases:

Real $v^\pm_{m,\bar{m}}(M)$ The $v^\pm_{m,\bar{m}}(M)$ is only real when $\lambda(m^2, \bar{m}^2, M^2) \geq 0$ which from (5.11) implies

$$M \geq m + \bar{m} \quad \text{or} \quad M \leq |m - \bar{m}|\,. \qquad (5.12)$$

When we are assured of real $v^\pm_{m,\bar{m}}(M)$ the solution of j_1 is related to the standard dilogarithm function,

$$j^a_{m,\bar{m}}(M) = -\sum_{k=\pm}\int_0^1 dx \frac{\ln\left|1 - v^k_{m,\bar{m}}(M)x\right|}{x} \qquad (5.13)$$

$$
\begin{aligned}
&\equiv \sum_{k=\pm} \mathrm{Li}_2(v^k_{m,\bar{m}}(M), 0) \\
&= \begin{cases} \sum_{k=\pm} \mathrm{Li}_2(v^k_{m,\bar{m}}(M)) \text{ for } v^k_{m,\bar{m}}(M) \leq 1 \\ \sum_{k=\pm} \mathrm{Li}_2(v^k_{m,\bar{m}}(M)) + i\pi \ln v^k_{m,\bar{m}}(M) \text{ for } v^k_{m,\bar{m}}(M) > 1, \end{cases}
\end{aligned}
$$

Complex $v^{\pm}_{m,\bar{m}}(M)$ The $v^k_{m,\bar{m}}(M)$ are complex if $\lambda(m^2, \bar{m}^2, M^2) < 0$. This results in the $j_{m,\bar{m}}(M)$ being related to a dilogarithm function with a complex argument. To show this, we express j_1 as

$$
\begin{aligned}
j_1(M) &= -\sum_{k=\pm} \int_0^1 \frac{dx}{x} \ln\left|1 - v^k_{m,\bar{m}}(M)x\right| \\
&= -\sum_{k=\pm} \int_0^{\rho(M)\exp(i\phi^k_{m,\bar{m}}(M))} dz \frac{\ln(1-z)}{z} \\
&= -\sum_{k=\pm} \frac{1}{2} \int_0^{\rho(M)} \frac{dx}{x} \ln(1 - 2x\cos\phi^k_{m,\bar{m}}(M) + x^2) \\
&\qquad + i \int_0^{\rho(M)} \frac{dy}{y} \arctan\left[\frac{y \sin\phi^k_{m,\bar{m}}(M)}{1 - y\cos\phi^k_{m,\bar{m}}(M)}\right] \\
&= -\int_0^{\rho(M)} \frac{dx}{x} \ln(1 - 2x\cos\phi^k_{m,\bar{m}}(M) + x^2) \\
&\equiv 2\mathrm{Li}_2(\rho(M), \phi_{m,\bar{m}}(M)),
\end{aligned} \tag{5.14}
$$

where

$$
\rho(M) = M/m, \quad \phi = \phi^+ = -\phi^- \text{ and } \cos\phi_{m,\bar{m}}(M) = \frac{m^2 - \bar{m}^2 + M^2}{2Mm}.
$$

Determination of $j^b_{m,\bar{m}}(M)$

$j^b_{m,\bar{m}}(M)$ is a simpler integral to evaluate as it does not contain the $1/u$ dependence. Recall,

$$
j^b_{m,\bar{m}}(M) = -\delta \int_0^1 dx \ln\left|1 - (1 - \bar{m}^2/m^2 + M^2/m^2)x + M^2x^2/m^2\right|,
$$

which, by standard techniques, reduces to

$$
\begin{aligned}
j^b_{m,\bar{m}}(M) &= \frac{m - \bar{m}}{m\,M^2} \left[(\bar{m}^2 - m^2 + M^2) \ln\left(\frac{\bar{m}}{m}\right)\right. \\
&\qquad \left. -\lambda^{1/2}(m^2, \bar{m}^2, M^2) \mathrm{arctanh}\left(\frac{\lambda^{1/2}(m^2, \bar{m}^2, M^2)}{\bar{m}^2 + m^2 - M^2}\right)\right],
\end{aligned}
$$

and is valid for all $m, \bar{m}, M$. It is also useful to express $j_2(M)$ in terms of real $v_{1,2}(M)$. Following a similar method to that used for deriving j_1, we find

$$j^b_{m,\bar{m}}(M) = -\delta \sum_{k=\pm} (1 - 1/v^k_{m,\bar{m}}(M)) \ln \left|1 - v^k_{m,\bar{m}}(M)\right| \text{ for } \lambda(m^2, \bar{m}^2, M^2) \geq 0.$$

General $J_{m,m,\bar{m}}(M_V, M_P, 0)$: comparison with covariant amplitude
To summarise, the final form of the loop integral is:

$$J_{m,m,\bar{m}}(M_V, M_P, 0) = \frac{m^2}{M_V^2 - M_P^2} \sum_{i=a}^{b} j^i(M_V) - j^i(M_P). \tag{5.15}$$

Here we have not considered the imaginary part in j_1 which is irrelevant to the decay process, and

$$j^a_{m,\bar{m}}(M) = \begin{cases} \sum_{k=\pm} \mathrm{Li}_2(v^k_{m,\bar{m}}(M), 0) & \text{if } \lambda(m^2, \bar{m}^2, M^2) \geq 0 \\ 2\mathrm{Li}_2(\rho(M), \phi_{m,\bar{m}}(M)) & \text{if } \lambda(m^2, \bar{m}^2, M^2) < 0, \end{cases} \tag{5.16}$$

where

$$v^k_{m,\bar{m}}(M) = [m^2 - \bar{m}^2 + M^2 \pm \lambda^{1/2}(m^2, \bar{m}^2, M^2)]/2m^2$$
$$\rho(M) = M/m, \ \cos\phi_{m,\bar{m}}(M) = (m^2 - \bar{m}^2 + M^2)/2Mm,$$

and

$$\begin{aligned} j^b_{m,\bar{m}}(M) \ = \ & \frac{m - \bar{m}}{m\, M^2} \left[(\bar{m}^2 - m^2 + M^2) \ln\left(\frac{\bar{m}}{m}\right) \right. \\ & \left. -\lambda^{1/2}(m^2, \bar{m}^2, M^2) \mathrm{arctanh}\left(\frac{\lambda^{1/2}(m^2, \bar{m}^2, M^2)}{\bar{m}^2 + m^2 - M^2}\right) \right]. \end{aligned}$$

If we compare our quark level amplitude (5.5) with the standard covariant amplitude,

$$A(V \to P\gamma) = i g_{VP\gamma} \epsilon_{\alpha\beta\mu\nu} P_V^\alpha P_\gamma^\beta \varepsilon^\mu \varepsilon^\nu$$

we see that the quark triangle approach leads to the $g_{VP\gamma}$ covariant coupling constant as

$$g_{VP\gamma} = \frac{eN_C}{4\pi^2} g_{Vq\bar{q}} g_{Pq\bar{q}} [Q J_{m,m,\bar{m}}(M_V, M_P, 0)/m + \bar{Q} J_{\bar{m},\bar{m},m}(M_V, M_P, 0)/\bar{m}]. \tag{5.17}$$

5.1.3 $P \to \gamma\gamma$ loop integral

The $P \to \gamma\gamma$ transition has the simplest corresponding one-loop integral as the decay to two photons imposes two very helpful conditions. Firstly, since the photons can only couple to quarks and antiquarks of the same flavour all the quark masses in the loop are identical so that $m_1 = m_2 = m_3 \equiv m$, and secondly $P_\gamma^2 = P_{\gamma'}^2 = 0$ as both external photons are on-shell. Despite the fact that the formulation of the Feynman quark triangle has an incoming spin 1 particle, the loop integral can be easily adapted to accommodate an incoming pseudoscalar meson. We simply need to substitute $M_1^2 \to M_P^2$, $M_{2,3}^2 \to 0$ in (5.3) and $\gamma_\mu \leftrightarrow \gamma_5$ in (5.1). Thus we solve $J_{m,m,m}(M_P, 0, 0)$,

$$\begin{aligned} J_{m,m,m}(M_P,0,0) &= \int_0^1 dx \int_0^{1-x} dy \frac{m^2}{m^2 - M_P^2 uv} \\ &= -\frac{m^2}{M_P^2} \int_0^1 \frac{dx}{x} \ln\left|(m^2 - M_P^2 u + M_P^2 u^2)/m^2\right| \\ &= \frac{m^2}{M_P^2} j^a_{m,m}(M_P). \end{aligned}$$

with the similar conditions on $j^a(M)$ as in (5.16) so that

$$J_{m,m,m}(M_P,0,0) = \frac{m^2}{M_P^2} \times \begin{cases} \sum_{k=\pm} \mathrm{Li}_2\left(v^k_{m,m}(M_P), 0\right) & \text{if } M_P \geq 2m, \\ 2\mathrm{Li}_2\left(\rho(M_P), \phi_{m,m}(M_P)\right) & \text{if } 0 \leq M_P < 2m. \end{cases} \tag{5.18}$$

The substitution $\gamma_\mu \leftrightarrow \gamma_5$ in (5.1) simply leads to a sign change in (5.6), so we find

$$A(P \to \gamma\gamma) = i\frac{N_C}{2\pi^2} g_{Pq\bar{q}} e^2 Q^2 \varepsilon^\mu \varepsilon'^\nu P_\gamma^\rho P_{\gamma'}^\sigma \epsilon_{\mu\nu\rho\sigma} J_{m,m,m}(M_P,0,0)/m,$$

which compares with the general covariant form

$$A(P \to \gamma\gamma) = i g_{P\gamma\gamma} \varepsilon^\mu \varepsilon'^\nu P_\gamma^\rho P_{\gamma'}^\sigma \epsilon_{\mu\nu\rho\sigma},$$

suggesting

$$g_{P\gamma\gamma} = \frac{N_C}{2\pi^2} g_{Pq\bar{q}} e^2 Q^2 J_{m,m,m}(M_P,0,0)/m. \tag{5.19}$$

5.2 Symmetry Limit Integrals

Although the derivations in Section 5.1 are free of dynamical approximations (except in (5.7) where $M_P \to 0$ was used) it is useful to derive some symmetry limit relations of the loop integral forms. Not only may they provide an insight into the workings of the quark triangles, they also give us some direct checks with other research. The two most appropriate simplifications to consider are a chiral limit form in which the pseudoscalar mass is assumed insignificant in the Feynman graph and a heavy quark limit where a quark mass is much larger than the other quarks.

5.2.1 Chiral symmetry limit of $J_{m,m,\bar{m}}(M_V, M_P, 0)$

The chiral symmetry limit is useful in the light meson sector, and allows us to directly compare our derivation against that of Bramon and Scadron [25]. The limit corresponds to a small pseudoscalar mass when compared to the vector mass, that is $M_V^2 >> M_P^2$. Such a limit is entirely appropriate for the study of the radiative decays of K^* mesons, and it is reassuring to know that our $J_{m,m,\bar{m}}(M_V, M_P, 0)$ reduces to the J_M of [25] in the chiral limit.

The chiral limit, corresponding to $M_P \to 0$ in $J_{m,m,\bar{m}}(M_V, M_P, 0)$, enables us to use the real form for $j^a_{m,\bar{m}}$ in (5.13) as $M_P \leq |m - \bar{m}|$.

$$v^{\pm}_{m,\bar{m}}(0) = 0, -\delta^2 - 2\delta$$

from (5.9) so that

$$j^a_{m,\bar{m}}(0) = \sum_{k=\pm} \mathrm{Li}_2(v^k_{m,\bar{m}}(0), 0) = \mathrm{Li}_2(0,0) + \mathrm{Li}_2(-\delta^2 - 2\delta, 0) = \mathrm{Li}_2(-\delta^2 - 2\delta, 0),$$

and

$$\begin{aligned} & j^b_{m,\bar{m}}(M_P \to 0) \\ &= -\delta \sum_{k=\pm} \left(1 - 1/v^k_{m,\bar{m}}(M_P \to 0)\right) \ln\left|1 - v^k_{m,\bar{m}}(M_P \to 0)\right| \\ &= -\delta \left(\lim_{\epsilon \to 0}(1 - 1/\epsilon) \ln|1 - \epsilon| + (1 + 1/(\delta^2 + 2\delta)] \ln\left|1 + 2\delta + \delta^2\right|\right) \\ &= -\delta - \frac{2(\delta+1)^2}{\delta+2} \ln|1 + \delta|\,. \end{aligned}$$

Thus $J_{m,m,\bar{m}}(M_V, M_P, 0)$ in the chiral limit $M_P \to 0$ becomes

$$J_{m,m,\bar{m}}(M_V,0,0) = \frac{m^2}{M_V^2}\left\{\delta + \sum_{k=\pm}\left[\mathrm{Li}_2(v^k_{m,\bar{m}}(M_V),0) - \delta(1-1/v^k_{m,\bar{m}}(M_V))\right.\right.$$
$$\left.\left.\times \ln\left|1-v^k_{m,\bar{m}}(M_V)\right|\right] - \mathrm{Li}_2(-\delta^2-2\delta,0) + \frac{2(1+\delta)^2}{2+\delta}\ln|1+\delta|\right\}, \quad (5.20)$$

where we have assumed $v^k_{m,\bar{m}}(M_V)$ is real. This form may be simplified even further near the isospin symmetry limit whereby $\bar{m} \simeq m$. In this instance δ is small and we ignore δ terms of order 2 and higher,

$$\begin{aligned}
\mathrm{Li}_2(-\delta^2-2\delta,0) &\to \mathrm{Li}_2(-2\delta,0), \\
\frac{2(1+\delta)^2}{2+\delta}\ln|1+\delta| &\to (\delta+\frac{1}{2})\ln|1+2\delta|, \\
v^{\pm}_{m,m(1+\delta)}(M_V) &\underset{\delta \text{ small}}{\to} -\tfrac{1}{2}\left\{2\delta - (M_V/m)^2\right. \\
&\quad \left.\mp[(2\delta+(M_V/m)^2)^2 - (2M_V/m)^2]^{1/2}\right\} \\
&= \frac{M_V^2}{2m^2} - \delta \pm \left[\left(\frac{M_V^2}{2m^2}-\delta\right)^2 - \frac{M_V^2}{m^2}\right]^{1/2}. \quad (5.21)
\end{aligned}$$

Thus we find $J_{m,m,\bar{m}}(M_V,0,0)$ incorporating isospin symmetry (say $\bar{m} = m+\epsilon$) between quark flavors reduces to

$$\begin{aligned}
J_{m,m,m(1+\delta)}(M_V,0,0) = \frac{m^2}{M_V^2}\Bigg\{\delta + \sum_{k=\pm}\Big[&\mathrm{Li}_2(v^k_{m,m(1+\delta)}(M_V),0) \\
&-\delta\left(1-1/v^k_{m,m(1+\delta)}(M_V)\right)\ln\left|1-v^k_{m,m(1+\delta)}(M_V)\right|\Big] \\
&-\mathrm{Li}_2(-2\delta,0) + (\delta+1/2)\ln|1+2\delta|\Bigg\},
\end{aligned}$$

with $v^{\pm}_{m,m(1+\delta)}(M_V)$ defined in Eq. (5.21). This form is very similar to the J_M of Bramon and Scadron [25] once the identifications $m = M$, $\bar{m} = \bar{M}$, $P^2 = M_V^2$, $v^{\pm}_{m,m(1+\delta)}(M_V) = v_{1,2}$ and $J_{m,m,m(1+\delta)}(M_V,0,0) = J_M$ are made. There is a subtle difference in their use of the dilogarithm function $\mathrm{Li}_2(z)$ versus our function $\mathrm{Li}_2(z,0)$ which is similar to the dilog, but which only allows real solutions (the term $i\pi \ln\left|v^k_{m,\bar{m}}(M)\right|$ in Eq. (5.13) ensures this). In the chiral limit with $M_V > m+\bar{m}$ these two functions are equivalent. In

addition their form finishes with the term $(\delta - 1/2)\ln|1+2\delta|$ whereas we have $(\delta+1/2)\ln|1+2\delta|$. We believe this difference is due to a typographical mistake as the argument of the natural log function is linked to the multiplier outside, so that there should be no difference between them (the missing multiplication factor of two is easily accounted for, but not the sign change).

5.2.2 Chiral symmetry limit of $J_{m,m,m}(M_P, 0, 0)$

There is a well-known chiral limit of the $P \to \gamma\gamma$ case which is applied to $\pi^0 \to \gamma\gamma$ [20, 4], namely $g_{\pi^0\gamma\gamma} = e^2 N_C g_{\pi^0} Q^2/4\pi^2 m$. This implies that $J_{m,m,m}(M_{\pi^0}, 0, 0) = 1/2$. We can establish this from our full formulae. With the chiral limit $M_P \to 0$ so that $M_P < 2m$ and the appropriate form of J from (5.18) is

$$J_{m,m,m}(M_P, 0, 0) = 2m^2 \mathrm{Li}_2(\rho(M_P), \phi_{m,m}(M_P))/M_P^2,$$

and we define $M_P/m = \epsilon$ with $\epsilon \to 0$ as $M_P \to 0$. We subsequently find $\rho(M_P) = \epsilon, \cos\phi_{m,m}(M_P) = \epsilon/2$ and therefore

$$\begin{aligned} J_{m,m,m}(M_P, 0, 0) &= \frac{2}{\epsilon^2}\left[-\frac{1}{2}\int_0^\epsilon \frac{dx}{x}\ln(1-\epsilon x + x^2)\right] \\ J_{m,m,m}(M_P \to 0, 0, 0) &\approx -\frac{1}{\epsilon^2}\int_0^\epsilon dx[-\epsilon + (1-\epsilon^2/2)x + \epsilon(\epsilon^2+3)x/3 + \ldots] \\ &= \frac{1}{2} - \epsilon^2/12 + \epsilon^4/9 + \ldots \end{aligned}$$

Consequently, we see $J_{m,m,m}(M_P \to 0, 0, 0)$ reproduces the $\pi^0 \to \gamma\gamma$ result in the chiral limit.

5.2.3 Heavy quark symmetry limit

Since we are particularly interested in the heavy meson decays $D^* \to D\gamma$ and $B^* \to B\gamma$ we feel it is of interest to examine the heavy quark expansion of our loop integral J. To derive this we consider an expansion in terms of the light to heavy quark mass ratio in each of the loop integrals. We make

the arbitrary choice of $m = m_q$ and $\bar{m} = m_Q$, where m_q is the light quark mass, and m_Q the heavy quark mass. These lead to the following definitions:

$$\frac{m}{\bar{m}} = \epsilon \tag{5.22}$$

$$M_P = \bar{m} + \Lambda_P, \tag{5.23}$$

$$M_V = \bar{m} + \Lambda_V \tag{5.24}$$

where $\epsilon \to 0$ in the heavy quark limit, and Λ_P, Λ_V is the combined binding energy and light quark mass for the pseudoscalar and vector meson, respectively.

Heavy quark limit of $J_{m,m,m/\epsilon}(M_V, M_P, 0)$

We consider the heavy quark limit of $J_{m,m,\bar{m}/\epsilon}(M_V, M_P, 0)$ and from (5.23) and (5.24) we make the extra definitions

$$M_{V,P}/m = r_{V,P} + 1/\epsilon$$

where $r_{V,P} = \Lambda_{V,P}/m = (M_{V,P} - \bar{m})/m$. Substituting these variable redefinitions in (5.8) and ignoring terms of order $\mathcal{O}(1)$ or higher

$$J_{m,m,m/\epsilon}(M_V, M_P, 0) \approx \int_0^1 dx \int_0^{1-x} dy \frac{x/\epsilon}{x/\epsilon^2 - 2(r_V - r_P)xy/\epsilon - (2r_P + 1/\epsilon)x(1-x)/\epsilon}.$$

This may be solved to

$$J_{m,m,m/\epsilon}(mr_V + \bar{m}, mr_P + \bar{m}, 0) = -\frac{\epsilon\,(r_V \ln|2r_V\epsilon| - r_P \ln|2r_P\epsilon|)}{(r_V - r_P)(1 + 2\epsilon(r_V + r_P))} \tag{5.25}$$

as the highest order terms in the expansion. Note that this term is of the form $\epsilon \ln \epsilon$ and we can thus expect slow convergence of the heavy quark limit form.

Heavy quark limit of $J_{\bar{m},\bar{m},\bar{m}\epsilon}(M_V, M_P, 0)$

The triangle diagram in which the role of m and $\bar{m}$ is swapped corresponds to $J_{\bar{m},\bar{m},m}$, which, with the notation (5.22) is expressed as $J_{\bar{m},\bar{m},\bar{m}\epsilon}$. With the

role of m and $\bar{m}$ reversed, we are now interested in the ratios $M_{V,P}/\bar{m}$ which are given by

$$M_{V,P}/\bar{m} = 1 + \Lambda_{V,P}/\bar{m} = 1 + r_{V,P}\epsilon.$$

If we reformulate (5.8) and ignore contributions of order ϵ^2 and higher we find

$$\begin{aligned} & J_{\bar{m},\bar{m},\bar{m}\epsilon}(M_V, M_P, 0) \\ & \quad \approx \int_0^1 dx \int_0^{1-x} dy \frac{1 + (\epsilon - 1)x}{1 - x - 2(r_V - r_P)\epsilon\, xy - (1 + 2r_P\epsilon)x(1-x)} \\ & \quad = [\mathrm{Li}_2(1 + 2r_V\epsilon, 0) - \mathrm{Li}_2(1 + 2r_P\epsilon, 0) \\ & \qquad + \frac{2\epsilon(1-\epsilon)}{1 + 2\epsilon(r_V + r_P)} (r_V \ln|2r_V\epsilon| - r_P \ln|2r_P\epsilon|)]\,. \end{aligned}$$

To simplify this form further, we consider an expansion of the dilogarithm. Since

$$\begin{aligned} & \mathrm{Li}_2(1 + 2r_V\epsilon, 0) - \mathrm{Li}_2(1 + 2r_P\epsilon, 0) \\ & \quad = -\int_{1+2r_P\epsilon}^{1+2r_V\epsilon} \frac{dx}{x} \ln|1 - x| \\ & \quad \approx -\int_{2r_P\epsilon}^{2r_V\epsilon} dz\, \ln z(1 - z + z^2 - z^3 + \ldots) \\ & \quad = -2\epsilon(r_V \ln 2r_V\epsilon - r_P \ln 2r_P\epsilon - (r_V - r_P) + \mathcal{O}(\epsilon)), \end{aligned}$$

to arrive at the final form

$$J_{\bar{m},\bar{m},\bar{m}\epsilon}(mr_V + \bar{m}, mr_P + \bar{m}, 0) = 1 - \frac{\epsilon}{r_V - r_P}(r_V \ln|2r_V\epsilon| - r_P \ln|2r_V\epsilon|). \tag{5.26}$$

Once again observe the $\epsilon \ln \epsilon$ dependence, indicative of slow convergence.

It appears that both expansions (5.25) and (5.26) will only converge slowly to their true counterparts $J_{m,m,\bar{m}}(M_V, M_P, 0)$ and $J_{\bar{m},\bar{m},m}(M_V, M_P, 0)$. Thus, unfortunately, they are not so useful approximations for either the c or b quark cases.

There are other possible expansions we could consider, namely that of the $P \to \gamma\gamma$ and $V \to P\gamma$ loop integrals where there is only one quark flavor in the loop (such as $\eta_c \to \gamma\gamma$, $\eta_b \to \gamma\gamma$, $J/\psi \to \eta_c\gamma$ or $\Upsilon \to \eta_b\gamma$) and consider

some expansion as the quark mass becomes large. Unfortunately, such an expansion fails to be a good approximation, simply due to the assumption one has to make about the pseudoscalar and/or vector mass. For example, in the $P \to \gamma\gamma$ case one would assume the pseudoscalar mass M_P would consist of the sum of the quark masses along with some binding energy so that $M_P = 2m + \Delta$. Then the loop integral could be expressed as

$$J_{m,m,m}(M_P, 0, 0) = \int_0^1 du \int_0^{1-u} \frac{dv}{1 - \rho^2 uv}$$

where $\rho = M_P/m = 2 + \Delta/m$ and one would attempt to do some sort of expansion near $\rho = 2$. Unfortunately such an expansion is impractical as the integral contains a pole at $\rho = 2, u = 1/2$.

5.3 Application to experimental measures

With the technology in place, we now apply it to physical processes involving the electromagnetic decays of the ground state mesons. We start by demonstrating the excellent agreement between the quark triangle prediction and experimental measure of the $K^* \to K\gamma$ neutral to charged width ratio.

5.3.1 $K^* \to K\gamma$ and the coupling ratio

The observed K^* branching fraction [13] of

$$\Gamma_{K^{*0}\to K^0\gamma}/\Gamma_{K^{*+}\to K^+\gamma} = 2.31 \pm 0.29,$$

which translates to the coupling constant ratio of

$$g_{K^{*0}K^0\gamma}/g_{K^{*+}K^+\gamma} = 1.514 \pm 0.125, \tag{5.27}$$

is far from its $SU(3)$ predicted value of 2, but is simply understood in the quark loop formalism as shown by Bramon and Scadron [25]. We quickly re–iterate this point. Using (5.17) and assuming $g_{Vus} = g_{Vds}$ and $g_{Pus} = g_{Pds}$ by isospin,

$$\frac{g_{K^{*0}K^0\gamma}}{g_{K^{*+}K^+\gamma}} = \frac{Q_d J_{d,s}(K^{*0}, K^0)/m_d + Q_s J_{s,d}(K^{*0}, K^0)/m_s}{Q_u J_{u,s}(K^{*+}, K^+)/m_u + Q_s J_{s,u}(K^{*+}, K^+)/m_s} = -1.47, \tag{5.28}$$

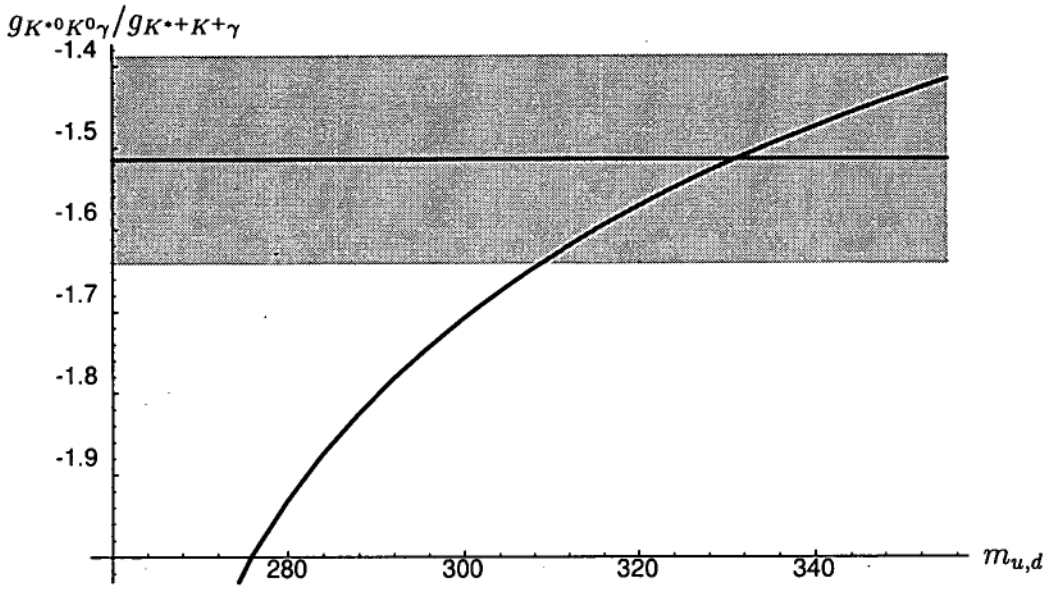

Figure 5.2: Variation of $g_{K^{*0}K^0\gamma}/g_{K^{*+}K^+\gamma}$ with light quark masses, $m_{u,d}$. It is assumed $m_s = 1.5m_{u,d}$.

where we use the shorter notation, $J_{q;q'}(V,P) \equiv J_{m_q,m_q,m_{q'}}(M_V, M_P, 0)$. The quark masses chosen were $m_u = m_d = 340$ MeV and $m_s = 510$ MeV, as used by Bramon and Scadron [25]. In fact the ratio $g_{K^{*0}K^0\gamma}/g_{K^{*+}K^+\gamma}$ is a sensitive measure of the $m_{u,d}$ and m_s masses. If we take $m_s = 1.5m_{u,d}$ which is entirely consistent with many results in the constituent quark model [26, 4, 111, 3, 56] the variation of (5.28) with $m_{u,d}$ (and hence m_s) allows us to constrain $m_{u,d}$ from the experimental result (5.27). This is seen in Figure 5.2, where the experimental result is indicated by the grey band. This plot shows that $310 < m_{u,d} < 360$ MeV and correspondingly $465 < m_s < 545$ MeV. Since an s quark mass of $m_s = m_\phi/2$ gives such a good comparison between the quark triangle diagram and the experimental measurement, we will continue to use this value throughout this work, along with $m_u = m_d = 340$ MeV.

The result (5.28) compares well with that of Bramon and Scadron [25], indicating their reliance on the chiral limit formulae is does not cause any loss of information. In fact we can observe the variation in the coupling relation

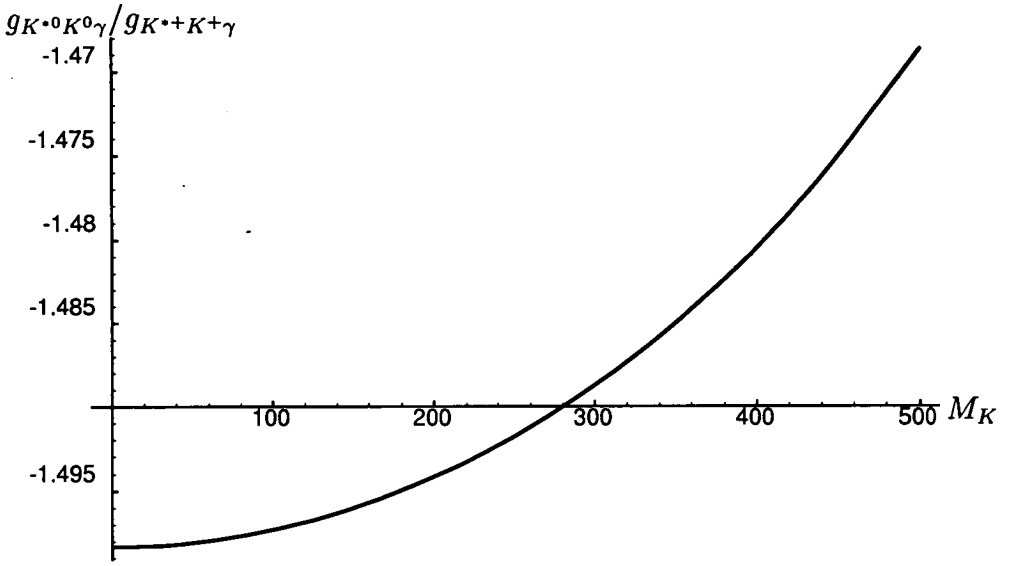

Figure 5.3: The lack of sensitivity of $g_{K^{*0}K^0\gamma}/g_{K^{*+}K^+\gamma}$ to the kaon mass as shown in this figure, emphasizes that a chiral limit form is applicable to this case.

(5.28) from the chiral limit $M_P = 0$ to $M_P = M_K$ using the approximation free $J_{m,m,\bar{m}}(M_V, M_P, 0)$; as Figure 5.3 shows there is very little change in the result.

We can also dramatically show how the s quark mass breaks the $SU(3)$ symmetry. Figure 5.4 displays the behaviour of $g_{K^{*0}K^0\gamma}/g_{K^{*+}K^+\gamma}$ from $m_s = m_u = m_d = 340$ MeV (the $SU(3)$ limit) to $m_s = 550$ MeV clearly indicating that it is the violation of constituent quark masses from $SU(3)$ symmetry that is responsible for the large deviation in K^* mesons from the expected symmetry.

The K^* radiative decays are particularly sensitive to $SU(3)$ violations as they involve the constituent masses of strange and non–strange quarks in the loop of the corresponding triangle diagram. The match achieved by the quark triangle scheme (5.28) to the experimental result (5.27) is far better than $SU(3)$ or broken $SU(3)$, as given by Equation (3.32). Subsequently, it appears the heavier meson cases, $D^* \to D\gamma$ and $B^* \to B\gamma$ which should

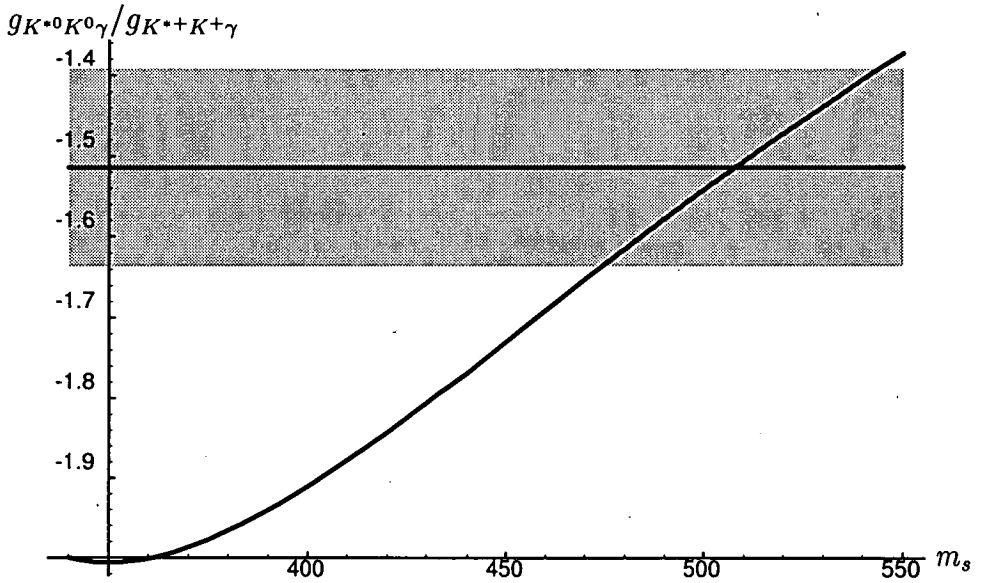

Figure 5.4: The breaking of $SU(3)$ by the s quark mass is clearly responsible for the deviation in the coupling ratio. The experimental measurement is also shown, supporting $m_s \simeq 500$ MeV.

also be sensitive to breaking effects caused by the c and b quark masses, would be best computed by the triangle diagram which can explicitly allow for different constituent masses in the loop, rather than in a broken $SU(4)$ or $SU(5)$ symmetry scheme.

5.3.2 Measurements of $g_{Pqq'}$

We may obtain estimates for the $g_{Pqq'}$ coupling constants using experimental measurements of the $P \to \gamma\gamma$ decay widths. In particular the widths for $\pi^0 \to \gamma\gamma$, $\eta \to \gamma\gamma$ and $\eta' \to \gamma\gamma$ processes are well known and we should be able to determine g_{Puu} and g_{Pss} to reasonable accuracy (we make the isosymmetric approximation $g_{Puu} = g_{Pdd}$, $m_u = m_d$).

Beginning with the π^0 meson which is the antisymmetric mixture $(u\bar{u} - d\bar{d})/\sqrt{2}$, we sum the contributions from both flavours to find the relation between the covariant coupling and the quark level coupling,

$$\begin{aligned} g_{\pi^0\gamma\gamma} &= \frac{6e^2}{4\pi^2}\left\{\left(\frac{2}{3}\right)^2 g_{\pi^0 uu}\frac{J_u(\pi^0)}{m_u} + \left(-\frac{1}{3}\right)^2 g_{\pi^0 dd}\frac{J_d(\pi^0)}{m_d}\right\} \\ &= \frac{e^2}{6\pi^2}\left\{4\frac{g_{Puu}}{\sqrt{2}} - \frac{g_{Pdd}}{\sqrt{2}}\right\} J_u(\pi^0)/m_u \\ &= \frac{e^2}{2\sqrt{2}\pi^2} g_{Puu} J_u(\pi^0)/m_u. \end{aligned} \tag{5.29}$$

For the cases η and $\eta' \to \gamma\gamma$ we obviously have to take into account the mixing of these states. We could do this in terms of the $SU(3)$ basis given in (3.19) and (3.20), but as we are working at the quark level, it is much more convenient to use a quark basis which describes the deviation from the ideal mixing case

$$\begin{aligned} \eta &= -\sin\varphi_P(u\bar{u} + d\bar{d})/\sqrt{2} - \cos\varphi_P s\bar{s}, \\ \eta' &= \cos\varphi_P(u\bar{u} + d\bar{d})/\sqrt{2} - \sin\varphi_P s\bar{s}, \end{aligned}$$

where $\varphi_P = \theta_P - \arctan\frac{1}{\sqrt{2}} \sim -45.8°$, a definition first introduced by Bramon and Greco [23, 24]. Following the methodology shown in (5.29) we obtain relations between the covariant amplitudes and meson–quark couplings which

are given in Table 5.1. These are then used along with the parameters $m_u = 340$ MeV, $m_s = 510$ MeV, $\varphi_P = -45.8°$ (in accordance with the quadratic Gell-Mann–Okubo relation) and the unnormalised covariant couplings from the measured decay rates

$$\Gamma_{P\to\gamma\gamma} = \frac{g^2_{P\gamma\gamma} M_P^3}{64\pi},$$

to obtain several estimates of the pseudoscalar–quark couplings as given in Table 5.2. We used the processes $\eta \to \gamma\gamma$ and $\eta' \to \gamma\gamma$ to simultaneously determine the u and d quark-pseudoscalar meson couplings. We comment that although there is some experimental and theoretical favouritism for a pseudoscalar mixing angle of $\theta_P \approx -20°$, representing a significant deviation from the GMO quadratic mass expectation, this is totally unfounded once some $SU(3)$ symmetry breaking is accounted for in terms of a constituent quark mass difference between the strange and non-strange quarks. With a mass ratio $m_s/m_{u,d} \simeq 1.5$ a vast majority of the experimental results are entirely consistent with $\theta_P = 14° \pm 2°$ [26] which is much closer to the GMO calculation. Hence we persist to use the GMO value and comment when the result appears to have a high sensitivity to the angle.

From the results, it appears g_{Puu} differs as determined from π^0, η and η' processes. The Goldberger–Treiman (GT) relation at the quark–level, gives us a good check of our results. For the pion, the relation reads

$$F_\pi g_{Puu}/\sqrt{2} = m_u. \tag{5.30}$$

Using $F_\pi = 92.42 \pm 0.07 \pm 0.25$ MeV [13] along with $m_u = 340$ MeV we predict $g_{Puu} = 5.203 \pm 0.004 \pm 0.014$ which compares well with the experimental result from $\pi^0 \to \gamma\gamma$. Hence it appears there is a problem with the η or η' determinations, for which there are several possible explanations:

- the η meson is about four times as massive as the pion, so it may be appropriate to allow for mass dependency in the coupling constant. Suppose we label the first coupling constant from $\pi^0 \to \gamma\gamma$

as $g_{Puu}(m^2_{\pi^0})$, while the second from $\eta \to \gamma\gamma$ and $\eta' \to \gamma\gamma$ as a coupling constant somewhere between m_η and $m_{\eta'}$. Numerically we took the appropriate mass as the equal weight average, $(m^2_\eta + m^2_{\eta'})/2$. By linearly interpolating between these two couplings, we estimate a value of $g_{Puu}(m^2_\eta) = 4.61 \pm 0.19$ for $\theta_P = -10.5°$

- the quark triangle diagram may not be successful in the description of $\eta \to \gamma\gamma$ and $\eta' \to \gamma\gamma$ where the heavier pseudoscalar parents are prone to introduce additional gluon-exchange effects. This may have such ramifications as producing admixtures of heavy-flavour $q\bar{q}$ states or gluonium in η' [74]

- the $U(1)$ anomaly may play an important role [37].

Also included in Table 5.2 is the estimate of g_{Pcc} using a charm quark mass of $m_c = 1550$ MeV along with the experimentally determined width [13] of $\Gamma_{\eta_c \to \gamma\gamma} = 3.96 \pm {}^{1.95}_{1.85}$ keV.

5.3.3 Measurements of $g_{Vqq'}$

There exist many useful decay channels $V \to P\gamma$ and corresponding data from which we can determine the product $g_{Vqq'}g_{Pqq'}$. To this end we proceed in two steps. Firstly, we interpret individual meson–meson–photon couplings in terms of meson–quark–antiquark couplings, deriving relations between them as shown in Table 5.1. Assuming isospin symmetry there are only three unknown products of couplings involved in the light meson sector; $g_{Vuu}g_{Puu}$, $g_{Vus}g_{Pus}$, and $g_{Vss}g_{Pss}$. Following this we extract individual meson–meson–photon couplings $g_{VP\gamma}$ from the most recently measured decay widths $\Gamma_{V\to P\gamma} = (M^2_V - M^2_P)^3 g^2_{VP\gamma}/(96\pi M^3_V)$ by simply removing the kinematic factors. The results are listed in the first column of Table 5.2. As one can see, they scatter over a relatively wide range.

We are able to determine $g_{Vuu}g_{Puu}$ solely from any one of the processes $\rho^0 \to \pi^0\gamma$, $\rho^+ \to \pi^+\gamma$, $\rho^0 \to \eta\gamma$, $\omega \to \pi^0\gamma$, $\omega \to \eta\gamma$ and $\eta' \to \rho^0\gamma$.

Process	Relation between covariant couplings and meson–quark couplings
$\pi^0 \to \gamma\gamma$	$g_{\pi^0\gamma\gamma} = \frac{e^2}{2\sqrt{2}\pi^2} g_{Puu} J_u(\pi^0)/m_u$
$\eta \to \gamma\gamma$	$g_{\eta\gamma\gamma} = -\frac{e^2}{6\sqrt{2}\pi^2}\{5\sin\varphi_P g_{Puu} J_u(\eta)/m_u + \sqrt{2}\cos\varphi_P g_{Pss} J_s(\eta)/m_s\}$
$\eta' \to \gamma\gamma$	$g_{\eta'\gamma\gamma} = \frac{e^2}{6\sqrt{2}\pi^2}\{5\cos\varphi_P g_{Puu} J_u(\eta')/m_u - \sqrt{2}\sin\varphi_P g_{Pss} J_s(\eta')/m_s\}$
$\eta_c \to \gamma\gamma$	$g_{\eta_c\gamma\gamma} = \frac{2e^2}{3\pi^2} g_{Pcc} J_c(\eta_c)/m_c$
$\rho^0 \to \pi^0\gamma$	$g_{\rho^0\pi^0\gamma} = \frac{e}{4\pi^2} g_{Vuu} g_{Puu} J_{u,u}(\rho^0, \pi^0)/m_u$
$\rho^+ \to \pi^+\gamma$	$g_{\rho^+\pi^+\gamma} = \frac{e}{4\pi^2} g_{Vud} g_{Pud} J_{u,d}(\rho^+, \pi^+)/m_u$
$\rho^0 \to \eta\gamma$	$g_{\rho^0\eta\gamma} = -\frac{3e}{4\pi^2}\sin\varphi_P g_{Vuu} g_{Puu} J_{u,u}(\rho^0, \eta)/m_u$
$\omega \to \pi^0\gamma$	$g_{\omega\pi^0\gamma} = \frac{3e}{4\pi^2}\cos\varphi_V g_{Vuu} g_{Puu} J_{u,u}(\omega, \pi^0)/m_u$
$\omega \to \eta\gamma$	$g_{\omega\eta\gamma} = -\frac{e}{4\pi^2}\{\cos\varphi_V \sin\varphi_P g_{Vuu} g_{Puu} J_{u,u}(\omega, \eta)/m_u$ $+2\sin\varphi_V \cos\varphi_P g_{Vss} g_{Pss} J_{s,s}(\omega, \eta)/m_s\}$
$\eta' \to \rho^0\gamma$	$g_{\eta'\rho^0\gamma} = \frac{3e}{4\pi^2}\cos\varphi_P g_{Vuu} g_{Puu} J_{u,u}(\eta', \rho^0)/m_u$
$\eta' \to \omega\gamma$	$g_{\eta'\omega\gamma} = \frac{e}{4\pi^2}\{\cos\varphi_P \cos\varphi_V g_{Vuu} g_{Puu} J_{u,u}(\eta', \omega)/m_u$ $-2\sin\varphi_P \sin\varphi_V g_{Vss} g_{Pss} J_{s,s}(\eta', \omega)/m_s\}$
$\phi \to \pi^0\gamma$	$g_{\phi\pi^0\gamma} = -\frac{3e}{4\pi^2}\sin\varphi_V g_{Vuu} g_{Puu} J_{u,u}(\phi, \pi^0)/m_u$
$\phi \to \eta\gamma$	$g_{\phi\eta\gamma} = \frac{e}{4\pi^2}\{\sin\varphi_V \sin\varphi_P g_{Vuu} g_{Puu} J_{u,u}(\phi, \eta)/m_u$ $-2\cos\varphi_V \cos\varphi_P g_{Vss} g_{Pss} J_{s,s}(\phi, \eta)/m_s\}$
$K^{*0} \to K^0\gamma$	$g_{K^{*0}K^0\gamma} = \frac{e}{4\pi^2} g_{Vds} g_{Pds}\left[J_{d,s}(K^{*0}, K^0)/m_d + J_{s,d}(K^{*0}, K^0)/m_s\right]$
$K^{*+} \to K^+\gamma$	$g_{K^{*+}K^+\gamma} = \frac{e}{4\pi^2} g_{Vus} g_{Pus}\left[2J_{u,s}(K^{*+}, K^+)/m_u - J_{s,u}(K^{*+}, K^+)/m_s\right]$
$J/\psi \to \eta_c\gamma$	$g_{J/\psi\eta_c\gamma} = \frac{e}{\pi^2} g_{Vcc} g_{Pcc} J_{c,c}(J/\psi, \eta_c)/m_c$
$\phi \to \rho\pi$	$g_{\phi\rho\pi} \simeq -\frac{3}{2\sqrt{2}\pi^2}\sin\varphi_V g_{Vuu}^2 g_{Puu}\left\{J_{u,u,u}(\phi, \rho^0, 0) + 4J_{u,u,u}(\phi, \rho^+, 0)\right\}/m_u$

Table 5.1: Relations between covariant couplings $g_{P\gamma\gamma}, g_{VP\gamma}$ or $g_{PV\gamma}$ and meson–quark–antiquark couplings $g_{Vq\bar{q}'}, g_{Pq\bar{q}'}$

Experimental result ($\times 10^{-4}\mathrm{MeV}^{-1}$)[13]	Meson–quark–antiquark coupling
$g_{\pi^0\gamma\gamma} = 0.2516 \pm 0.0091$	$g_{Puu} = 5.14 \pm 0.19$
$g_{\eta\gamma\gamma} = 0.239 \pm 0.011$ $g_{\eta'\gamma\gamma} = 0.312 \pm 0.016$	$g_{Puu} = 4.03 \pm 0.14$, $g_{Pss} = 6.45 \pm 0.67$
$g_{\eta_c\gamma\gamma} = 0.055 \pm {}^{0.014}_{0.013}$	$g_{Pcc} = 1.52 \pm {}^{0.38}_{0.36}$
$g_{\rho^0\pi^0\gamma} = 2.95 \pm 0.37$	$g_{Vuu}g_{Puu} = 14.88 \pm 1.89$
$g_{\rho^+\pi^+\gamma} = 2.24 \pm 0.13$	$g_{Vuu}g_{Puu} = 11.23 \pm 0.63$
$g_{\rho^0\eta\gamma} = 5.66 \pm 0.52$	$g_{Vuu}g_{Puu} = 10.94 \pm 1.02$
$g_{\omega\pi^0\gamma} = 7.04 \pm 0.21$	$g_{Vuu}g_{Puu} = 12.52 \pm 0.38$
$g_{\omega\eta\gamma} = 1.82 \pm 0.23$ $g_{\phi\eta\gamma} = 2.100 \pm 0.051$	$g_{Vuu}g_{Puu} = 12.2 \pm 1.5$, $g_{Vss}g_{Pss} = 6.89 \pm 0.17$
$g_{\phi\pi^0\gamma} = 0.417 \pm 0.021$	$g_{Vuu}g_{Puu} = 25.4 \pm 1.3$
$g_{K^{*0}K^0\gamma} = 3.84 \pm 0.17$	$g_{Vds}g_{Pds} = 8.43 \pm 0.37$
$g_{K^{*+}K^+\gamma} = 2.53 \pm 0.11$	$g_{Vus}g_{Pus} = 8.21 \pm 0.37$
$g_{\eta'\rho^0\gamma} = 3.91 \pm 0.18$	$g_{Puu}g_{Vuu} = 15.98 \pm 0.74$
$g_{\eta'\omega\gamma} = 1.369 \pm 0.087$	$\bar{g}_{Puu}\bar{g}_{Vuu} \underset{\downarrow}{=} 11.95 \pm 0.49$ $g_{Pss}g_{Vss} = -36.9 \pm 4.8$
$g_{J/\psi\eta_c\gamma} = 1.66 \pm 0.26$	$g_{Vcc}g_{Pcc} = 1.88 \pm 0.30$
$g_{\phi\rho\pi} = 10.71 \pm 0.30$	$g^2_{Vuu}g_{Puu} = 27.53 \pm 0.76$

Table 5.2: Determination of meson–quark–antiquark couplings.

In addition, the decays $\omega \to \eta\gamma$, $\phi \to \eta\gamma$ and $\eta' \to \omega\gamma$ can be used to simultaneously solve for $g_{Vuu}g_{Puu}$ and $g_{Vss}g_{Pss}$. Our numerical results are shown in the second column of Table 5.2 where we use the same quark masses as previously along with the quark basis mixing angles φ_V and φ_P which are related to the standard mixing angles via $\varphi_{V,P} = \theta_{V,P} - \arctan(1/\sqrt{2})$. We also have at our disposal data from the decay $\phi \to \rho\pi$ and because of the small experimental uncertainty in the width $\Gamma_{\phi\to\rho\pi}$ it provides an accurate estimate of $g^2_{Vuu}g_{Puu}$.

The values of the product $g_{Vuu}g_{Puu}$ turn out to lie in a quite small range, except for that derived from the $\phi \to \pi^0\gamma$ and $\eta' \to \rho^0\gamma$. The result from $\phi \to \pi^0\gamma$ would fall into this range had we chosen a mixing angle of about $\varphi_V \simeq 8°$, a change of 3.5°. Such an extreme sensitivity to change in mixing angle leads us to exclude this channel from our analysis. Recalling the couplings of pseudoscalar meson with quark–antiquark pairs discussed previously, we now obtain g_{Vuu}.

Since the estimate $g_{Puu} = 5.14 \pm 0.19$ from $\pi^0 \to \gamma\gamma$ agrees so well with the GT relation (5.30) we adopt this value as the best measure of g_{Puu}. This along with the $g_{Vuu}g_{Puu}$ and $g^2_{Vuu}g_{Puu}$ measures in Table 5.2 lead to a weighted average value $\bar{g}_{Vuu} = 2.33 \pm 0.04$ which differs from g_{Puu}, revealing a substantial violation of the spin symmetry in the triangle scheme.. This average excludes the measures from $\phi \to \pi^0\gamma$ and $\eta' \to \rho^0\gamma$, the first which is sensitive to the vector mixing angle while the second involves the η' meson, which as mentioned earlier may be susceptible to the $U(1)$ anomaly or other effects. We present an ideogram of this weighted average in Figure 5.5. It shows the $\phi \to \rho\pi$ process gives a very accurate measure of g_{Vuu}, with most of the other results also in compliance with the average. We also note that the weighted average has not been scaled as $\sqrt{\chi^2/(N-1)} = 0.98$.

We repeat this procedure in the analysis of g_{Vss}, but with fewer channels to determine a result. Tentatively taking $g_{Pss} = 6.45 \pm 0.67$ (from $\eta, \eta' \to \gamma\gamma$) we obtain $g_{Vss} = 1.07 \pm 0.11$ from $\omega, \phi \to \eta\gamma$, indicating a large $SU(3)_V$ symmetry breaking once again. We do not use data from $\eta' \to \omega\gamma$ where the

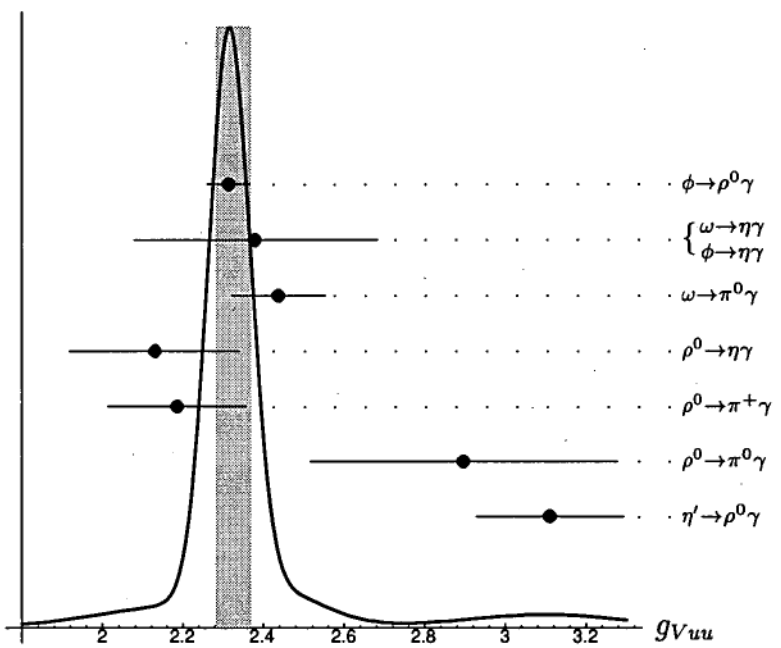

Figure 5.5: Ideogram of the weighted average fit for g_{Vuu}. The result from $\eta' \to \rho^0\gamma$ is not included in the average.

qq'	$g_{Pqq'}$	$g_{Vqq'}$
uu, dd	5.14 ± 0.19	2.33 ± 0.04
us, ds	3.76 ± 0.04	2.21 ± 0.10
ss	6.45 ± 0.67	1.07 ± 0.11
cc	1.52 ± 0.52	1.24 ± 0.18

Table 5.3: Average quark-meson couplings from experimental measures

average product $g_{Vuu}g_{Puu}$ has been used to determine $g_{Vss}g_{Pss}$. Estimates for g_{Vcc} using the $J/\psi \to \eta_c\gamma$ channel yield $g_{Vcc} = 1.24 \pm 0.18$. Note that g_{Vcc} and g_{Pcc} are not substantially different, perhaps indicative of a limit $g_{Vqq} = g_{Pqq}$ as m_q gets large.

For completeness, we wish to obtain a measure of g_{Vus} using the product $g_{Vus}g_{Pus}$. However, we have no means of getting g_{Pds} for the kaon in the triangle scheme. This is because unlike π^0, the $K^0 \to \gamma\gamma$ decay is not mediated by pure electromagnetic interactions. However assuming the Goldberger–Treiman relation at the quark level

$$f_K g_{Pus}(m_K^2) = (m_u + m_s)/2$$

we find $g_{Pus} = 3.761 \pm 0.035$ where we have used $f_K = 113.0 \pm 1.0 \pm 0.3$ MeV [13]. Subsequently, $g_{Vus} = 2.21 \pm 0.10$ (averaged over the charged and neutral processes).

In summary we provide the average quark-meson couplings in Table 5.3. The most noticeable difference between these values and those of a similar study [77, 85] based on the 1994 Particle Data Tables is in the values of g_{Vcc} and g_{Pcc} (which were $g_{Vcc} = 0.92 \pm 0.23$ and $g_{Pcc} = 2.02 \pm 0.38$). The updated experimental measures of $\Gamma_{J/\psi\to\eta_c\gamma}$ and $\Gamma_{\eta_c\to\gamma\gamma}$ are responsible for the change.

5.4 Predictions

The stability of the quark-meson couplings, particularly for the u quark, enable the prediction of several decay widths. It also provides a very simple means to predict heavy meson coupling ratios like (5.28) where the only free parameter is the c and b quark mass.

5.4.1 $\phi \to \eta'\gamma$ coupling constant and branching fraction

We can use our best fit estimates of the meson–quark coupling constants to predict the decay width for the decay $\phi \to \eta'\gamma$.

$$\begin{aligned} g_{\phi\eta'\gamma} &= -\frac{e}{4\pi^2}\{\sin\varphi_V \cos\varphi_P g_{Vuu} g_{Puu} J_{u,u}(\phi,\eta')/m_u \\ &\quad +2\cos\varphi_V \sin\varphi_P g_{Vss} g_{Pss} J_{s,s}(\phi,\eta')/m_s\} \end{aligned}$$

and using $m_u = 340$ MeV, $m_s = 510$ MeV and mixing angles $\varphi_P = -45.8°$, $\varphi_V = 4.08°$ along with our couplings from Table 5.3, we compute the coupling to be $g_{\phi\eta'\gamma} \simeq 5.55 \times 10^{-4}$ MeV^{-1}. This gives a branching ratio of

$$Br(\phi \to \eta'\gamma) \simeq 3.94 \times 10^{-4}$$

which is slightly below the experimental upper limit of $Br(\phi \to \eta'\gamma) < 4.1 \times 10^{-4}$ at 90% confidence level [13]. We point out that the result displays very sensitive dependence on the choice of s quark mass. Also we remain cautious of predictions involving the η' meson due to its association with the $U(1)$ anomaly.

5.4.2 $D^* \to D\gamma$ and $B^* \to B\gamma$ coupling ratios

Since the derivation of $J_{m,m,\bar{m}}(M_V, M_P, 0)$ is free of approximations we can safely apply it to the D^* and B^* meson radiative decays. To do so we must assume $g_{Vuq} = g_{Vdq}$ and $g_{Puq} = g_{Pdq}$ where q is either the c or b quark (much like we did in the $K^* \to K\gamma$ case). With this quite reasonable assumption the coupling ratio $g_{H^{*0}H^0\gamma}/g_{H^{*+}H^+\gamma}$ ($H = D$ or B) is given by

$$\frac{g_{D^{*0}D^0\gamma}}{g_{D^{*+}D^+\gamma}} = \frac{Q_u J_{u,c}(D^{*0}, D^0)/m_u + Q_c J_{c,u}(D^{*0}, D^0)/m_c}{Q_d J_{d,c}(D^{*+}, D^+)/m_d + Q_c J_{c,d}(D^{*+}, D^+)/m_c}, \qquad (5.31)$$

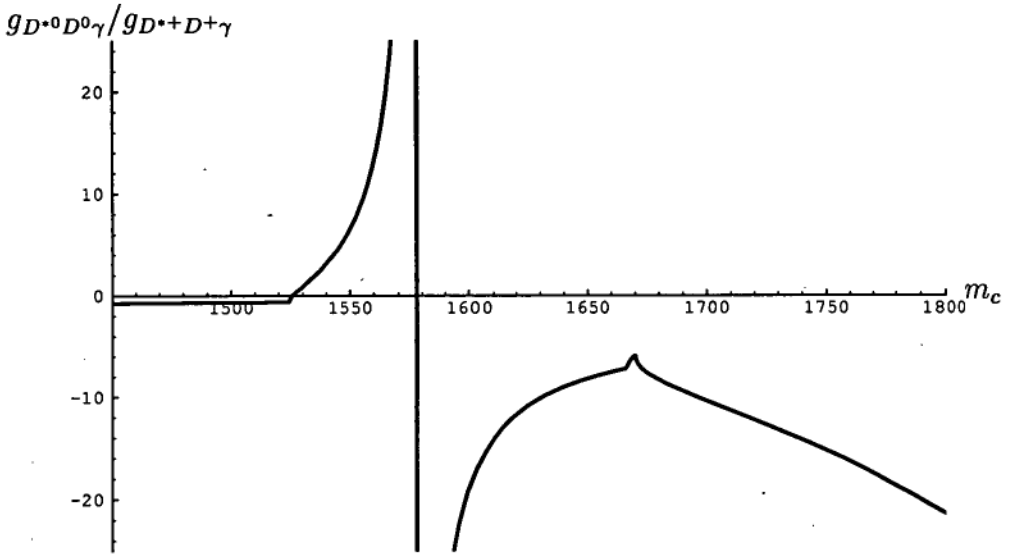

Figure 5.6: Variation of coupling ratio $g_{D^{*0}D^0\gamma}/g_{D^{*+}D^+\gamma}$ with c quark mass.

and

$$\frac{g_{B^{*0}B^0\gamma}}{g_{B^{*+}B^+\gamma}} = \frac{Q_d J_{d,b}(B^{*0}, B^0)/m_d + Q_b J_{b,d}(B^{*0}, B^0)/m_b}{Q_u J_{u,b}(B^{*+}, B^+)/m_u + Q_b J_{b,u}(B^{*+}, B^+)/m_b}. \tag{5.32}$$

Relations (5.31) and (5.32) allow us examine the coupling constant ratios as a function of the c and b quark mass, respectively.

The behaviour appears in Figures 5.6 and 5.7. In order to give actual values we use a c quark mass of 1550 MeV (approximately half the J/ψ mass) yielding $g_{D^{*0}D^0\gamma}/g_{D^{*+}D^+\gamma} = 6.47$ and a b quark mass of 4730 MeV (approximately half the Υ mass) which gives $g_{B^{*0}B^0\gamma}/g_{B^{*+}B^+\gamma} = 0.018$. We can compare our results with those of other workers. These are presented in Table 5.4. We hoped that our study of $g_{Vqq'}, g_{Pqq'}$ measurements would enable us to make some reasonable estimates of $g_{Vuc}g_{Puc}$ and $g_{Vub}g_{Pub}$, but the data does not allow this. Thus we cannot make predictions about actual decay widths.

From the table we see that our estimate of $g_{D^{*0}D^0\gamma}/g_{D^{*+}D^+\gamma} = 6.47$ is of within the range of other predictions, while $g_{B^{*0}B^0\gamma}/g_{B^{*+}B^+\gamma} = 0.018$ is small compared to the few theoretical expectations available. Nonetheless,

Ref.	$\frac{g_{D^{*0}D^0\gamma}}{g_{D^{*+}D^+\gamma}}$	$\frac{g_{B^{*0}B^0\gamma}}{g_{B^{*+}B^+\gamma}}$	Parameters and/or Model[a] (masses in GeV)
This	6.47	0.018	$m_{u,d} = 0.34,\ m_c = 1.55,\ m_b = 4.73$
(3.33) (3.34)	60	0.8	broken $\tilde{U}(4N_f)$
[118]	7.6 ± 2.2	0.588 ± 0.078	$\{m_{u,d} = 0,\ m_c = 1.3,\ m_b = 4.7\}$ QCDSR
[75]	6.17	0.571	$\left\{ \begin{array}{l} m_{u,d} = 0.25,\ m_s = 0.37, \\ m_c = 1.445,\ m_b = 4.64 \end{array} \right\}$ RQM
[29]	4.06	0.583	$\left\{ \begin{array}{l} m_u = 0.338,\ m_c = 1.6, \\ m_d = 0.322,\ m_b = 5 \end{array} \right\}$ HQET
[38]	8.48	-	Bethe-Salpeter approach
[89]	5.5 ± 2.8	0.60 ± 0.16	HHCT
[1]	3.05	0.488	$\{m_{u,d} = 0,\ m_b = 4.7\}$QCDSR
[109]	5.10	0.685	$\{m_{u,d,s} = 0.25,\ m_c = 1.44,\ m_b = 4.8\}$ RQM
[48]	$6.3 \pm {}^{14.1}_{2.7}$	0.64 ± 0.14	$\{m_c = 1.45 \pm 0.05,\ m_b = 4.7 \pm 0.03\}$ QCDSR
[28]	12.9	-	$\{m_{u,d} = 0.35,\ m_c = 1.5\}$ RQM
[2]	3.28 ± 0.47	-	$\{m_{u,d} = 0,\ m_s = 0.15,\ m_c = 1.35\}$ QCDSR
[56]	3.36	0.479	$\left\{ \begin{array}{l} m_{u,d} = 0.385,\ m_c = 1.52, \\ m_s = 0.545,\ m_b = 4.8 \end{array} \right\}$ VMD+KRSF
[100]	3.81		$\{m_u = 0.31,\ m_s = 0.485,\ m_c = 1.662\}$H-LS
[73]	5.32	0.576	HHCT
[92]	6.71	-	$\{m_{u,d} = 0.3,\ m_c = 1.6\}$ RLFQM
[32]	6.61	0.62	$\left\{ \begin{array}{l} m_{u,d,s} = 0.48,\ m_c = 1.57 \text{ for } D^* \\ m_{u,d,s} = 0.59,\ m_b = 4.93 \text{ for } B^* \end{array} \right\}$RPM
[31]	5.5 ± 2.8	0.59 ± 0.16	$\{m_{u,d} = 0.55\}$ HQET+VMD
[30]	1.0 ± 1.1	0.44 ± 0.47	$\{m_c = 1.5,\ m_b = 4.5\}$ HHCT
[79]	3.50	-	SQM
[108]	-	0.676	$\{m_s = 0.279,\ m_b = 5.2\}$ Bag
[98]	3.84 ± 0.80	-	
[86]	4.54	-	$\left\{ \begin{array}{l} m_{u,d} = 0,\ m_s = 0.279 \\ m_c = 1.5,\ \lambda = 1 \end{array} \right\}$ Bag
[113]	3.93 ± 0.20	-	$SU(4)$
[113]	4.49 ± 0.23	-	broken $SU(4)$
[113]	3.92 ± 0.21	-	broken $SU(4)$ by $1/M_V^2$
[95]	2.00	-	QM + PCAC
[50]	3.72	0.55	$\{m_{u,d} = 0.335,\ m_c = 1.84\}$ QM
[112]	0.57 ± 0.20		Finite Energy Sum Rules

[a]Abbreviations: R=Relativistic, QM=Quark Model, SQM=Simple QM, H-LS=Heavy-Light System, HHCT=Heavy Hadron Chiral Theory, QCDSR=QCD Sum Rules, PM=Potential Model, LF=Light Front

Table 5.4: Summary of theoretical estimates of radiative coupling ratio.

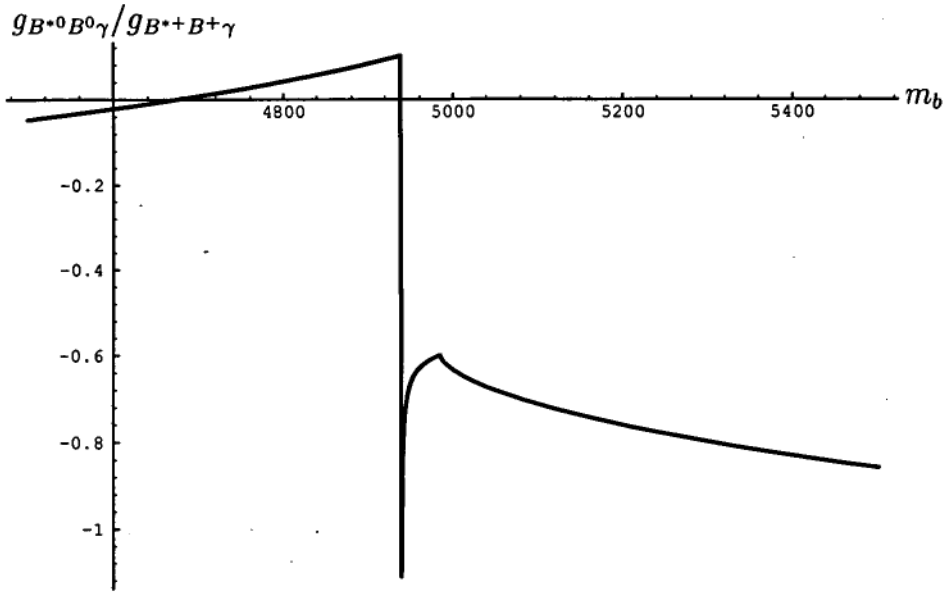

Figure 5.7: Variation of coupling ratio $g_{B^{*0}B^0\gamma}/g_{B^{*+}B^+\gamma}$ with b quark mass.

Figure 5.7 shows a value $g_{B^{*0}B^0\gamma}/g_{B^{*+}B^+\gamma} \simeq 0.6$ is easily achieved with a small change of the b quark mass to $m_b \simeq 5000$ MeV. Hence our method is quite sensitive to m_b so that accurate experimental measure of the ratio $g_{B^{*0}B^0\gamma}/g_{B^{*+}B^+\gamma}$ would in turn constrain the b quark constituent mass.

5.5 Summary

We have successfully evaluated $V \to P\gamma$ and $P \to \gamma\gamma$ processes in a quark triangle diagram scheme which is valid for arbitrary vector or pseudoscalar masses, as well as $V \to PV'$ processes for light pseudoscalar mass with same quark masses in the loop. By comparison with available experimental data, we found that this scheme works well for all radiative processes involving the light mesons (no charm or bottom quarks), except for $\phi \to \pi^0\gamma$ (due to the sensitivity of this channel to the mixing angle) and the channels $\eta' \to \rho^0(\omega)\gamma$.

The scheme produces well determined estimates of the meson–quark–antiquark couplings for the light mesons and which preserve universality of a

given quark flavour. However, this adherence to universality is at the expense of a prolification of meson–quark–antiquark couplings. The large difference between $g_{Vqq'}$ and $g_{Pqq'}$ indicates a substantial violation of spin symmetry in the quark triangle formalism.

A number of predictions have been made based on the scheme. Firstly we note that our theoretical result for the $\phi \to \eta'\gamma$ decay width is around the present experimental upper limit and awaits comparison with further measurement. Secondly our prediction for $g_{D^{*0}D^0\gamma}/g_{D^{*\pm}D^{\pm}\gamma} = 6.47$ with $m_c \approx m_{J/\psi}/2$ is within range of other theoretical estimates, while $g_{B^{*0}B^0\gamma}/g_{B^{*\pm}B^{\pm}\gamma} = 0.018$ for $m_b \approx m_\Upsilon/2$ is small compared with the few results in the literature. We expect future measurements of these radiative decays will distinguish between these predictions.

Chapter 6

Conclusions

6.1 Summary

This thesis has sought universal couplings in the two-body strong and electromagnetic decays of the mesons. We have used two quite distinct techniques to derive these couplings from the experimental measures of the decay widths, one acting at the meson level while the other at the quark level.

Chapter 2 detailed the historical development of the $SU(6)$ symmetry of elementary particles from arguments akin to those of Wigner's $SU(4)$ theory of nuclear interactions. We contrasted the predictions of the $SU(6)$ scheme with the well-known ones of $SU(3)$, or the "eightfold way." These included the particle classifications, the mass relations and baryon magnetic moments. In most cases the $SU(6)$ predictions were well matched by experiment. We also discussed the many salient features of the $SU(6)$ scheme, in particular its more intuitive basis and the fact that it requires the existence of the 'colour' quantum number. These beneficial aspects of the symmetry are offset by the difficulties in obtaining a relativistic generalisation of it, but nonetheless we detailed a useful covariant theory based on $\tilde{U}(4N_f)$. It provides meson wavefunctions and interaction Lagrangians which are invariant under an extended symmetry group. We also discussed the similarities between this approach and many modern techniques.

The advantage of the $\tilde{U}(4N_f)$ scheme is that by virtue of its extended symmetry, it reduces the number of coupling constants required to calculate interactions. This is perfect for establishing universal coupling constants, and this was the focus of Chapter 3. In this chapter we applied the supermultiplet scheme to the ground state meson decays using 'world averaged' experimental data. We found reasonably uniform coupling constants for VPP interactions, but most significantly our method easily identified a simple symmetry breaking deviation which could be incorporated into the scheme. The direct study of VVP vertex type interactions was restricted to the process $\phi \to \rho\pi$, but we examined them indirectly via vector meson dominance and electromagnetic interactions. It was not as easy to identify a symmetry breaking mechanism, possibly because of the uncertainties of the VMD approach. The $\tilde{U}(4N_f)$ scheme relates the couplings from VPP and VVP interactions, and an excellent match was obtained with reasonable averages of masses and couplings. The last part of the chapter was concerned with demonstrating the predictive power of the supermultiplet method, particularly in the heavy meson arena. Our results were consistent with many other theoretical techniques.

The excited mesons have not been the focus of much theoretical study. We have tried to partly rectify this with a comprehensive analysis of the two-body strong decays of all orbitally excited mesons, as given in Chapter 4. Our motivation is still to determine coupling constants from decay widths, and since the $\tilde{U}(4N_f)$ scheme was seen to perform well in the ground state cases, the version of the scheme suitable for orbital excitation states was used, namely $\tilde{U}(4N_f) \otimes O(3,1)_L$. Once again, because it is has supermultiplet particle structure it requires much fewer coupling constants than lower symmetry schemes. Following the derivation of numerous interaction and decay rate formulae, the coupling constants for OZI allowed two-body strong decays of $L = 1$ to $L = 3$ parent meson to ground state mesons were calculated from experimental data. The results were very encouraging and support the $\tilde{U}(4N_f) \otimes O(3,1)_L$ wavefunctions from the universality of the coupling

constants. However, there were many results which would benefit from more accurate experimental data to truly test the scheme. Toward the end of the chapter we once again demonstrated the power of the supermultiplet method by supplying several predictions about the strong decays of the $L = 1$ charm mesons. In some cases we could compare our predictions with other work and there was usually good agreement. Importantly, our work has detailed some predictions for these decay widths not witnessed elsewhere.

Chapter 5 saw the development of a complementary technique. It was mainly concerned with trying to improve the understanding of electromagnetic interactions of the ground states in the context of universal couplings at vertices in a quark triangle diagram. We applied the approximation free form of the corresponding loop integral to several processes, $V \to P\gamma$, $P \to \gamma\gamma$ and $\phi \to \rho\pi$ and typically returned very uniform meson–quark–antiquark couplings from analysis of experimental rates. We could once again extract some predictions from the method, but they were only of neutral to charged coupling ratios. It would seem that the quark triangle method is highly accurate in most situations that it can be applied, but this is offset by the number of coupling constants required to describe a given interaction from the quark flavours involved in the loop.

6.2 Outlook

There have been some very encouraging and unique results obtained in this thesis, some of which deserve better study. Of considerable worth would be examination of the origin of the observed behaviour $g_{LSS}/g_{(L+1)SS} \sim 2000$ MeV which could be intimately linked to the parameters in the confining quark potential and may reveal information about the nature of quark binding in the mesons. One could also attempt to merge the ideas learned in Chapter 5 where the importance of the constituent quark mass differences was shown, with those of the scaling behaviour in g_{VPP}. Some researchers have already tried this [42] in an approximate way, but nonetheless with some

fruitful outcomes. However, the ultimate test of such a technique would be in its prediction of the ratio $g_{K^{*0}K^0\gamma}/g_{K^{*+}K^+\gamma}$. The author has attempted this and achieved some match with experiment, but unfortunately the technique was not gauge invariant.

This study has mainly exploited the machinery of the $\tilde{U}(4N_f) \otimes O(3,1)_L$ symmetry to examine the two-body strong and electromagnetic decays of mesons and has shown this to be very valuable and accurate. This suggests there are still plenty of processes which could be analysed for universal couplings using this approach. The simplest next step would be to include three-body strong and electromagnetic decays of the mesons. This would be particularly useful in the orbitally excited meson realm, as the increasing phase space makes such processes more likely. The baryon states are also embodied in the $\tilde{U}(4N_f) \otimes O(3,1)_L$ scheme along with baryon-meson interactions and this too would be a fruitful field of study. Finally, the weak transitions could also be studied in the context of the supermultiplet scheme, as advocated by several workers [70].

Appendix A

Groups, relations and identities

A.1 Unitary symmetry groups

A.1.1 The $SU(3)$ algebra

The λ-matrices are

$$\lambda_1 = \begin{pmatrix} 0 & 1 & 0 \\ 1 & 0 & 0 \\ 0 & 0 & 0 \end{pmatrix}, \qquad \lambda_2 = \begin{pmatrix} 0 & -i & 0 \\ i & 0 & 0 \\ 0 & 0 & 0 \end{pmatrix},$$

$$\lambda_3 = \begin{pmatrix} 1 & 0 & 0 \\ 0 & -1 & 0 \\ 0 & 0 & 0 \end{pmatrix}, \qquad \lambda_4 = \begin{pmatrix} 0 & 0 & 1 \\ 0 & 0 & 0 \\ 1 & 0 & 0 \end{pmatrix},$$

$$\lambda_5 = \begin{pmatrix} 0 & 0 & -i \\ 0 & 0 & 0 \\ i & 0 & 0 \end{pmatrix}, \qquad \lambda_6 = \begin{pmatrix} 0 & 0 & 0 \\ 0 & 0 & 1 \\ 0 & 1 & 0 \end{pmatrix},$$

$$\lambda_7 = \begin{pmatrix} 0 & 0 & 0 \\ 0 & 0 & -i \\ 0 & i & 0 \end{pmatrix}, \qquad \lambda_8 = \frac{1}{\sqrt{3}} \begin{pmatrix} 1 & 0 & 0 \\ 0 & 1 & 0 \\ 0 & 0 & -2 \end{pmatrix}.$$

A.1.2 The $U(2,2)$ algebra

The sixteen 4×4 Dirac matrices

$$\gamma_R = \begin{cases} 1 \\ \gamma_\mu \\ \sigma_{\mu\nu} = \frac{i}{2}[\gamma_\mu, \gamma_\nu] \\ i\gamma_\mu\gamma_5 \\ \gamma_5 = \gamma_0\gamma_1\gamma_2\gamma_3 \end{cases}, \; R = 1, \ldots, 16; \; \mu, \nu = 0, 1, 2, 3$$

with metric $g_{\mu\nu} = (1, -1, -1, -1)_{\text{diag}}$ and $\{\gamma_\mu, \gamma_v\} = 2g_{\mu\nu}$ obey the multiplication rules

$$\begin{aligned}
\gamma_\mu\gamma_\nu &= -i\sigma_{\mu\nu} + g_{\mu\nu}, \\
\gamma_\lambda\sigma_{\mu\nu} &= i(g_{\lambda\mu}\gamma_\nu - g_{\lambda\nu}\gamma_\mu) + \epsilon_{\kappa\lambda\mu\nu}i\gamma^\kappa\gamma_5, \\
\gamma_\mu i\gamma_\nu\gamma_5 &= ig_{\mu\nu}\gamma_5 + \tfrac{1}{2}\epsilon_{\mu\nu\kappa\lambda}\sigma^{\kappa\lambda}, \\
\sigma_{\kappa\lambda}\sigma_{\mu\nu} &= i(g_{\kappa\nu}\sigma_{\lambda\mu} + g_{\lambda\mu}\sigma_{\kappa\nu} - g_{\kappa\mu}\sigma_{\lambda\nu} - g_{\lambda\nu}\sigma_{\kappa\mu}) \\
&\quad +(g_{\kappa\mu}g_{\lambda\nu} - g_{\lambda\mu}g_{\kappa\nu} - \epsilon_{\kappa\lambda\mu\nu}\gamma_5), \\
\sigma_{\kappa\lambda}i\gamma_\mu\gamma_5 &= i(g_{\lambda\mu}i\gamma_\kappa\gamma_5 - g_{\kappa\mu}i\gamma_\lambda\gamma_5) - \epsilon_{\kappa\lambda\mu\nu}\gamma^\nu, \\
\sigma_{\kappa\lambda}\gamma_5 &= \tfrac{1}{2}\epsilon_{\kappa\lambda\mu\nu}\sigma^{\mu\nu}, \\
\gamma_\mu\gamma_5\gamma_\nu\gamma_5 &= g_{\mu\nu} - i\sigma_{\mu\nu}.
\end{aligned}$$

The generators of the group J_R, normalised so that $J_R = \frac{1}{2}\gamma_R$ constitutes the fundamental representation, satisfy the commutation relations:

$$\begin{aligned}
[J_{\mu\nu}, J_5] &= 0, \\
[J_\mu, J_\nu] = -[J_{\mu 5}, J_{\nu 5}] &= -iJ_{\mu\nu}, \\
[J_\mu, J_{\nu 5}] &= ig_{\mu\nu}J_5, \\
[J_\lambda, J_{\mu\nu}] &= i\left(g_{\lambda\mu}J_\nu - g_{\lambda\nu}J_\mu\right), \\
[J_{\lambda 5}, J_{\mu\nu}] &= i\left(g_{\lambda\mu}J_{\nu 5} - g_{\lambda\nu}J_{\mu 5}\right), \\
[J_{\kappa\lambda}, J_{\mu\nu}] &= i\left(g_{\kappa\nu}J_{\lambda\mu} + g_{\lambda\mu}J_{\kappa\nu} - g_{\kappa\mu}J_{\lambda\nu} - g_{\lambda\nu}J_{\kappa\mu}\right), \\
[J_\mu, J_5] &= -iJ_{\mu 5}, \\
[J_{\mu 5}, J_5] &= -iJ_\mu.
\end{aligned}$$

A.2 Dirac trace algebra

The general properties of traces, as shown for the same dimensional matrices A and B,

$$\begin{aligned} \mathrm{Tr}[A+B] &= \mathrm{Tr}[A]+\mathrm{Tr}[B], \\ \mathrm{Tr}[AB] &= \mathrm{Tr}[BA] \end{aligned}$$

are often used along with the specific results for the γ–matrices in Dirac's representation,

$$\begin{aligned} \mathrm{Tr}[\gamma_\mu] &= 0 \\ \mathrm{Tr}[\gamma_5] &= 0, \\ \mathrm{Tr}[\gamma_5(\gamma)^n] &= 0, \text{for } n<4, \\ \mathrm{Tr}[(\gamma)^{2n+1}] &= 0, \forall n \end{aligned} \tag{A.1}$$

$$\begin{aligned} \mathrm{Tr}[1] &= 4, \\ \mathrm{Tr}[\gamma_\mu\gamma_\nu] &= 4g_{\mu\nu}, \\ \mathrm{Tr}[\gamma_\mu\gamma_\nu\gamma_\rho\gamma_\sigma] &= 4(g_{\mu\nu}g_{\rho\sigma}-g_{\mu\rho}g_{\nu\sigma}+g_{\mu\sigma}g_{\nu\rho}), \\ \mathrm{Tr}[\gamma_5\gamma_\mu\gamma_\nu\gamma_\rho\gamma_\sigma] &= -4\epsilon_{\mu\nu\rho\sigma}. \end{aligned} \tag{A.2}$$

A.3 Antisymmetric Tensor Identities

$$\begin{aligned} \epsilon_{\mu\nu\rho\sigma}\epsilon^{\mu\nu\rho\sigma} &= -4! \\ \epsilon_{\mu\nu\rho\sigma}\epsilon_{\mu'}{}^{\nu\rho\sigma} &= -3!\, g_{\mu\mu'} \\ \epsilon_{\mu\nu\rho\sigma}\epsilon_{\mu'\nu'}{}^{\rho\sigma} &= -2!\begin{vmatrix} g_{\mu\mu'} & g_{\nu\mu'} \\ g_{\mu\nu'} & g_{\nu\nu'} \end{vmatrix} \\ \epsilon_{\mu\nu\rho\sigma}\epsilon_{\mu'\nu'\rho'}{}^{\sigma} &= -1!\begin{vmatrix} g_{\mu\mu'} & g_{\nu\mu'} & g_{\rho\mu'} \\ g_{\mu\nu'} & g_{\nu\nu'} & g_{\rho\nu'} \\ g_{\mu\rho'} & g_{\nu\rho'} & g_{\rho\rho'} \end{vmatrix} \end{aligned} \tag{A.3}$$

Bibliography

[1] T. M. Aliev, D. A. Demir, E. Iltan, and N. K. Pak. Radiative $B^* \to B\gamma$ and $D^* \to D\gamma$ decays in light cone QCD sum rules. *Phys. Rev. D*, 54(1):857–862, 1996.

[2] T. M. Aliev, E. Iltan, and N. K. Pak. Radiative D^* meson decays in QCD sum rules. *Phys. Lett. B*, 334:169–174, 1994.

[3] Ll. Ametller, C. Ayala, and A. Bramon. $SU(3)$ breaking mechanisms for pseudoscalar–meson charge radii. *Phys. Rev. D*, 24(1):233–235, 1981.

[4] Ll. Ametller, C. Ayala, and A. Bramon. Constituent–quark and baryon loops in pseudoscalar transitions. *Phys. Rev. D*, 29(5):916–920, 1984.

[5] James F. Amundson, C. Glenn Boyd, Elizabeth Jenkins, Michael Luke, Aneesh V. Manohar, Jonathan L. Rosner, Martin J. Savage, and Mark B. Wise. Radiative D^* decay using heavy quark and chiral symmetry. *Phys. Lett. B*, 296:415–419, 1992.

[6] D. Aston et al. Spin-parity determination of the $\phi_J(1850)$ from $K - p$ interactions at 11 GeV/c. *Phys. Lett. B*, 208:324–330, 1988.

[7] D. Aston et al. A study of $K^-\pi^+$ scattering in the reaction $K^-p \to K^-\pi^+n$ at 11-GeV/c. *Nucl. Phys. B*, 296:493, 1988.

[8] K. Bardakci, J. M. Cornwall, P. G. O. Freund, and B. W. Lee. Intrinsically broken $U(6) \otimes U(6)$ symmetry for strong interactions. *Phys. Rev. Lett.*, 13(23):698–701, 1964.

[9] K. Bardakci, J. M. Cornwall, P. G. O. Freund, and B. W. Lee. Intrinsically broken $U(6) \otimes U(6)$ symmetry for strong interactions II. *Phys. Rev. Lett.*, 14(2):48–51, 1965.

[10] William A. Bardeen and Christopher T. Hill. Chiral dynamics and heavy quark symmetry in a solvable toy field theoretic model. *Phys. Rev. D*, 49(1):409–425, 1994.

[11] V. Bargmann and E. P. Wigner. Group theoretical discussion of relativistic wave equations. *Proc. Nat. Acad. Sci. Wash.*, 34:211, 1948.

[12] S. Barlag et al. ACCMOR Collaboration. Measurement of the mass and width of the charmed meson $D^{*+}(2010)$. *Phys. Lett. B*, 278:481–484, 1992.

[13] R. M. Barnett et al. Review of Particle Properties. Particle Data Group. *Phys. Rev. D*, 54(1):1, 1996.

[14] D. A. Bauer et al. TPC/Two Gamma Collaboration. Measurement of the kaon content of three-prong τ decays. *Phys. Rev. D*, 50(1):R13–R17, 1994.

[15] M. A. B. Bég, B. W. Lee, and A. Pais. $SU(6)$ and electromagnetic interactions. *Phys. Rev. Lett.*, 13(16):514–517, 1964.

[16] M. A. B. Bég and A. Pais. Covariance, $SU(6)$ and unitarity. *Phys. Rev. Lett.*, 14(13):509–512, 1965.

[17] M. A. B. Bég and A. Pais. Relativistic, crossing-symmetric, $SU(6)$-invariant S-matrix theory. *Phys. Rev. Lett.*, 14(8):267–270, 1965.

[18] Mirza A. Baqi Bég and Virendra Singh. Splitting of spin-unitary spin supermultiplets. *Phys. Rev. Lett.*, 13(13):418–421, 1964.

[19] V. M. Belyaev, V. M. Braun, A. Khodjamirian, and R. Rückl. $D^*D\pi$ and $B^*B\pi$ couplings in QCD. *Phys. Rev. D*, 51(11):6177–6195, 1995.

[20] J. Bernabéu, R. Tarrach, and F. J. Yndurain. Quark masses, isospin breaking and the vector piece of $\pi \to e\nu\gamma$. *Phys. Lett. B*, 79:464–468, 1978.

[21] R. Blankenbecler, M. L. Golderger, K. Johnson, and S. B. Treiman. Some tests of relativistic $SU(6)$ schemes. *Phys. Rev. Lett.*, 14(13):518–520, 1965.

[22] Harry G. Blundell, Stephen Godfrey, and Brian Phelps. Properties of the strange axial mesons in the relativized quark model. *Phys. Rev. D*, 53(7):3715–3722, 1996.

[23] A. Bramon and M. Greco. Radiative decays of mesons and an extended vector-meson dominance model. *Nuovo Cimento*, 14A(2):323–334, 1973.

[24] A. Bramon and M. Greco. Quark model predictions for radiative decays of mesons. *Phys. Lett. B*, 48:137–, 1974.

[25] A. Bramon and M. D. Scadron. Breaking of $SU(3)$ in vector-meson radiative decays. *Phys. Rev. D*, 40(11):3779–3781, 1989.

[26] A. Bramon and M. D. Scadron. Pseudoscalar $\eta - \eta'$ mixing and $SU(3)$ breaking. *Phys. Lett. B*, 234:346–348, 1990.

[27] J. M. Charap and P. T. Matthews. On the covariant extension of $SU(6)$. *Proc. Roy. Soc.*, 286A:300–311, 1965.

[28] Nan-Guang Chen and Kuang-Ta Chao. The quark axial vector coupling and heavy meson decays. *Phys. Lett. B*, 345:67–73, 1995.

[29] Hai-Yang Cheng, Chi-Yee Cheung, Guey-Lin Lin, Y. C. Lin, Tung-Mow Yan, and Hoi-Lai Yu. Chiral lagrangians for radiative decays of heavy hadrons. *Phys. Rev. D*, 47(3):1030–1042, 1993.

[30] Peter Cho and Howard Georgi. Electromagnetic interactions in heavy hadron chiral theory. *Phys. Lett. B*, 296:408–414, 1992.

[31] P. Colangelo, F. De Fazio, and G. Nardulli. Radiative heavy meson transitions. *Phys. Lett. B*, 316:555–560, 1993.

[32] P. Colangelo, F. De Fazio, and G. Nardulli. D^* radiative decays and strong coupling of heavy mesons with soft pions in a QCD relativistic potential model. *Phys. Lett. B*, 334:175–179, 1994.

[33] P. Colangelo, F. De Fazio, G. Nardulli, N. Di Bartolomeo, and R. Gatto. Strong coupling of excited heavy mesons. *Phys. Rev. D*, 52(11):6422–6434, 1995.

[34] P. Colangelo, G. Nardulli, A. Deandrea, N. Di Bartolomeo, R. Gatto, and F. Feruglio. On the coupling of heavy mesons to pions in QCD. *Phys. Lett. B*, 339:151–159, 1994.

[35] Sidney Coleman. Trouble with relativistic $SU(6)$. *Phys. Rev.*, 138(5B):1262–1267, 1965.

[36] J. M. Cornwall, P. G. O. Freund, and K. T. Mahanthappa. Meson-Baryon scattering in the intrinsically broken $M(12)$ scheme. *Phys. Rev. Lett.*, 14(13):515–517, 1965.

[37] R. J. Crewther. Status of the $U(1)$ problem. *Riv. Nuovo Cim.*, 2(8):63–117, 1979.

[38] Yuan-Ben Dai, Chao-Shang Huang, and Hong-Ying Jin. The $1/M$ expansion in the B-S formalism and the decay of 1^- and 0^+ heavy mesons to order $1/M$. *Z. Phys. C*, 65:87–92, 1995.

[39] Yuan-Ben Dai and Hong-Ying Jin. Decay widths of excited heavy mesons in leading order of the $1/M_Q$ expansion. *Phys. Rev. D*, 52(1):236–241, 1995.

[40] R. Delbourgo. Covariant supermultiplet theory, the Zweig rule and the ψ particles. *Phys. Lett. B*, 59:357–360, 1975.

[41] R. Delbourgo and Dongsheng Liu. Heavy quark supermultiplet excitations. *Phys. Rev. D*, 49(11):5979–5983, 1994.

[42] R. Delbourgo and Dongsheng Liu. Strong and electromagnetic interactions of heavy baryons. *Phys. Rev. D*, 53:6576–6581, 1996.

[43] R. Delbourgo, M. A. Rashid, A. Salam, and J. Strathdee. The $\tilde{U}(12)$ symmetry. In *Proceedings of the International Seminar in High-Energy Physics and Elementary Particles, Trieste, 1965*, pages 455–529, Vienna, 1965. International Atomic Energy Agency.

[44] R. Delbourgo, A. Salam, and J. Strathdee. Relativistic structure of $SU(6)$. *Phys. Rev.*, 138(2B):420–423, 1965.

[45] R. Delbourgo and Abdus Salam. Reggeization in supermultiplet theories. *Phys. Rev.*, 186(5):1516–1528, 1969.

[46] A. Denner. Techniques for the calculation of electroweak radiative corrections at the one loop level and results for W physics at LEP200. *Fortschr. Phys.*, 41:307–420, 1993.

[47] A. Donnachie and A. B. Clegg. Eta Rho in diffractive photoproduction and e^+e^- annihilation. *Z. Phys. C.*, 34:257–260, 1987.

[48] H. G. Dosch and S. Narison. $B^*B\pi(\gamma)$ couplings and $D^*D\pi(\gamma)$- decays within a $1/M$-expansion in full QCD. *Phys. Lett. B*, 368:163–170, 1996.

[49] Freeman J. Dyson. *Symmetry Groups in Nuclear and Particle Physics.* W.A. Benjamin Inc., New York and Amsterdam, 1966.

[50] E. Eichten, K. Gottfried, T. Kinoshita, K.D. Lane, and T.M. Yan. Charmonium: comparison with experiment. *Phys. Rev. D*, 21(1):203–233, 1980.

[51] Estia E. Eichten, Christopher T. Hill, and Chris Quigg. Properties of orbitally excited heavy-light ($Q\bar{q}$) mesons. *Phys. Rev. Lett.*, 71(25):4116–4119, 1993.

[52] V.L. Eletsky and Y.A.I. Kogan. Calculation of $D^* \to D\gamma$ and $D^* \to D\pi$ decay witdths from QCD sum rules. *Z. Phys. C*, 28:155–161, 1985.

[53] Adam F. Falk and Michael Luke. Strong decays of excited heavy mesons in chiral perturbation theory. *Phys. Lett. B*, 292:119–127, 1992.

[54] Adam F. Falk and Thomas Mehen. Excited heavy mesons beyond leading order in the heavy quark expansion. *Phys. Rev. D*, 53(1):231–240, 1996.

[55] Fayyazuddin and Riazuddin. Heavy-quark spin symmetry and D mesons. *Phys. Rev. D*, 48(5):2224–2229, 1993.

[56] Fayyazuddin and Riazuddin. Radiative D^* decay using vector meson dominance. *Phys. Lett. B*, 337:189–191, 1994.

[57] R. P. Feynman, M. Gell-Mann, and G. Zweig. Group $U(6) \otimes U(6)$ generated by current components. *Phys. Rev. Lett.*, 13(22):678–681, 1964.

[58] M. Gell-Mann. Isotopic spin and new unstable particles. *Phys. Rev.*, 92(2):833L–834L, 1953.

[59] M. Gell-Mann. Symmetries of baryons and mesons. *Phys. Rev.*, 125(3):1067–1084, 1962.

[60] M. Gell-Mann. A schematic model of baryons and mesons. *Phys. Lett.*, 8(3):214–215, 1964.

[61] M. Gell-Mann, D. Sharp, and W. G. Wagner. Decay rates of neutral mesons. *Phys. Rev. Lett.*, 8(6):261–262, 1962.

[62] Benjamin Grinstein. Light–quark, heavy–quark systems. *Annu. Rev. Nucl. Part. Sci.*, 42:101–145, 1992.

[63] A. G. Grozin and O. I. Yakovlev. Couplings of heavy hadrons with pions from QCD sum rules. Preprint BudkerINP-94-3, hep-ph/9401267, 1994.

[64] F. Gürsey, A. Pais, and L. A. Radicati. Spin and unitary spin independence of strong interactions. *Phys. Rev. Lett.*, 13(8):299–301, 1964.

[65] F. Gürsey and L. A. Radicati. Spin and unitary spin independence of strong interactions. *Phys. Rev. Lett.*, 13(5):173–175, 1964.

[66] Haim Harari. Duality diagrams. *Phys. Rev. Lett.*, 22(11):562–565, 1969.

[67] W. Heisenberg. *Zeits. f. Physik*, 77:1, 1932.

[68] K Hikasa et al. Review of Particle Properties. Particle Data Group. *Phys. Rev. D*, 45(S1), 1992.

[69] F. Hussain, J. G. Körner, K. Schilcher, G. Thompson, and Y.L. Wu. Heavy-light hadrons and current induced transitions among them. *Phys. Lett. B*, 249:295–302, 1990.

[70] F. Hussain, J. G. Körner, and G. Thompson. Relativistic $SU(6)$ wave functions as the basis of modern approaches to hadronic wave functions. *Ann. Phys.*, 206:334–367, 1991.

[71] Nathan Isgur and Mark B. Wise. Weak decays of heavy mesons in the static quark approximation. *Phys. Lett. B*, 232:113–117, 1989.

[72] Nathan Isgur and Mark B. Wise. Weak transition form factors between heavy mesons. *Phys. Lett. B*, 237:527–530, 1990.

[73] Pankaj Jain, Arshad Momen, and Joseph Schechter. Heavy meson radiative decays and light vector meson dominance. *Int. J. Mod. Phys. A*, 10:2467–2478, 1995.

[74] Wolfgang Jaus. Relativistic constituent-quark model of electroweak properties of light mesons. *Phys. Rev. D*, 44(9):2851–2859, 1991.

[75] Wolfgang Jaus. Semileptonic, radiative, and pionic decays of B, B^* and D, D^* mesons. *Phys. Rev. D*, 53(3):1349–1365, 1996.

[76] N. R. Jones and R. Delbourgo. Meson supermultiplet decay constants. *Aust. J. Phys.*, 48:55–69, 1995.

[77] N. R. Jones and Dongsheng Liu. Radiative decays of heavy and light mesons in a quark triangle approach. *Phys. Rev. D*, 53(11):6334–6343, 1996.

[78] A. B. Kaidalov and A. V. Nogteva. Predictions of the model of quark-gluon strings for boson masses and widths. Systems consisting of light and heavy quarks. *Sov. J. Nucl. Phys.*, 47(2):321–325, 1988.

[79] A. N. Kamal and Q. P. Xu. Total width of the D^*. *Phys. Lett. B*, 284:421–426, 1992.

[80] N. Kemmer. *Proc. Roy. Soc.*, 173A:91, 1939.

[81] A. Khodjamirian and R. Rückl. Heavy meson form factors, couplings and exclusive decays in QCD. *Nucl. Phys. B*, 39BC:396–398, 1995.

[82] T.K. Kuo and Tsu Yao. Mass formulas in the $SU(6)$ symmetry scheme. *Phys. Rev. Lett.*, 13(13):415–417, 1964.

[83] R. Levi Setti and Thomas Lasinski. *Strongly Interacting Particles.* The University of Chicago Press, Chicago, 1973.

[84] L. Lewin and J. C. P. Miller. *Dilogarithms and associated functions.* Macdonald, London, 1958.

[85] Dongsheng Liu and N. R. Jones. Quark triangle diagram and radiative meson decays. *Aust. J. Phys.*, 50:155–162, 1997.

[86] Gerald A. Miller and Paul Singer. Radiative and pionic decays of the D^* mesons and the magnetic moment of the charmed quark. *Phys. Rev. D*, 37(9):2564–2569, 1988.

[87] L. Montanet et al. Review of Particle Properties. Particle Data Group. *Phys. Rev. D*, 50(3):1173–1823, 1994.

[88] Tadao Nakano and Kazuhiko Nishijima. Charge independence for V-particles. *Prog. Theor. Phys.*, 10:581L–582L, 1953.

[89] G. Nardulli. Chiral effective theory for heavy mesons. In Casalbouni, G. Domokos, S. Kovesi-Domokos, and B. Monteleoni, editors, *Johns Hopkins Workshop on Current Problems in Particle Theory, 18th: Theory Meets Experiment, Florence, Italy, Aug 31 - Sep 2, 1994.*, page 308, Florence, 1995. Scientific.

[90] Y. Ne'eman. Derivation of strong interactions from a gauge invariance. *Nucl. Phys.*, 26:222–229, 1961.

[91] Shmuel Nussinov and Werner Wetzel. Comparison of exclusive decay rates for $b \to u$ and $b \to c$ transitions. *Phys. Rev. D*, 36(1):130–136, 1987.

[92] Patrick J. O'Donnell and Q. P. Xu. Strong and radiative D^* decays. *Phys. Lett. B*, 336:113–118, 1994.

[93] S. Okubo. Note on unitary symmetries in strong interactions. *Prog. Theoret. Phys.*, 27(5):949–966, 1962.

[94] A. Pais. Implications of spin-unitary spin independence. *Phys. Rev. Lett.*, 13(5):175–177, 1964.

[95] T. N. Pham. Partially conserved axial–vector current condition in the quark model: G_A/G_V for vector mesons and the $\omega\rho\pi$ coupling constant. *Phys. Rev. D*, 25(11):2955–2959, 1982.

[96] Vladimir Privman and Paul Singer. The width and decay modes of charmed tensor mesons. *Phys. Lett. B*, 91:436–440, 1980.

[97] P. Roman and J. J. Aghassi. Covariant merging of spin and unitary spin. *Phys. Lett.*, 14(1):68–70, 1965.

[98] J. L. Rosner. In *Particles and Fields 3, Proc. Banff Summer Institute (Banff, Canada, 1988)*, page 395, Singapore, 1989. World Scientific.

[99] Jonathan L. Rosner. Graphical form of duality. *Phys. Rev. Lett.*, 22(13):689–692, 1969.

[100] Jonathan L. Rosner. P-wave mesons with one heavy quark. *Comments Nucl. Part. Phys.*, 16(3):109–130, 1986.

[101] B. Sakita. Supermultiplets of elementary particles. *Phys. Rev.*, 136(6B):1756–1760, 1964.

[102] Bunji Sakita and Kameshwar C. Wali. Relativistic formulation of the $SU(6)$ symmetry scheme. *Phys. Rev.*, 139(5B):B1355–B1367, 1965.

[103] J. J. Sakurai. Theory of strong interactions. *Ann. Phys.*, 11:1–48, 1960.

[104] A. Salam, R. Delbourgo, M. A. Rashid, and J. Strathdee. The covariant theory of strong interaction symmetries. II. *Proc. Roy. Soc.*, 286A:312–318, 1965.

[105] A. Salam, R. Delbourgo, and J. Strathdee. The covariant theory of strong interaction symmetries. *Proc. Roy. Soc.*, 284A:146–158, 1965.

[106] A. Salam, J. Strathdee, J. M. Charap, and P. T. Matthews. P and C properties of the $\tilde{U}(12)$ multiplets. *Phys. Lett.*, 15(2):184–185, 1965.

[107] M. D. Scadron. *Advanced Quantum Theory and Its Applications Through Feynman Diagrams.* Springer-Verlag, New York, 1979.

[108] Paul Singer and G. A. Miller. $B^* \to B\gamma$ decays in a bag model for heavy–light–quark states. *Phys. Rev. D*, 39(3):825–827, 1989.

[109] M. Sutherland, B. Holdom, S. Jaimungal, and Randy Lewis. What can a relativistic quark model tell us about charmed mesons? *Phys. Rev. D*, 51(9):5053–5063, 1995.

[110] Mahiko Suzuki. Strange axial-vector mesons. *Phys. Rev. D*, 47(3):1252–1255, 1993.

[111] R. Tarrach. Meson charge radii and quarks. *Z. Phys. C*, 2:221–223, 1979.

[112] R. L. Thews. Comparison of symmetry and duality constraints for radiative transitions of mesons. *Phys. Rev. D*, 17(11):3038–3049, 1978.

[113] R.L. Thews and A.N. Kamal. D^* decays: Do theory and experiment agree? *Phys. Rev. D*, 32(3):810–812, 1985.

[114] W. Thirring. Electromagnetic properties of hadrons in the static $SU(6)$ model. *Acta Physica Austriaca*, Suppl II:205–211, 1966.

[115] Nils A. Törnqvist and Matts Roos. Confirmation of the sigma meson. *Phys. Rev. Lett.*, 76(10):1575–1578, 1996.

[116] John Weinstein and Nathan Isgur. $K\bar{K}$ molecules. *Phys. Rev. D*, 41(7):2236, 1990.

[117] E. Wigner. On the consequences of the symmetry of the nuclear hamiltonian on the spectroscopy of nuclei. *Phys. Rev.*, 51:106–119, 1937.

[118] Shi-lin Zhu, W-Y. P. Hwang, and Ze-sen Yang. $D^* \to D\gamma$ and $B^* \to B\gamma$ as derived from QCD sum rules. e-print hep-ph/9610412, 1996.

[119] M. Zielinski et al. Evidence for the electromagnetic production of the A_1. *Phys. Rev. Lett.*, 52(14):1195–1198, 1984.

[120] G. Zweig. An $SU(3)$ model for strong interaction symmetry. Preprint CERN-TH-412, Centre Européen de la Recherche Nucléaire, 1964.